

T.C.
YEDİTEPE UNIVERSITY
INSTITUTE OF HEALTH SCIENCES
DEPARTMENT OF PHARMACOGNOSY

***IN VITRO* EFFECTS OF
SOME PLANTS WHICH ARE USED IN TRADITIONAL
MEDICINE IN TURKEY ON SEVERAL
INFLAMMATORY PARAMETERS**

IN THE PARTIAL FULFILMENT OF THE REQUIREMENTS
FOR THE DEGREE OF DOCTOR OF PHILOSOPHY

İrem Atay, Pharm.

Advisors

Prof. Dr. Erdem Yeşilada

Prof. Dr. Hasan Kırmızıbekmez

ISTANBUL
FEBRUARY 2014

T.C.
YEDİTEPE UNIVERSITY
INSTITUTE OF HEALTH SCIENCES
DEPARTMENT OF PHARMACOGNOSY

***IN VITRO* EFFECTS OF
SOME PLANTS WHICH ARE USED IN TRADITIONAL
MEDICINE ON SEVERAL INFLAMMATORY
PARAMETERS**

IN THE PARTIAL FULFILMENT OF THE REQUIREMENTS
FOR THE DEGREE OF DOCTOR OF PHILOSOPHY

İrem Atay, Pharm.

Advisors

Prof. Dr. Erdem Yeşilada

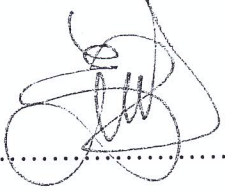
Prof. Dr. Hasan Kırmızıbekmez

ISTANBUL
FEBRUARY 2014

Doktora öğrencisi İrem Atay'ın çalışması jürimiz tarafından Farmakognozi Anabilim Dalı doktora tezi olarak uygun görülmüştür.

İMZA

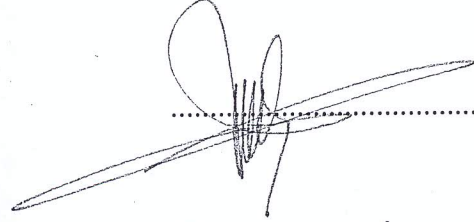
Başkan : Prof. Dr. Erdem YEŞİLADA
Üniversite : Yeditepe Üniversitesi



Üye : Prof. Dr. Hasan KIRMIZİBEKMEZ
Üniversite : Yeditepe Üniversitesi



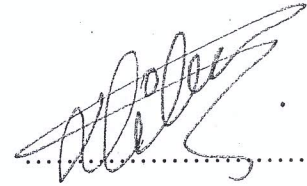
Üye : Prof. Dr. Ekrem SEZİK
Üniversite : Yeditepe Üniversitesi



Üye : Prof. Dr. Esra Küpeli AKKOL
Üniversite : Gazi Üniversitesi



Üye : Doç. Dr. Dilek TELCİ
Üniversite : Yeditepe Üniversitesi




ONAY

Yukarıdaki jüri kararı Enstitü Yönetim Kurulu'nun .21./02./2014
sayılı kararı ile onaylanmıştır.

tarikh ve4-6.....

Prof. Dr. Bayram YILMAZ
Sağlık Bilimleri Enstitü Müdürü V.



Dedication

*The work behind this thesis is dedicated to my family,
with serenity, peace, joy
and love...*

Acknowledgements

First and foremost, I would like to express the deepest appreciation to my advisor, Prof. Dr. Erdem Yeşilada, for his encouragement, generosity, guidance and support during this study. I really appreciate for all the advice, help, and opportunities he has given to me. His wisdom, knowledge and commitment to the highest standards inspired and motivated me.

I also would like to thank Prof. Dr. Hasan Kırmızıbekmez for his guidance and support. His endless support has been precious all these years. He always showed me patience and understanding during the exhausting chromatographic isolation and structure elucidation studies.

I would like to express my gratitude to Assoc. Prof. Dr. Dilek Telci for her guidance on activity assays. I am deeply grateful to her for giving me the opportunity to learn the bioassays conducted in her laboratory and reviewing this thesis.

I would also like to thank Assoc. Prof. Dr. Ahmet Ceyhan Gören of TÜBİTAK National Meteorology Institute (TÜBİTAK UME) for providing us with NMR spectra of the isolates.

My friends and colleagues in Department of Pharmacy and Department of Genetics and Bioengineering deserve warm thanks for giving hand in solving problems, providing a pleasant atmosphere and giving and sharing experience, strength and hope.

Last but not the least, I would like to thank my family, my mother Demet Atay and my sister Ikbal Atay for their endless patience. Without their support this work would not be possible. And precious thanks goes to my father who left us too early for giving me the first idea of attending this Ph.D programme.

TUBITAK is greatly acknowledged for their support. This study is funded by TUBITAK-SBAG (Project no: 110S197) research grant.



Sambucus ebulus L.



Sambucus nigra L.



Cistus laurifolius L.

Abstract

The leaves of *Sambucus ebulus* L, *S. nigra* L. (Caprifoliaceae) and *Cistus laurifolius* L. (Cistaceae) were used against inflammatory problems in Turkish folk medicine. Previous investigations have proven their *in vivo* potent anti-inflammatory activity. The aim of the present study was to investigate their effects on various inflammatory parameters by using *in vitro* methods to provide evidences on their activity mechanisms and to isolate the active ingredients through activity-guided procedures.

Active components were isolated from extracts by using an *in vitro* bioassay model based on the inhibition of nuclear factor-kappa B in Lipopolysaccharide (LPS)-induced Raw 264.7 macrophages and their chemical structures were elucidated by spectroscopic techniques. Flavonoids; Isorhamnetin-3-*O*-glucopyranoside, isorhamnetin-3-*O*-rutinoside, quercetin-3-*O*-glucopyranoside, quercetin-3-*O*-galactopyranoside and two new iridoids; Sambulin A, Sambulin B were identified from *S. ebulus*, a sterol mixture (SNH-1) and remaining water subextract (CL-R-H₂O) were determined to be active components of *S. nigra* and *C. laurifolius*, respectively. These active molecules or fractions were further investigated for their effects on several inflammatory mediators [i.e. TNF α , IL-1 α , IL-1 β , IL-2, IL-6, PGE₂ (ELISA)], nitric oxide (Griess Assay). Effects on the protein levels (iNOS/COX-2) or phosphorylations [Mitogen-Activated Protein Kinases (MAPK) and inhibitor of kappa-B protein (I κ B α)] were studied by Western Blot.

As conclusion, among the isolated flavonoids; isorhamnetin-3-*O*-glucopyranoside and isorhamnetin-3-*O*-rutinoside inhibited NO, iNOS, TNF α , isorhamnetin-3-*O*-rutinoside inhibited PGE₂/COX-2. Both flavonoids inhibited p38/I κ B α phosphorylations. Iridoid type constituents suppressed iNOS/COX-2, NO/PGE₂ and TNF α as well as JNK/I κ B α phosphorylations. The active fractions, SNH-1 and CL-R-H₂O, decreased the levels of NO/PGE₂ and inhibited JNK/I κ B α phosphorylations.

Keywords: *Cistus laurifolius*, *Sambucus ebulus*, *Sambucus nigra*, Nuclear Factor-kappa B, Anti-inflammatory

Özet

Sambucus ebulus L. *S. nigra* L., (Caprifoliaceae) ve *Cistus laurifolius* L. (Cistaceae) bitkilerinin yaprakları Türkiye’de halk arasında enflamatuvar durumlara karşı kullanılmaktadır. Bitkiler üzerinde yürütülen önceki çalışmalar, bu bitkilerin *in vivo* potent antienflamatuvar etkilere sahip olduğunu göstermiştir. Bu çalışmanın amacı bu bitkilerin etki mekanizmalarını açıklamak amacıyla, çeşitli enflamasyon parametreleri üzerindeki etkilerini *in vitro* metotlar kullanarak ortaya koymak ve aktivite yönlendirmeli fraksiyonlama tekniği ile etkili bileşenleri izole etmektir.

Lipopolisakkarit (LPS) ile indüklenmiş Raw 264.7 makrofaj hücrelerinin nükleer faktör-kappa B inhibisyonuna dayanan aktivite modeli kullanılarak hazırlanan ekstrelerden etkili aktif bileşenler izole edilmiş ve yapıları spektroskopik yöntemler ile aydınlatılmıştır. *S. ebulus* bitkisinden; flavonoit yapısında (izoramnetin-3-*O*-glukopiranozit, izoramnetin-3-*O*-rutinozit, kersetin-3-*O*-glukopiranozit, kersetin-3-*O*- β -D-galaktopiranozit) ve iridoit yapısında iki yeni bileşik; Sambulin A ve Sambulin B elde edilmiştir. *S. nigra* ve *C. laurifolius*’un aktif bileşenleri olarak ise, sırasıyla, bir sterol karışımı (SNH-1) ve kalan su alt ekstresi (CL-R-H₂O) belirlenmiştir. Ayrıca tanımlanan aktif molekül veya fraksiyonların enflamatuvar mediyatörler [TNFalfa, IL-1alfa, IL-1beta, IL-2, IL-6, PGE₂ (ELIZA)], ve nitrik oksit (Griess Yöntemi) üzerindeki etkileri incelenmiştir. Protein seviyeleri (iNOS/COX-2) ve protein fosforilasyonları [Mitojen Aktive Protein Kinazlar (MAPK) ve kappa B protein inhibitörü (I κ Balfa)] üzerindeki etkiler Western Blot yöntemiyle araştırılmıştır.

Sonuç olarak, izole edilen flavonoitlerden; izoramnetin-3-*O*-glukopiranozit ve izoramnetin-3-*O*-rutinozit NO, iNOS, TNFalfa üretimini inhibe etmiştir. İzoramnetin-3-*O*-rutinozit ayrıca PGE₂ ve COX-2 inhibisyonu da sağlamıştır. Her iki flavonoit p38/I κ Balfa fosforilasyonlarını inhibe etmiştir. İridoit tipi bileşikler iNOS/COX-2 seviyelerini baskılamış NO/PGE₂ ve TNFalfa üretimlerini azaltmış, JNK ve I κ Balfa fosforilasyonlarını engellemiştir. Diğer taraftan SNH-1 ve CL-R-H₂O aktif fraksiyonları NO, PGE₂ seviyeleri ile JNK ve I κ Balfa fosforilasyonlarını inhibe etmiştir.

Anahtar Kelimeler: *Cistus laurifolius*, *Sambucus ebulus*, *Sambucus nigra*, Nükleer Faktör-kappa B, Antienflamatuvar

Contents

<i>Dedication</i>	I
Acknowledgements.....	II
Abstract.....	IV
Özet.....	V
Contents	VI
Abbreviations/Kısaltmalar	X
List of Tables	XI
List of Figures	XIII
1. INTRODUCTION and AIM.....	1
2. GENERAL DESCRIPTION.....	4
2.1. Botanical Chapter	5
2.1.1. <i>Sambucus</i> L.....	6
2.1.1.1. Caprifoliaceae	6
2.1.1.2. The <i>Sambucus</i> genus.....	7
2.1.1.3. <i>Sambucus ebulus</i> L.	7
2.1.1.4. <i>Sambucus nigra</i> L.	8
2.1.2. <i>Cistus</i> L.	8
2.1.2.1. Cistaceae	8
2.1.2.2. The <i>Cistus</i> L. Genus.....	9
2.1.2.3. <i>Cistus laurifolius</i> L.	10
2.2. Ethnobotanical and Ethnopharmacological Information	11
2.2.1. Traditional Medicinal Uses of <i>Sambucus</i> species.....	12
2.2.2. Biological Activity Studies on <i>Sambucus</i> Species	15
2.2.2.1. Anti-inflammatory and Antinociceptive activity.....	15
2.2.2.2. Cytotoxic and Antiangiogenic activity	17
2.2.2.3. Antioxidative activity	17
2.2.2.4. Anti- <i>Helicobacter pylori</i> activity.....	18
2.2.2.5. Antimicrobial activity	18
2.2.2.6. Immunomodulatory activity:	20
2.2.2.7. Antiosteoporotic Activity	20

2.2.2.8. Wound-healing activity	21
2.2.2.9. Antidiabetic activity.....	21
2.2.3. Traditional Medicinal Uses of <i>Cistus</i> species.....	22
2.2.4. Biological Activity Studies on <i>Cistus</i> species	24
2.2.4.1. Anti-inflammatory activity	24
2.2.4.2. Antioxidative activity	25
2.2.4.3. Cytotoxic activity.....	26
2.2.4.4. Antiviral and Antimicrobial activity.....	27
2.2.4.5. Anti- <i>Helicobacter pylori</i> and Antiulcer activity.....	28
2.2.4.6. Spasmolytic Activity.....	28
2.2.4.7. Antidiabetic Activity.....	29
2.2.4.8. Other Biological Activities	29
2.3. Phytochemical Information.....	30
2.3.1. Phytochemical studies on <i>Sambucus</i> genus	31
2.3.1.1. Phenolic Compounds	31
2.3.1.2. Terpenic Compounds.....	45
2.3.1.3. Steroidal Compounds.....	53
2.3.1.4. Other Compounds	56
2.3.2. Phytochemical Studies on <i>Cistus</i> species	57
2.3.2.1. Phenolic Compounds	57
2.3.2.2. Terpenic Compounds.....	63
2.3.2.3. Essential Oils	73
2.4. General Information on Inflammation and Related Inflammatory Parameters ...	74
2.4.1. Inflammation.....	75
2.4.2. Cytokines	76
2.4.3. Nitric oxide and iNOS enzyme.....	77
2.4.4. PGE ₂ and COX-2	78
2.4.5. NF-κB Signalling.....	80
2.4.6. Mitogen-Activated Protein Kinases (MAPK).....	82
2.4.7. LPS and Macrophage Cells.....	84
3. MATERIALS AND METHODS.....	85
3.1. Materials	86

3.1.1. Plant Materials	86
3.1.2. Bioreagents, Chemicals and Solvents	86
3.1.3. Equipment	88
3.1.4. Instruments.....	88
3.1.5. Kits.....	89
3.1.6. Antibodies	90
3.2. Methods	91
3.2.1. Phytochemical Studies.....	91
3.2.1.1.Extraction.....	91
3.2.1.2. Solvent-Solvent Fractionation of the Extracts	91
3.2.1.3. Chromatographic Methods	97
3.2.1.4. Chromatographic Fractionation Procedures for the Isolation of the Active Constituents from <i>S. ebulus</i> EtOAc Subextract (SE-EtOAc).....	98
3.2.1.5. Chromatographic Fractionation Procedures for the Isolation of the Active Constituents from <i>S. ebulus</i> CHCl ₃ Subextract (SE- CHCl ₃)	103
3.2.1.6. Chromatographic fractionation procedures for the isolation of the active constituents from <i>S. ebulus</i> Hexane subextract (SE-Hex)	107
3.2.1.7. Chromatographic fractionation procedures for the isolation of the active constituents from <i>S. nigra</i> Hexane subextract (SN-Hex)	110
3.2.1.8. Chromatographic fractionation procedures for the isolation of the active constituents from <i>C. laurifolius</i> remaining water subextract (CL-R-H ₂ O)	113
3.2.2. Activity Studies.....	114
3.2.2.1. Cells and Cell Culture.....	114
3.2.2.2. Cell Passaging and Counting	114
3.2.2.3. Cryopreservation of the Cell Line	114
3.2.2.4. Cell Thawing.....	115
3.2.2.5. WST-1 Assay for Cell Viability	115
3.2.2.6. Preparation of Nuclear Proteins and Electromobility Shift Assay (EMSA).....	115
3.2.2.7. Nitrite Assay	116
3.2.2.8. Enzyme Immunoassay for Quantification of PGE ₂ and Cytokines (TNF α , IL-1 α , IL-1 β , IL-2, IL-6).....	117
3.2.2.9. Western Blotting	117

3.2.2.10. RNA Isolation and Quantification	118
3.2.2.11. cDNA synthesis	118
3.2.2.12. Quantitative Polymerase Chain Reaction	119
3.2.2.13. Statistical Analysis.....	119
4. RESULTS	120
4.1. Phytochemical Results	121
4.1.1. Structure Elucidation of SE-1 and SE-4 (mixtures of Quercetin-3- <i>O</i> - β -D-glucopyranoside and Quercetin-3- <i>O</i> - β -D-galactopyranoside).....	122
4.1.2. Structure Elucidation of SE-2 (Isorhamnetin-3- <i>O</i> - β -D-glucopyranoside) .	131
4.1.3. Structure Elucidation of SE-6 (Isorhamnetin-3- <i>O</i> -rutinoside)	136
4.1.4. Structure Elucidation of SECP-2 and SEH-1 (Sambulin A and Sambulin B)	141
4.1.5. The structure elucidations of SECP-1, SECP-3 and SECP-4.....	153
4.1.6. The structure Elucidation of SNH-1 and SNH-2	153
4.2. Biological Activity Results	154
4.2.1. Cytotoxicity Assay.....	155
4.2.2. Activity-guided Isolation Procedures	157
4.2.3. The Effects of the Compounds on PGE ₂ , Nitric Oxide Productions and Protein and mRNA levels of Related Enzymes	182
4.2.4. Effects of the Active Compounds on Inflammatory Cytokines.....	201
4.2.5. The Effects of Bioactive Compounds on MAPK's and I κ -B α phosphorylation	209
5. DISCUSSION & CONCLUSION	215
6. REFERENCES	233
7. CURRICULUM VITAE.....	252

Abbreviations

Abbreviations	
COX-2	Cyclooxygenase-2
ELISA	Enzyme-linked Immunosorbent Assay
EMSA	Electromobility Shift Assay
ERK	Extracellular signal-regulated kinase
RT-PCR	Real Time Polymerase Chain Reaction
IL	Interleukin
iNOS	inducible Nitric Oxide Synthase
JNK	c-JUN-N-terminal kinase
MAP kinase	Mitogen Activated Protein Kinases
NF- κ B	Nuclear Factor kappa B
NMR	Nuclear Magnetic Resonance
NO	Nitric Oxide
PGE ₂	Prostaglandin E ₂
TNF α	Tumor Necrosis Factor-alpha
UV	Ultraviolet
MS	Mass Spectrometry

List of Tables

Table 1: Phenylpropane derivatives from <i>Sambucus</i> genus	31
Table 2: Phenolic glycosides from <i>Sambucus</i> genus	32
Table 3: Phenolic acids from <i>Sambucus</i> genus.....	33
Table 4: Flavonoids from <i>Sambucus</i> genus	34
Table 5: Anthocyanins from <i>Sambucus</i> genus.....	35
Table 6: Anthocyanins from <i>Sambucus</i> genus.....	36
Table 7: Anthocyanins from <i>Sambucus</i> genus.....	37
Table 8: Flavan-3-ols from <i>Sambucus</i> genus.....	37
Table 9: Lignans from <i>Sambucus</i> genus	38
Table 10: Lignans from <i>Sambucus</i> genus	39
Table 11: Lignans from <i>Sambucus</i> genus	39
Table 12: Lignans from <i>Sambucus</i> genus	40
Table 13: Lignans from <i>Sambucus</i> genus	41
Table 14: Lignans from <i>Sambucus</i> genus	42
Table 15: Lignans from <i>Sambucus</i> genus	42
Table 16: Lignans from <i>Sambucus</i> genus	43
Table 17: Lignans from <i>Sambucus</i> genus	44
Table 18: Lignans from <i>Sambucus</i> genus	45
Table 19: Monoterpenes from <i>Sambucus</i> genus	45
Table 20: Iridoids from <i>Sambucus</i> genus	46
Table 21: Iridoids from <i>Sambucus</i> genus	47
Table 22: Iridoids from <i>Sambucus</i> genus	48
Table 23: Valerian type iridoid glycosides from <i>Sambucus</i> genus.....	49
Table 24: Sesquiterpenes from <i>Sambucus</i> genus.....	50
Table 25: Triterpenoids from <i>Sambucus</i> genus	50
Table 26: Triterpenoids from <i>Sambucus</i> genus	51
Table 27: Triterpenoids from <i>Sambucus</i> genus	52
Table 28: Phytosterols from <i>Sambucus</i> genus	53
Table 29: Phytosterols from <i>Sambucus</i> genus	54
Table 30: Cyanogenins and cyanohydrines from <i>Sambucus</i> genus.....	55
Table 31: Fatty acid and fatty acid esters from <i>Sambucus</i> genus	56
Table 32: Phenolic acids from <i>Cistus</i> genus	57
Table 33: Phenolic acids from <i>Cistus</i> genus	58
Table 34: Flavonoids from <i>Cistus</i> genus	59
Table 35: Flavonoids from <i>Cistus</i> genus	60
Table 36: Flavan-3-ols from <i>Cistus</i> genus.....	60
Table 37: Prodelphinidins from <i>Cistus</i> genus.....	61
Table 38: Dimeric prodelphinidines from <i>Cistus</i> genus	62
Table 39: Dimeric prodelphinidines from <i>Cistus</i> genus	63

Table 40: Labdane type diterpenes from <i>Cistus</i> genus	63
Table 41: Labdane type diterpenes from <i>Cistus</i> genus	64
Table 42: Labdane type diterpenes from <i>Cistus</i> genus	64
Table 43: Labdane type diterpenes from <i>Cistus</i> genus	65
Table 44: Labdane type diterpenes from <i>Cistus</i> genus	65
Table 45: Labdane type diterpenes from <i>Cistus</i> genus	66
Table 46: Labdane type diterpenes from <i>Cistus</i> genus	66
Table 47: Labdane type diterpenes from <i>Cistus</i> genus	67
Table 48: Labdane type diterpenes from <i>Cistus</i> genus	68
Table 49: Labdane type diterpenes from <i>Cistus</i> genus	69
Table 50: Labdane type diterpenes from <i>Cistus</i> genus	69
Table 51: Labdane type diterpenes from <i>Cistus</i> genus	70
Table 52: Clerodane type diterpenes from <i>Cistus</i> genus	70
Table 53: Neo-clerodane type diterpenes from <i>Cistus</i> genus	71
Table 54: Neo-clerodane type diterpenes from <i>Cistus</i> genus	72
Table 55: Compositions of essential oils obtained from <i>Cistus</i> genus	73
Table 56: ¹ H (600 MHz, MeOD) and ¹³ C-NMR (150 MHz, MeOD) data of Quercetin-3- <i>O</i> -β-D-glucopyranoside	125
Table 57: ¹ H (600 MHz, MeOD) and ¹³ C-NMR (150 MHz, MeOD) datas of SE-2 (Isorhamnetin-3- <i>O</i> -β-D-glucopyranoside)	133
Table 58: ¹ H (600 MHz, MeOD) and ¹³ C-NMR (150 MHz, MeOD) datas of SE-6 (Isorhamnetin-3- <i>O</i> -β-rutinoside)	138
Table 59: ¹ H (600 MHz, MeOD) and ¹³ C-NMR (150 MHz, MeOD) data of SEH-1 (Sambulin B) and SECP-2 (Sambulin A)	144
Table 60: Non-toxic concentrations of samples	155
Table 61: Summary of the inhibitory activities of the active components on NF-κB and IκBα/MAPK phosphorylations	224
Table 62: Summary of the results of the <i>in vitro</i> inhibitory activities of the active components on inflammatory parameters	227

List of Figures

Figure 1: Phospholipase cascade	80
Figure 2: LPS induced NF- κ B and Mitogen Activated Protein Kinase (MAPK) pathways	81
Figure 3: Mitogen-Activated Protein Kinase (MAPK) pathways	83
Figure 4: Fractionation of <i>C. laurifolius</i> EtOH (CL-EtOH) extract by successive solvent-solvent extractions.	94
Figure 5: Fractionation of <i>S. ebulus</i> MeOH (SE-MEOH) extract by successive solvent-solvent extractions.	95
Figure 6: Fractionation of <i>S. nigra</i> MeOH (SN-MEOH) extract by successive solvent-solvent extractions.	96
Figure 7: Activity-guided isolation of active compounds from <i>S. ebulus</i> EtOAc subextract (SE-EtOH).	102
Figure 8: Activity-guided isolation of active compounds from <i>S. ebulus</i> CHCl ₃ subextract (SE-CHCl ₃).	106
Figure 9: Activity-guided isolation of active compounds from <i>S. ebulus</i> hexane subextract (SE-Hex).	109
Figure 10: Activity-guided isolation of active compounds from <i>S. nigra</i> hexane subextract (SN-Hex).	112
Figure 11: ¹ H-NMR (600 MHz, MeOD) spectrum of SE-1 (Quercetin-3- <i>O</i> - β -D-glucopyranoside/Quercetin-3- <i>O</i> - β -D-galactopyranoside (3/2)).	126
Figure 12: ¹ H-NMR (600 MHz, MeOD) spectrum of SE-4 (Quercetin-3- <i>O</i> - β -D-glucopyranoside/Quercetin-3- <i>O</i> - β -D-galactopyranoside (2/3)).	127
Figure 13: ¹³ C-NMR (150 MHz, MeOD) spectrum of SE-4 (Quercetin-3- <i>O</i> - β -D-glucopyranoside/Quercetin-3- <i>O</i> - β -D-galactopyranoside (2/3)).	128
Figure 14: HR-ESI-MS spectra of SE-1 (Quercetin-3- <i>O</i> - β -D-glucopyranoside/Quercetin-3- <i>O</i> - β -D-galactopyranoside (3/2)).	129
Figure 15: HR-ESI-MS spectra of SE-4 (Quercetin-3- <i>O</i> - β -D-glucopyranoside/Quercetin-3- <i>O</i> - β -D-galactopyranoside (2/3)).	130
Figure 16: ¹ H-NMR (600 MHz, MeOD) spectrum of SE-2 (Isorhamnetin-3- <i>O</i> - β -D-glucopyranoside).	134
Figure 17: ¹³ C-NMR (150 MHz, MeOD) spectrum of SE-2 (Isorhamnetin-3- <i>O</i> - β -D-glucopyranoside).	135
Figure 18: ¹ H-NMR (600 MHz, MeOD) spectrum of SE-6 (Isorhamnetin-3- <i>O</i> -rutoside).	139
Figure 19: ¹³ C-NMR (150 MHz, MeOD) spectrum of SE-6 (Isorhamnetin-3- <i>O</i> -rutoside).	140
Figure 20: The HMBC correlations of SEH-1 (Sambulin B) and SECP-2 (Sambulin A) (C \rightarrow H).	145
Figure 21: The ¹ H-NMR (300 MHz, CDCl ₃) spectrum of SEH-1 (Sambulin B)	146

Figure 22: The ¹³ C-NMR (150 MHz, CDCl ₃) of SEH-1 (Sambulin B).	147
Figure 23: The ESI-MS spectrum of SEH-1 (Sambulin B)	148
Figure 24: The ¹³ C-NMR (150 MHz, CDCl ₃) of SECP-2 (Sambulin A).	149
Figure 25: The HMBC spectrum of SECP-2 (Sambulin A)	150
Figure 26: The HSQC spectrum of SECP-2 (Sambulin A)	151
Figure 27: The ESI-MS spectrum of SECP-2 (Sambulin A)	152
Figure 28: EMSA images of the total extracts and subextracts.	161
Figure 29: Densitometric analysis of NF-κB inhibitory activities obtained for total extracts and subextracts.	163
Figure 30: The NF-κB inhibitory activities of the fractions obtained from CL-R-H ₂ O.	164
Figure 31: The concentration-dependent NF-κB inhibitory activity of CL-R-H ₂ O.	165
Figure 32: The NF-κB inhibitory activities of the fractions obtained from polyamide column chromatography of SE-EtOAc.	166
Figure 33: EMSA image showing the effects of the flavonoids obtained from SE-EtOAc on the activation of NF-κB.	167
Figure 34: The concentration-dependent NF-κB inhibitory activity of the flavonoid mixture SE-1.	168
Figure 35: The concentration-dependent NF-κB inhibitory activity of the SE-2.	169
Figure 36: The concentration-dependent NF-κB inhibitory activity of the flavonoid mixture SE-4.	170
Figure 37: The concentration-dependent NF-κB inhibitory activity of SE-6.	171
Figure 38: The EMSA images showing the NF-κB inhibitory activities of the fractions obtained from SE-CHCl ₃ , SN-Hex by silica gel column chromatographies.	172
Figure 39: The NF-κB inhibitory effects of the fractions obtained from SE-CHCl ₃ , SN- Hex by silica gel column chromatographies and subfractions obtained from fraction SE _{CHCl₃} I Fr 14-16.	174
Figure 40: The concentration-dependent NF-κB inhibitory activity of SNH-1.	175
Figure 41: The concentration-dependent NF-κB inhibitory activity of SNH-2.	176
Figure 42: The concentration-dependent NF-κB inhibitory activity of SECP-2.	177
Figure 43: The concentration-dependent NF-κB inhibitory activity of SECP-4.	178
Figure 44: The NF-κB inhibitory effects of the fractions obtained from SE-Hex.	179
Figure 45: EMSA image showing the effects of the compounds obtained from SE- CHCl ₃ and SN-Hex on the activation of NF-κB.	180
Figure 46: The concentration-dependent NF-κB inhibitory activity of SEH-1.	181
Figure 47: Effects of isorhamnetin-3- <i>O</i> -rutinoside (SE-6) on the productions of NO, PGE ₂ and iNOS/COX-2 protein expression levels.	186
Figure 48: Effects isorhamnetin-3- <i>O</i> -β-D-glucopyranoside (SE-2) on the productions of NO, PGE ₂ and iNOS/COX-2 protein expression levels.	188
Figure 49: Effects of Sambulin B (SEH-1) on the productions of NO, PGE ₂ and iNOS/COX-2 protein expression levels.	190

Figure 50: Effects of Sambulin A (SECP-2) on the productions of NO, PGE2 and iNOS/COX-2 protein expression levels.....	192
Figure 51: Effects of CL-R-H ₂ O on the productions of NO, PGE2 and iNOS/COX-2 protein expression.	194
Figure 52: Effects of SNH-1 on the productions of NO, PGE2 and iNOS/COX-2 protein expression levels.	196
Figure 53: The effects of SE-2 (isorhamnetin-3- <i>O</i> -D-glucoopyranoside) on mRNA levels of iNOS.....	197
Figure 54: The effects of SE-6 (isorhamnetin-3- <i>O</i> -rutinoside) on mRNA levels of iNOS and COX-2.....	198
Figure 55: The effects of SEH-1 (Sambuln B) on mRNA levels of iNOS and COX-2.	199
Figure 56: The effects of SECP-2 (Sambuln A) on mRNA levels of iNOS and COX-2.	200
Figure 57: The inhibitory effects of the isolates on LPS induced TNF α secretion.	202
Figure 58: The concentration-dependent inhibitory effects of the active compounds on LPS-induced TNF α secretion.	205
Figure 59: The inhibitory effects of the isolates on LPS induced IL-6 secretion.....	206
Figure 60: The concentration-dependent inhibitory effects of the SEH-1 (Sambulin B) on LPS induced IL-6 secretion.	206
Figure 61: The inhibitory effects of the isolates on LPS induced IL-2 secretion.....	207
Figure 62: The inhibitory effects of the isolates on LPS induced IL-1 α secretion.....	207
Figure 63: The inhibitory effects of the isolates on LPS induced IL-1 β secretion.....	208
Figure 64: Effect of SE-2 (isorhamnetin-3- <i>O</i> -D-glucoopyranoside) on MAPKs activation (p38, JNK and ERK phosphorylation) and I κ -B α phosphorylation.	212
Figure 65: Effect of SE-6 (isorhamnetin-3- <i>O</i> -rutinoside) on MAPKs activation (p38, JNK and ERK phosphorylation) and I κ B α phosphorylation.	212
Figure 66: Effect of SECP-2 (Sambulin A) on MAPKs activation (p38, JNK and ERK phosphorylation) and I κ B α phosphorylation.	213
Figure 67: Effect of SEH-1 (Sambulin B) on MAPKs activation (p38, JNK and ERK phosphorylation) and I κ B α phosphorylation.	213
Figure 68: Effect of SNH-1 on MAPKs activation (p38, JNK and ERK phosphorylation) and I κ B α phosphorylation.....	214
Figure 69: Effect of CL-R-H ₂ O on MAPKs activation (p38, JNK and ERK phosphorylation) and I κ B α phosphorylation	214

1. INTRODUCTION and AIM

INTRODUCTION and AIM

Inflammation is the host defence system against various stress factors (physical, chemical, or biological). Although acute inflammation is an essential defence mechanism of the body, when it becomes persistent as in chronic inflammation, it leads to the development of several chronic inflammatory disorders such as chronic asthma, rheumatoid arthritis, multiple sclerosis and inflammatory bowel disease. Chronic inflammatory diseases are debilitating and are becoming increasingly common in society (1-4). In fact, recent investigations revealed that several cancers might be linked to chronic inflammation (5). Although many agents are in medical practice to treat inflammatory disorders, prolonged use of these agents is undesirable due to severe adverse/side effects and high costs. For that reason, there is a need to develop new anti-inflammatory agents with minimum side effects and low costs (6). In this regard plants used in traditional medicine offer a rich source for drug discovery and development (7).

Inflammation is a complex process and various mediators such as nitric oxide (NO), prostaglandins and cytokines involve in its pathogenesis (1, 2). Nuclear Factor kappa-B (NF- κ B) is a transcription factor which is responsible for the transcription of various inflammatory interleukins (IL-1, IL-2, IL-6), cytokines such as tumor necrosis factor-alpha (TNF α), cyclooxygenase-2 (COX-2) and inducible nitric oxide synthase (iNOS) (8, 9). NF- κ B involves in the pathogenesis of inflammatory disorders such as rheumatoid arthritis and asthma (10).

The aim of this study is to provide additional evidences to support the claimed ethnopharmacological usages and mechanisms of the *in vivo* anti-inflammatory activities of the aforementioned plants with a molecular approach as well as to isolate and identify the compounds which are responsible for the anti-inflammatory activity.

Sambucus ebulus L., *S. nigra* L. and *Cistus laurifolius* L. are used traditionally against rheumatism and related inflammatory disorders in Turkey. The decoctions prepared from the leaves or aerial parts of these plants had been reported to be used externally as bath or by applying the poultices prepared on the affected limbs (11-13). Eventually, *in vitro* methods might be a powerful tool to investigate the claimed effects. Firstly methanol or ethanol extracts were prepared from the leaves. The total extracts were then subjected to liquid-liquid extraction with solvents in increasing polarities. Preliminary screening on these subextracts to investigate their inhibitory effects on the activity of NF- κ B was performed by using Electromobility Shift Assay. LPS-induced Raw 264.7 macrophages were employed as a model to study inflammation. The extracts with potent inhibitory activities were further studied by activity-guided fractionation (AGF) procedures. Active compounds were isolated by using common chromatographic techniques (column chromatography, medium pressure liquid chromatography). Structure elucidation of the compounds was achieved by spectroscopic techniques i.e., UV, IR, NMR (1D, 2D) and MS. Compounds exerted high activity were further investigated for their anti-inflammatory activity profiles on the productions of NO, PGE₂, TNF α , IL-1 α , IL-1 β , IL-2 and IL-6 by ELISA and Griess Assays. The effects of the active compounds on COX-2 and iNOS protein and mRNA expressions were analysed by RT-PCR and Western Blotting. The mechanism of anti-inflammatory activity was investigated on I κ B α phosphorylation and MAP kinases including extracellular signal-regulated kinases (ERK1/2), c-JUN-N-terminal kinases (JNK) and p38 kinases phosphorylation by Western blotting.

2. GENERAL DESCRIPTION

This section includes two parts; Botanical Part and Theoretical Part.

Botanical part consists of botanical information about *S. ebulus*, *S. nigra* and *C. laurifolius* along with general characteristic properties of their genera and families.

Theoretical part is divided into two parts the first part is a review on the previous ethnopharmacological, biological activity and phytochemical studies on *Sambucus* and *Cistus* genera. Second part contains general information on inflammation and inflammatory parameters.

2.1. Botanical Chapter

This section includes botanical information on *S. ebulus*, *S. nigra* and *C. laurifolius* along with the botanical characteristics of genera *Sambucus*, *Cistus* and their families; Caprifoliaceae and Cistaceae respectively.

2.1.1. *Sambucus* L.

This section includes botanical information about the genus *Sambucus*. Phylogenetic studies based both on morphological and molecular characteristics of Dipsacales suggested that *Sambucus* should no longer belong to Caprifoliaceae and recently genus *Sambucus* was transferred to Adoxaceae. Although this new classification for *Sambucus* gender has led to many controversial arguments, in this section we present the characteristics of gender as it belonged to Caprifoliaceae family in the Flora of Turkey and the East Aegean Islands. (14-18).

2.1.1.1. Caprifoliaceae

Caprifoliaceae consists of shrubs or herbs with opposite leaves. Stipules may be absent or if present they might be small and adnate to the petiole. Flowers are hermaphrodite and paired on long peduncles or in cymes, heads or whorls, actinomorphic or zygomorphic with five sepals. Corolla is gamopetalous and usually consists five petals. Stamens are usually 5, alternating with petals, inserted on the corolla tube. Ovary is inferior, 1-5-locular, placentation axile, ovules 1 and many in each loculus. Fruit (in Turkey) is a drupe or few-seeded berry; seeds are with fleshy endosperm (18). Caprifoliaceae is represented by three genera in Turkey. The key to these three genera in 'The Flora of Turkey and the East Aegean Islands' is as follows (18);

- 1. Leaves pinnate*Sambucus*

- 1. Leaves simple
 - 2. Flowers in compound cymes.....*Viburnum*
 - 2. Flowers in pairs, heads or whorls..... *Lonicera*

2.1.1.2. The *Sambucus* genus

Herbs or shrubs with large pith. Leaves imparipinnate and opposite; stipules may be present or absent. Flowers are compound many-flowered umbellate or paniculate cymes and usually 5-merous; corolla regular, rotate; ovary 3-5-celled; stigmas 3-5. Fruit is a drupe (18). There are two species of *Sambucus* in Turkey and the key to the species is presented below (18):

1. Herbs; stipules ovate, 8-30 mm.....*ebulus*

1. Shrubs or small trees; stipules absent or subulate, c. 4 mm.....*nigra*

2.1.1.3. *Sambucus ebulus* L.

S. ebulus is a glabrous, foetid perennial herb which grows 0.5-2 m high with erect, usually unbranched stems with a creepy rhizome. The leaves are opposite, pinnate, 15 - 30 cm long, with 5-9 finely-toothed and lobed leaflets. Leaflets 3-6 paired, lanceolate to elliptic, 7-15x2-6 cm, serrate. Stipulates ovate, 8-30 mm. Inflorescence with 3 primary rays, flat topped, 7-10 cm diameter. The flowers are self-fertile and hermaphrodite, white, sometimes tinged with pink. Anthers are purple. The fruit is black drupe globose that is 5 - 6 mm in diameter (18).

Flowering: 7-8. months

Habitat: Deciduous forest, roadside banks

Altitude: 500-2000m

Turkish names: Sultanotu, cüce mürver, aziotu, pıyran, haptovina, ademotu, piran, mulver, şahmelik, buzka, ancura, şahmehlemi, yağdan, yıldıgın (11, 12, 19)

Other languages: Bazak -Bulgarian, daneworth, dwarf elder-English (20, 21)

2.1.1.4. *Sambucus nigra* L.

Shrub or small trees about 4-10 m long, foetid. Leaflets are ovate-lanceolate or ovate elliptic, (1-)2-3(-4)-paired, 3-12x3-6 cm, serrate, sparsely hairy on the veins on the underside, otherwise glabrous; stipules absent or subulate, c. 4 mm. Inflorescence usually with 5 primary rays, flat topped, 10-20 cm diam. Flowers are cream, c. 5mm; anthers cream. Drupe globose 6-8 mm, blackish-purple (18).

Flowering: 4-7. months

Habitat: Amongst scrub, forest margins, etc.

Altitude: sea level-1700 m.

Turkish names: Mürver, mürver çiçeği, mülver, kara mürver, mülver ağacı, patırık, patlangoz (12, 19).

Other languages: Sauko -Italian (22), black elderberry -English (23), astunpa, intsusa, sabuko, saúco-Basque (24), angure koli-Azarbaijani (25).

2.1.2. *Cistus* L.

This section includes botanical information on the genus *Cistus* and *Cistus laurifolius*.

2.1.2.1. Cistaceae

Cistaceae family consists of shrubs, perennial or annual herbs, with simple and often opposite leaves. The leaves are stipulate or not. Sepals are 5 or 3 and often very unequal. Corolla is actinomorphic. Petals 5, free, pink, yellow, evanescent. The flower has too many stamens which are free. Ovary is superior, 3-10 carpellate, with a single style which matures to a loculicidal capsule containing 3 to numerous seeds. Cistaceae is represented by five genus in Turkey. The key to these five genera in ‘The Flora of Turkey and the East Aegean Islands’ is as follows (26);

1. Carpels 5 or 10; inner sepals not much larger than the outer; shrubs.....**1. *Cistus***

1. Carpels 3; inner sepals much larger than the outer; shrubs or herbs

2. Stigmas borne on ± elongate, geniculate styles; nerves of sepals are prominent; shrubs or herbs with yellow, unblotched petals

3. All stamens fertile; leaves opposite; dwarf shrubs or annual herbs with numerous seeds and per capsule.....**2. *Helianthemum***

3. Outer stamens sterile, moniliform; leaves usually alternate (except *F. Thmifolia*); dwarf shrubs with 3-12 seeds per capsule.....**3. *Fumana***

2. Stigmas sessile, or borne on short, straight styles; sepals with inconspicuous nerves; shrublets or herbs with petals yellow and blotched at base or white and unblotched

4. Dwarf shrubs with linear leaves and flowers in umbels; petals white, unblotched.....**4. *Halimium***

4. Annual herbs with broad leaves and flowers in lax racemes; petals yellow, blotched at base.....**5. *Tuberaria***

2.1.2.2. The *Cistus* L. Genus

The genus *Cistus* contains shrubs. The leaves are opposite, exstipulate, petiolate. Sepals 5 or 3, the outer sepals are not smaller than the inner ones. Petals are pink or white. Stamens are all fertile. Stigma is sessile or on a straight style. Carpels 5 or 10. The key to the species is presented below (26).

1. Flowers pink; cymes terminal; sepals 5, rounded at base, ± equal

2. Cymes lax; flowers 3-5(-6) cm across; leaves greenish above; style equal to stamens.....**1. *creticus***

2. Cymes compact; flowers 2-3 cm across; leaves grey on both sides; style shorter than stamens.....**2. *parviflorus***
1. Flowers white; cymes lateral; sepals 3, or if 5 then cordate at base and outer 3 much broader than inner 2
3. Sepals 5, cordate at base; petioles free; upper leaf-surface covered with stellate hairs.....**3. *salviifolius***
3. Sepals 3, rounded at base; petioles connate at base; upper leaf-surface glabrous.....**4. *laurifolius***

2.1.2.3. *Cistus laurifolius* L.

Cistus laurifolius is a shrub with 1-3 m height. The leaves may be ovate or sometimes lanceolate, acute, with basal-connate petioles. The upper surface of the leaves is glabrous and very sticky and the lower surface is grey and densely tomentose. Cymes are lateral, 3-5 flowered, with long peduncles. Flowers 3-4 cm across and white. Sepals 3 (-4), not cordate at base. Styles are short or absent (26).

Flowering: 5-6. months

Habitat: Submediterranean macchie

Altitude: 50-1200 m.

Turkish names: Karahan, laden, pamuk out (19).

2.2. Ethnobotanical and Ethnopharmacological Information

This chapter is a review on the previous ethnopharmacological, biological activity and ethnobotanic studies on *Sambucus* and *Cistus* genera. Last part contains general information on inflammation and inflammatory parameters.

2.2.1. Traditional Medicinal Uses of *Sambucus* species

There are two species of *Sambucus* in Turkey and both of them are frequently used in traditional medicine. The fresh leaves or poultice made from the leaves, roots or aerial parts of *S. ebulus* are wrapped in a cloth and applied externally to treat burns, infectious wounds, snake bites, edema, eczema, urticaria, rheumatic and other inflammatory problems (11, 12). Bathing inside the decoction of roots is also suggested against rheumatic pain in Kırklareli. The decoction of roots or fruits are used internally as a remedy for hemorrhoids or stomachaches (12). The fresh leaves of *S. ebulus* are cooked inside milk to obtain a poultice is then applied externally on wounds in Kastamonu (27).

The fruits of *S. ebulus* are mixed with walnuts and eaten to treat asthma, while decoction of the fruits is combined with the whole plant of *Urtica dioica* and applied externally to treat rheumatism (11).

S. ebulus was shown to be the most widely used medicinal plant against rheumatism in the Northern Anatolia. Mostly the fresh leaves are wilted over fire and applied on limbs or decoction of leaves, roots or aerial parts is used as bath to treat rheumatic pain. Fruits are widely used against hemorrhoids; the black fruits are swallowed on an empty stomach like a pill or chewed. The poultice made from aerial parts is applied on burns after mixing with olive oil. The flowers of the plant is consumed as tea to strengthen the eyes (13). The traditional use of *S. ebulus* in veterinary medicine is also common in the Northern Anatolia. Aerial parts are externally applied on abdomen of the cattles to treat inflammatory swellings or leaves are used as analgesic after castration operation (13).

The flowers of *S. nigra* are used as decoction or infusion to treat respiratory system disorders such as bronchitis, cold, cough, and asthma (28). The fruits of the plant are eaten once a day for a week to treat prostatitis (12).

In vicinity of Erzincan leaves of *S. nigra* are used for maturation of abscess. Tea prepared from the flowers is used internally against diabetes (29), to treat asthma, bronchitis and as expectorant in Elazığ (30).

A reference survey has also revealed that *Sambucus* species have been used in folk medicines throughout the Europe, North and South America and China. In Bulgarian folk medicine fruits, flowers and roots of *S. ebulus* is used as diuretic, antitussive and antipyretic(31). Albanians use aerial parts of *S. ebulus* as antirheumatic, (32).

On the other hand, in spite of widespread use of the *S. ebulus* fruits in traditional medicine consumption of fruits in higher amounts may induce vomitory intoxications, particularly in children (33).

In Italy, flowers, leaves and fruits of *S. nigra* were used traditionally as anti-inflammatory, antirheumatic, analgic. The tea prepared from the flowers was used internally against rheumatism, whereas decoction of the leaves was used as mouthwash against toothache. The poultice of leaves and flowers were mixed with olive oil and applied externally on painful body parts to treat muscular and rheumatic pain (22). Flowers and fruits of *S. nigra* are used as diuretic and to stimulate perspiration in Bulgaria (31).

In Israel the flowers of *S. nigra* were marketed and used against asthma, to ease breathing in respiratory diseases (23).

In Northern Navvara (Spain) *S. nigra* was traditionally used for dermatological problems such as wounds, furuncles, boils, pimples, eczema, burns, seborrheic dermatitis, herpes infections and respiratory problems such as as catarrh, congestion, and sore throat (24).

In west Azerbaijan (Iran), *S. nigra* is known as ‘angure koli’ and infusions prepared from the different parts of the plant were used for various purposes. Flowers were used to treat fevers, rheumatism and scrophulosis, while leaves and barks were used for respiratory ailments and fruits as laxative (25).

The leaves and flowers of *S. nigra* were used to treat sore throat and insect bites in Albania (32). In Serbia, *S. nigra* was used as diuretic, antiseptic and antiscatarrhal, and expectorant. It was used to diminish fever in common colds and influenza (34).

In Eastern Cuba, *S. simpsonii* which is known as ‘sauca blanco’ participates in many multiherbal recipes against pneumonia and catarrh (35). In Bolivia *S. peruviana* was used against swellings (36). In Argentine *S. australis* was used as digestive, diuretic and diaphoretic, while in Peru *S. peruviana* was suggested as emetic (37, 38).

The poultice made from the leaves of *S. chinensis* which is known as ‘akha ka wu’ was used against rheumatoid arthritis by Akha people living in China and Thailand (39). In China, *S. adnata* is also used against rheumatismal diseases (40).

2.2.2. Biological Activity Studies on *Sambucus* Species

In this section, investigations on the biological effects of various *Sambucus* species will be compiled.

2.2.2.1. Anti-inflammatory and Antinociceptive activity

Yeşilada et al. investigated the *in-vitro* anti-inflammatory effects of the extracts of the flower buds and leaves of *S. ebulus* on LPS induced human peripheral mononuclear cells. The effects of the extracts on the production of IL-1 α , IL-1 β and TNF α was measured by ELISA. Besides methanol extracts; hexane, chloroform, *n*-butanol and remaining aqueous subextracts of the methanol extracts were tested. The methanol extract exerted significant inhibitory activity on the productions of IL-1 α and IL-1 β (33% and 40% inhibitions, respectively), but the inhibitory effects decreased upon fractionation. Although methanol extract of *S. ebulus* caused no decrease on TNF α , hexane subextract showed the highest inhibitory activity (50%) over tested *Sambucus* extracts and fractions. Methanol extract from the flower buds only led to a 32% decrease of IL-1 α and the inhibitory ratio reached 39% for its hexane subextract (6). Opposite to the promising anti-inflammatory activity of the flower extracts of *S. ebulus*, the MeOH extract of the seeds of *S. nigra* had no effect on the production of NO of LPS induced macrophage cells (41).

Schwaiger et al. isolated ursolic acid, a pentacyclic triterpenoid, from the diethyl ether subextract of ethanol extract of the leaves as active principal by using a bioassay model based on the inhibition of TNF α induced expression of vascular cell adhesion molecule-1 (VCAM-1) on the surface of human umbilical vein endothelial cells (HUVECs). Ursolic acid reduced TNF α induced VCAM-1 expression of HUVEC cells in a concentration-dependent manner with an IC₅₀ value of 12.5 μ M. It also (IC₅₀ 3.13-6.25 μ M) inhibited expression of ICAM-1 upon stimulation with TNF α in a concentration-dependent manner (20).

Ebrahimzadeh et al. investigated the anti-inflammatory and antinociceptive activities of different parts of *S. ebulus* by using hot plate, writhing and carrageenan-induced inflammation models in mice and rats. Fruits, leaves and roots were separately extracted with solvents with hexane, ethyl acetate and methanol successively. All extracts showed a dose-dependent and marked analgesic and anti-inflammatory activities (42). Methanol extracts significantly inhibited carrageenan-induced edema at 600 mg/kg dose; the fruits inhibited the inflammation 86% and leaves 71%, respectively. This inhibition was close to diclofenac which is a well-known non-steroidal anti-inflammatory drug (43).

On the other hand, Ahmadiani et al. investigated the analgesic and anti-inflammatory effects of the methanol extract of *S. ebulus* rhizome. For the assessment of analgesic activity acute (tail flick) and chronic (formalin test) pain models and for anti-inflammatory activity acute and subacute paw edema models of inflammation in rats were used (44). The extract applied at 100 and 200 mg/kg doses, increased tail flick latency compared to sodium salicylate which showed no effect at a dose of 300 mg/kg. In formalin test, the extract (100 mg/kg) relieved nociception in animals. In this study, it was shown that the methanol extract of rhizome produced a significant anti-inflammatory activity in both acute and chronic inflammatory tests at 200 mg/kg. The anti-inflammatory action of the extract was not reversed by naloxone (an opioid antagonist) suggesting that the anti-inflammatory effect might be unrelated to the opioid system (44) .

Yeşilada et al. investigated the anti-inflammatory and antiarthritic activities of methanol and aqueous extracts of the aerial parts of *S. ebulus*. Both extracts showed potent *in vivo* anti-inflammatory activity against carrageenan-induced hind paw edema model in mice, as well as adjuvant-induced chronic arthritis model in rats. The active metabolite of the methanol extract was isolated and identified as chlorogenic acid (45, 46). Hexane subextracts of the flowering aerial parts and root extracts produced statistically significant and dose-dependent inhibition of edema induced by carrageenan at all doses. However, hexane subextract of the leaves did not show any activity up to 600 mg/kg i.p. The highest activity was shown in the aerial parts and roots at 600 mg/kg

which reduced inflammation by 80% comparable to diclofenac (78% for diclofenac at 100 mg /kg) .

2.2.2.2. Cytotoxic and Antiangiogenic activity

Cytotoxic effect ethyl acetate extract of the fruits of *S. ebulus* was evaluated on hepatocarcinoma (HepG2) and colon carcinoma (CT26) cells. IC₅₀ values of the extract on HepG2 and CT26 cancer cell lines were much lower than that on fibroblast and ovary (CHO) normal cells. The lowest and highest IC₅₀ values of the extract were also determined on HepG2 (97.03 ± 1.52 µg/ml) and CHO (346.2 ± 3.02 µg/ml) cell lines (47).

2.2.2.3. Antioxidative activity

In order to determine the antioxidative potential of methanol and aqueous extractss of *S. ebulus* fruit, several methods including DPPH radical-scavenging activity assay, nitric oxide-scavenging activity assay, metal chelating activity assay, scavenging of hydrogen peroxide, reducing power determination and FTC methods were applied. The IC₅₀ value for DPPH radical-scavenging activity was 228 ± 12 g/ml. In another study it was shown that methanol extract of the whole plant of *S. ebulus* showed 91% and the methanol extract of the seeds showed 82% inhibition of DPPH at 0.8 mg/ml and 167 µg/ml concentrations respectively (41, 48). The extracts showed weak activity in nitric oxide assay. Methanol extract of *S. ebulus* flowers also showed antioxidative activities evaluated by Fe²⁺ chelating ability test. The iron chelating activity of the extract was very weak. The extracts were highly capable of scavenging hydrogen peroxide in a concentration-dependent manner (IC₅₀:59.5± 3.3 µg/ml). The peroxidation inhibition of the extract was 86%, in FTC test (49). Another study conducted by Ebrahimzadeh et al. showed that methanol and aqueous fractions of *S. ebulus* fruits showed less DPPH scavenging activity than ascorbic acid and quercetin. Aqueous extracts were found to be more effective than methanol extract in the nitrite scavenging assay. The antioxidative effect of methanol and aqueous extract of fruits showed weak Fe²⁺ chelating ability by 48 and 21% inhibition, respectively (49).

2.2.2.4. Anti-*Helicobacter pylori* activity

Chloroform subextract of the alcoholic extract prepared from aerial parts of *S. ebulus* exerted significant *in vitro* activity against *Helicobacter pylori* with MIC = 31.2 µg/ml while aqueous, methanol extracts and *n*-butanol subextract were not active (50). Berry extracts of *S. nigra* inhibited the growth *H. pylori in vitro* and also enhanced its susceptibility to clarythromisin (51).

2.2.2.5. Antimicrobial activity

Literature survey revealed that various commercially available standardized preparations containing elderberry flowers (*S. nigra*) as an active ingredient were evaluated for their antiviral or antiinfluenza activities. A standardized elderberry extract (Rubini, BerryPharma AG) showed antimicrobial activity against both Gram-(+) bacteria (*Streptococcus pyogenes* and group C and G *Streptococci*), and Gram (-) bacterium (*Branhamella catarrhalis*) in microtitre broth micro-dilution assay. These strains are responsible for upper respiratory track infections. Antiviral activity was also investigated with cell-culture experiments, towards two different strains of influenza virus: H5N1-type influenza A and an influenza B. The extract also exerted inhibitory effect on the propagation of human pathogenic influenza viruses (52). Two products (Sinupret oral drops and Sinupret dry extract) containing a mixture of the extracts of Sambuci Flos along with Gentianae Radix, Primulae Flos, Rumicis Herba and Verbenae Herba tested *in vitro* against a panel of human pathogenic viruses which are responsible for the upper respiratory tract infections: influenza A, Chile 1/83 (H1N1) virus, Porcine Influenza A/California/07/2009 (H1N1) virus, parainfluenza type 3 virus, respiratory syncytial virus, strain Long, human rhinovirus B subtype 14, coxsackievirus subtype A9, and adenovirus C subtype 5. These products were only found to be active against FluA, Para 3 and CA9 at high concentrations. The effects against pFluA HRV 14, RSV and Adeno 5 were significant (53). A nasal spray (TheraMax[®]) containing green tea extract and elderberry extract was tested on influenza A/NWS/33 (H1N1) infected mice and the authors informed a delay on symptoms during animal infections (54).

Lariciresinol obtained from *S. williamsii* was tested against *Candida albicans*, *Malassezia furfur* and *Trichosporon beigelii*. It displayed activity against all tested species with MIC values lower than 30 µg/ml without any hemolytic effect on human erythrocytes. The fungicidal activity was suggested to be the result of membrane disrupting property of the compound (55). Similarly pinoresinol isolated from *S. williamsii*, exerted antifungal activities towards the same microorganisms and the mechanism of action was suggested to be due to the depolarization effect of the fungal membrane pores (56).

Feline immunodeficiency virus (FIV) infections of cat is accepted to be an animal model of human immunodeficiency virus (HIV) infections. *S. nigra* showed significant anti-FIV activity tested on Crandell feline kidney cells infected with FIV (57). In another study, the branch extract of *S. racemosa* exerted significant antiviral activity against respiratory syncytial virus (58).

The extract of *S. nigra* berries showed inhibitory activity on Human Influenza A (H1N1) virus with an IC₅₀ value of 252 ± 34 µg/ml. Two compounds were identified as active principles: 5, 7, 3',4'-tetra-*O*-methylquercetin and 5,7-dihydroxy-4-oxo-2-(3,4,5-trihydroxyphenyl) chroman-3-yl-3,4,5-trihydroxycyclohexanecarboxylate (59).

The juice of *S. nigra* berries as well as fractions obtained according to molecular weights by ultrafiltration were tested against Human Influenza virus A. The condensed extract had a strong antiviral activity in infected mice. High molecular weight fractions suppressed viral replication in bronchoalveolar lavage fluids and increased the level of human influenza virus A neutralising antibody concentration in serum (60).

During an influenza outbreak, a placebo-controlled, double blind study was conducted to assess the efficacy of a standardized elderberry extract (Sambucol®). The extract improved the symptoms such as fever within two days and a complete recovery ratio was 90% which was four days shorter than placebo control group (61). Another randomized, double blind, placebo controlled study carried on 60 patients with

influenza infection also supported these findings. Symptoms were relieved 4 days earlier and use of rescue medication was significantly decreased compared to placebo (62).

A study was designed to evaluate the *in vitro* antiviral activity of aqueous-methanol extracts of 70 medicinal plants. Among the tested extracts *S. racemosa* extract showed the most promising activity against HIV-reverse transcriptase with an IC₅₀ value of 0.017 mg/ml (63).

2.2.2.6. Immunomodulatory activity:

Sambucol[®], a standardized extract of *S. nigra* fruits which were found to be an efficient agent against influenza infections was also tested for immunomodulatory activity on monocytes isolated from healthy volunteers. Sambucol preparations were found to activate the immune system by increasing cytokines such as TNF α , IL-1 β and IL-6. Therefore it was suggested that it may be beneficial in patients with influenza, cancer and HIV (64).

2.2.2.7. Antiosteoporotic Activity

Xie et al. investigated the antiosteoporotic effects of *S. williamsi* 60% ethanol extract on ovariectomized rats and rat osteoblast like UMR 106 cell line. The ethanol extract administered orally (30 or 60 mg/100 g body weight/day) significantly increased blood Ca⁺ levels while decreasing urine levels of calcium in ovariectomized rats. Treatment with the extract also affected the markers of bone resorption. Serum alkaline phosphatase and serum osteoclastin levels were repaired and were similar to the levels of the estrogen treated control group. Bone mineral density increased within four months of treatment. The ethanol extract was fractionated with solvent-solvent extraction and their effects on mRNA expression of osteoprotegerin (OPG) and Receptor Activated NF- κ B Ligand (RANKL) in Rat Osteoblast-Like UMR106 cells were investigated. Chloroform and ethyl acetate subextracts were reported to inhibit osteoclastogenesis as a result of the increased ratio of OPG/RANKL (65, 66). Following

this discovery authors attempted to define the active fractions and compounds responsible for the mentioned activity, and several lignans were identified in the active fraction by HPLC analysis (66, 67). In another study to isolate the active compounds, ten lignans were isolated from the 60% ethanol extract of the stems of *S. williamsi* and tested on UMR106 cells which is an *in vitro* model to study the physiology of osteoblast as well as compounds and hormones related to osteoporosis. Pinoresinol, dihydrodehydrodiconiferyl alcohol, buddlenol G showed stimulating effects on UMR106 cell proliferation and alkaline phosphatase activity (68).

2.2.2.8. Wound-healing activity

The methanol extract and the subfractions of the leaves of *S. ebulus* were tested for their *in vivo* wound healing activity. The wound healing activity of the methanol extract was close to the reference drug Madecassol[®] in circular excision model. On incision wound model, a significant increase in the wound tensile strength was determined with the same extract. Subfractions showed significant but reduced wound healing activity on both *in vivo* wound models. Activity-guided fractionation led to the isolation of a flavonoid glycoside “quercetin 3-*O*- β -glucoside” as one of the active principles (69).

2.2.2.9. Antidiabetic activity

A polyphenol enriched extract of *S. nigra* berries caused a significant improvement in the antioxidative capacity of the serum in diabetic rats restoring the normal concentration of reduced glutathione (GSH) and remarkably reduced the serum malondialdehyde concentration in streptozosin-induced diabetic rats. The extract caused a decrease in blood glucose levels after 16 weeks of the induction of diabetes mellitus (70).

2.2.3. Traditional Medicinal Uses of *Cistus* species

Cistus sp. was reported to be used as bath against rheumatism. The poultice prepared from the boiled leaves was externally applied on the body part at kidney level to treat urinary infections (71, 72).

The aerial parts of *C. laurifolius* were used as antialgic, anti-inflammatory and antiseptic and applied externally as lotion. The decoctions prepared from branches of *C. laurifolius* were used against diabetes in vicinity of Edremit (28). The preparations prepared like tisanes were used orally against ulcers in Spanish traditional medicine in Catalonia (73).

C. salviifolius which is known as Ghabra in Lebanon was used against rheumatism by external application of the leaf decoctions as compress (74). The aerial parts of the same plant were used against skin inflammations in Italy (75). Flower decoctions of *C. salviifolius* were used orally against ulcer in vicinity of Marmaris (76). Fresh leaves of the same plant were applied externally on wounds in Kirklareli region (12). It has been reported that the decoctions prepared from branches of the same plant were used against diabetes in vicinity of Edremit (28).

Oral infusions prepared from the aerial parts of *C. monspeliensis* were reported to be used traditionally as antiulcerogenic and antihelminthic in Catalonia (77). An alcoholic macerate of the leaves of the same plant was also used externally for the healing of burns, sores, superficial edemas, dermatitis, insect bites in Tuscany (Italy) (78).

Flower decoctions of *C. creticus* were used orally against ulcer in vicinity of Marmaris while the leaves of *C. creticus* were applied externally on wounds as hemostatic in vicinity of Edremit region (28). In Italy infusions prepared from the leaves of *C. creticus* were used as tonic and stimulant (79).

The preparations from the leaves of *C. albidus* was used against Parkinson disease and the tisane prepared from the flowers was used internally as antitussif in Eastern Mallorca (80). Decoctions of *C. clusii* fruits were used internally against inflammation and pain in Spanish traditional medicine (81).

2.2.4. Biological Activity Studies on *Cistus* species

This section includes the survey of the literatures on the biological activities of *Cistus* species.

2.2.4.1. Anti-inflammatory activity

The leaves of *C. laurifolius* were tested for prostaglandin (PG) inhibitory activity. The methanol extract showed inhibitory effect on PGE₁ and PGE₂-induced contractions in guinea pig ileum at dose of 300 µg/ml. Sixteen compounds were isolated by activity-guided isolation and they were evaluated for their PG inhibitory activities. The identified compounds were; 3-*O*-methylquercetin (**1**), 3,7-*O*-dimethylquercetin (**2**), genkwanin (**3**), 3,7-*O*-dimethyl kaempferol (**4**), 3,4'-*O*-dimethylquercetin (**5**), apigenin (**6**), 3,4'-*O*-dimethylkaempferol (**7**), ellagic acid (**8**), β-sitosterol-3-*O*-β-glucoside (**9**), quercetin-3-*O*-α-rhamnoside (**10**), 5-*O*-*p*-coumaroyl quinic acid methyl ester (**11**), 1-(4-hydroxy-3-methoxyphenyl)-2-[4-(3-α-l-rhamnopyranoxypropyl)-2-methoxyphenoxy]-1,3-propanediol (**12**), 2, 3-dihydro-2-(4'-α-l-rhamnopyranosyloxy-3'-methoxyphenyl)-3-hydroxymethyl-7-methoxy-5-benzofuranpropanol (**15**). New lignan glycosides **13** and **14** were determined to be olivil 9-*O*-β-D-xyloside and berchemol-9-*O*-rhamnoside, respectively. Compound **16** was isolated as a 2:1 mixture of two diastereomers, the major one of which was determined to be (7*S*,8*R*)-dihydrodehydrodiconiferyl alcohol 9'-*O*-α-L-rhamnoside. The known PG inhibitory effect was observed in **1**, **5**, **10**, **12** and **16** at 30 µg/ml. These findings showed that flavonoids and lignans may contribute to the efficacy of the herb against inflammatory disorders (82, 83).

Effects of extracts and fractions from the leaves with non-woody branches of *C. laurifolius* were studied using two *in vivo* models: carrageenan induced hind-paw edema and acetic acid-induced increased vascular permeability. EtOH extract was significantly active in both at 250 and 500 mg/kg doses. The ethanol extract was submitted to subsequent solvent extractions (hexane, CHCl₃, EtOAc, *n*-BuOH, R-H₂O) and CHCl₃ and EtOAc subextracts were found significantly active against both models. The compounds responsible from the activity in the most active fraction (CHCl₃ subextract) were isolated as; 3-*O*-methylquercetin; 3,7-*O*-dimethylquercetin; 3,7-*O*-

dimethylkaempferol. To investigate the potent antinociceptive activity, these flavonoids were also assessed through inhibition of *p*-benzoquinone-induced writhing test in mice. All the isolated compounds showed potent antinociceptive activity without inducing any gastric lesions (83).

Pre-incubation of the human monocytes with *C. clusii* extracts 30 mins prior to LPS induction induced a significant inhibition of IL-6, while petroleum ether extract was effective on TNF α secretion (84).

2.2.4.2. Antioxidative activity

Sadhu et al. investigated the antioxidant activity of the methanol extract of the leaves of *Cistus laurifolius* by measuring the DPPH radical scavenging effect on TLC plates. Several spots on the reddish-purple background of the TLC plate were reacted positively. Sixteen compounds (flavonoids and lignans) were then isolated through activity-guided processing (PGE₁ and PGE₂-induced contractions in guinea pig ileum and DPPH radical scavenging assays) and they were also evaluated for their radical scavenging activity. The results indicated that catechol structure of the B ring was essential for the radical scavenging activity of the flavonoids (82).

A complete set of antioxidant assays such as; TEAC (Trolox equivalent antioxidant capacity), FRAP assay (ferric ion reducing antioxidant power), TBARS assay (2-thiobarbituric acid reactive substances) and ORAC assay (Oxygen radical absorbance capacity) was performed to characterize the antioxidant potential of *C. ladanifer* and *C. populifolius*. *C. populifolius* aqueous extract exhibited a higher antioxidant capacity than *C. ladanifer* in TEAC, FRAP, TBARS assays correlated to its higher phenolic content determined through Folin-Ciocalteu reagent. In contrast to the results obtained in previous assays, *C. ladanifer* extract was more potent than *C. populifolius* when tested by ORAC method (85).

2.2.4.3. Cytotoxic activity

The cytotoxic activity of the aqueous extracts of the leaves of *C. ladanifer* and *C. populifolius* were determined on different cell lines including pancreatic, colon and breast cancer cells. *Cistus* extracts exhibited similar activities against pancreatic cancer cells. HS-766T and M186 cells were resistant to these extracts, whereas M220 cells were highly sensitive with CC₅₀ values of 0.49 and 0.66 mg/ml for *C. ladanifer* and *C. populifolius* extracts, respectively. Breast cancer cells, MCF7/HER2 and JIMT-1 cells were the most sensitive cells to *Cistus* extracts: CC₅₀ values within the range of 0,5-1 mg/ml for MCF7/HER2 and 1.6-2 mg/ml for JIMT-1 cells. SKBr3 breast cancer cells and HT29 colon cancer cells were more resistant to these extracts (85).

Labdane-type diterpenes appear to be the predominant compounds of the resin 'ladano' which is secreted from the leaves and stems of *Cistus creticus* subsp. *creticus* (86). In an effort to identify compounds with cytotoxic activity, labdane type diterpenes isolated from the aerial parts and resin of *C. creticus*. After that they were investigated for their biological activity (87, 88). The authors attributed a significant cytotoxic activity to a number of labdane-type diterpenoid compounds from the aerial parts and resin of *C. creticus* against several cell line systems including KB, P-388, NSCLC-N6, MOLT 3, RAJI, H9. Nine labdane type compounds isolated from the plant and studied against 14 human leukemic cell lines including; CCRF-CEM, H33AJ-JA13, HUT78, KM3, NAMALWA, DAUDI, SDK, JIYOYE, CCRF-SB, HL60, K562, U937 (89). The most active compound (13*E*)-labd-13-ene-8 α , 15-diol exhibited cytotoxic activity against 13 of the cell lines tested. It was also studied for its effect on the uptake of (³H)-thymidine as a marker of DNA synthesis and declared to affect the DNA synthesis in all cell lines (89). Demetzos et al. also designed liposomal formulations for a number of biologically active diterpenes isolated from *C. creticus* subsp. *creticus* or resin 'ladano' to overcome the water solubility in order to prepare suitable formulation for *in vivo* administration. Liposomes were designed for labd-7,13-dien-15-ol, labd-13(*E*)-ene-8 α ,15-diol and its derivative labd-13(*E*)-ene-8 α -ol-15-yl-acetate. The cytotoxic activities of free and liposomal forms were also studied (86, 90). The cytotoxic activity of both liposome and free form of labd-7,13-dien-15-ol were

found to be identical (90). Sclareol and *ent*-3 β -hydroxy-13-epi-manoyl oxide isolated from the leaves and fruits of *C. creticus* were found to be active against human leukemic cell lines. The latter was converted to its thiomidazolide derivative. *Ent*-3 β -hydroxy-13-epi-manoyl and its thiomidazolide derivative were found to induce apoptic cell death in human T cell leukemia lines. The effects of these compounds on the activation and/or suppression of critical genes such as *c-myc* and *bcl-2* which plays a key role in apoptozis were also studied in the two different leukemic cell lines; MOLT3 and H33AJ-JA1. It's declared that induction of apoptosis by these compounds is preceded by *c-myc* down regulation and being not affected, *bcl-2* could not prevent apoptosis induced by the two different diterpenes (91).

2.2.4.4. Antiviral and Antimicrobial activity

The aqueous extracts of the leaves of *C. ladanifer* and *C. populifolius* were studied against two types of bacteria; Gram-positive (*Staphylococcus aureus*) and Gram-negative (*Escherichia coli*). The extract of *C. ladanifer* showed significant antibacterial activity against *Staphylococcus aureus* (MIC₅₀: 154 μ g/ml), whereas *C. populifolius* (MIC₅₀: 123 μ g/ml) was effective against *Escherichia coli* (4). In another study the antibacterial effect of two *Cistus* species (*C. villosus*, *C. monspeliensis*) was tested against a panel of bacteria (*S. aureus*, *Enterococcus hirea*, *E. coli*, *Pseudomonas aeruginosa*), yeast (*Candida albicans*, *C. krusei*, *C. glabrata*) and mold (*Aspergillus fumigates*) by using the standard M27-T broth microdilution technique. The leaf extracts showed antimicrobial activities with MIC values ranging from 0.78 to 50 mg/ml for bacteria and 0.19 to 200 mg/ml for fungi. *Cistus villosus* extracts showed the lowest MIC values. *C. villosus* extracts showed interesting activity when used on *S. aureus* (MIC=0.78 mg/ml) and *Candida glabrata* (MIC=0.19 mg/ml) (92).

A polyphenol rich extract (CYSTUS052) prepared from *C. creticus* was found to possess antiviral activity against influenza virus in cell culture and mice. Treatment with the extract reduced the pyrogenity of the virus in A549 or MDCK cells infected with avian and human influenza strains. Mice treated with the extract had no change in the body temperature and no histological alterations observed on bronchiolus epithelial

cells (93, 94). A randomised, placebo controlled prospective study conducted on 160 patients with upper respiratory track infections to evaluate the effects of CYTUS052 lozenges. The symptoms were remarkably reduced by CYTUS052 treatment and C-reactive protein was significantly decreased in patients (95).

2.2.4.5. Anti-*Helicobacter pylori* and Antiulcer activity

Extracts of *C. laurifolius* flowers and solvent fractions of the extract showed a remarkable anti-*Helicobacter pylori* activity. The MIC value of chloroform subextract (1,95 µg/ml) was very close to the reference compound ofloxacin (11). Through activity-guided procedures quercetin-3-methyl ether (isorhamnetin) was isolated from the chloroform subextract as the active component involved in the anti-*H. pylori* activity (96).

A fraction obtained by EtOH precipitation from the EtOH extract of *C. laurifolius* was reported to be active against various ulcer models in rats and mice including pylorus ligation-, ethanol-, indomethacin-, indomethacin plus HCL/EtOH-induced gastric and cysteamine-induced duodenal lesions. The extract also exerted antacid activity (50).

2.2.4.6. Spasmolytic Activity

The water extracts of *C. creticus* and *C. monspeliensis* were evaluated for their myorelaxant activities using isolated smooth muscle of rat ileum and aorta. Both extracts inhibited the contractile response to acetylcholine, phenylephrine and KCl suggesting their spasmolytic activities on intestinal and vascular smooth muscle cells (97). Aziz et al, studied the antispasmodic activity of *C. ladaniferus* aqueous extract on rodent jejunum. The extract of leaves and stems caused the inhibition of the spontaneous motility of the rabbit jejunum and K⁺ induced contractions in rabbit and rat jejunum (98).

2.2.4.7. Antidiabetic Activity

In a screening study aimed to investigate the inhibitory effects of 38 plants from traditional Turkish folk medicine on human aldose reductase (h-AR) enzyme, the plant extracts from *Cistus* genus (*C. laurifolius*, *C. creticus*, *C. monspeliensis*, *C. salviifolius*, *C. parvifolius*) exhibited potent inhibitory activity. *C. laurifolius* extract also exerted strong inhibition in the blood coagulation assay. Quercetin-3-*O*-methyl ether was isolated from *C. laurifolius* and was found to be as potent as that of eparlestat, which is prescribed for treating diabetic complications (99). Ethanol extract of *C. laurifolius* was shown to reduce the blood glucose levels of streptozosine-induced diabetic rats ranging from 16% to 34% at 250 and 500 mg/kg doses. The extract also exerted potent inhibition on α -glucosidase and α -amylase (100).

2.2.4.8. Other Biological Activities

Quercetin-3-7-dimethylether was isolated from *C. laurifolius* leaves and found to possess potent antioxidant activity on lipid peroxidation in liver and plasma, cellular glutathione levels (GSH) and plasma AST (aspartate aminotransferase) and ALT (alanine aminotransferase) enzyme activities in acetaminophen-induced liver damage in mice (101).

Anticholinesterase and antioxidant effects of EtOH extract and fractions along with isolated flavonoids from *C. laurifolius* were evaluated. Ethanol extract was the most active on acetylcholinesterase inhibition and ethyl acetate and *n*-butanol fractions were active on DPPH and FRAP assays (102).

2.3. Phytochemical Information

This section is a review on previous phytochemical studies on *Cistus* and *Sambucus* genera.

2.3.1. Phytochemical studies on *Sambucus* genus

Previous phytochemical work on the genus *Sambucus* revealed that it is rich in lignans, iridoids, flavonoids and cyanogenins. The results of the literature survey of the compounds isolated from *Sambucus* genus is summarised in **Tables 1-31**.

2.3.1.1. Phenolic Compounds

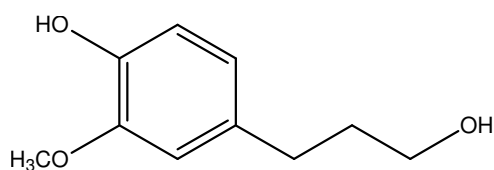


Table 1: Phenylpropane derivatives from *Sambucus* genus

Compounds	Species	Reference
Coniferyl alcohol	<i>williamsi</i> (stems and branches)	(67)

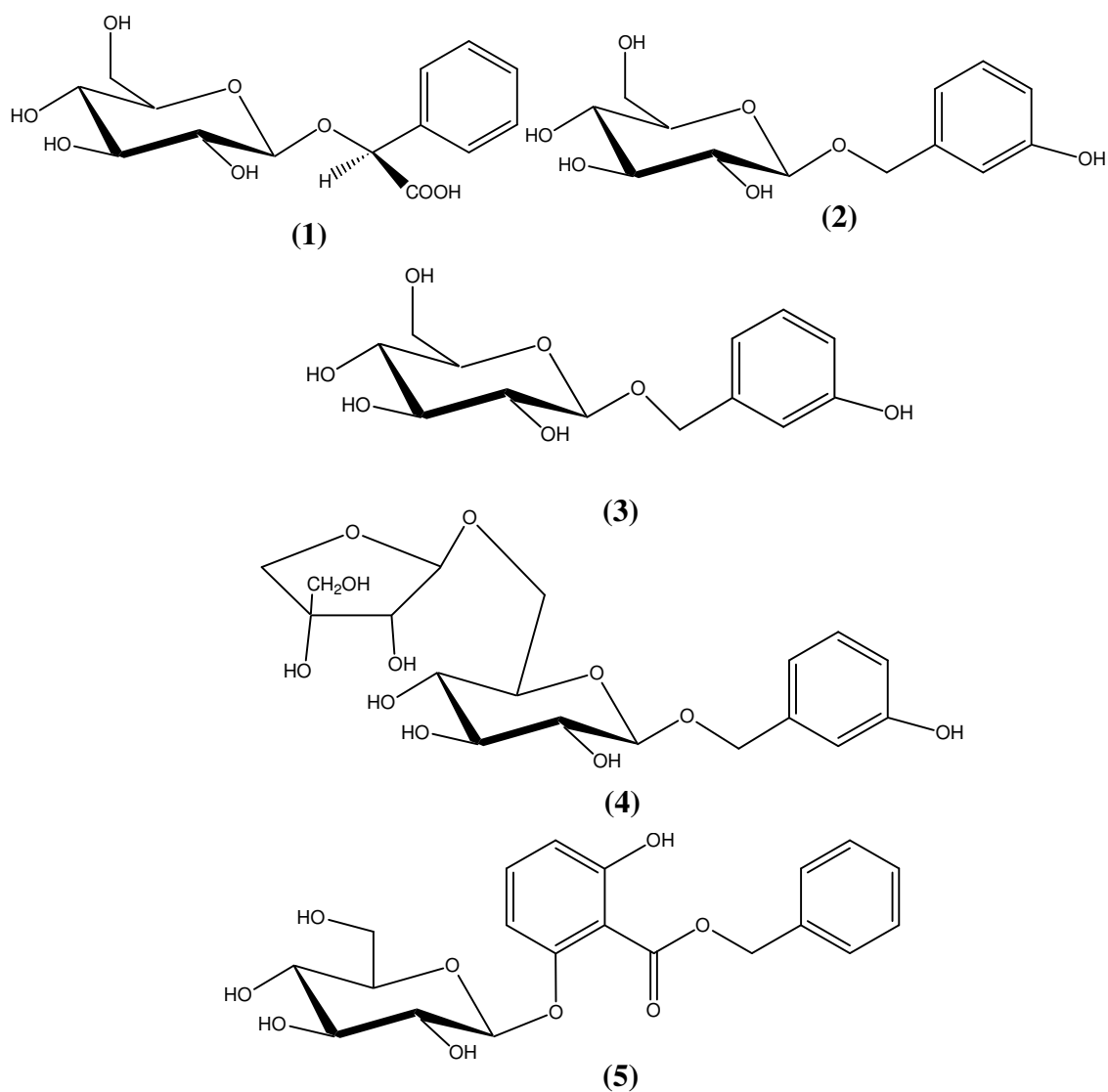
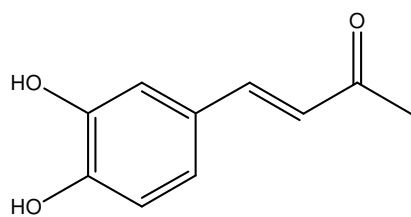
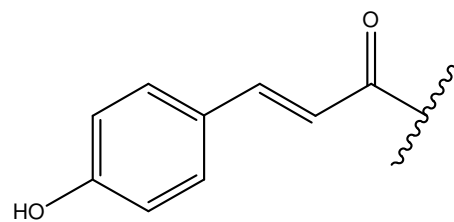


Table 2: Phenolic glycosides from *Sambucus* genus

Compounds	Species	Reference
(2S)-2-O-β-D -glucopyranosyl-2-hydroxy-phenyl-acetic acid (1)	<i>nigra</i> (leaves)	(103)
3-Hydroxybenzyl-1-O-β-D-glucopyranoside (2)	<i>nigra</i> (leaves)	(103)
1-O-β-D-glucopyranosyl-2-(3-hydroxyphenyl)-ethanol (3)	<i>nigra</i> (leaves)	(103)
Benzyl alcohol-β-D-apiofuranosyl-(1→6)-β-D-glucopyranoside (Icariside F) (4)	<i>nigra</i> (leaves)	(103)
Benzyl 2-O-β-D-glucopyranosyl-2,6-dihydroxy-benzoate (5)	<i>nigra</i> (leaves)	(103)



Caffeoyl



***p*-Coumaroyl**

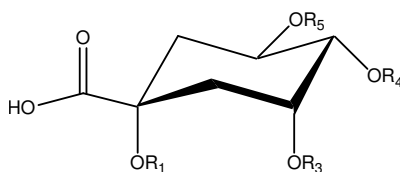


Table 3: Phenolic acids from *Sambucus* genus

Compounds	R ₁	R ₃	R ₄	R ₅	Species	Reference
3- <i>O</i> -caffeoylquinic acid	H	Caf	H	H	<i>nigra</i> (flowers)	(104)
3- <i>O</i> - <i>p</i> -coumaroylquinic acid	H	<i>p</i> -cou	H	H	<i>nigra</i> (flowers)	(104)
5- <i>O</i> -caffeoylquinic acid	H	OH	H	Caf	<i>nigra</i> (flowers)	(104)
5- <i>O</i> - <i>p</i> -coumaroylquinic acid	H	OH	H	<i>p</i> -Cou	<i>nigra</i> (flowers)	(104)
3,5-di- <i>O</i> -caffeoylquinic acid	H	Caf	H	Caf	<i>nigra</i> (flowers)	(104)

Caf: Caffeoyl, *p*-cou: *p*-coumaroyl

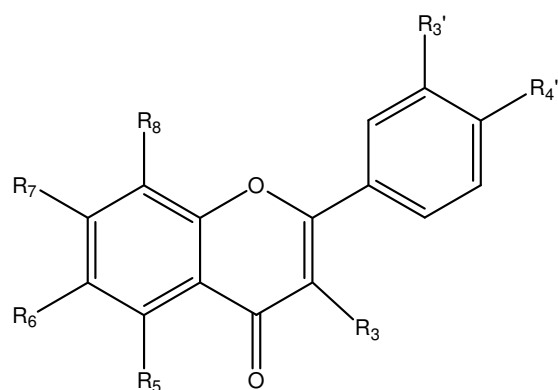


Table 4: Flavonoids from *Sambucus* genus

Compounds	R ₃	R ₅	R ₆	R ₇	R ₈	R _{3'}	R _{4'}	Species	Reference
Apigenin	H	OH	H	OH	H	H	OH	<i>adnata</i> (whole plant)	(105)
Kaempferol	OH	OH	H	OH	H	H	OH	<i>adnata</i> (whole plant)	(106)
Kaempferol-3- <i>O</i> -neohesperoside	ONeohes	OH	H	OH	H	H	OH	<i>nigra</i> (leaves)	(103)
Kaempferol-3- <i>O</i> -glucoside (Astragalin)	OGlc	OH	H	OH	H	H	OH	<i>nigra</i> (leaves)	(103)
Kaempferol 3- <i>O</i> -rutinoside	ORut	OH	H	OH	H	H	OH	<i>nigra</i> (flowers)	(104)
Luteolin	H	OH	H	OH	H	OH	OH	<i>adnata</i> (whole plant)	(105)
Quercetin	OH	OH	H	OH	H	OH	OH	<i>adnata</i> (whole plant) <i>nigra</i> (berries)	(105) (107)
Quercetin 3- <i>O</i> -glucoside (Isoquercitrin)	OGlc	OH	H	OH	H	OH	OH	<i>adnata</i> (whole plant) <i>ebulus</i> (leaves) <i>nigra</i> (leaves, flowers, berries)	(69) (103, 104, 107)
Quercetin-3- <i>O</i> -neohesperoside	ONeohes	OH	H	OH	H	OH	OH	<i>nigra</i> (leaves)	(103)
Quercetin 3- <i>O</i> -rutinoside	ORut	OH	H	OH	H	OH	OH	<i>nigra</i> (flowers) <i>nigra</i> (berries)	(104) (107)
Rhamnetin 3- <i>O</i> -glucoside	OGlc	OH	H	OCH ₃	H	OH	OH	<i>nigra</i> (leaves)	(103)
Isorhamnetin 3- <i>O</i> -glucoside	OGlc	OH	H	OH	H	OCH ₃	OH	<i>nigra</i> (flowers)	(104)

Glc:β-Glucose, Neohes: Neohesperidose, Rut: Rutinose

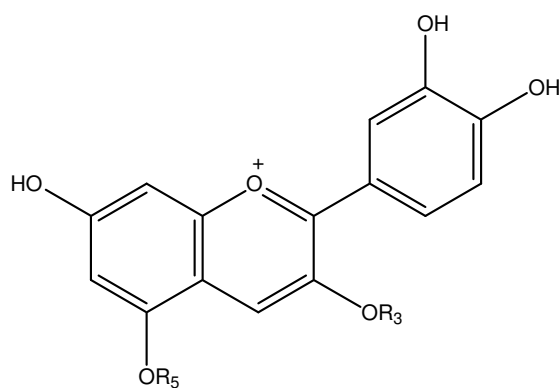


Table 5: Anthocyanins from *Sambucus* genus

Compounds	R3	R5	Species	Reference
Cyanidin-3-sambubioside-5-glucoside	Sambu	Glc	<i>nigra</i> (berries) <i>canadensis</i> (berries)	(107) (108-110)
Cyanidin-3-glucoside	Glc	H	<i>canadensis</i> (berries)	(108-110)
Cyanidin-3,5-diglucoside	Glc	Glc	<i>nigra</i> (berries) <i>canadensis</i> (berries)	(107) (108-110)
Cyanidin-3-sambubioside	Sambu	H	<i>nigra</i> (berries) <i>canadensis</i> (berries)	(107) (108-110)
Cyanidin-3-rutinoside	Rut	H	<i>nigra</i> (berries)	(107)

Glc: β -Glucose, Rut: Rutinose, Sambu: Sambubiose

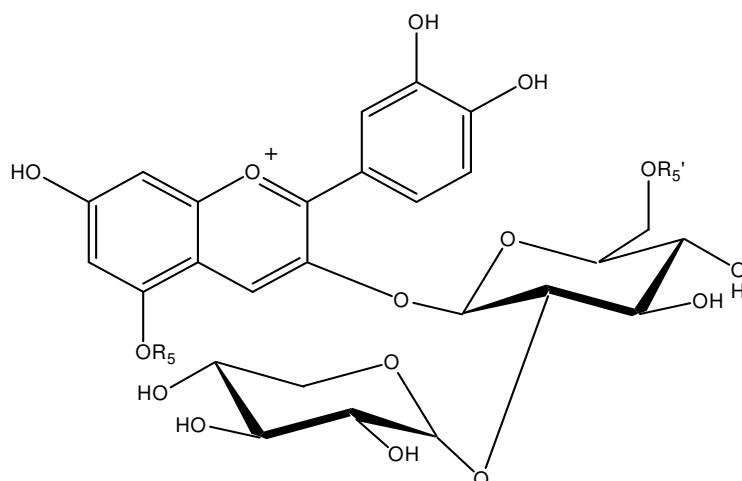


Table 6: Anthocyanins from *Sambucus* genus

Compounds	R ₅	R _{5'}	Species	Reference
Cyanidin-3- <i>O</i> -(2''- <i>O</i> -xylosylglucoside)	H	H	<i>nigra</i> (berries) <i>caerulea</i> (berries)	(107) (108)
Cyanidin-3- <i>O</i> -(2''- <i>O</i> -xylosylglucoside)-5- <i>O</i> -glucoside	Glc	H	<i>nigra</i> (berries) <i>sachalinensis</i> (berries) <i>sibirica</i> (berries) <i>racemosa</i> (berries) <i>racemosa</i> ssp. <i>pubens</i> <i>racemosa</i> ssp. <i>sieboldii</i> <i>racemosa</i> ssp. <i>callicarpa</i> <i>canadensis</i> (berries)	(107) (108) (108) (108) (108) (108) (108) (108-110)
Cyanidin-3- <i>O</i> -(2''- <i>O</i> -xylosyl-6''- <i>O</i> - <i>Z</i> - <i>p</i> -coumaroylglucoside)-5- <i>O</i> -glucoside	Glc	<i>p</i> (<i>Z</i>)-cou	<i>sachalinensis</i> (berries) <i>sibirica</i> (berries) <i>racemosa</i> (berries) <i>racemosa</i> ssp. <i>pubens</i> (berries) <i>racemosa</i> ssp. <i>sieboldii</i> (berries) <i>racemosa</i> ssp. <i>ctgallicarpa</i> <i>canadensis</i> (berries)	(108) (108) (108) (108) (108) (108) (108-110)
Cyanidin-3- <i>O</i> -(2''- <i>O</i> -xylosyl-6''- <i>O</i> - <i>E</i> - <i>p</i> -coumaroylglucoside)-5- <i>O</i> -glucoside	Glc	<i>p</i> -(<i>E</i>)-cou	<i>sachalinensis</i> (berries) <i>sibirica</i> (berries) <i>racemosa</i> (berries) <i>racemosa</i> ssp. <i>pubens</i> (berries) <i>racemosa</i> ssp. <i>sieboldii</i> (berries) <i>racemosa</i> ssp. <i>callicarpa</i> (berries)	(108) (108) (108) (108) (108) (108-110)

Glc: β-Glucose, Xyl:xylose, Cou: Coumaroyl

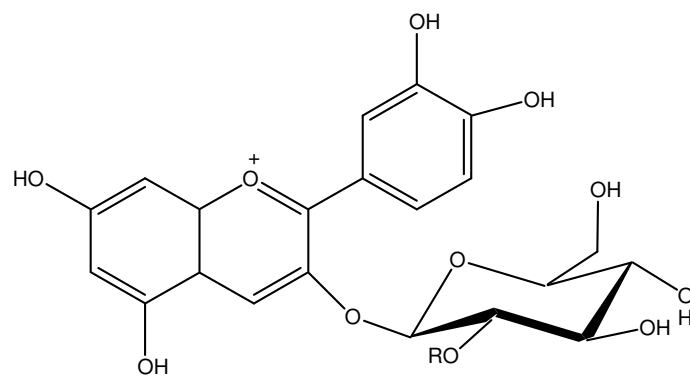


Table 7: Anthocyanins from *Sambucus* genus

Compounds	R	Species	Reference
Cyanidin-3-O-(2''-O-xylosylgalactoside)	Xyl	<i>cerulea</i> (berries)	(108)

Xyl: xylose

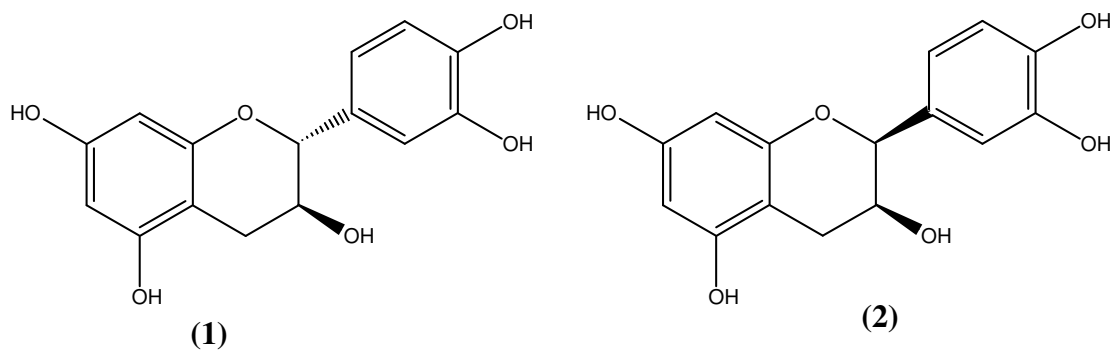


Table 8: Flavan-3-ols from *Sambucus* genus

Compounds	Species	Reference
(+)-Catechin (1)	<i>cerulea</i> (fruits)	(111)
(+)-Epicatechin (2)	<i>cerulea</i> (fruits)	(111)

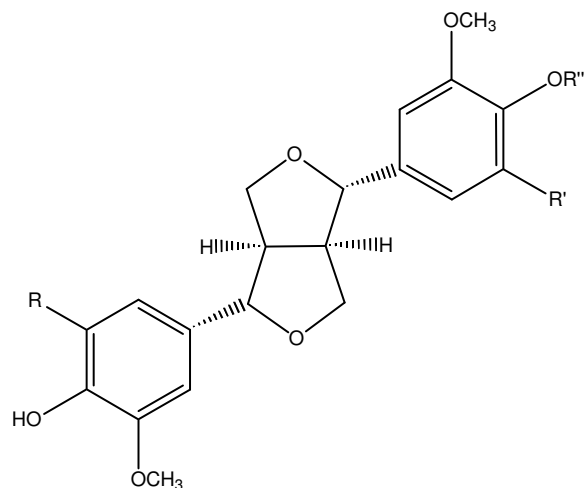


Table 9: Lignans from *Sambucus* genus

Compounds	R	R'	R''	Species	Reference
(+) Pinoresinol	H	H	H	<i>nigra</i> (leaves)	(103)
				<i>adnata</i> (whole plant)	(106)
				<i>williamsi</i> (stems)	
(+) Medioresinol	H	OH	H	<i>nigra</i> (leaves)	(103)
(+) Syringaresinol- <i>O</i> - β -D-glucopyranoside	OCH ₃	OCH ₃	Glc	<i>sieboldiana</i> (leaves)	(112)

Glc: β -Glucose

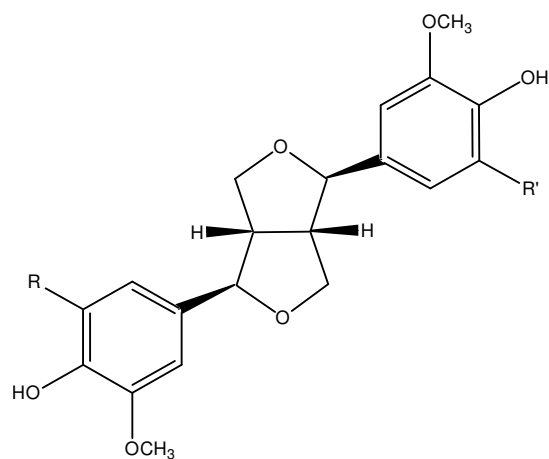


Table 10: Lignans from *Sambucus* genus

Compounds	R	R'	Species	Reference
(-) pinoresinol	H	H	<i>williamsii</i> (stems)	(68)
(-)-syringaresinol	OCH ₃	OCH ₃	<i>williamsii</i> (stems)	(68)

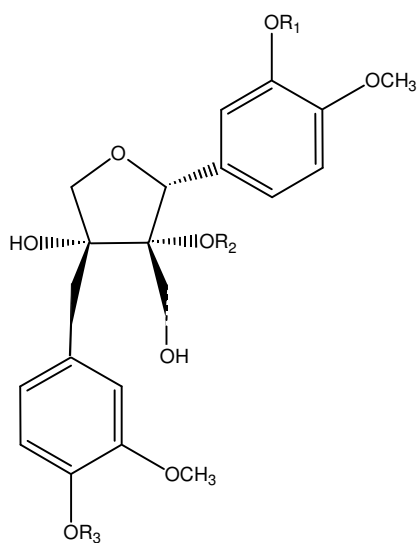


Table 11: Lignans from *Sambucus* genus

Compounds	R ₁	R ₂	R ₃	Species	Reference
(-)-olivil 4''-O-β-D-glucopyranoside	H	H	Glc	<i>sieboldiana</i> (leaves)	(112)
(-)-massoniresinol 4''-O-β-D- glucopyranoside	H	H	Glc	<i>sieboldiana</i> (leaves)	(112)
(-)-massoniresinol 4'-O-β-D- glucopyranoside	Glc	H	H	<i>sieboldiana</i> (leaves)	(112)

Glc: β-Glucose

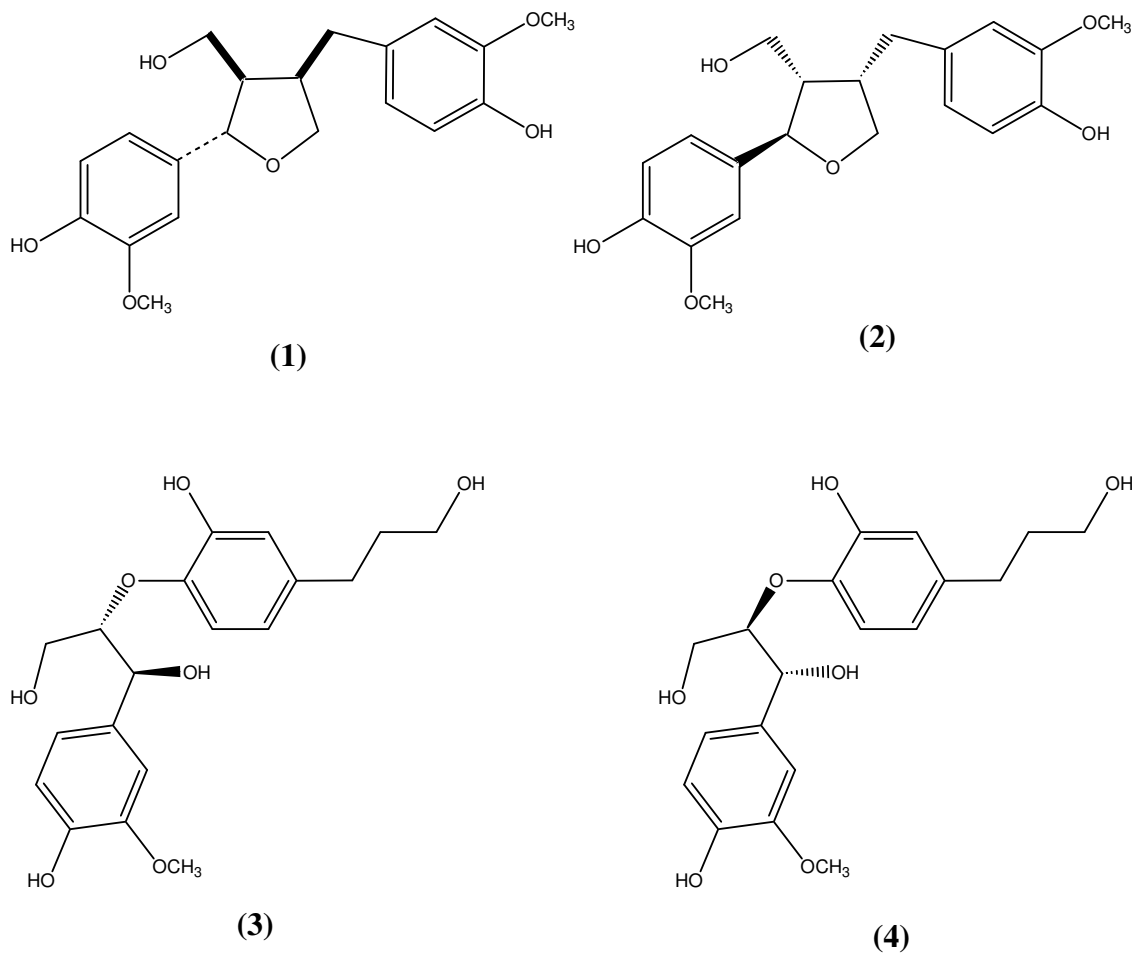
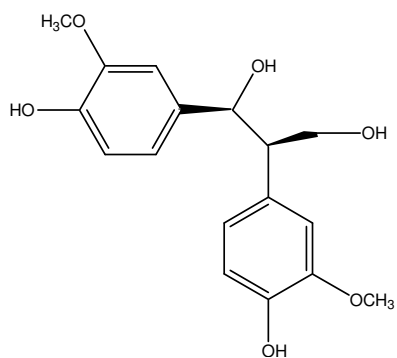
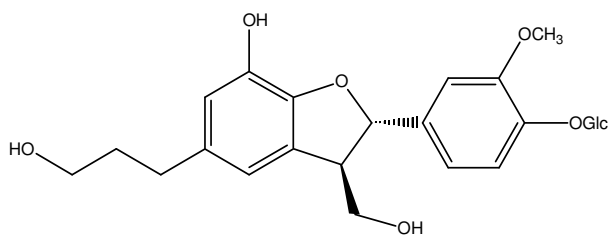


Table 12: Lignans from *Sambucus* genus

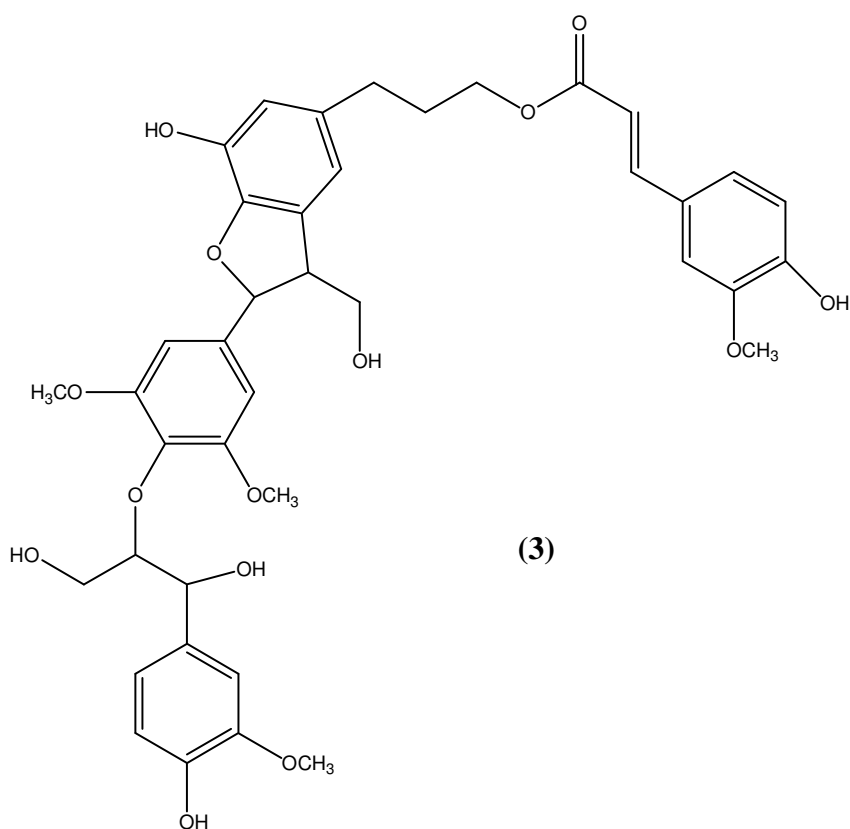
Compounds	Species	Reference
(+) lariciresinol (1)	<i>nigra</i> (leaves)	(103)
(-) lariciresinol (2)	<i>williamsi</i> (stems)	(55, 113)
Erythro-1-(4-hydroxy-3-methoxyphenyl)-2-[2-hydroxy-4-(3-hydroxypropyl) phenoxy]-1,3-propanediol (3)	<i>williamsi</i> (leaves)	(114)
Threo-1-(4-hydroxy-3-methoxyphenyl)-2-[2-hydroxy-4-(3-hydroxypropyl) phenoxy]-1,3-propanediol (4)	<i>williamsi</i> (leaves)	(114)



(1)



(2)



(3)

Table 13: Lignans from *Sambucus* genus

Compounds	Species	Reference
1, 2-bis (4-hydroxy-3-methoxy phenyl)-1, 3-propanediol (1)	<i>williamsi</i> (stems)	(68)
2-1-(4-hydroxy-3-methoxy- phenyl)-1,3-propanediol (Buddlenol G) (2)	<i>williamsi</i> (stems)	(68)
(2 <i>S</i> ,3 <i>R</i>)-2,3-dihydro-7-hydroxy-2-(4'-hydroxy-3'-methoxyphenyl)-3-hydroxy- methyl-5-benzofuranpropanol 4'- <i>O</i> -β-D-glucopyranoside (3)	<i>sieboldiana</i> (leaves)	(112)

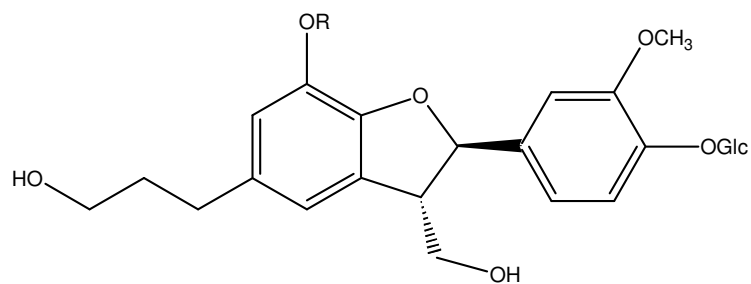


Table 14: Lignans from *Sambucus* genus

Compounds	R	Species	Reference
(2 <i>R</i> ,3 <i>S</i>)-2,3-dihydro-7-hydroxy-2-(4'-hydroxy-3'-methoxyphenyl)-3-hydroxy- methyl-5-benzofuranpropanol 4'- <i>O</i> - β-D-glucopyranoside	H	<i>sieboldiana</i> (leaves)	(112)
(2 <i>R</i> ,3 <i>S</i>)-2,3-dihydro-2-(4''-hydroxy-3'-methoxyphenyl)-3-hydroxymethyl-7-methoxy-5-benzofuran- propanol 4'- <i>O</i> - β-D-glucopyranoside	CH ₃	<i>sieboldiana</i> (leaves)	(112)

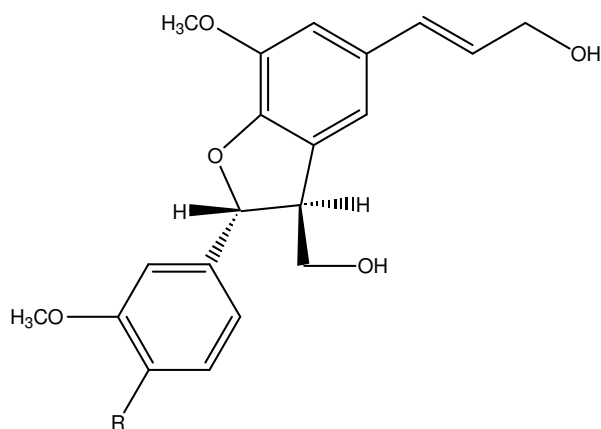


Table 15: Lignans from *Sambucus* genus

Compounds	R	Species	Reference
Dehydrodiconiferyl alcohol-4- <i>O</i> -β-D-glucopyranoside	OGlc	<i>williamsi</i> (stems)	(114)
Dehydrodiconiferyl alcohol	H	<i>williamsi</i> (stems)	(67)

Glc: β-Glucose

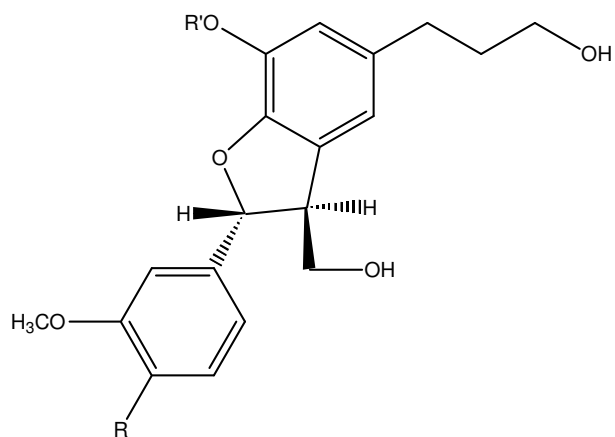
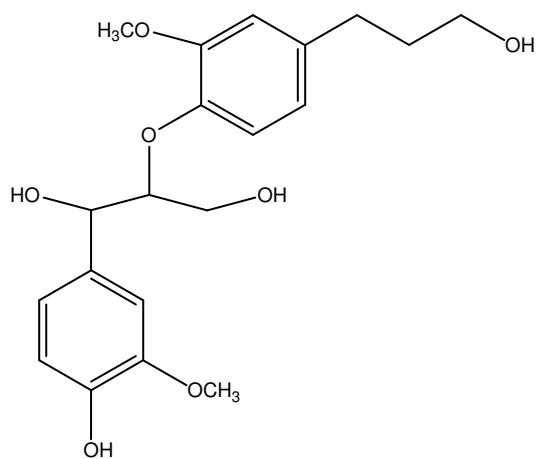


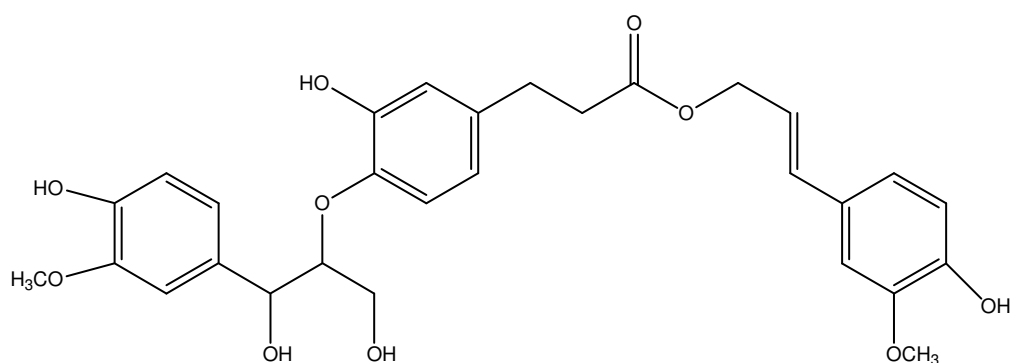
Table 16: Lignans from *Sambucus* genus

Compounds	R	R'	Species	Reference
Dihydrodehydrodiconiferyl alcohol-4- <i>O</i> - β -D-glucopyranoside	OGlc	CH ₃	<i>williamsi</i> (stems)	(114)
(7 <i>S</i> , 8 <i>R</i>)-dihydro-3'-hydroxy- 8-hydroxy-methyl-7-(4-hydroxy-3-methoxy-phenyl)-1'-benzofuranpropanol	H	H	<i>williams I</i> (stems)	(114)
Dihydrodehydrodiconiferyl alcohol	H	H	<i>williamsi</i> (stems)	(67)

Glc: β -Glucose



(1)



(2)

Table 17: Lignans from *Sambucus* genus

Compounds	Diastereomers	Species	Reference
(-)-erythro-1-(4-hydroxy-3-methoxyphenyl)-2-[4-(3-hydroxypropanyl)-2-methoxyphenoxy]-1,3-propanediol (1)	erythro	<i>williamsi</i> (stems)	(68)
(-)-threo-1-(4-hydroxy-3-methoxyphenyl)-2-[4-(3-hydroxypropanyl)-2-methoxyphenoxy]-1,3-propanediol (1)	threo	<i>williamsi</i> (stems)	(68)
Erythro-1-(4-hydroxy-3-methoxyphenyl)-2-[4-(4-hydroxy-3-methoxy-cinnamoyloxypropanyl)-2-hydroxyphenoxy]-1,3-propanediol (Sambucunol A) (2)	erythro	<i>williamsi</i> (stems)	(68)
Threo-1-(4-hydroxy-3-methoxyphenyl)-2-[4-(4-hydroxy-3-methoxy-cinnamoyloxypropanyl)-2-hydroxyphenoxy]-1,3-propanediol (Sambucunol B) (2)	threo	<i>williamsi</i> (stems)	(68)

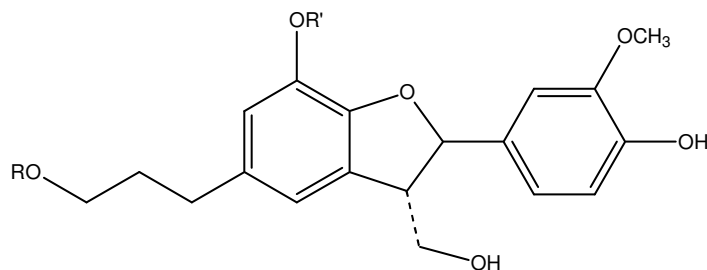


Table 18: Lignans from *Sambucus* genus

Compounds	R	R'	Species	Reference
(2 <i>R</i> -trans) 2,3-dihydro-2-(4-hydroxy-3-methoxyphenyl)-3-(hydroxymethyl)-7-methoxy-5-benzofuranpropanol acetate	OAc	CH ₃	<i>nigra</i> (leaves)	(103)
(2 <i>R</i> -trans)-2,3-dihydro-2-(4-hydroxy-3-methoxyphenyl)-3-(hydroxymethyl)-7-hydroxy-5-benzofuranpropanol	H	CH ₃	<i>nigra</i> (leaves)	(103)
(2 <i>R</i> -trans)-2,3-dihydro-2-(4-hydroxy-3-methoxyphenyl)-3-(hydroxymethyl)-7-methoxy-5-benzofuranpropanol	H	H	<i>nigra</i> (leaves)	(103)

Ac: Acetyl

2.3.1.2. Terpenic Compounds

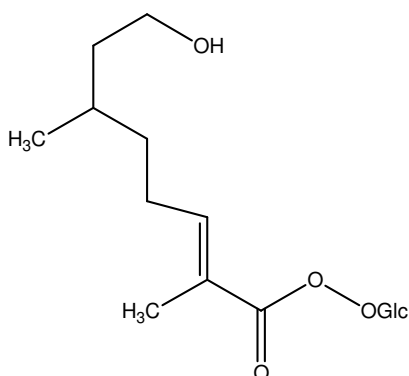


Table 19: Monoterpenes from *Sambucus* genus

Compounds	Species	Reference
(β-D-glucopyranosyl)-8-hydroxy-2,6-dimetyloct-2-enoat	<i>ebulus</i> (root)	(115)

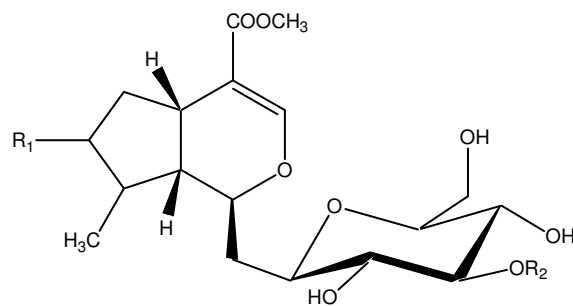
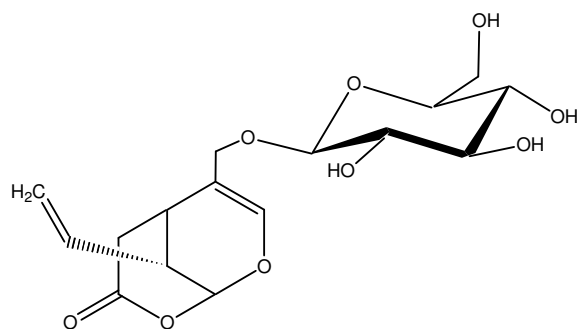


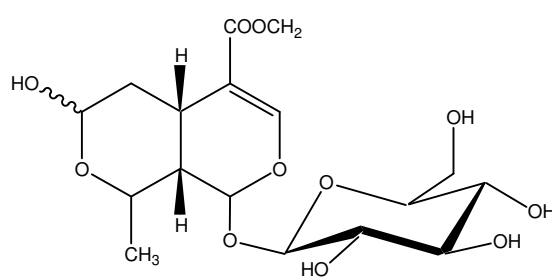
Table 20: Iridoids from *Sambucus* genus

Compound	R ₁	R ₃	Species	Reference
Williamsoside A	H	Api	<i>williamsi</i> (root bark)	(116)
Williamsoside B	OH	Api	<i>williamsi</i> (root bark)	(116)

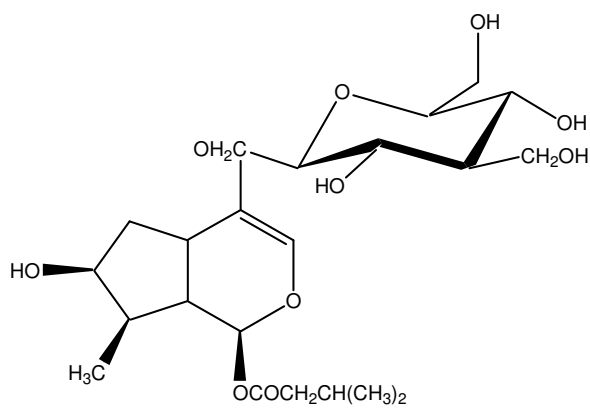
Api: Apiose



(1)



(2)



(3)

Table 21: Iridoids from *Sambucus* genus

Compound	Species	Reference
Isosweroside (1)	<i>ebulus</i> (leaves)	(117)
Morronoside (2)	<i>ebulus</i> (leaves) <i>ebulus</i> (root bark)	(117) (114)
7,7- <i>O</i> -dihydroebuloside (3)	<i>ebulus</i> (roots)	(118)

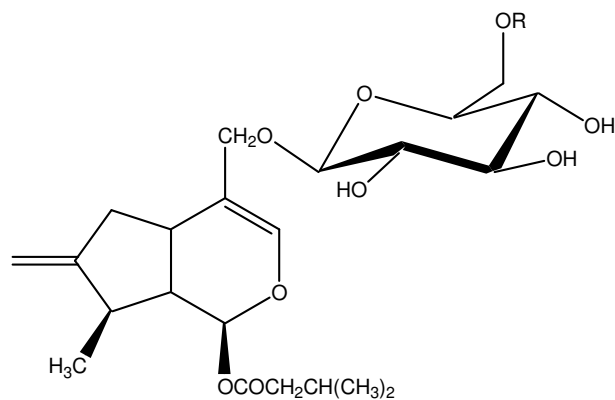


Table 22: Iridoids from *Sambucus* genus

Compounds	R	Species	Reference
Ebuloside	H	<i>ebulus</i> (leaves)	(117, 119)
6'- <i>O</i> -apiosylebuloside	Api	<i>ebulus</i> (roots)	(115)

Api: Apiose

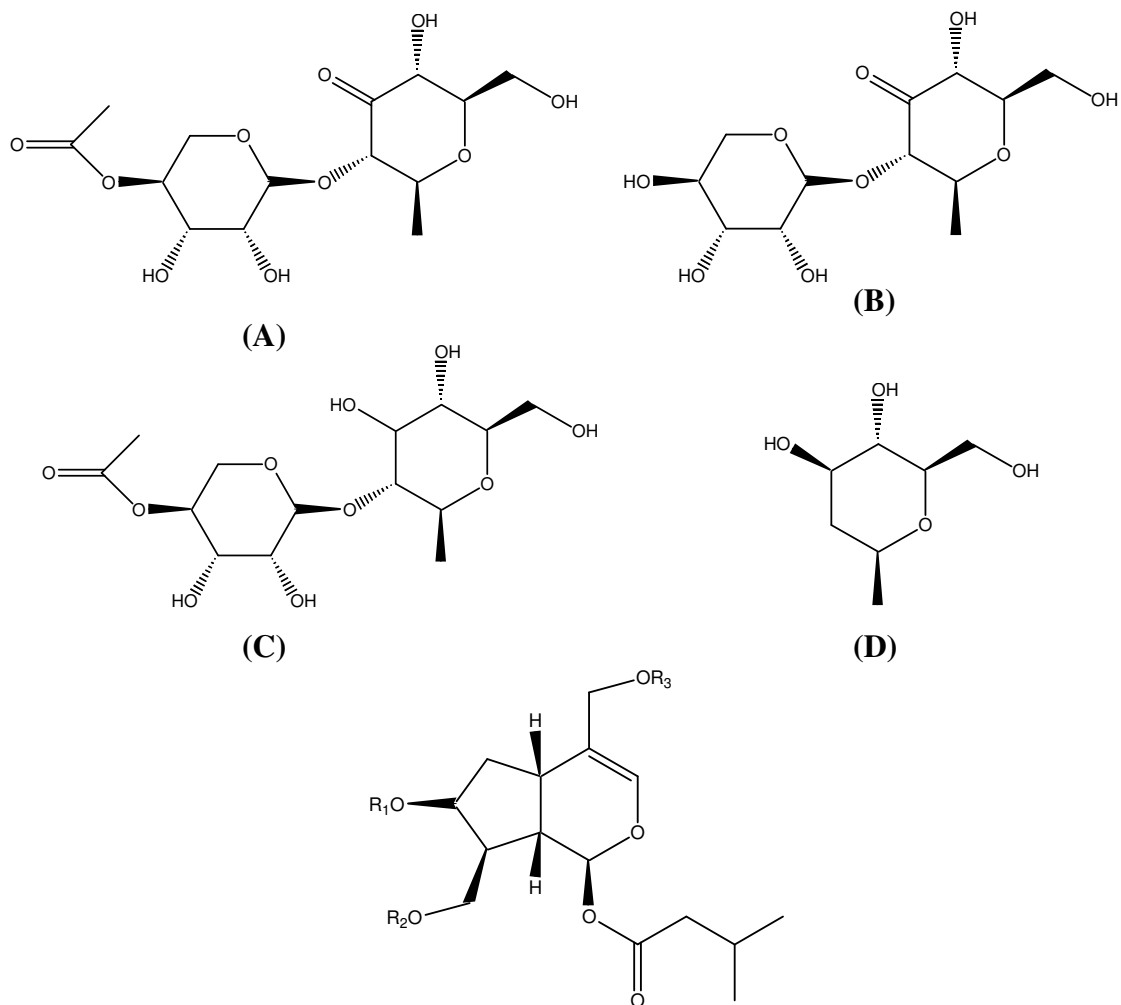


Table 23: Valerian type iridoid glycosides from *Sambucus* genus

Compound	R ₁	R ₂	R ₃	Species	Reference
10- <i>O</i> -acetylpatrinin aglycone-11- <i>O</i> -[4''- <i>O</i> -acetyl- α -L-rhamnopyranosyl-(1-2)- β -D-ribohexo-3-ulopyranoside]	H	Ac	A	<i>ebulus</i> (leaves)	(120)
7- <i>O</i> -acetylpatrinin aglycone-11- <i>O</i> -[4''- <i>O</i> -acetyl- α -L-rhamnopyranosyl-(1-2)- β -D-ribohexo-3-ulopyranoside]	Ac	H	A	<i>ebulus</i> (leaves)	(120)
10- <i>O</i> -acetylpatrinin aglycone-11- <i>O</i> -[α -L-rhamnopyranosyl-(1-2)- β -D-ribohexo-3-ulopyranoside]	H	Ac	B	<i>ebulus</i> (leaves)	(120)
Patrinin aglycone-11- <i>O</i> -[4''- <i>O</i> -acetyl- α -L-rhamnopyranosyl-(1-2)- β -D-ribohexo-3-ulopyranoside]	H	H	A	<i>ebulus</i> (leaves)	(120)
10- <i>O</i> -acetylpatrinin aglycone-11- <i>O</i> -[4''- <i>O</i> -acetyl- α -L-rhamnopyranosyl-(1-2)- β -D-glucopyranoside]	H	Ac	C	<i>ebulus</i> (leaves)	(120)
Patrinin aglycone-11- <i>O</i> -2'-deoxy- β -D-glucopyranoside	H	H	D	<i>ebulus</i> (leaves)	(120)

Ac: Acetyl

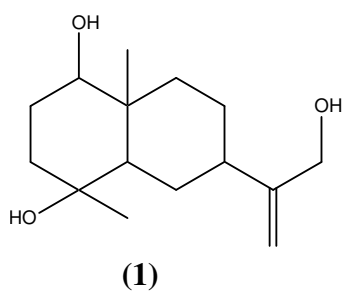


Table 24: Sesquiterpenes from *Sambucus* genus

Compounds	Species	Reference
1,4,13-Trihydroxy-eudesm-11(12)-ene (1)	<i>Williamsii</i> (stems)	(121)

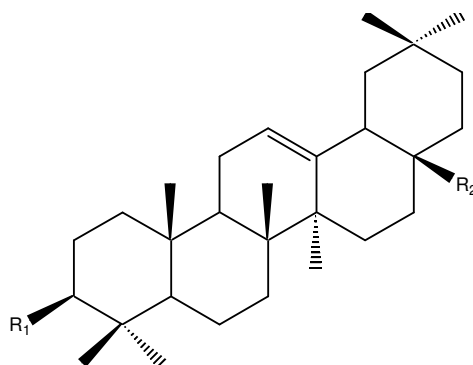


Table 25: Triterpenoids from *Sambucus* genus

Compounds	R ₁	R ₂	Species	Reference
α -amyrol acetate	CH ₃ COO	CH ₃	<i>adnata</i> (whole plant)	(105)
α -amyrin	H	CH ₃	<i>adnata</i> (whole plant)	(105)
			<i>williamsii</i> (?)	(122)
			<i>nigra</i> (barks)	(123)
Oleanolic acid	OH	COOH	<i>nigra</i> (barks)	(123)

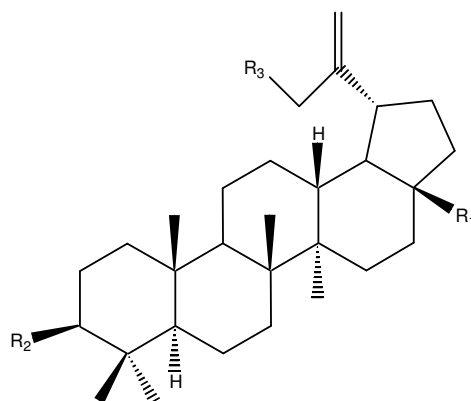
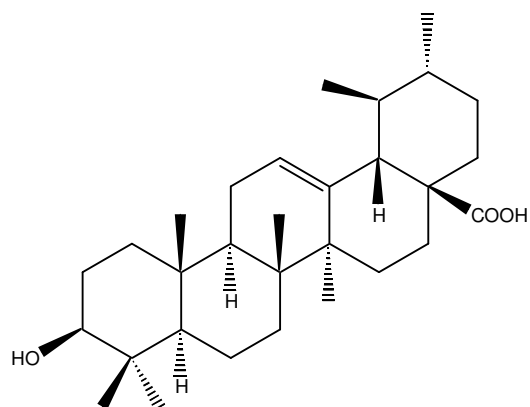
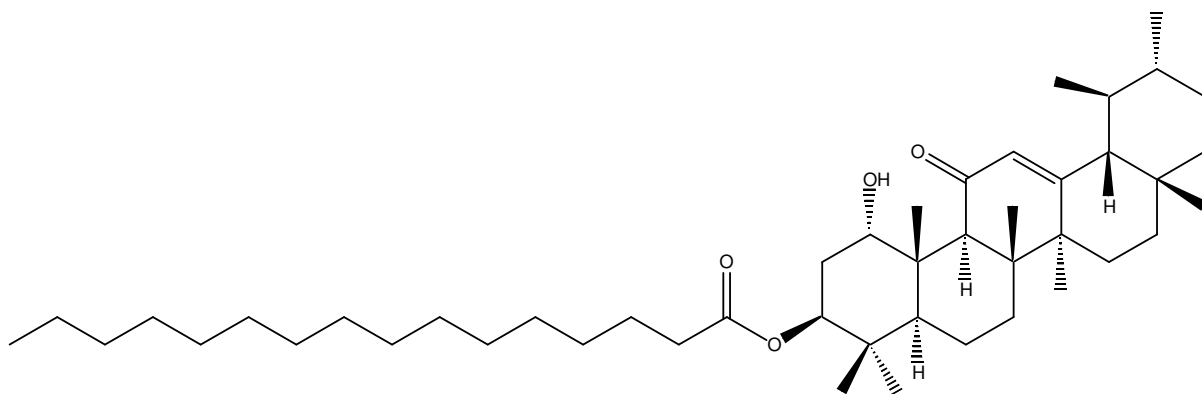


Table 26: Triterpenoids from *Sambucus* genus

Compounds	R ₁	R ₂	R ₃	Species	Reference
Betulinic acid	COOH	OH	H	<i>adnata</i> (whole plant)	(105)
3,28,29-trihydroxylupan	CH ₂ OH	OH	OH	<i>adnata</i> (whole plant)	(105)
Lupeol 3-acetate	CH ₃	CH ₃ COO	H	<i>adnata</i> (whole plant)	(106)
Lupeol-3-palmitate	CH ₃	CH ₃ COO	H	<i>williamsi</i> (?)	(122)
Betulin	CH ₂ OH	OH	H	<i>nigra</i> (barks)	(123)



(1)



(2)

Table 27: Triterpenoids from *Sambucus* genus

Compounds	Species	Reference
Ursolic acid (1)	<i>ebulus</i> (leaves)	(20)
	<i>adnata</i> (whole plant)	(106)
	<i>australis</i> (aerial parts)	(124)
	<i>williamsii</i> (?)	(122)
Sambucilate (2)	<i>adnata</i> (whole plant)	(106)

2.3.1.3. Steroidal Compounds

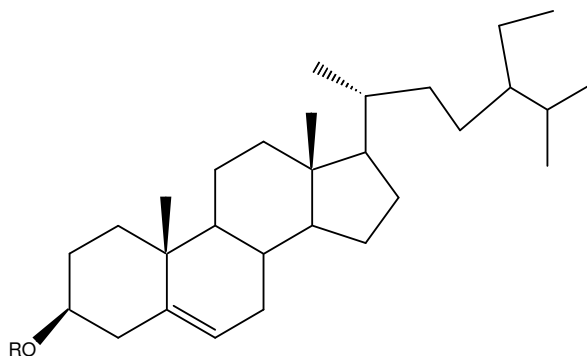


Table 28: Phytosterols from *Sambucus* genus

Compounds	R	Species	Reference
β -sitosterol	H	<i>adnata</i> (whole plant)	(106)
		<i>nigra</i> (barks)	(123)
		<i>williamsii</i> (?)	(122)
β -sitosterol-3- <i>O</i> - β -D-glucopyranoside	Glc	<i>williamsii</i> (?)	(122)

Glc: β -Glucose

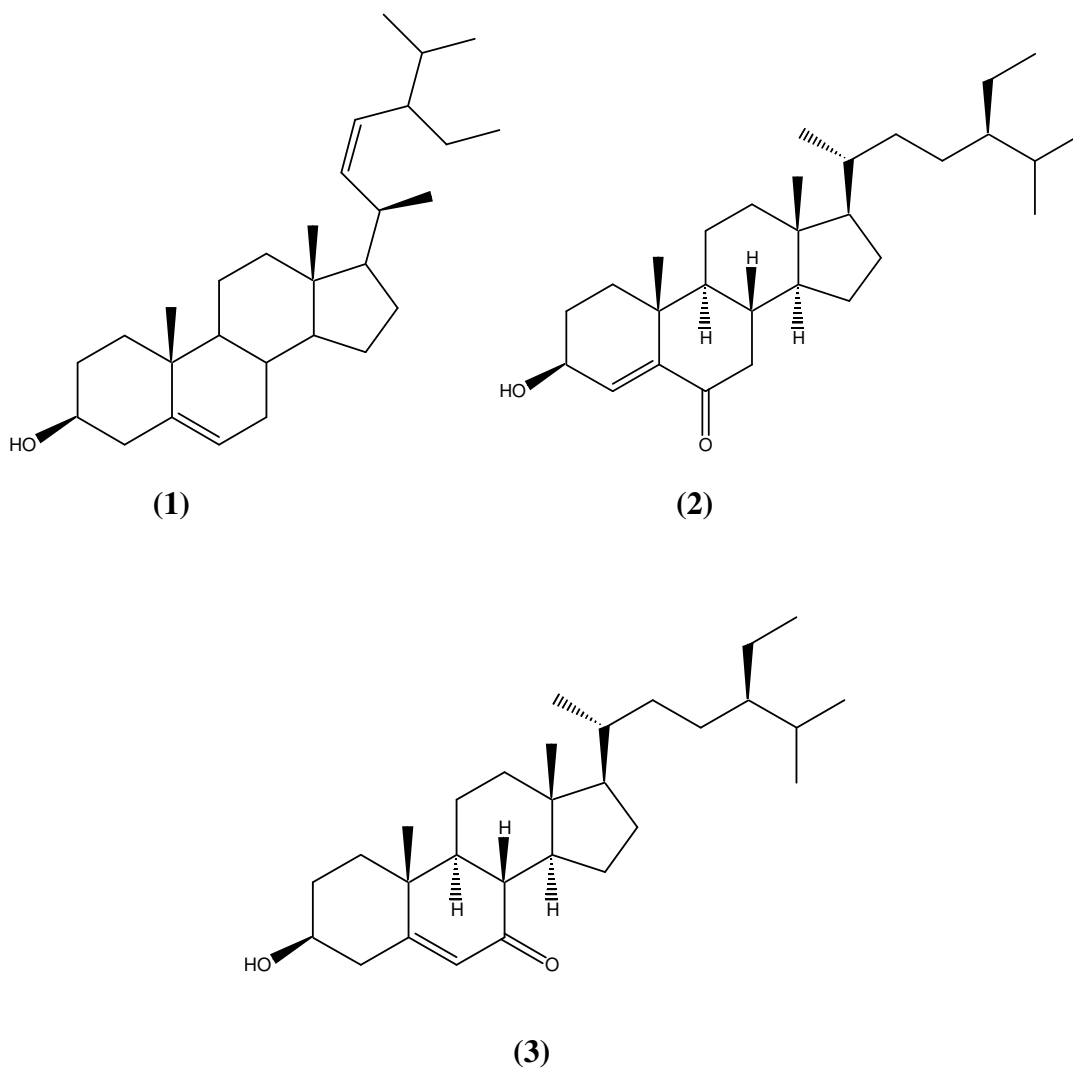
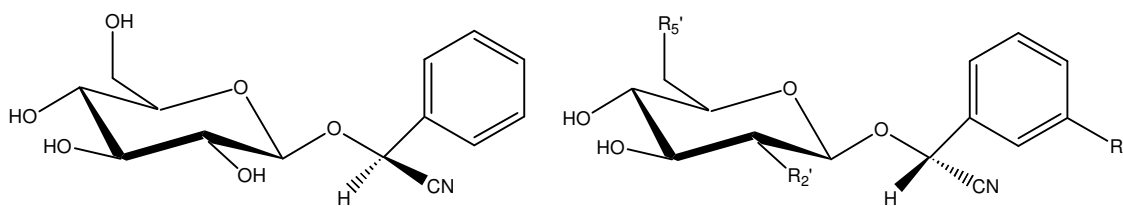


Table 29: Phytosterols from *Sambucus* genus

Compounds	Species	Reference
Stigmasterol (1)	<i>adnata</i> (whole plant)	(105, 106)
Stigmast-4-en-3 β -ol-6-one (2)	<i>adnata</i> (whole plant)	(105, 106)
7-keto-sitosterol (3)	<i>adnata</i> (whole plant)	(105, 106)



(1)

Table 30: Cyanogenins and cyanohydrines from *Sambucus* genus

Compounds	R	R ₂ '	R ₅ '	Species	Reference
Sambunigrin (1)				<i>nigra</i> (leaves)	(103)
Prunasin	H	H	H	<i>nigra</i> (leaves)	(103)
Holocalin	OH	H	H	<i>nigra</i> (leaves)	(103)
6-acetyl holocalin	OH	Ac	H	<i>nigra</i> (leaves)	(103)
(2S)-[β-D-apiofuranosyl-(1-2)]-β-D-glucopyranosyl-mandelonitrile	H	Api	H	<i>nigra</i> (leaves)	(103)

Ac: Acetyl, Api: Apiose

2.3.1.4. Other Compounds

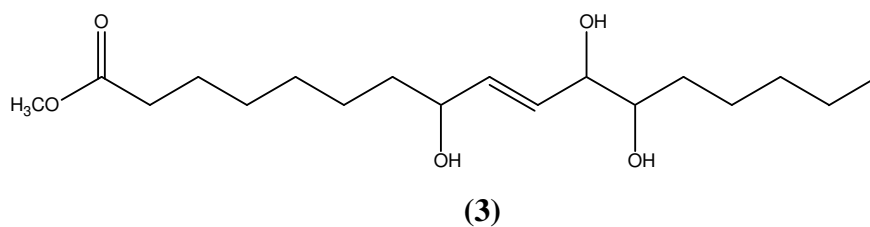
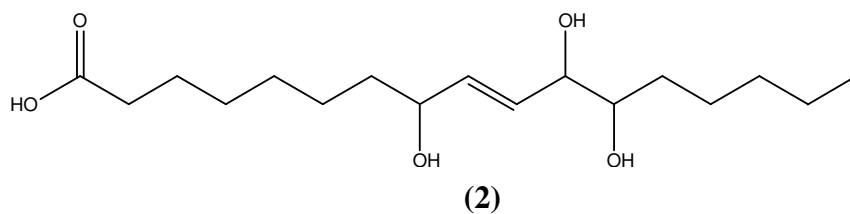
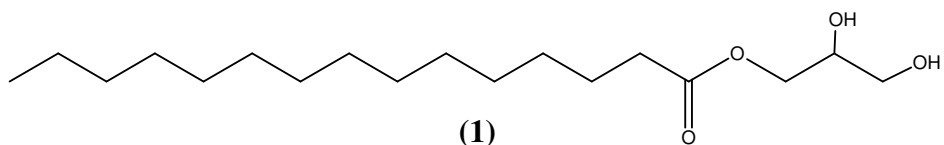


Table 31: Fatty acid and fatty acid esters from *Sambucus* genus

Compounds	Species	Reference
Glycerol monopalmitat (1)	<i>adnata</i> (whole plant)	(105)
Tianshic acid (2)	<i>williamsii</i> (stems)	(121)
(9E)-8,11,12-trihydroxyoctadecenoic acid methyl ester (3)	<i>williamsii</i> (stems)	(121)

2.3.2. Phytochemical Studies on *Cistus* species

A survey of literatures on the chemical constituents of *Cistus* species revealed that this genus is rich in diterpenoids, flavonoids and proanthocyanidins. Compounds identified in *Cistus* genus are classified according to their groups and laid out between **Tables 32-54**.

2.3.2.1. Phenolic Compounds

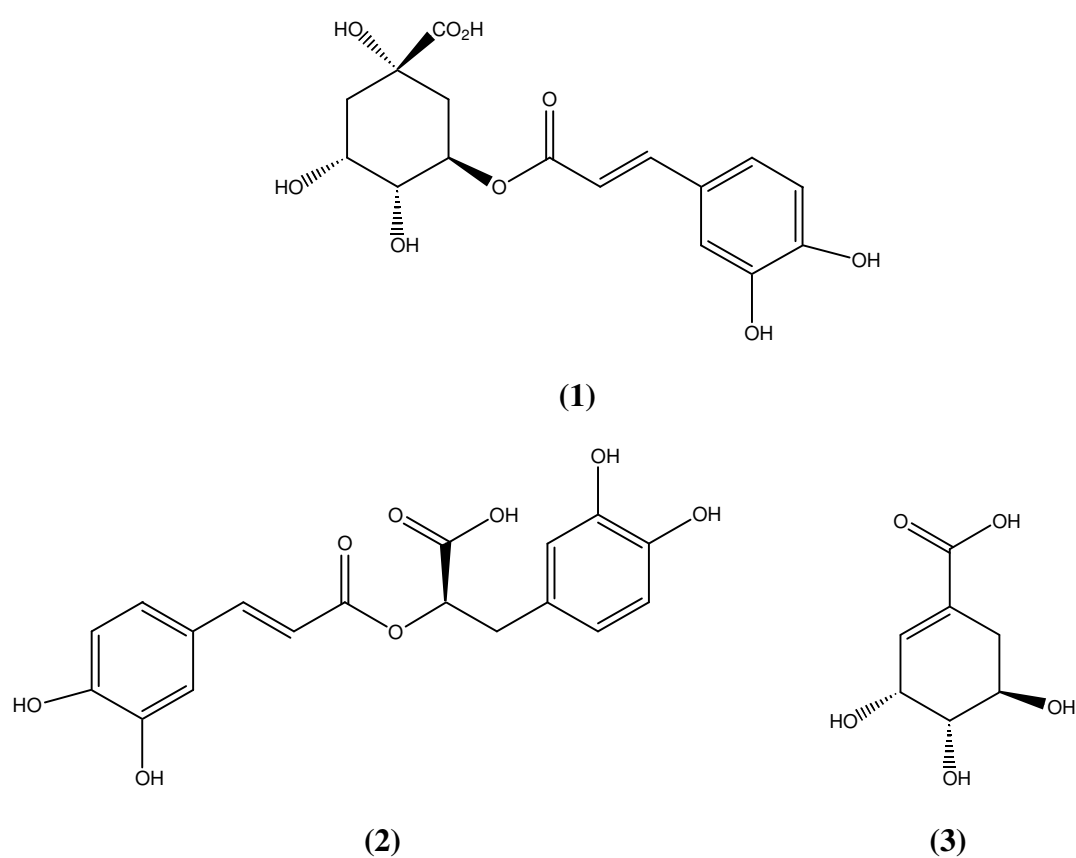
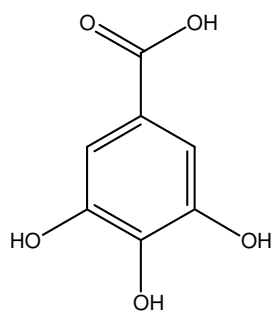
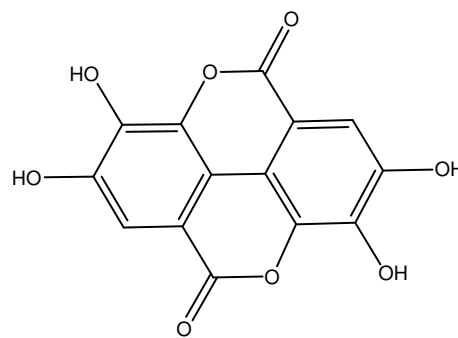


Table 32: Phenolic acids from *Cistus* genus

Compounds	Species	Reference
Chlorogenic acid (1)	<i>laurifolius</i> (leaves)	(100)
Rosmarinic acid (2)	<i>creticus</i> (?)	(125)
Shikimic acid (3)	<i>creticus</i> (aerial parts)	(126)



(1)



(2)

Table 33: Phenolic acids from *Cistus* genus

Compounds	Species	Reference
Gallic acid (1)	<i>creticus</i> (?)	(125)
	<i>laurifolius</i> (leaves)	(100)
Ellagic acid (2)	<i>creticus</i> (?)	(125)

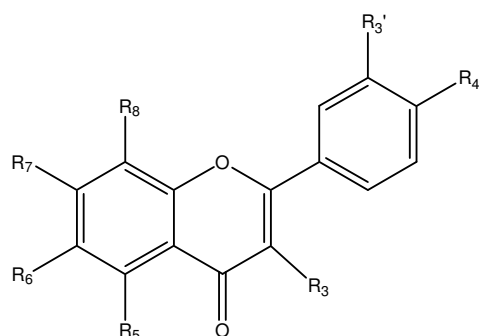


Table 34: Flavonoids from *Cistus* genus

Compounds	R ₃	R ₅	R ₆	R ₇	R ₈	R _{3'}	R _{4'}	Species	Reference
Apigenin	H	OH	H	OH	H	H	OH	<i>ladanifer</i> (leaves) <i>laurifolius</i> (leaves)	(127) (100)
Apigenin-4'-methyl ether	H	OH	H	OH	H	H	OCH ₃	<i>ladanifer</i> (leaves)	(127)
Apigenin-7-methyl ether	H	OH	H	OCH ₃	H	H	OH	<i>ladanifer</i> (leaves)	(127)
Apigenin-7,4'-dimethyl ether.	H	OH	H	OCH ₃	H	H	OCH ₃	<i>ladanifer</i> (leaves)	(127)
Kaempferol-3-methyl ether								<i>ladanifer</i> (leaves)	(127)
	OCH ₃	OH	H	OH	H	H	OH	<i>paliniae</i> (aerial)	(128)
Kaempferol-3,4'-dimethyl ether	OCH ₃	OH	H	OH	H	H	OH	<i>ladanifer</i> (leaves)	(127)
Kaempferol-3,7-dimethyl ether								<i>ladanifer</i> (leaves) <i>laurifolius</i> (leaves) <i>paliniae</i>	(127) (83, 96) (128)
	OCH ₃	OH	H	OCH ₃	H	H	OH		
Kaempferol-3,7,4'-trimethyl ether	OCH ₃	OH	H	OCH ₃	H	H	OCH ₃	<i>ladanifer</i> (leaves)	(127)
Quercetin	OH	OH	H	OH	H	OH	OH	<i>laurifolius</i> (leaves)	(100)
Quercetin-3-methyleter	OCH ₃	OH	H	OH	H	OH	OH	<i>laurifolius</i> (leaves)	(83, 96, 100)
Quercetin-3,7-dimethyleter	OCH ₃	OH	H	OCH ₃	H	OH	OH	<i>laurifolius</i> (leaves)	(83, 96)
Quercetin 5,3'-dimethyl ether	OH	OCH ₃	H	OH	H	OCH ₃	OH	<i>laurifolius</i> (leaves)	(129)
Quercetin 3,5,3'-trimethyl ether	OCH ₃	OCH ₃	H	OH	H	OCH ₃	OH	<i>laurifolius</i> (leave)	(129)
Quercetin-3-O-galactoside	OGal	OH	H	OH	H	OH	OH	<i>Creticus</i> (?)	(125)
Quercetin-3-O-glucoside	OGlc	OH	H	OH	H	OH	OH	<i>creticus</i> (?)	(125)
Quercetin-3-O- α -rhamnoside	ORha	OH	H	OH	H	OH	OH	<i>laurifolius</i> (leaves) <i>creticus</i> (?)	(100) (125)
Rutin	ORut	OH	H	OH	H	OH	OH	<i>creticus</i> (?)	(125)

Gal: Galactoside, Rha: Rhamnoside, Rut: Rutoside

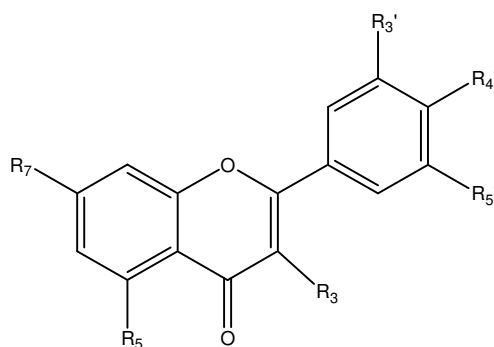


Table 35: Flavonoids from *Cistus* genus

Compounds	R ₃	R ₅	R ₇	R _{3'}	R _{4'}	R _{5'}	Species	Reference
Genkwanin (5,4'-dihydroxy-7-methoxyflavone)	H	OH	OCH ₃	H	OH	H	<i>palinhae</i> (aerial)	(128)
Myricetin-3- <i>O</i> -galactoside	OGal	OH	OH	OH	OH	OH	<i>creticus</i> (?)	(125)
Myricitrin	ORha	OH	OH	OH	OH	OH	<i>creticus</i> (?)	(125)

Gal: Galactose, Rha: Rhamnose

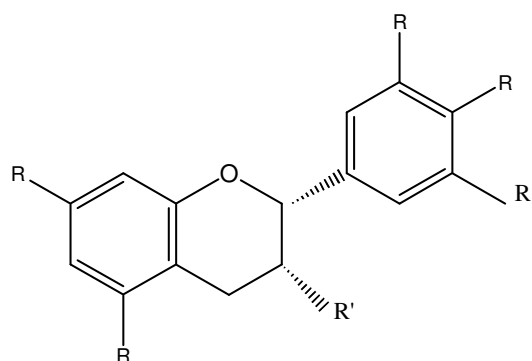


Table 36: Flavan-3-ols from *Cistus* genus

Compounds	R	R'	Species	Reference
Epigallocatechin	OH	OH	<i>creticus</i> (aerial parts) <i>salviifolius</i> (herbs)	(125, 126) (130)
Epigallocatechin 3- <i>O</i> -gallate	OH	OGalloyl	<i>salviifolius</i> (herbs)	(130)
3- <i>O</i> - <i>p</i> -hydroxybenzoyl ester of epigallocatechin	OH	<i>p</i> -(OH)- benzoyl	<i>salviifolius</i> (herbs)	(130)

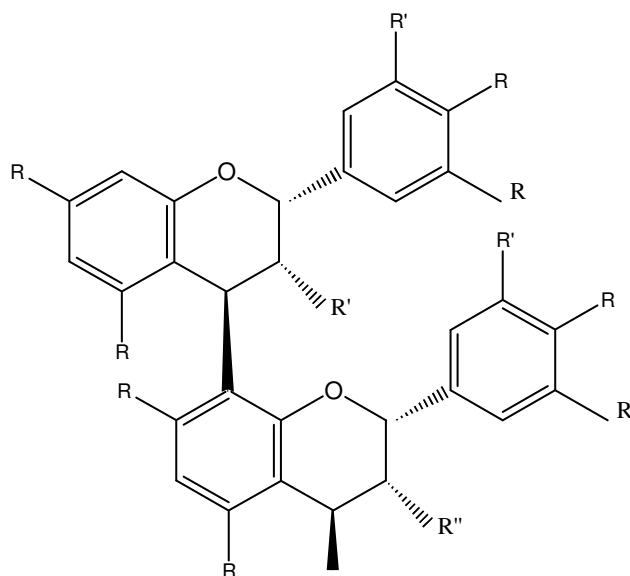


Table 37: Prodelphinidins from *Cistus* genus

Compounds	R	R'	R''	Species	Reference
Epigallocatechin-(4 β →8)-epigallocatechin	OH	OH	OH	<i>salviifolius</i> (herbs)	(130)
Epigallocatechin-3- <i>O</i> -gallate-(4 β →8)-epigallocatechin	OH	OGalloyl	OH	<i>salviifolius</i> (herbs)	(130)
Epigallo-catechin-(4 β →8)-epigallocatechin-3- <i>O</i> -gallate	OH	OH	OGalloyl	<i>salviifolius</i> (herbs)	(130)

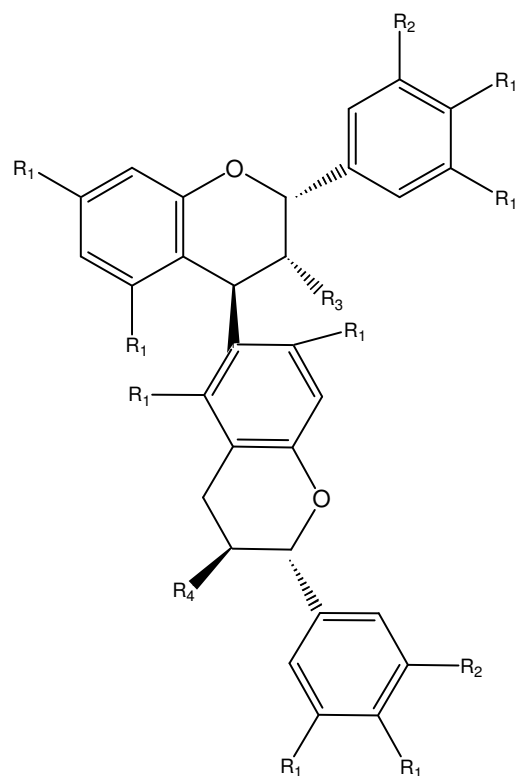


Table 38: Dimeric prodelphinidines from *Cistus* genus

Compounds	R ₁	R ₂	R ₃	R ₄	Species	Reference
Epicatechin-(4β→6)-catechin	OH	H	OH	OH	<i>creticus</i> (aerial parts)	(126)
Epigallocatechin-3- <i>O</i> -gallate-(4β→6)-gallocatechin	OH	OH	OGalloyl	OH	<i>creticus</i> (aerial parts)	(126)

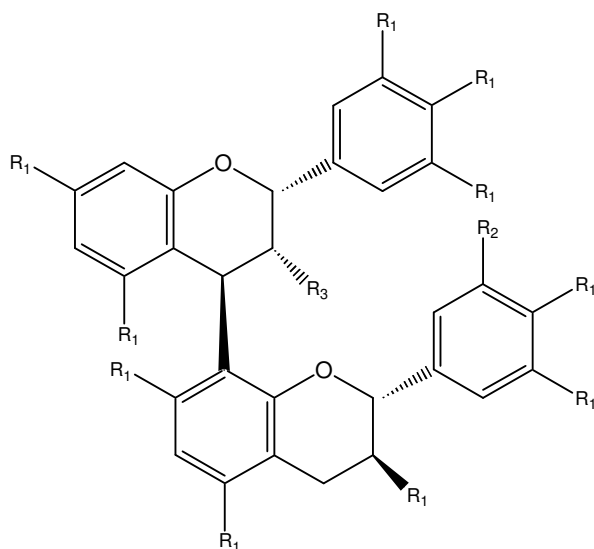


Table 39: Dimeric prodelphinidines from *Cistus* genus

Compounds	R ₁	R ₂	R ₃	Species	Reference
Epigallocatechin-(4β→8)-catechin	OH	H	OH	<i>creticus</i> (aerial parts)	(126)
Epigallocatechin-(4β→8)-gallocatechin	OH	OH	OH	<i>creticus</i> (aerial parts)	(126)
Epigallocatechin-3- <i>O</i> -gallate-(4β→8)-gallocatechin	OH	OH	OGalloyl	<i>creticus</i> (aerial parts)	(126)

2.3.2.2. Terpenic Compounds

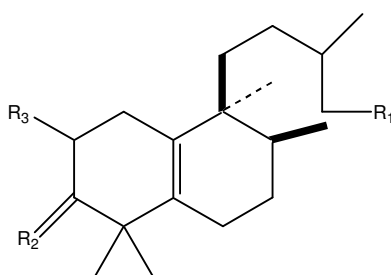


Table 40: Labdane type diterpenes from *Cistus* genus

Compounds	R ₁	R ₂	R ₃	Species	Reference
Salmantic acid	COOH	O	H, H	<i>laurifolius</i> (aerial)	(131)
Salmantidiol	CH ₂ OH	HαOH	H, H	<i>laurifolius</i> (aerial)	(131)

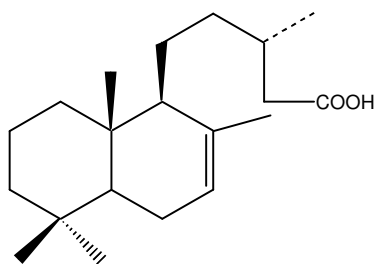


Table 41: Labdane type diterpenes from *Cistus* genus

Compounds	Species	Reference
Caticic acid	<i>palinhae</i> (aerial)	(128)
	<i>symphytifolius</i> (aerial)	(132)

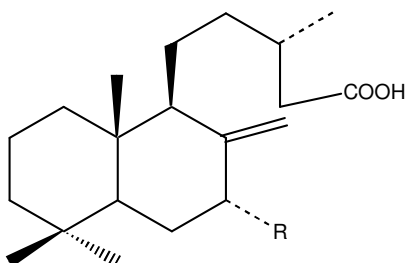


Table 42: Labdane type diterpenes from *Cistus* genus

Compounds	R	Species	Reference
Labdenic acid	H	<i>symphytifolius</i> (aerial)	(132)
		<i>palinhae</i> (aerial)	(128)
Cistenolic acid	OH	<i>symphytifolius</i> (aerial)	(132)

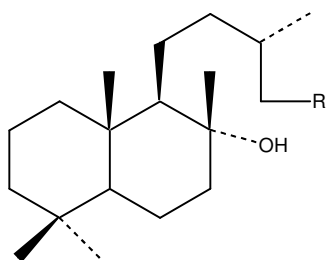


Table 43: Labdane type diterpenes from *Cistus* genus

Compounds	R	Species	Reference
Labdanolic acid	COOH	<i>symphytifolius</i> (aerial)	(132)
		<i>palinhae</i> (aerial)	(128)
		<i>ladaniferus</i>	(133)
Labdan-8 α ,15-diol	CH ₂ OH	<i>symphytifolius</i> (aerial)	(132)

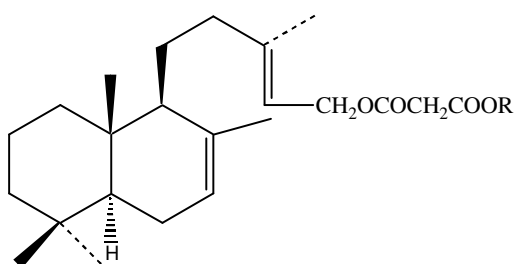
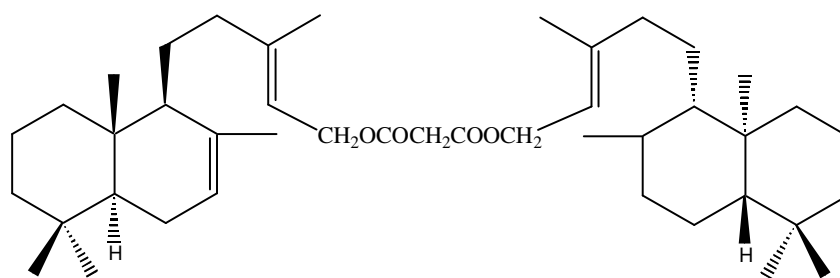
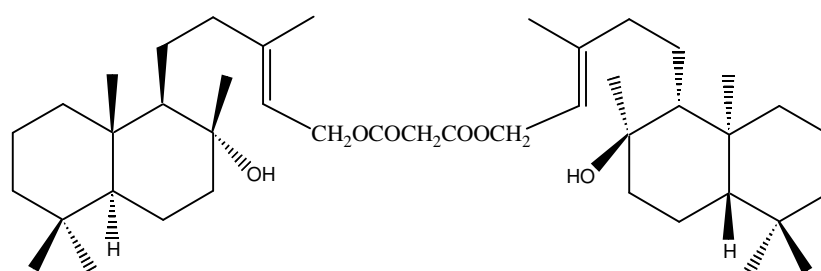


Table 44: Labdane type diterpenes from *Cistus* genus

Compounds	R	Species	Reference
(13 <i>E</i>)-labd-7,13-diene-15-yl malonic acid.	H	<i>creticus</i> (resin)	(134)
(13 <i>E</i>)-labd-7,13-diene-15-yl methyl malonic acid diester	CH ₃	<i>creticus</i> (resin)	(134)



(1)



(2)

Table 45: Labdane type diterpenes from *Cistus* genus

Compounds	Species	Reference
[(13 <i>E</i>)-labd-7,13-diene-15-yl] malonate (1)	<i>creticus</i> (resin)	(134)
Di-[(13 <i>E</i>)-labd-13-ene, 8a-ol-15yl] malonate (2)	<i>creticus</i> (resin)	(134)

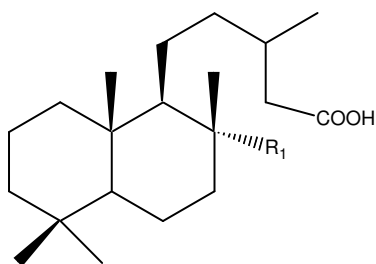
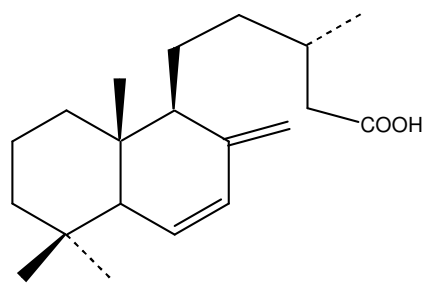
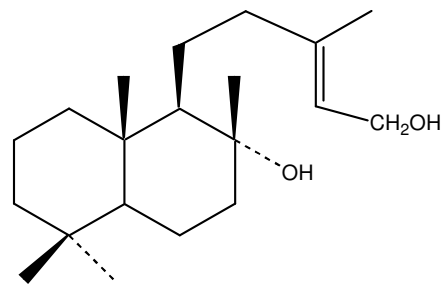


Table 46: Labdane type diterpenes from *Cistus* genus

Compounds	R ₁	Species	Reference
8α-methoxy-labda-15-oic acid	OCH ₃	<i>ladaniferus</i> (aerial)	(133)
		<i>palinhae</i> (aerial)	(128)
Labdanolic acid	OH	<i>ladaniferus</i> (aerial)	(133)
		<i>palinhae</i> (aerial)	(128)



(1)



(2)

Table 47: Labdane type diterpenes from *Cistus* genus

Compounds	Species	Reference
Cistadienic acid (1)	<i>symphytifolius</i> (aerial)	(132)
Labd-13(<i>E</i>)-ene-8 α ,15-diol (2)	<i>symphytifolius</i> (aerial)	(132)

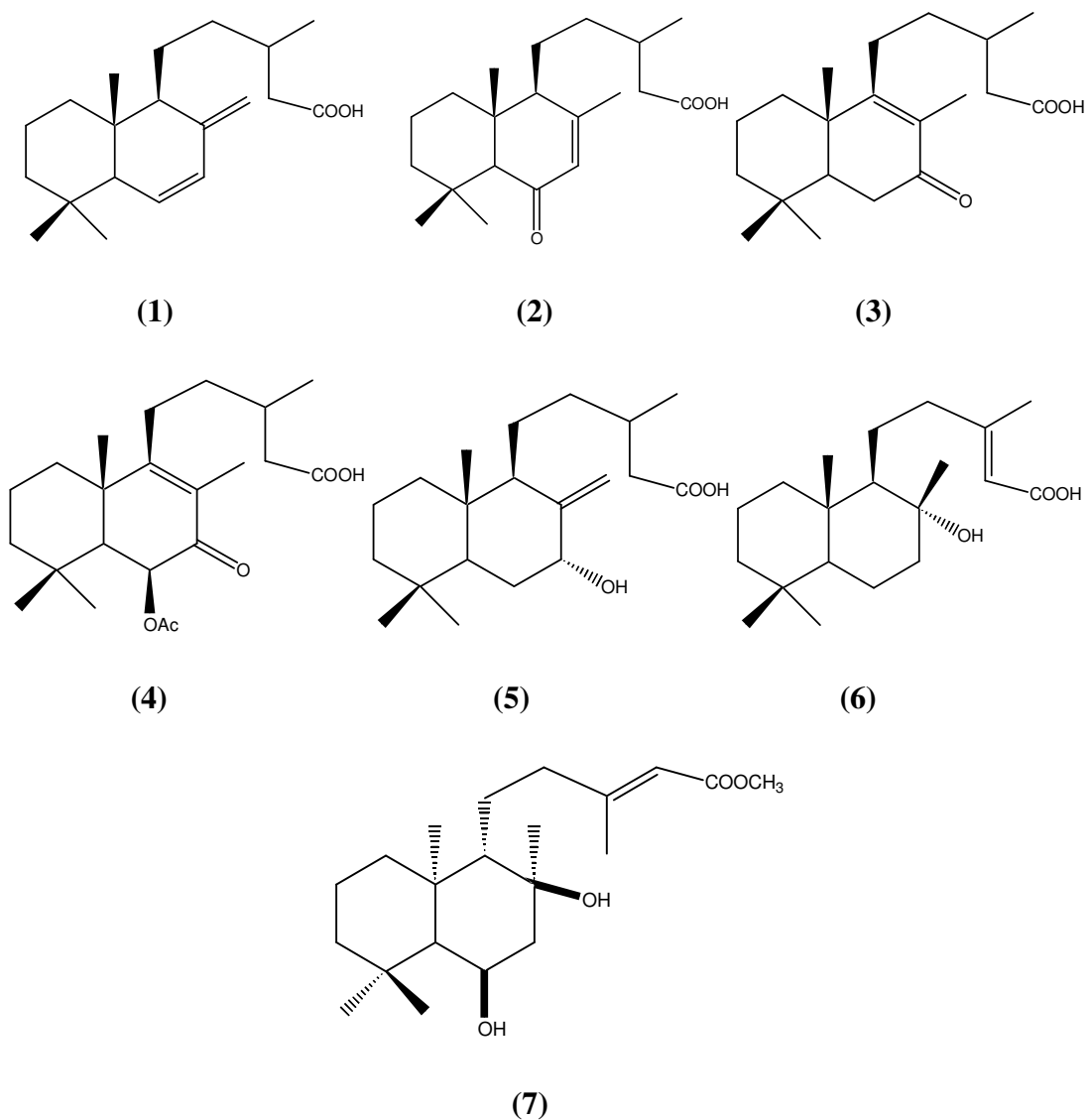


Table 48: Labdane type diterpenes from *Cistus* genus

Compounds	Species	Reference
6,8(17) labdadien-15-oic acid (1)	<i>ladaniferus</i> (aerial)	(133)
6-oxocaticic acid (2)	<i>ladaniferus</i> (aerial)	(133)
7-oxo-8-labden-15-oic acid (3)	<i>ladaniferus</i> (aerial)	(133)
6 β -acetoxy-7-oxo-8-labden-15-oic acid (4)	<i>ladaniferus</i> (aerial)	(133)
7 α -hydroxy-8(17)-labden-15-oic acid (5)	<i>ladaniferus</i> (aerial)	(133)
8 α -hydroxy-13(E)-labden-15-oic acid (6)	<i>ladaniferus</i> (aerial) <i>palinhae</i> (aerial)	(133) (128)
6 β ,8-dihydroxy-ent-13E-labden-15-oic acid (Laurifolic acid) (7)	<i>laurifolius</i> (aerial)	(135)

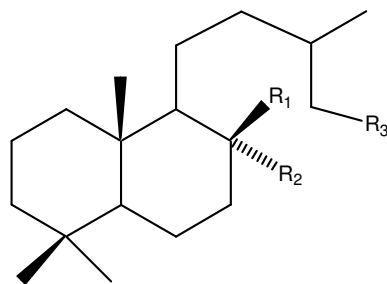


Table 49: Labdane type diterpenes from *Cistus* genus

Compounds	R ₁	R ₂	R ₃	Species	Reference
8,15-labdane-1,10-diol	CH ₃	OH	CH ₂ OH	<i>palinhae</i> (aerial)	(128)
8 α -hydroxy-15-acetoxy-labdane	CH ₃	OH	CH ₂ OAc	<i>palinhae</i> (aerial)	(128)
8- <i>epi</i> -15-labdane-1,10-diol	OH	CH ₃	CH ₂ OH	<i>palinhae</i> (aerial)	(128)
8 α -hydroxy-15-phenylpropionyloxy-labdane	CH ₃	OH	CH ₂ OCO(CH ₂) ₂ C ₆ H ₅	<i>palinhae</i> (aerial)	(128)

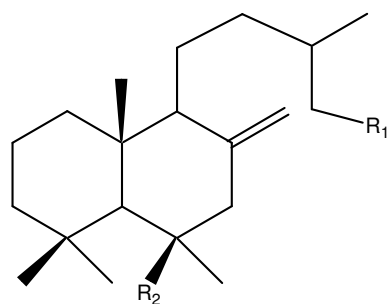
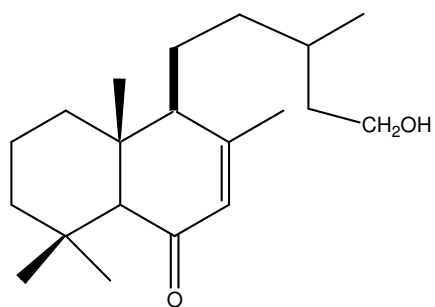
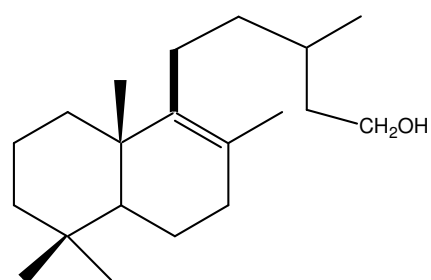


Table 50: Labdane type diterpenes from *Cistus* genus

Compounds	R ₁	R ₂	Species	Reference
8(17)labden-15-ol	CH ₂ OH	OH	<i>palinhae</i> (aerial)	(128)
6 β -hydroxy-8(17)-labden-15-ol	CH ₂ OH	H	<i>palinhae</i> (aerial)	(128)



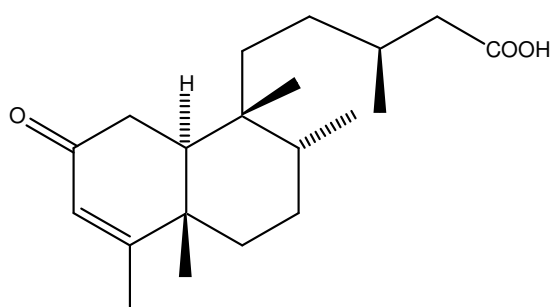
(1)



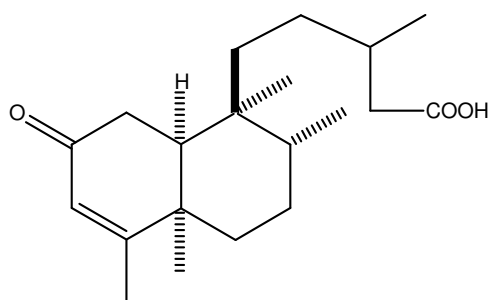
(2)

Table 51: Labdane type diterpenes from *Cistus* genus

Compounds	Species	Reference
6-oxo-7-labden-15-ol (1)	<i>palinhae</i> (aerial)	(128)
8-labden-15-ol (2)	<i>palinhae</i> (aerial)	(128)



(1)



(2)

Table 52: Clerodane type diterpenes from *Cistus* genus

Compounds	Species	Reference
2 α ,3 β -dihydroxy-4(18)- <i>neo</i> -cleroden-15-oate	<i>populifolius</i>	(136)
(5S,8R,9R,10S,13S)-2-oxo-3-cleroden-15-oic (1)	<i>palinhae</i> (aerial)	(137)
(5R, 8R, 9S, 10S)-2-oxo-3- <i>cis</i> -cleroden-15-oic (2)	<i>palinhae</i> (aerial)	(128)

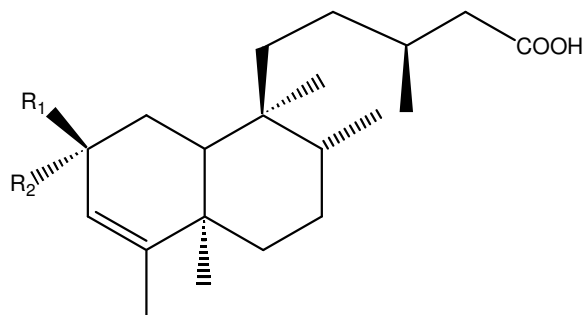
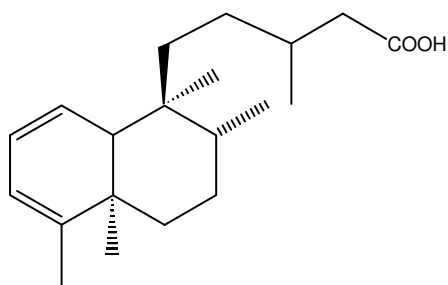


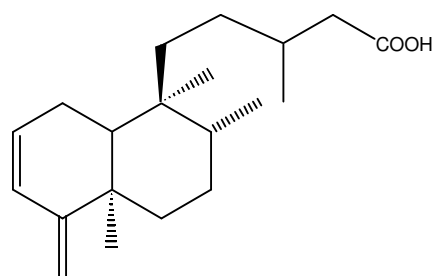
Table 53: Neo-clerodane type diterpenes from *Cistus* genus

Compounds	R ₁	R ₂	Species	Reference
3-neo-cleroden-15-oic acid	H	H	<i>populifolius</i>	(136)
2 α -methoxy-3-neo-cleroden-15-oic acid	H	OCH ₃	<i>populifolius</i>	(136)
2 α -acetoxy-3-neo-cleroden-oic acid	H	OAc	<i>populifolius</i>	(136)
2 α -hydroxy-3-neo-cleroden-15-oic acid	H	OH	<i>populifolius</i>	(136)

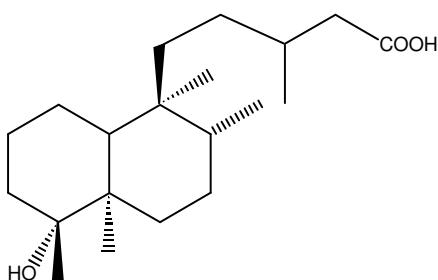
Ac: Acetyl



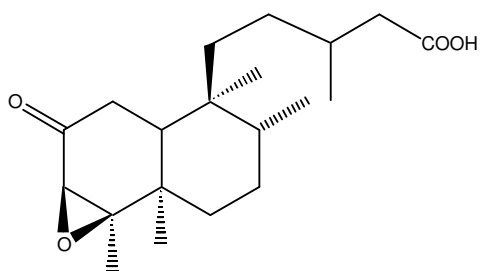
(1)



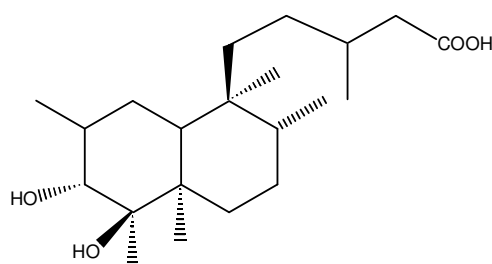
(2)



(3)



(4)



(5)

Table 54: Neo-clerodane type diterpenes from *Cistus* genus

Compounds	Species	Reference
1, 3-neo-clerodadien-oic acid (1)	<i>populifolius</i>	(136)
2, 4(18)-neo-clerodadien-15-oic acid (2)	<i>populifolius</i>	(136)
2β-hydroxy-3-neo-cleroden-15-oic acid (3)	<i>populifolius</i>	(136)
2α-hydroxy-3-neo-cleroden-15-oic acid (4)	<i>populifolius</i>	(136)
3α, 4β-dihydroxy-neo-clerodan-15-oic acid (5)	<i>populifolius</i>	(136)

2.3.2.3. Essential Oils

Table 55: Compositions of essential oils obtained from *Cistus* genus

Plant name/Part	Method	yield of essential oil (%)	Major componenets of the essential oil	Reference
<i>C. albidus</i> / leaves	Steam distillation	0.13% ±0.06	α-zingiberen δ-cadinene α-cucurmene β-caryophyllen α-humulen	(138)
<i>C. monspeliensis</i> / leaves	Steam distillation	0.0178±0.007	α-bisabolol α-cadinol β-caryophyllen Spathulenol 3-nonen-2-one	(139)
<i>C.ladanifer</i> / aerial parts	Steam distillation	0.34	trans-pinocarveol bornyl acetate terpinen-4-ol Viridiflorol ledol α-pinene	(140)
<i>C. laurifolius</i> / leaves	Steam distillation	0.1	Borneol Nanocosane	(141)
<i>C. parvifolius</i> /leaves	Steam distillation	0.2	α-13-oxy-14-ene-epilabdane manoyl oxide δ-cadinene	(142)

2.4. General Information on Inflammation and Related Inflammatory Parameters

2.4.1. Inflammation

Inflammation is the host defence response against inflammatory stimuli. Various factors may lead to inflammation such as traumatic, infectious, post-ischaemic, toxic or autoimmune injury. Inflammation is the cumulative result of genetic factors and multiple physiological responses. Although inflammatory responses may differ in various inflammatory diseases, they can be characterised by a common spectrum of endogenous mediators such as growth factors, prostaglandins, chemokines, matrix metalloproteinases, inflammatory cytokines such as interleukins IL-1, IL-6, IL-8, tumour necrosis factor (TNF α), and toxic molecules such as nitric oxide and free radicals (1, 2).

In response to an inflammatory stimuli, immune cells such as macrophages, dendritic cells, and mast cells are activated and release inflammatory mediators which generates the clinical signs of inflammation; redness, elevated heat, swelling, pain and loss of function. During inflammation, vasodilatation occurs and blood flow increases to the inflammatory site to transport high amount of immune cells to the sites. Some mediators increase the sensitivity to pain while some mediators alter blood vessels to allow leukocyte migration from blood vessels to tissue (143, 144).

Acute inflammation is characterised initially by mostly neutrophilic leukocyte infiltration, after 24 to 48 hours monocytic cells predominate. In contrast, chronic inflammation is characterized by the presence of mononuclear cells, such as macrophages and lymphocytes (3). Acute inflammation is mediated by eicosanoids and vasoactive amines. These mediators initiate the early response of the immune system against inflammatory stimuli by increasing the movement of plasma and leukocytes into inflammatory site. Various cytokines and growth factors are released in chronic inflammation and immune cells such as leukocytes, lymphocytes and fibroblasts are recruited (3).

Although acute inflammation is a beneficial host response against various inflammatory stimuli, chronic inflammation is persistent and can lead to tissue damage. Chronic inflammation lies in the etiology of many diseases such as rheumatoid arthritis,

chronic inflammatory bowel diseases, neurodegenerative disorders, septic shock syndrome, heart attacks, Alzheimer's disease, and cancers (4, 145) .

2.4.2. Cytokines

Cytokines are regulators of host responses to infection, immune responses, inflammation, and trauma. They are produced by every kind of cell but mainly by macrophages and T-cells. Cytokines are classified into two groups depending on their ability to induce or reduce inflammation: proinflammatory cytokines and anti-inflammatory cytokines. Interleukin (IL)-1's and tumor necrosis factor (TNF) are proinflammatory cytokines, they produce fever, inflammation, tissue destruction, and, in some cases, shock and death as well as inducing the transcription of proinflammatory genes and endothelial adhesion molecules. IL-4, IL-10, and IL-13 are potent anti-inflammatory cytokines which suppress the genes for proinflammatory cytokines such as IL-1, TNF α , and the chemokines (146, 147).

TNF α (cachectin) involves in inflammation, immune system development and apoptosis (148-150). TNF α is also involved in a number of pathological conditions including asthma, Crohn's disease, rheumatoid arthritis, neuropathic pain, autoimmunity, and cancers (150-154). Monoclonal antibodies against TNF have been shown to be clinically active against Crohn's disease (155).

IL-1 α and IL-1 β are cytokines that participate in the regulation of immune responses, inflammatory reactions, and hematopoiesis. They induce acute phase protein synthesis, prostaglandin and collagenase synthesis by fibroblasts and chondrocytes, induces the transcription of COX-2 and seems to have little effect on the increased production of COX-1, induce gene expression for type II phospholipase A₂ and induces pyrogenicity (147, 156).

IL-6 mediates the acute phase responses but when its activity as a proinflammatory cytokine persists, acute inflammation turns into chronic inflammation that includes immune responses. In chronic inflammation, IL-6 provides mononuclear cell accumulation at the site of injury, through continuous MCP-1 secretion, angioproliferation and antiapoptotic functions on T cells. It is important as a marker of

the transition from acute to chronic inflammation by signaling a change from neutrophils to macrophages. Macrophages are the main source of proinflammatory cytokines. Levels of circulating IL-6 are elevated in several inflammatory diseases including rheumatoid arthritis, systemic juvenile idiopathic arthritis, systemic lupus erythematosus, ankylosing spondylitis, psoriasis and Crohn's disease. (3).

It has been shown that levels of $\text{TNF}\alpha$, $\text{IL-1}\beta$ and IL-6 are significantly high in joint lesions of rheumatoid arthritis patients (157). Neurodegenerative diseases such as Alzheimer's disease are initiated by the expression of cytokines or inflammatory mediators such as prostanooids and nitric oxide. Recent studies indicate that inhibition of $\text{IL-1}\beta$ and $\text{TNF}\alpha$ leads to a decrease in neuronal damage (158, 159).

IL-2 promotes the proliferation and differentiation of T cells. IL-2 has been used clinically to enhance T cell immunity in patients with AIDS or cancer, and inhibit T cell responses against transplanted tissues. This cytokine offers new hope for the rational control of T cell responses in patients with malignant and infectious diseases (8, 160).

2.4.3. Nitric oxide and iNOS enzyme

Nitric oxide (NO) is an important intracellular and intercellular signalling molecule and is produced by many types of cells to contribute physiological and pathological function of many organs. In neuronal system it serves as a biological mediator like neurotransmitters while it regulates blood vessel tone in vascular system, and it is an important defense molecule for immune cells. NO is synthesized by nitric oxide synthases (NOS), thus there are three isoforms neuronal NOS (nNOS or NOSI), inducible NOS (iNOS or NOSII) and endothelial NOS (eNOS or NOSIII) and there is also some evidence of a different NOS enzyme; mitochondrial NOS (mtNOS). This family of enzymes catalyzes the nicotinamide adenine dinucleotide phosphate hydrogen (NADPH)-dependent oxidation of L-arginine, to produce NO and L-citrulline. nNOS and eNOS are constitutively expressed in neuronal and endothelial cells, iNOS is not constitutively present, it can be rapidly induced by inflammatory stimuli, bacterial lipopolysaccharide (LPS) and cytokines (161). The half life of NO in biological fluids is

very short and it is rapidly oxidized to nitrite and nitrate. NO production can be measured by its end products (162). Monocytes, macrophages, and neutrophils produce nitric oxide when immune system is activated. NO couples with superoxide (O_2^-) to form peroxynitrite ($ONOO^-$) which is extremely reactive, comparing with NO or O_2^- alone. NO has also been known as a chemically potential molecule causing DNA damage by nitration and oxidation (163).

The transcription of the iNOS gene shows different signalling pathways such as protein kinase C, tyrosine kinase, janus kinases, raf-1 protein kinase, mitogen activated protein kinases (MAP kinase), depending on the stimulator or cell type (164-167). The promoter region of the mouse iNOS gene contains several binding sites for transcription factors like NF- κ B as well as Jun/Fos heterodimers, some C/EBT, CREB and the STAT family of transcription factors (168-171). Transcription factors like NF- κ B and AP-1 (activating protein-1) mediate the expression of iNOS (172). Stimulators such as LPS, cytokines, interferon-gama (IFN γ), TNF α , facilitate the translocation of NF- κ B from cytosol to the nucleus and the induction of iNOS gene expression (166, 173, 174). The cytokines TNF α , IL-1 α and IL-1 β are endogen inducers of iNOS (174).

NO produced by iNOS contributes to the antimicrobial activity of macrophages. However, high concentrations of NO and its reactive derivatives, such as peroxynitrite and nitrogen dioxide, are found to play important roles in infammation and carcinogenesis (175). NO have also been defined as an important molecule in inflammation and sepsis. Inhibiton of NO production induced by iNOS may and provide a measure to assess the activity of drugs against inflammation (176).

2.4.4. PGE₂ and COX-2

Prostaglandins (PG's) are prostanoid fatty acid derivatives of arachidonic acid. Arachidonic acid which is produced from membrane phospholipids by phospholipases (**Figure 1**), metabolized by cyclooxygenases (COX-1 or COX-2) to form PGG₂ and PGH₂ which is then converted into PGE₂ by prostaglandin E synthetase (PGES) (177).

COX-1 constitutively presents in every cell and provides PGs that are required for homeostatic functions, including gastric cytoprotection and hemostasis. COX-2 is

induced in cells during inflammation and plays role in PG formation during inflammation. Selective COX-2 inhibition is important to have anti-inflammatory activity without the gastrointestinal side effects of traditional nonsteroidal anti-inflammatory drugs (178) .

COX-1-derived PGE₂ plays a protective role for gastric mucosa. PGE₂ production in the kidney is critical for normal renal function by modulating salt and water transport, and stimulating renin release. PGE₂ promotes either smooth muscle relaxation or contraction depending on the tissue. PGE₂ has also been shown to play a role in the maintenance of blood pressure (179). PGE₂ acts as a potent relaxant of vascular smooth muscle cells, increasing blood flow and therefore potentiating edema. PGE₂ also promotes inflammatory pain by sensitizing afferent nerve endings to the actions of bradykinin and histamine (180). COX-2 is induced by proinflammatory stimuli, including bacterial LPS, and produces proinflammatory prostaglandins at the inflammatory site (181). Besides its role in inflammation, COX-2 also plays important roles in the pathogenesis of diseases such as colon carcinoma, Alzheimer's disease, heart failure, and hypertension. Therefore, there is an increasing interest in research for new COX-2 inhibitors (182).

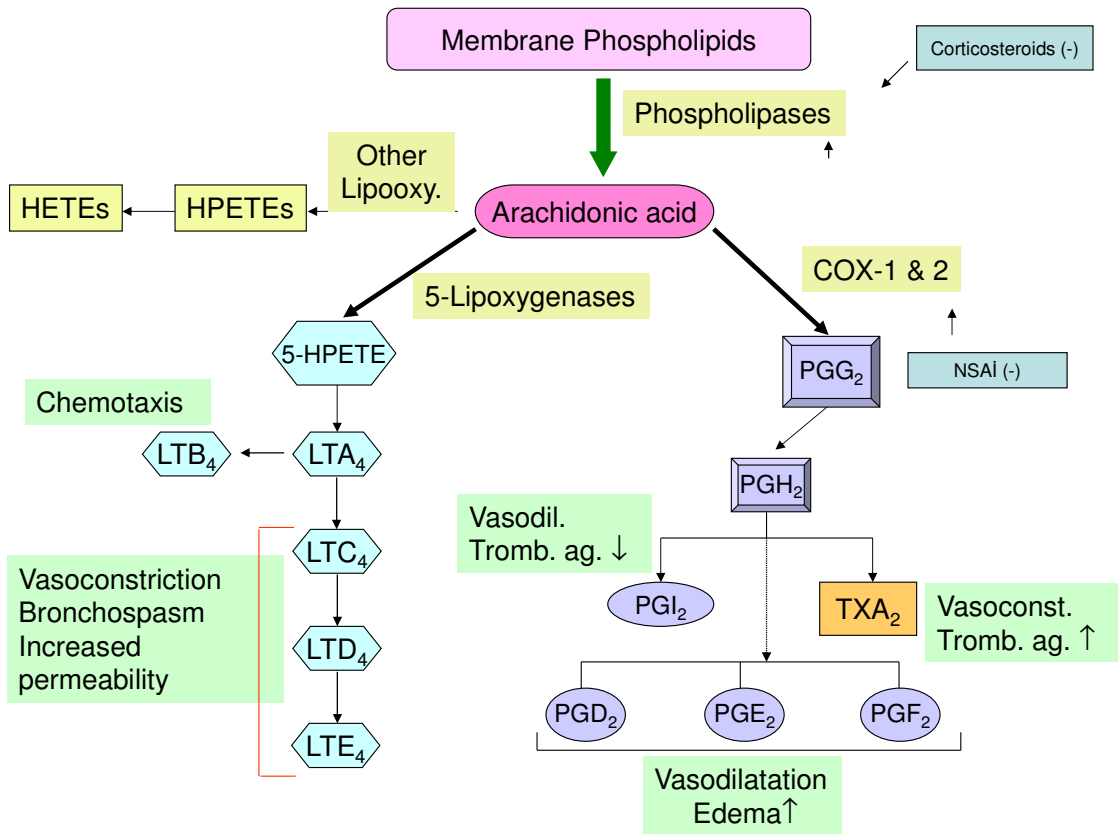


Figure 1: Phospholipase cascade

HETE: 5-Hydroxyeicosatetraenoic acid, **HPETE:** 5-hydroperoxyeicosatetraenoic acid, **LT:** Leukotriene
PG: Prostaglandin, **TX:** Tromboxane

2.4.5. NF- κ B Signalling

NF- κ B is a heterodimeric transcription factor composed of p50 and p65 (RelA), but a variety of other Rel-containing dimers are also known to exist. In unstimulated cells NF- κ B is located in cytosol in its inactive form where it is bound to the inhibitor protein I kappa B (I κ B). Two kinases responsible for phosphorylating I κ B's are IKK α and IKK β . I κ B proteins are rapidly phosphorylated on two critical amino-terminal serine residues (Ser³² and Ser³⁶ in I κ B α , Ser¹⁹ and Ser²³ in I κ B β) (183, 184). In response to the stimulation such as LPS, I κ Bs are rapidly ubiquitinated and degraded by 26S proteasome complex. The free NF- κ B dimers translocate to the nucleus, bind with high affinity to specific sites in the promoter regions of target genes and stimulate their transcription (**Figure 2**). Activation of TNF and Toll-like receptors results in activation of I κ B kinases which phosphorylate I κ B at two serine residues (Ser32 and 36) (185).

The NF- κ B family consists of five transcription factors that play key roles in inflammation. Besides its role in inflammation, NF- κ B plays an important role both in immune system and proliferation and survival of many types of animal cells. Members of this family are activated by various stimuli including growth factors, DNA damage, bacterial and viral infections and cytokines. This phosphorylation leads ubiquitination and degradation of I κ B by the proteasome and free NF- κ B translocates to nucleus (186)

The NF- κ B pathway is a therapeutic target in inflammatory diseases as NF- κ B plays an important role in the transcription of TNF α , IL-1 α , IL-2, IL-6, IL-8, acute phase proteins, COX-2, and iNOS (8, 9).

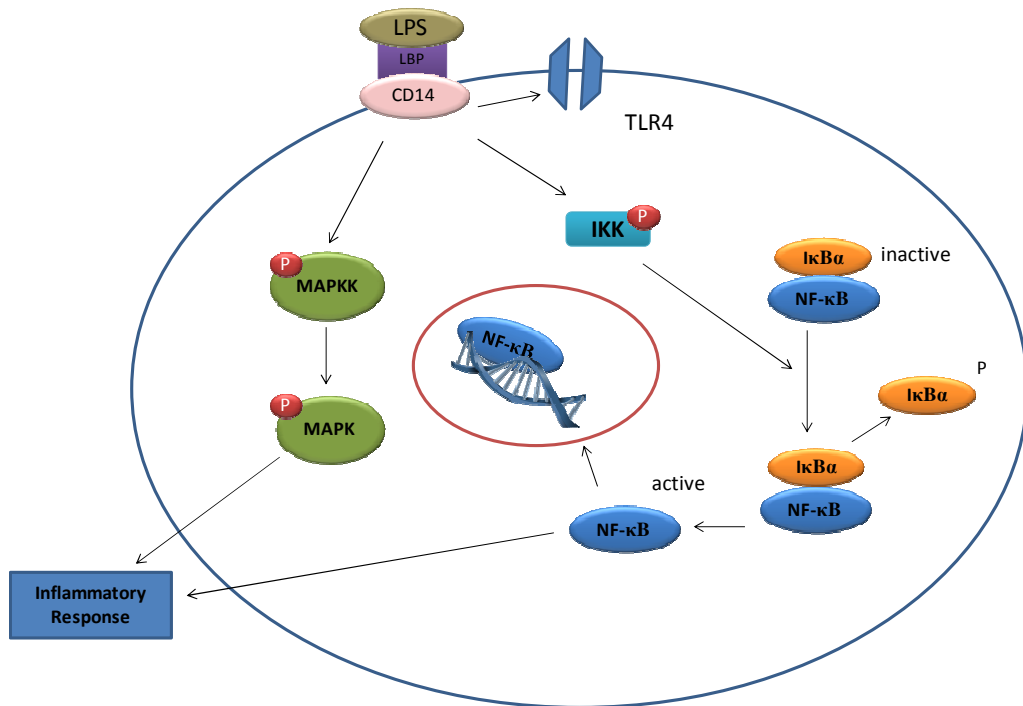


Figure 2: LPS induced NF- κ B and Mitogen Activated Protein Kinase (MAPK) pathways
LPS: Lipopolysaccharide, **LBP:** Lipopolysaccharide Binding Protein, **MAPKK:** Mitogen Activated Protein Kinase Kinases, **MAPK:** Mitogen Activated Protein Kinase, **IKK:** I kappa-B Kinases, **I κ B α :** I Kappa-B, **NF- κ B:** Nuclear Factor Kappa-B

2.4.6. Mitogen-Activated Protein Kinases (MAPK)

The MAP kinases are from a family of serine/threonine protein kinases which are activated by a variety of growth factors and other signaling molecules. They play central roles in signal transduction (186). Mammalian cells have multiple MAP kinase pathways that control distinct cellular responses. Each cascade consists of three protein kinases: a terminal MAP kinase and two upstream kinases (186). These enzymes are regulated by a characteristic phosphorelay system in which a series of three protein kinases phosphorylate and activate one another and like their substrates, MAPKs are regulated by phosphorylation (**Figure 3**). MAPK's are substrates for MAPK kinases (MKK's, MAP2K or MEK). MKK's phosphorylates and activates MAPK to activate its own substrates. The third component of the phosphorelay system; MKKK's (MAPKKK's or MAP3K) activates specific MKK's. In mammalian cells, three major groups of MAP kinases identified: ERK (ERK-1, ERK-2), JNK (JNK-1, JNK-2, JNK-3) and p38 (p38 α , p38 β , p38 γ , p38 δ) MAP kinases (186, 187).

Activation of ERK is mediated by two upstream protein kinases which are coupled to growth factor receptors by the Ras GTP-binding protein. Ras interacts with Raf protein kinase Raf phosphorylates and activates MEK (MAP kinase/ERK kinase), a dual specificity protein kinase that activates ERK by phosphorylation on both threonine and tyrosine residues (Thr-183 and Tyr-185). ERK then phosphorylates a variety of nuclear and cytoplasmic target proteins including other protein kinases and transcription factors. The Ras proteins are guanine nucleotide-binding proteins that function analogously to the α subunits of G proteins. Ras activation is mediated by guanine nucleotide exchange factors that stimulating the release of bound GDP and it exchange for GTP. GTP hydrolysis is stimulated by GTPase-activating proteins which terminates the Ras-GTP activity. JNK and p38 kinases are activated in response to inflammatory cytokines and cellular stress. JNK and p38 kinases are activated by Rho subfamily of small GTP-binding proteins (Rac, Rho, Cdc42) rather than by Ras. ERK signalling principally leads to cell proliferation, survival and differentiation while JNK and p38 MAP kinase pathways lead to inflammation and cell death (186).

The c-Jun amino-terminal kinases (JNKs) are critical regulators of transcription, and JNK inhibitors may be effective in control of rheumatoid arthritis. The p38 MAPKs

are activated by inflammatory cytokines and environmental stress and may contribute to the onset of diseases like asthma and autoimmunity (186).

The involvement of MAPK's in the regulation of the synthesis of many inflammatory mediators at the level of transcription and translation make them potential targets for anti-inflammatory researches (145). p38 MAPK regulates expression many inflammatory genes such as $TNF\alpha$, $IL-1\beta$, $IL-6$ and cyclooxygenases (145). It has been shown that p38 MAP kinase is required for gene expression mediated by $NF-\kappa B$. The activation of p38 MAPK was found to be involved in iNOS expression in LPS-induced mouse macrophages (188).

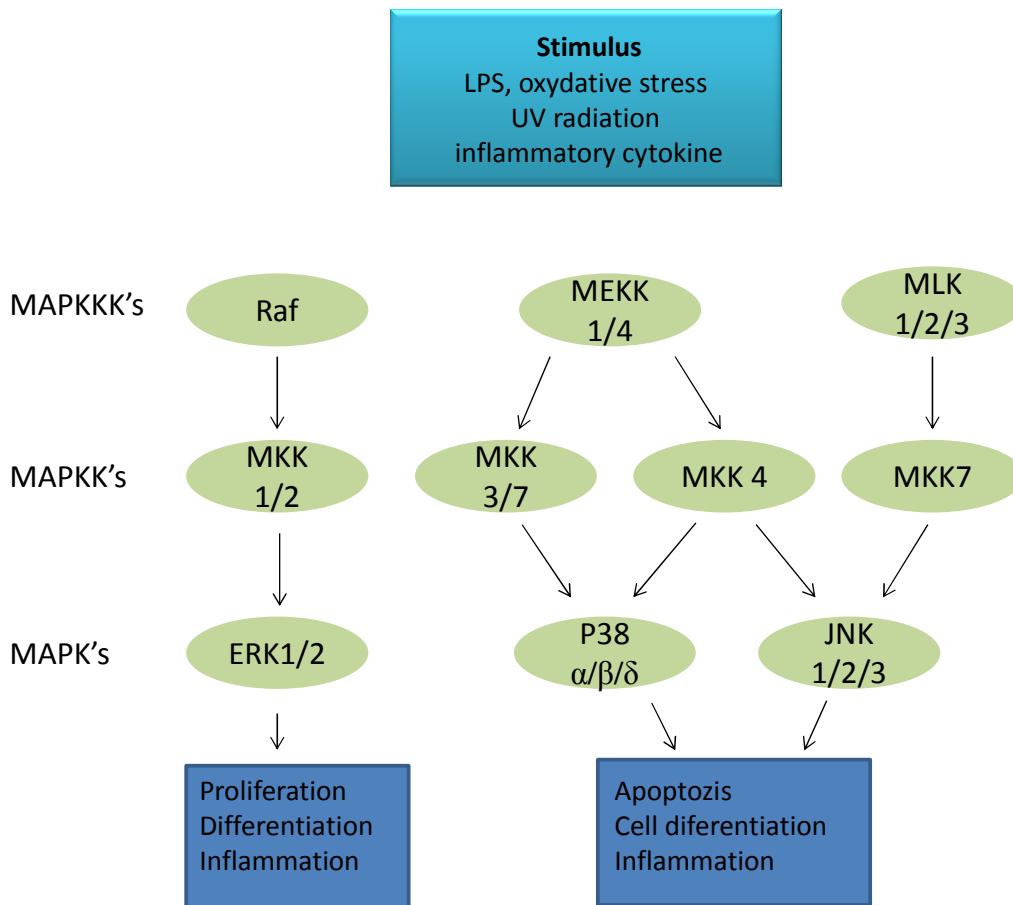


Figure 3: Mitogen-Activated Protein Kinase (MAPK) pathways
 MAPKKK: Mitogen Activated Protein Kinase Kinase, MAPKK (MKK,): Mitogen Activated Protein Kinase Kinase, MAPK: Mitogen Activated Protein Kinase, MEKK: MAPK/ERK Signal Regulated Kinase

2.4.7. LPS and Macrophage Cells

LPS is the principal component of the outer membrane of gram negative bacteria. LPS and LPS containing molecules form complexes with LBP (Lipopolysaccharide binding protein); a plasma protein (189). LBP is needed for the response to LPS. LPS and LBP complexes binds to CD14 which is a differentiation antigen of monocytes, and in this way LPS may induce responses (190). LPS then interacts with TLR4, a signaling receptor and the accessory protein MD-2 (190, 191). Macrophages are among the first cells responding to microbial infection. They detect pathogenic substances through their pattern-recognition receptors and initiate and regulate inflammation using a wide range of soluble proinflammatory mediators. LPS is one of the most powerful activators of macrophages, and macrophages and monocytes induced by LPS are known to be activated for the production of inflammatory mediators, such as NO, cytokines including TNF α , IL-1 α and IL-6. Raw 264.7 macrophages are murine macrophage cell lines which are used frequently in studies of inflammation. Numerous anti-inflammatory activity studies have been reported using LPS-stimulated Raw 264.7 macrophages *in vitro* (192-194).

LPS stimulates phosphorylation of inhibitor κ B (I κ B) resulting in its degradation and activated translocation of NF- κ B to the nucleus (195). LPS activates mitogen-activated protein kinases (MAPKs) such as extracellular signal-regulated kinases (ERK) 1 and 2, c-Jun N-terminal kinase (JNK), and p38. The activated MAPKs increase in inflammatory disease states by transcription activation of the iNOS gene (196). LPS treatment of Raw 264.7 macrophages, murine bone marrow-derived macrophages and human THP-1 monocytes resulted in a rapid increase of p46 and p54 isoforms of JNK (197). Members of ERK pathway was shown to involve in the LPS induced TNF α production moreover JNK/SAPK is required for LPS-induced translation of TNF α mRNA (198, 199). TNF α production by LPS-stimulated macrophages is regulated at the levels of both transcription and translation. LPS activates extracellular-signal-regulated kinases 1 and 2 (ERK1 and ERK2), p38, and Jun N-terminal kinase/stress-activated protein kinase (JNK/SAPK) in Raw 264.7 macrophages and human THP-1 monocytes (198, 200).

3. MATERIALS AND METHODS

3.1. Materials

3.1.1. Plant Materials

The leaves of *C. laurifolius*, *S. ebulus* and *S. nigra* were collected from Uludağ-Bursa (Turkey) in June, 2009. The plants were identified by Prof. Dr. Erdem Yeşilada (Department of Pharmacognosy, Faculty of Pharmacy, Yeditepe University, İstanbul, Turkey). Voucher specimens for *Sambucus ebulus* (YEF 09017), *S. nigra* (YEF 09021) and *Cistus laurifolius* (YEF 09019) were deposited at the Herbarium of Yeditepe University. The plant materials were dried in shade and powdered prior to extraction.

3.1.2. Bioreagents, Chemicals and Solvents

4-(2-Hydroxyethyl) piperazine-1-ethansulfonic acid, N-(2-Hydroxyethyl) piperazine-N'-(2-ethanesulfonic acid) (HEPES) (Sigma Aldrich; H4034)

β-glycerolphosphate (Sigma Aldrich; G6376)

Aceton (Sigma Aldrich; S261108)

Acrylamide/bis-acryamide solution (Sigma Aldrich; A3574)

Agarose (Sigma Aldrich; A9539)

Antibiotic Antimycotic Solution (Sigma Aldrich; A5955)

Bovine Serum Albumine (Sigma Aldrich; A7030)

Chloroform (Analar Normapur; 22711.324)

Dexamethasone (Sigma Aldrich; D4902)

Dichloromethane (Merck; 1.06044.2500)

Dithiothreitol (DTT) (Fisher scientific; BP172)

Dulbecco's Modified Eagles Medium (DMEM) (Gibco-Invitrogen; 41966-029)

Dimethylsulfoxide (DMSO) (Sigma Aldrich; D2438)

Dulbecco's Phosphate Buffer Saline (Invitrogen; 14200)

Enhanced Chemiluminescans (ECL) Reagent (Amersham; RPN2232)

Ethanol (Merck; 1.00971)

Ethidium Bromide Solution (Sigma Aldrich; E1510)

Ethyl Acetate (Sigma Aldrich; 27227)

Ethylendiamintetraacetic acid (EDTA) (Merck; 108418)

Ethylene glycol-bis (2-aminoethylether)-N,N,N',N'-tetraacetic acid (EGTA) (Sigma Aldrich ; E0396)

Fetal Bovine Serum (Sigma Aldrich; F9665)

Gel Loading Dye for Nucleic acids (Sigma Aldrich; G7654)

Glycine for electrophoresis (Merck; 64271)

Griess Reagent (Promega; G2930)

Molecular Weight DNA Ladder (Fermantas; SM0311)

Molecular Weight Protein Marker (Healthcare; RPN800E)

Nucleic Acid Stain (Phenix Research; RGB-4103)

Hybond-N+ nylon membrane (Amersham; RPN203B)

Membrane optimized for nucleic acid transfer

NF- κ B primer (forward 5'-ACAATCAGTTGAGGGGACTTTCCCAGGCAA-3-Elips)

NF- κ B primer (reverse 5'-TTGCCTGGGAAAGTCCCCTCAACTGATTGT-3- Elips)

Nitrocellulose Membrane-Hybond ECL (Amersham; RPN303D)

Laemmli Buffer (Sigma Aldrich; S3401)

Parthenolide (EMD Milipore; 512732)

Kieselgel 60 F₂₅₄ (Merck; 1.10757.1000)

Lipopolysaccharides from Escherichia coli 0111:B4 (Sigma Aldrich; L4391)

Methanol (Sigma Aldrich; SZE9365S)

Phenylmethanesulfonyl fluoride (PMSF) (Sigma Aldrich; P7626)

Polyamide for column chromatography (Merck; 0001447805)

Protease Inhibitor Cocktail (Sigma Aldrich; P8340)

RNA extraction reagent (PeQlab; 30-1020)

Sodium Dodecil Sulfate (SDS) (Merck; 56/3/550044)

Lowry Assay Reagent A (BioRad; 500-0113)

Lowry Assay Reagent B (BioRad; 500-0114)

L-N₆-(1-Iminoethyl) lysine hydrochloride (L-NIL) (Cayman; 80310)

N-[2-(Cyclohexyloxy)-4-nitrophenyl] methanesulfonamide (NS-398) (Sigma Aldrich; N194)

n-Butanol (Fluka; 52150)

n-Hexane (Sigma Aldrich; SZBA0655)

Radioimmunoprecipitation (RIPA) Lysis Buffer (Santa Cruz; sc-24948)

Sephadex LH-20 (Sigma Aldrich; LH20100)

Silicagel 60 F₂₅₄ Aluminium Sheets (Merck; 1.107571000)

Sodium fluoride (NaF) (Sigma Aldrich; S7920)

Sodium Orthovanadate (Na₃VO₄) (Sigma Aldrich; S6508)

Sulphuric acid (98%) (Riedel de Haen; 62260)

Trypsin Solution 10X (Biochrome AG; L2153)

Tris Base (Fisher BioReagents; BP152-500)

Tris-HCL (Sigma Aldrich; T5941)

Vanillin (Fluka;1435805)

3.1.3. Equipment

Beaker 100 ml, 200ml, 500 ml (Isotherm, Turkey)

Cryovials (TPP, Switzerland)

Erlenmayer Flasks 100 ml, 200ml, 500 ml (Isotherm, Turkey)

Micro pipettes 1000, 200, 100, 10, 2,5 µL (Thermo Scientific)

Micro pipette tips 1000, 200, 100, 10 µL (Capp, USA)

Sterile Cell Culture Flasks, T-25, T-75 and Cell Culture plates, 6 well, 12 well, 96 well (TPP, Switzerland)

Serological Pipets 2 ml, 5ml, 10 ml or 25 ml (TPP, Switzerland)

Filter Syringe 0,2 µm (TPP; MC-99722)

Polypropylen Centrifuge Tubes 0,5 ml, 1 ml, 2ml, 15 ml, 50 ml (Isolab, Germany or Axygen, Canada)

Tissue Culture Petri Dishes 100mm, 60 mm (TPP, Switzerland)

3.1.4. Instruments

Balance (Ohaus Explorer, USA)

Centrifuge (Hettich Micro 22R, Germany)

CO₂ incubator (Nuair NU55510/E/G, USA)

ELISA Plate Reader (Bio-Tek Elx800, USA)

FT-IR (Perkin Elmer, USA)

Gel-Imager (Bio Rad Gel Doc XR, USA)

Laminar Flow Cabinet (ESCO Labculture Class II Biohazard Safety Cabinet Type 2A, Singapore)

Lyophilizator (Christ Alpha 2-4 LD, Germany)

Medium Pressure Liquid Chromatography Apparatus (MPLC) (Combi Flash Companion, Isco, USA)

Microscope (inverted) (Nikon Eclipse TS100)

Molecular- Imager (BioRad Molecular- Imager FX, USA)

NMR (JEOL Eclipse-Virginia Tech)

Oven (Binder, Germany)

PCR Thermal Cycler (BioRad Mycycler, USA)

pH meter (Hanna Instruments PH211, Germany)

Real Time PCR Thermal Cycler (BioRad iCycler iQ Multicolor Detection System, USA)

Rotary Evaporator (Heildoph, Germany)

Spectrophotometer (Implen Nanophotometer, USA)

Liquid Nitrogen Tank (Arpece 110, France)

Ultrasonic Bath (Sonorex RK156BH, Germany)

UV (HP Aglient 8453, USA)

Water Bath (Grant OLS 200, UK)

Vacuum Dryer (Eppendorf Concentrator 5301, Germany)

Vortex (Stuart SA8, UK)

- 80°C Freezer (Thermo Forma- 86C ULT Freezer, USA)

3.1.5. Kits

Biotin 3' End DNA Labeling Kit (Pierce; 89818)

Cell proliferation reagent WST-1 (Roche05015944001)

Gapdh_3 qRT-PCR Primer Set, SYBR (Qiagen; QT01658692)

IL-1 α Immunoassay (eBioscience; BMS611)

IL-1 β Immunoassay (eBioscience; BMS6002)

IL-2 Immunoassay (eBioscience; BMS601)
IL-6 Immunoassay (R&D; M6000B)
Lightshift Chemiluminescent EMSA Kit (Pierce; 20148)
Omniscript RT Kit (Qiagen; 205113)
Oligo-dT Primers (Qiagen; 79237)
PGE₂ Immunoassay (Enzo; ADI-900-001)
QuantiTect Primer Assay Actb_2 (Qiagen; QT01136772)
QuantiTect Primer Assay Ptgs2 (Qiagen; QT00165347)
QuantiTect Primer Assay Rn18s (Qiagen; QT02448075)
QuantiTect Primer Assay Nos2 (Qiagen; QT00100275)
TNF α Immunoassay (R&D; MTA00B)
WST-1 Reagent (Roche Diagnostics; 05 015 944 001)
QuantiTect SYBR Green PCR Kit (Qiagen; 204145)

3.1.6. Antibodies

β -Actin Mouse Monoclonal IgG1 Antibody (Santa Cruz; sc-47778)
Cox-2 Mouse Monoclonal IgG1 antibody (Santa cruz; sc-166475)
I κ B α Rabbit Polyclonal IgG Antibody (Santa cruz; sc-371)
NOS2 Rabbit Polyclonal IgG Antibody (Santa Cruz; sc-8310)
p38 MAPK Rabbit Polyclonal Antibody (Cell signalling; 9212S)
p44/42 MAPK Rabbit Polyclonal Antibody (Cell Signalling; 9102S)
Phospho-I κ B α Antibody (Cell Signalling; 9246L)
Phospho-p38 Mouse Monoclonal IgG1 MAPK Antibody (Cell signalling; 9216S)
Phospho-p44/42 MAPK Mouse Monoclonal IgG1 (Cell Signalling Cat no; 9106S)
Phospho-SAPK/JNK Rabbit Monoclonal IgG1 (Cell signalling ; 4671S)
SAPK/JNK Rabbit Polyclonal Antibody (Cell Signalling; 9252)

3.2. Methods

3.2.1. Phytochemical Studies

Methanol or ethanol extracts were prepared from the leaves of the plants and fractionated with solvent-solvent extractions for preliminary activity screening. The active fractions were investigated by following the activity-guided fractionation (AGF) procedures in order to determine the components responsible for the activity of the extracts.

3.2.1.1. Extraction

The dried and powdered leaves of *C. laurifolius* (211 g) were extracted with ethanol (EtOH) (96 %, 1 L) by stirring in a water bath adjusted at 60 °C for 7 days, the ethanol extract was filtered through a filter paper, evaporated to dryness under reduced pressure. All extracts were combined to give the crude EtOH extract (**CL-EtOH** 39.3 g, yield: 18.6%).

The dried and powdered leaves of *S. ebulus* (330 g) and *S. nigra* (131 g) were individually extracted by maceration with methanol (MeOH) (2.3 L and 0.9 L respectively) for 24 hr's, stirring in a water-bath adjusted to 40°C. Each methanol extract was filtered through a filter paper, evaporated to dryness under reduced pressure to give the crude MeOH extract of *S. ebulus* (**SE-MeOH** 60.5 g, yield: 18.3%) and that of *S. nigra* (**SN-MeOH** 37.31 g, yield: 12.8%).

3.2.1.2. Solvent-Solvent Fractionation of the Extracts

The EtOH extract of *C. laurifolius* (**CL-EtOH**) was dissolved in 150 ml of methanol (MeOH) (90% in H₂O) and extracted with *n*-hexane (7x50 ml) in a separatory funnel. Combined *n*-hexane sublayer was evaporated under reduced pressure to yield “*n*-hexane subextract.” (**CL-Hex** 5.7 g, yield: 14.4%). After that MeOH was removed from the remaining extract and diluted with distilled water (H₂O) to 200 ml and further fractionated by successive solvent extractions with chloroform (CHCl₃) (7x50 ml), ethyl

acetate (EtOAc) (4x25 ml), and *n*-butanol (BuOH) saturated with H₂O (4x25 ml). Each extract after solvent extractions was evaporated to dryness under reduced pressure to yield “CHCl₃ subextract.” (**CL-CHCl₃** 12.4 g, yield: 31.7%), “EtOAc subextract.” (**CL-EtOAc** 2 g, yield: 5%), and “*n*-BuOH subextract.” (**CL-*n*-BuOH** 4 g, yield: %10), while remaining water phase was lyophilised (**CL-R-H₂O** 12 g, yield: 30.5%) respectively. The extraction and fractionation process was repeated several times to increase the extract yields before activity-guided procedures.

The MeOH extract of *S. ebulus* (**SE-MeOH**) was dissolved in 200 ml of H₂O in MeOH (10%) and extracted with *n*-hexane (9x200 ml) in a separatory funnel. Combined *n*-hexane extracts were evaporated under reduced pressure to yield “*n*-hexane subextract.” (**SE-Hex**, 8 g, yield: 13.8%). After that, MeOH was removed from the remaining extract and diluted with distilled water and further fractionated by successive solvent extractions with CHCl₃ (4x200 ml), EtOAc (4x200 ml), and *n*-BuOH saturated with H₂O (4x100 ml). Each subextract after solvent extractions was evaporated to dryness under reduced pressure to yield: “CHCl₃ subextract.” (**SE-CHCl₃**, 22.5 g, yield: 39.2%), “EtOAc subextract.” (**SE-EtOAc** 2.5 g, yield: 4.3%), and “*n*-BuOH subextract.” (**SE-*n*-BuOH** 9 g yield: 15.5 %), and “remaining aqueous subextract” (**SE-R-H₂O**, 11.5 g, yield: 19.8%), respectively. The extraction and fractionation process was repeated several times to increase the extract yields before submitting to activity-guided processing (**Figure 5**).

The MeOH extract of *S. nigra* (**SN-MeOH**) was dissolved in 70 ml of H₂O in MeOH (10%) and extracted with *n*-hexane (14x100 ml) in a separatory funnel. Combined *n*-hexane extract was evaporated under reduced pressure to yield “*n*-hexane subextract.” (**SN-Hex** 9.5 g, yield: 42.2%). After that, MeOH was removed from the remaining extract and diluted with distilled water H₂O and further fractionated by successive solvent extractions with CHCl₃ (3x100 ml), EtOAc (4x100 ml), and *n*-butanol saturated with H₂O (3x100 ml). Each of subextract after solvent extractions was evaporated to dryness under reduced pressure to yield “CHCl₃ subextract.” (**SN-CHCl₃** 780 mg, yield: 3.5%), “EtOAc subextract.” (**SN-EtOAc** 1.2 g, yield: 5.3%), and “*n*-BuOH subextract.” (**SN-*n*-BuOH** 2.5 g yield: 1.1 %), and “remaining aqueous

subextract” (SN-R-H₂O 7.7 g, yield: 34.2%), respectively. The extraction and fractionation process was repeated several times to increase the extract yields before activity-guided procedures (**Figure 6**).

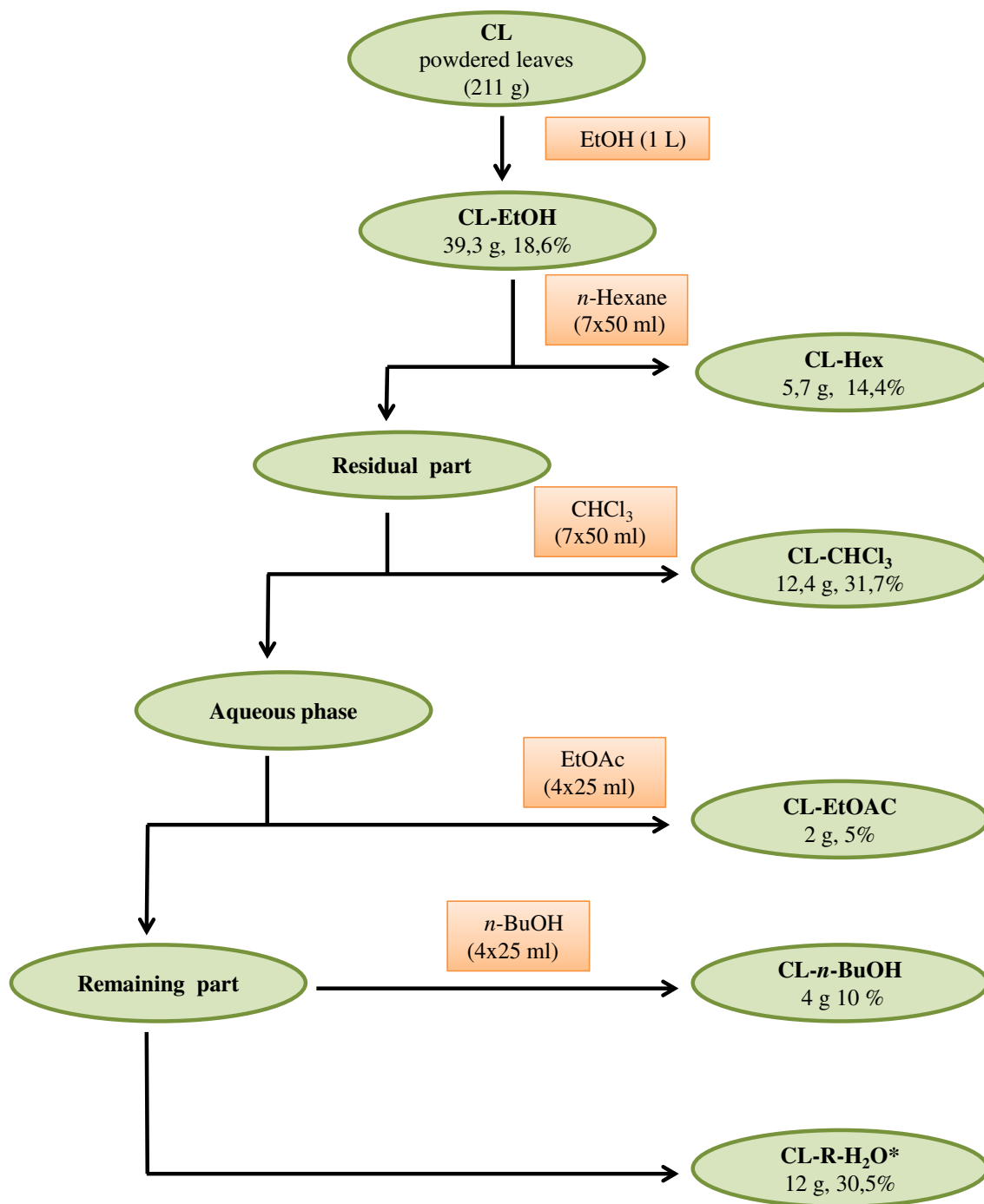


Figure 4: Fractionation of *C. laurifolius* EtOH (CL-EtOH) extract by successive solvent-solvent extractions. Active subextracts were indicated with an (*) asterisk.

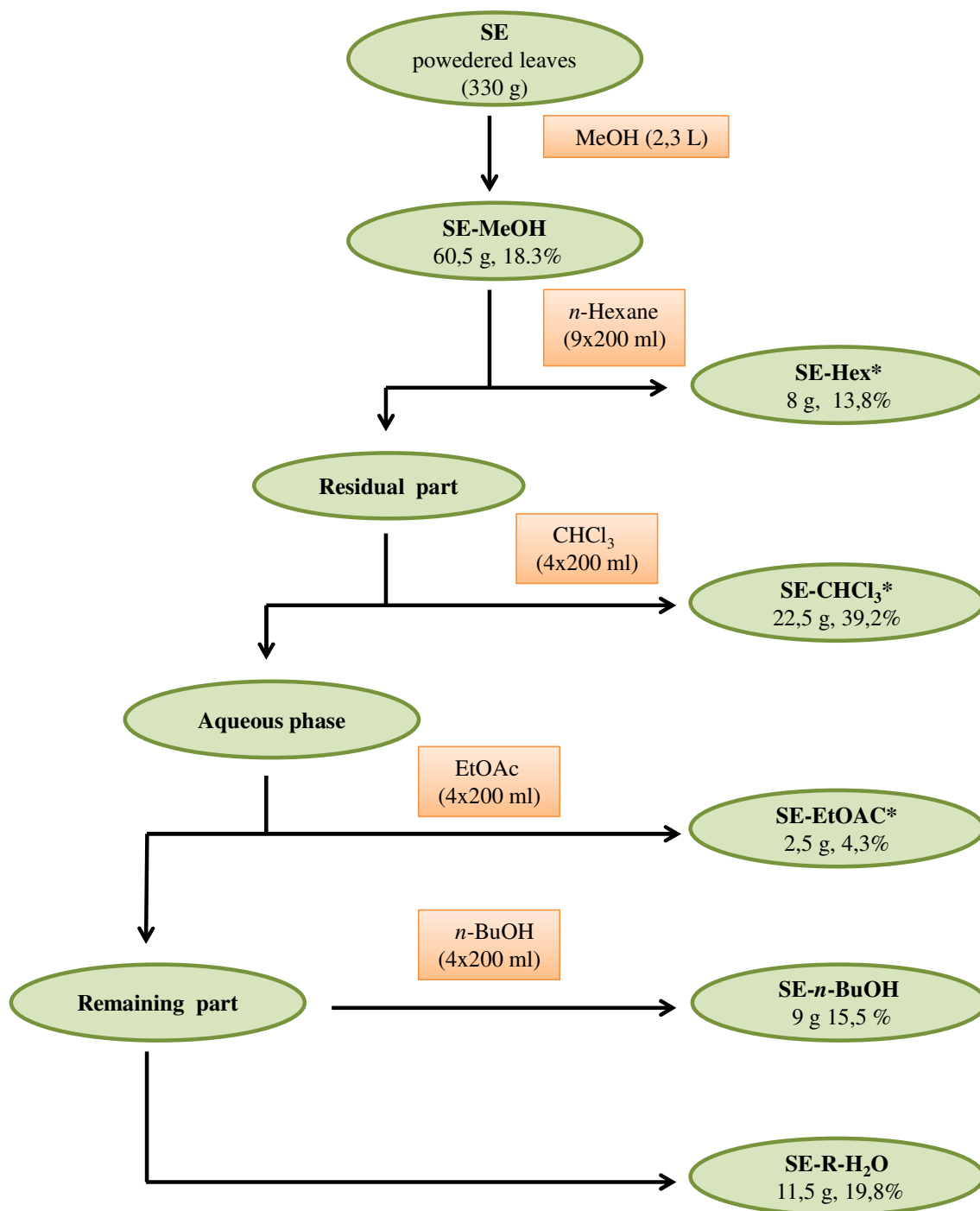


Figure 5: Fractionation of *S. ebulus* MeOH (SE-MEOH) extract by successive solvent-solvent extractions. Active subextracts were indicated with an (*) asterisk

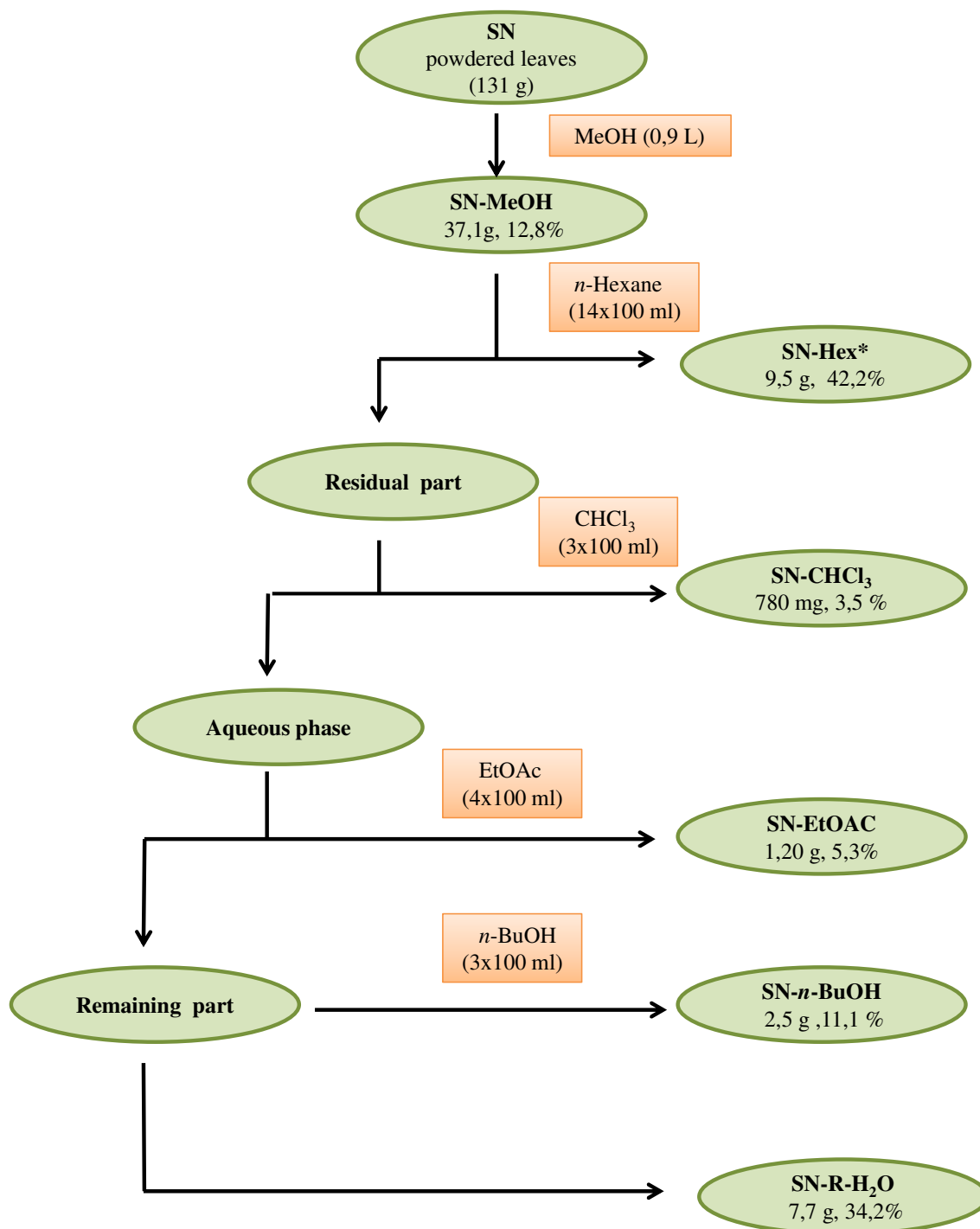


Figure 6: Fractionation of *S. nigra* MeOH (SN-MEOH) extract by successive solvent-solvent extractions. Active subextracts were indicated with an (*)asterisk.

3.2.1.3. Chromatographic Methods

Thin Layer Chromatography (TLC)

The optimisation of chromatographic fractionation and isolation procedure was made based on thin layer chromatography results. Crude extracts, fractions and pure compounds were monitored by TLC. Samples were spotted on precoated 0.20 mm thick silica gel 60 F₂₅₄ alumina plates (Merck, Darmstadt, Germany). A variety of solvent combinations were used for development including: CHCl₃-MeOH-H₂O (80:20:2-70:30:3-61:32:7), hexan; EtOAc (9:1, 8:2, 7:3, 1:1), hexan: acetone (9:1, 8:2, 7:3, 1:1). Chromatograms were visualised by exposing to UV at 254 and 366 nm (Camag UV lamp) or by using derivatization agents such as vanillin-sulphuric acid (1%) or sulphuric acid-EtOH (%5) and Antimon (III) chloride-CHCl₃ for terpenic compounds.

Open Column Chromatography

Fractionation of crude extracts or purification of compounds from fractions was achieved by open column chromatography methods using variety of stationary phase materials including: polyamide (Polyamide SC for column chromatography-Macherey Nagel), Sephadex LH 20 (Sigma) and silica gel (Kieselgel 60, 70-230 mesh, Merck). While polyamide column chromatography was used for initial fractionation of crude extracts; silica gel and sephadex column chromatographies were generally used for isolation of pure compounds from fractions. Mobile phases for these chromatographic techniques were as follows:

Polyamide Column Chromatography: Stepwise gradient elution with MeOH in H₂O (0-100%).

Silica Gel Column Chromatography: Organic solvents were combined to obtain solvent mixtures with different polarities.

Sephadex LH 20 Column Chromatography: MeOH or MeOH:CHCl₃ (1:1) mixture was used for elution from the column.

3.2.1.4. Chromatographic Fractionation Procedures for the Isolation of the Active Constituents from *S. ebulus* EtOAc Subextract (SE-EtOAc)

SE-EtOAc which showed significant *in vitro* inhibitory activity on NF-κB transcription factor was subjected to activity-guided fractionation (AGF) to isolate the compounds responsible for the activity.

Fractionation of SE-EtOAc by Polyamide Column Chromatography (SE_{EtOAc} I)

Column size: 2.5 x 30 cm

Stationary phase: Polyamide (Macherey Nagel MN Polyamid Sc particle size: 0.05-0.16 mm for column chromatography)

Procedure: 25 g of polyamide was mixed with H₂O and was transferred to a glass column. SE-EtOAc (2 g) was dissolved in H₂O, and was subjected to a polyamide column chromatography eluting with H₂O/MeOH mixtures (0-100%). Thin-layer chromatography (TLC) was used to monitor the fractions and they were combined under five fractions: [SE_{EtOAc} I Fr.1-4] (746 mg), [SE_{EtOAc} I Fr.5-10] (400 mg), [SE_{EtOAc} I Fr.12-14] [415 mg], [SE_{EtOAc} I Fr.15-20] (227 mg).

Isolation of Active Compounds from [SE_{EtOAc} I Fr.12-14] fraction with Reverse Phase Medium Pressure Liquid Chromatography (RP-MPLC) (SE_{EtOAc} II)

[SE_{EtOAc} I Fr.12-14] showed potent inhibitory activity on NF-κB and TLC of this fraction showed two major yellow spots after visualization with vanillin-H₂SO₄ reagent. This fraction was further subjected to successive separation on RP-MPLC and then opens column chromatography on silica gel.

Chromatography Apparatus: CombiFlash Companion (Teledyne Isco)

Column: 130 g. RediSep[®] Rf Reversed-phase C18 column (Teledyne Isco)

Flow rate: 10 ml/min

Procedure: 720 mg [SE_{EtOAc} I Fr.12-14] was dissolved in 4 ml 15% MeOH in H₂O and applied to column. Elution was started with 15% MeOH in H₂O and the MeOH ratio was gradually increased to finally reach 100% MeOH (171 mins). The fractions were monitored by TLC and similar fractions were combined. TLC of SE_{EtOAc} I Fr.12-14 showed two major yellow spots after visualization with vanillin-H₂SO₄ reagent. These two molecules were then separated from each other on RediSep column and combined under two fractions; [SE_{EtOAc} II Fr.26-34] and [SE_{EtOAc} II Fr.35-49]. The minor impurities in these fractions were removed by Silica gel column chromatography.

Isolation of Active Compounds from [SE_{EtOAc} II Fr.26-34] by Silica Gel Column Chromatography (SE_{EtOAc} III)

TLC analysis of the [SE_{EtOAc} II Fr.26-34] revealed a major yellow spot after visualization with 5% H₂SO₄ reagent. Final purification of the major component was achieved by silica gel column chromatography.

Column size: 1.5 x 20 cm

Stationary phase: Silica gel (Kieselgel 60, 70-230 mesh, Merck)

Procedure: 12 g silica gel was mixed with CHCl₃:MeOH (9:1) solvent mixture and transferred into glass column. [SE_{EtOAc}-II Fr. 26-34] (92 mg) was dissolved in the same solvent mixture and applied to column. 150 ml of CHCl₃:MeOH (85:15) and 250 ml CHCl₃:MeOH (90:10) was used to yield **SE-1** (37 mg).

Isolation of Active Compounds from [SE_{EtOAc} II Fr.35-49] by Silica gel Column Chromatography (SE_{EtOAc} IV)

Column size: 1.5 x 20

Stationary phase: Silica gel (Kieselgel 60, 70-230 mesh, Merck)

Procedure: 15 g of silica gel was mixed with CHCl₃:MeOH (98:2) and transferred into glass column. [SE_{EtOAc} II Fr.35-49] (132 mg) was dissolved in the same solvent and eluted with 50 ml CHCl₃:MeOH (98:2), 50 ml CHCl₃:MeOH (95:5), 350 ml CHCl₃:MeOH (90:10) and 150 ml CHCl₃:MeOH (80:20) successively as mobil phases and (SE-2) (5 mg) was obtained. The same procedure was repeated to obtain sufficient material for bioassays.

Isolation of Active Compounds from by [SE_{EtOAc} I Fr.15-20] with Medium Pressure Liquid Chromatography (SE_{EtOAc} V):

Chromatography Apparatus: CombiFlash Companion-Teledyne Isco

Column: 12 g Flash Column RediSep Silica (Teledyn Isco)

Flow rate: 5 ml/min

Procedure: 100 mg of [SE_{EtOAc} I Fr.15-20] was dissolved in 1 ml CHCl₃ and applied to column. Through gradient elution with MeOH in CHCl₃ solvent system (0-80% 200 mins.) SE-4 (18 mg) was obtained.

Isolation of Active Compounds from [SE_{EtOAc} I Fr.5-10] with RP-Medium Pressure Liquid Chromatography (SE_{EtOAc} VI)

Chromatography Apparatus: CombiFlash Companion (Teledyne Isco)

Column: C18 RediSep 13 g Reverse phase column (Teledyn Isco)

Flow rate: 5 ml/min

Procedure: 100 mg of [SE_{EtOAc} I Fr.5-10] was dissolved in 5% (MeOH) in H₂O and applied to RP-column. Increasing amounts of MeOH in H₂O was used for stepwise gradient elution in 120 mins. Elution was terminated with 70% MeOH. Fractions were combined according to their TLC profiles and [SE_{EtOAc} VI Fr.32-37] was obtained which was then purified by sephadex column chromatography to yield (SE-6).

Sephadex Column Chromatographic separation of [SE_{EtOAc} VI Fr.32-37] (SE_{EtOAc} VII)

Column size: 1 x 15 cm

Stationary phase: Sephadex LH-20 (Lipophilic Sephadex, 25-100 μ , Sigma-Aldrich)

Procedure: 5 g Sephadex LH-20 was suspended in MeOH and transferred into glass column. 25 mg [SE_{EtOAc} VI Fr.32-37] was dissolved in MeOH and applied to column, then eluted with 50 ml MeOH to give final pure compound.

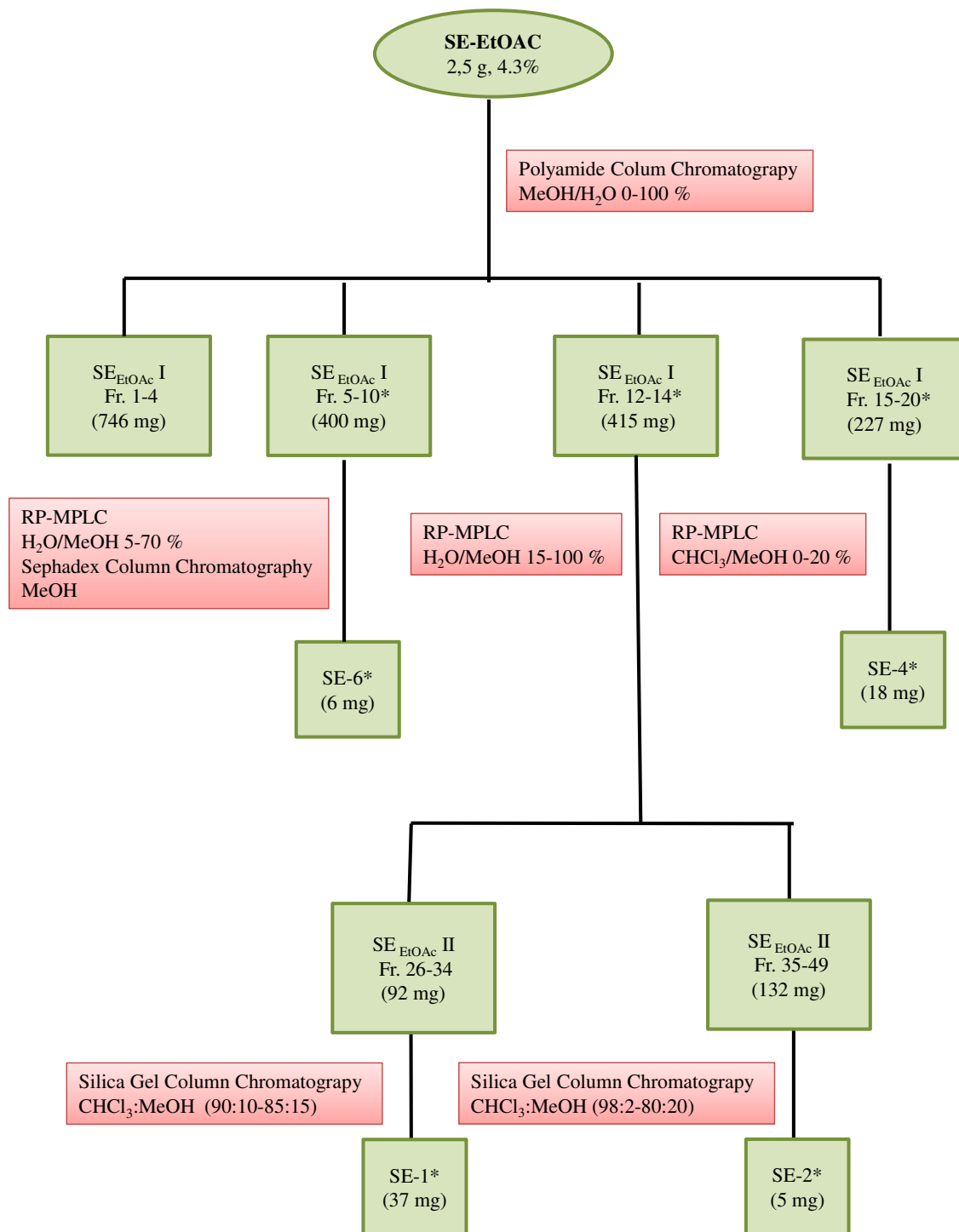


Figure 7: Activity-guided isolation of active compounds from *S. ebulus* EtOAc subextract (SE-EtOH). Active fractions were indicated with an asterisk (*).

3.2.1.5. Chromatographic Fractionation Procedures for the Isolation of the Active Constituents from *S. ebulus* CHCl₃ Subextract (SE- CHCl₃)

SE-CHCl₃ was subjected to activity-guided fractionation to isolate the component(s) responsible for the NF-κB inhibitory activity.

Fractionation of SE-CHCl₃ by Silica Gel Column Chromatography (SE_{CHCl₃} I):

Column size: 2.5 x 28 cm

Stationary phase: Silica gel (Kieselgel 60, 70-230 mesh, Merck)

Procedure: 200 g. of silica gel was suspended in *n*-hexane-EtOAc (8:2) solvent mixture and transferred into a glass column. 10 g of SE-CHCl₃ was dissolved in the same solvent mixture and applied to column. Elution solvent mixtures and ratios was as follows: 200 ml EtOAc: *n*-hexane (2:8), 200 ml EtOAc: *n*-hexane (4:6), 400 ml EtOAc: *n*-hexane (6:4), 300 ml EtOAc: *n*-hexane (7:3), 200 ml EtOAc: *n*-hexane (8:2), 200 ml EtOAc, 200 ml MeOH: CHCl₃ (1:9), 200 ml MeOH: CHCl₃ (2:8), 400 ml MeOH: CHCl₃ (3:7), 200 ml MeOH: CHCl₃ (4:6), 1000 ml MeOH: CHCl₃ (1:1). Fractions were monitored by TLC and similar fractions were combined to give four fractions: [SE_{CHCl₃} I Fr.2-7] (332 mg), [SE_{CHCl₃} I Fr.8-13] (794 mg), [SE_{CHCl₃} I Fr.14-16] (6.4 g), [SE_{CHCl₃} I Fr. 17-23] (806 mg). Fractions were tested on LPS-induced Raw 264.7 cells for their inhibitory effects on NF-κB transcription factor and only [SE_{CHCl₃} I Fr.14-16] exhibited significant activity. For that reason this fraction was further fractionated with silica gel column chromatography.

Fractionation of [SE_{CHCl₃} I Fr.14-16] by Silica Gel CC (SE_{CHCl₃} II)

Column size: 2 x 32 cm

Stationary phase: Silica gel (Kieselgel 60, 70-230 mesh, Merck)

Procedure: 150 g of silica gel was suspended in CHCl_3 and transferred in a glass column. 2.5 g [$\text{SE}_{\text{CHCl}_3}$ I Fr.14-16] was dissolved in CHCl_3 and applied to column. Elution was started with CHCl_3 (400 ml) and then a mixture of CHCl_3 :MeOH with gradually increased ratio of MeOH. 300 ml CHCl_3 :MeOH (97.5:2.5), 400 ml CHCl_3 :MeOH (90:10), 400 ml CHCl_3 :MeOH (85:15), 400 ml CHCl_3 :MeOH (70:30), 200 ml CHCl_3 :MeOH (40:60). Fractions were combined according to their TLC profiles: [$\text{SE}_{\text{CHCl}_3}$ II Fr.59-63] (1,289 g), [$\text{SE}_{\text{CHCl}_3}$ II Fr.71-72] (273 mg), [$\text{SE}_{\text{CHCl}_3}$ II Fr.73-74] (180 mg) and [$\text{SE}_{\text{CHCl}_3}$ I Fr.78-86] (615 mg). Fractions were tested for their inhibitory effects on NF- κ B transcription factor and only first two fractions exhibited significant activity, and these fractions were then submitted to chromatographic separations to isolate the active components.

Isolation of Active Compounds from [$\text{SE}_{\text{CHCl}_3}$ II Fr.59-63] by Silica Gel CC [$\text{SE}_{\text{CHCl}_3}$ III]

On TLC examination of $\text{SE}_{\text{CHCl}_3}$ II Fr.59-63 two brown spots, a major and a minor, were detected when visualized with 5% H_2SO_4 reagent. These compounds were then separated by successive column chromatography on silica gel ($\text{SE}_{\text{CHCl}_3}$ III) and by MPLC ($\text{SE}_{\text{CHCl}_3}$ IV).

Column size: 1.5x20 cm

Stationary phase: Silica gel (Kieselgel 60, 70-230 mesh, Merck)

Procedure: Silica gel (18 g) was suspended in EtOAc and transferred to a glass column. 200 mg of [$\text{SE}_{\text{CHCl}_3}$ II Fr.59-63] was dissolved in EtOAc and applied to column. The column was eluted with 100 ml CHCl_3 :EtOAc (7:3), 100 ml CHCl_3 :EtOAc (6:4), 100 ml CHCl_3 :EtOAc (5:5), 100 ml CHCl_3 :EtOAc (6:4), 100 ml CHCl_3 :EtOAc (7:3), 100 ml CHCl_3 :EtOAc (8:2), 100 ml CHCl_3 :EtOAc (9:1). Finally **SECP-1** (5 mg) was isolated as pure component.

Isolation of Active Compounds from [$\text{SE}_{\text{CHCl}_3}$ II Fr.59-63] by MPLC [$\text{SE}_{\text{CHCl}_3}$ IV]

Chromatography Apparatus: CombiFlash Companion (Teledyne Isco)

Column: RediSep Silica 40 g Flash Column (Teledyn Isco)

Flow rate: 5 ml/min

Procedure: [SE_{CHCl₃} II Fr.59-63] (180 mg) was dissolved in acetone:CHCl₃ (15:85) mixture. The column was eluted with increasing concentrations of acetone in CHCl₃ (15-90 %) in 300 mins. A pure compound was obtained in 32 mg (**SECP-2**).

Isolation of pure compounds from [SE_{CHCl₃} II Fr.71-72] by MPLC [SE_{CHCl₃} V]

The fraction was subjected to TLC and two major brown spots were detected by visualizing with H₂SO₄ reagent. The two major compounds were separated by repeated MPLC.

Chromatography Apparatus: CombiFlash Companion (Teledyne Isco)

Column: RediSep Silica Flash Column 40 g (Teledyn Isco)

Flow rate: 5 ml/min

Procedure: 200 mg SE_{CHCl₃} II Fr. 71-72 was dissolved in acetone:CHCl₃ (15:85) mixture. The column was eluted with increasing concentrations of acetone in CHCl₃ (15-90%) in 290 mins. Two fractions were obtained SE_{CHCl₃} V Fr. 50-60 (81 mg), SE_{CHCl₃} V Fr. 60-73 (25 mg) which were further chromatographed to yield **SECP-3** and **SECP-4**. **SECP-3** (40 mg) was isolated from SE_{CHCl₃} V Fr. 50-60 by using 12g RediSep Silica Flash Column eluted with increasing concentrations of acetone in CHCl₃ (20-60%) in 120 mins. **SECP-4** (8.5 mg) was obtained from a 4 g RediSep Silica Flash Column eluted with increasing concentrations of acetone in CHCl₃ (20-40%) in 120 mins.

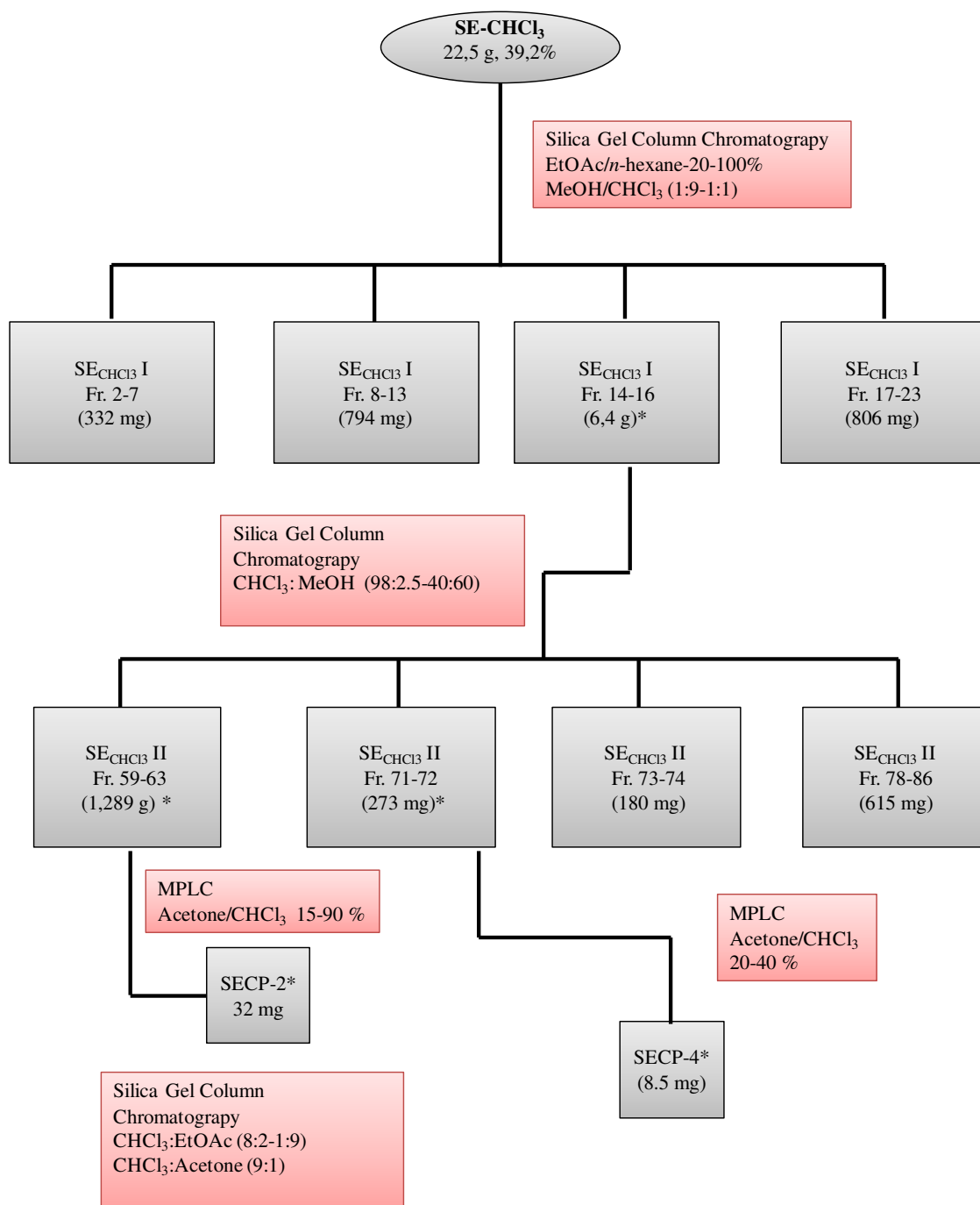


Figure 8: Activity-guided isolation of active compounds from *S. ebulus* CHCl₃ subextract (SE-CHCl₃). Active fractions were indicated with an asterisk (*).

3.2.1.6. Chromatographic fractionation procedures for the isolation of the active constituents from *S. ebulus* Hexane subextract (SE-Hex)

The subextracts of *S. ebulus* were tested for their inhibitory activity on NF- κ B transcription factor and SE-Hex exhibited significant inhibitory activity. After that this subextract was further fractionated by sephadex column chromatography.

Fractionation of SE-Hex by Sephadex LH-20 CC (SE_{Hexane} I)

Column size: 2.5 x 27 cm

Stationary phase: Sephadex LH-20 (Lipophylic Sephadex, 25-100 μ , Sigma-Aldrich)

Procedure: 16 g of Sephadex was mixed with CHCl₃:MeOH (1:1) mixture and transferred into glass column. SE-Hex was dissolved in the same mixture and eluted with 200 ml of CHCl₃:MeOH (1:1). The eluents were then combined under two fractions: [SE_{Hexane} I Fr. 9-12] (38 mg), [SE_{Hexane} I Fr. 13-15] (75 mg).

Fractionation of SE_{Hexane} I Fr. 9-12 by MPLC (SE_{Hexane} II)

Chromatography Apparatus: CombiFlash Companion (Teledyne Isco)

Column: RediSep Silica Flash Column 4 g (Teledyn Isco)

Flow rate: 5 ml/min

Procedure: SE_{Hexane} I Fr. 9-12 (38 mg) was dissolved in EtOAc:*n*-Hexane (15:80) mixture and submitted to RediSep Silica Flash Column. The column was eluted with increasing concentrations of EtOAc in *n*-Hexane (15-80 %) in 175 mins. Two fractions were obtained: SE_{Hexane} II Fr. 33-37-(12 mg) and SE_{Hexane} II Fr. 41-49 (5 mg). Only the first fraction which was composed of a single component exhibited a NF- κ B inhibitory

activity and the structure of this compound was then elucidated by spectroscopic techniques (**SEH-1**)

Fractionation of SE_{Hexane} I Fr. 13-15 by MPLC (SE_{Hexane} III)

Chromatography Apparatus: CombiFlash Companion (Teledyne Isco)

Column: RediSep Silica Flash Column 4 g (Teledyn Isco)

Flow rate: 5 ml/min

Procedure: SE_{Hexane} I Fr. 13-15 (75 mg) was dissolved in EtOAc: *n*-Hexane (20:80) mixture. The column was eluted with increasing concentrations of EtOAc in *n*-Hexane (20-50%) in 125 mins. Three fractions were obtained: [SE_{Hexane} III Fr. 16-19] (6 mg), [SE_{Hexane} III Fr. 23-25] (4 mg), [SE_{Hexane} III Fr. 48-52] (5.4 mg).

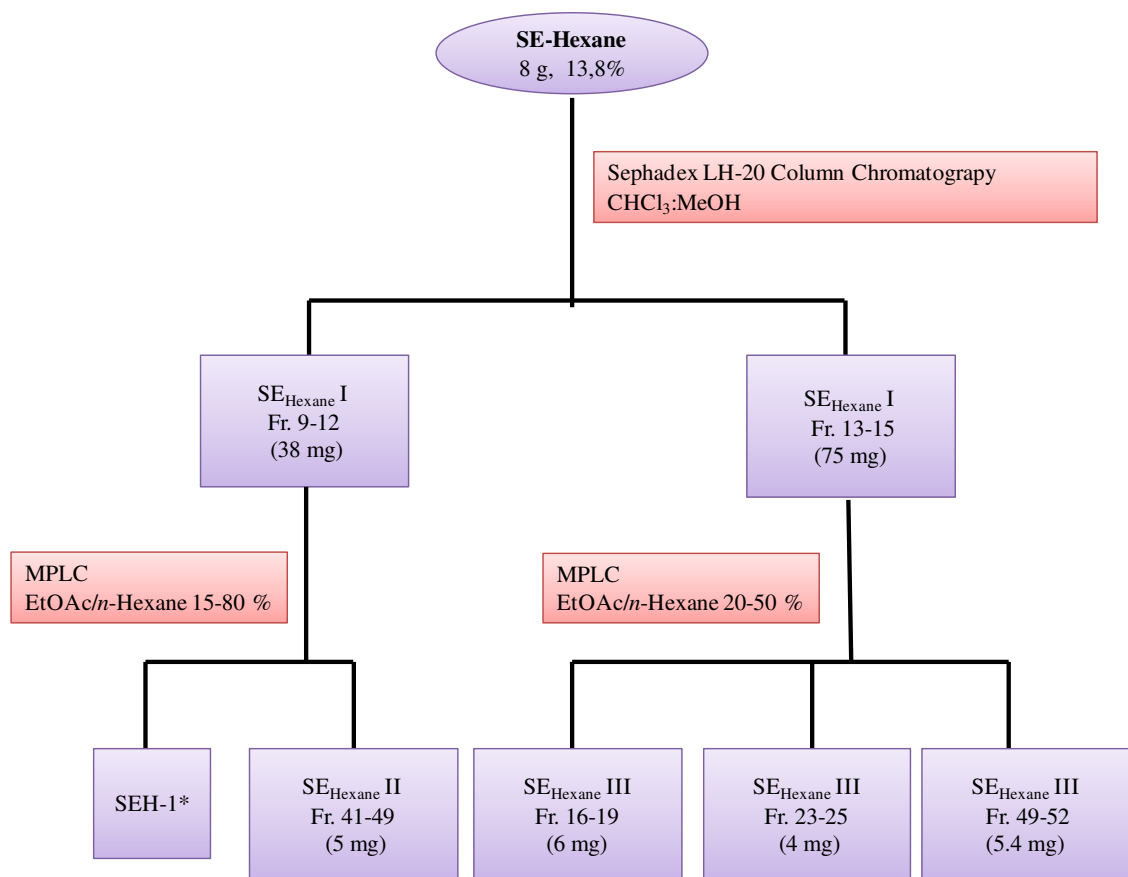


Figure 9: Activity-guided isolation of active compounds from *S. ebulus* hexane subextract (SE-Hex). Active fractions were indicated with an asterisk (*).

3.2.1.7. Chromatographic fractionation procedures for the isolation of the active constituents from *S. nigra* Hexane subextract (SN-Hex)

SN-Hex was the only active subextract on NF- κ B transcription factor and it was fractionated by silica gel column chromatography.

Fractionation of SN-Hex by Silica Gel CC (SN_{Hexane} I)

Column size: 2.5 x 27 cm

Stationary phase: Silica gel (Kieselgel 60, 70-230 mesh, Merck)

Procedure: 200 g. of silica gel was mixed with *n*-hexane and transferred into glass column. SN-Hex (5 g) was dissolved in *n*-hexane and applied to column. Elution solvent combinations were as follows: 200 ml *n*-hexane, 200 ml EtOAc: *n*-hexane (2:8), 200 ml EtOAc: *n*-hexane (4:6), 200 ml EtOAc: *n*-hexane (6:4), 200 ml EtOAc: *n*-hexane (8:2), 200 ml EtOAc, 200 ml MeOH: EtOAc (2:8), 200 ml MeOH: EtOAc (1:1). Fractions are combined to give four main fractions: SN_{Hexane} I Fr. 1-6 (520 mg), SN_{Hexane} I Fr. 7-10 (1.5 g), SN_{Hexane} I Fr. 11-16 (418 mg), SN_{Hexane} I Fr. 17-25 (1.95 g.). SN_{Hexane} I Fr. 11-16 and SN_{Hexane} I Fr. 17-25 was active on NF- κ B transcription factor. The fractions were examined by TLC and it revealed that SN_{Hexane} I Fr. 17-15 was including only one major pink spot after derivatisation with vanillin-H₂SO₄ reagent with very minor impurities on front line [solvent system: *n*-hexane:EtOAc (7:3)] which was later isolated by silica gel column chromatography. Fr. 11-16 was also including the same pink spot and besides several minor green spots probably of chlorophylls.

Isolation of Active Constituents from SN_{Hexane} I Fr. 17-25 by Silica Gel CC (SN_{Hexane} II)

Column size: 1 x 15 cm

Stationary phase: Silica gel (Kieselgel 60, 70-230 mesh, Merck)

Procedure: 9 g of silica gel was mixed with *n*-hexane:EtOAc mixture (8:2) and transferred into glass column. SN_{Hexane} I Fr. 17-25 (400 mg) was dissolved in *n*-hexane:EtOAc mixture (8:2) and applied to column. Elution was started with 200 ml *n*-hexane:EtOAc mixture (8:2) and the EtOAc in *n*-hexane was gradually increased (10% in every step) to reach final concentration of 80%. A pure compound (143 mg) which was a pink spot after derivatisation with sulphuric acid 5% reagent was obtained from this column (**SNH-1**).

Fractionation of SN_{Hexane} I Fr. 11-16 by Sephadex CC (SN_{Hexane} III)

Column size: 1 x 15 cm

Stationary phase: Sephadex LH-20 (Lipophilic Sephadex, 25-100 μ , Sigma-Aldrich)

Procedure: 50 g of Sephadex LH-20 was mixed with *n*-hexane:EtOAc mixture (8:2) and transferred into glass column. SN_{Hexane} I Fr. 11-16 (400 mg) was dissolved in CHCl₃:MeOH mixture and eluted with 300 ml of the same mixture. Two fractions were combined according to TLC profiles: SN_{Hexane} III Fr. 5-12 (144 mg) and SN_{Hexane} III Fr. 12-29 (389 mg). When the first fraction was investigated by TLC (SN_{Hexane} III Fr. 5-12) several spots were observed which were giving green color after derivatisation with vanillin-sulphuric acid reagent. The fraction was further chromatographed on Sephadex and Silica gel chromatographies but the separation could not be achieved. So this fraction was chosen for further investigations on the mechanism of anti-inflammatory activity and was named as **SNH-2**. SN_{Hexane} III Fr. 12-29 was the same compound as **SNH-1**.

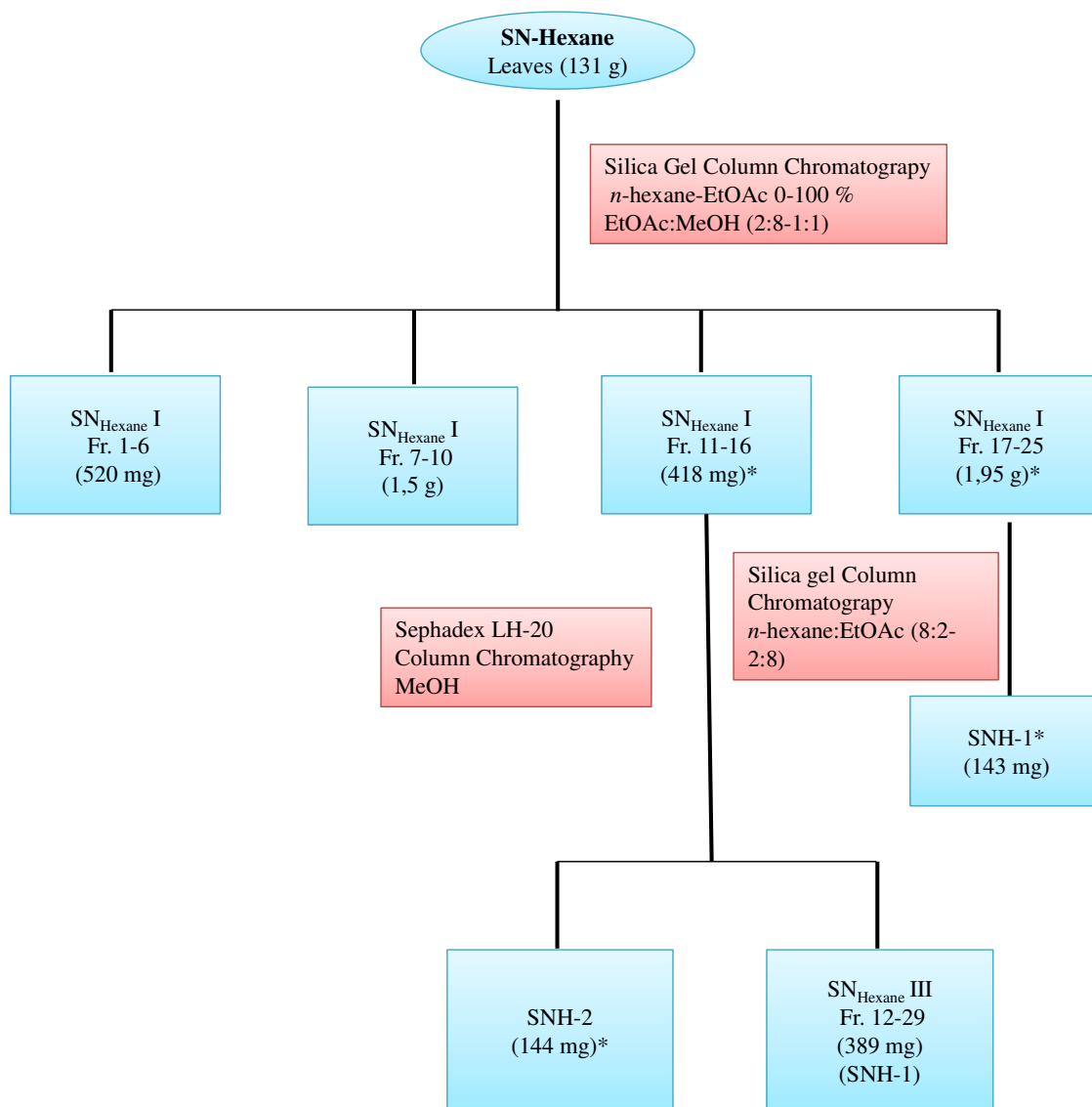


Figure 10: Activity-guided isolation of active compounds from *S. nigra* hexane subextract (SN-Hex). Active fractions were indicated with an asterisk (*).

3.2.1.8. Chromatographic fractionation procedures for the isolation of the active constituents from *C. laurifolius* remaining water subextract (CL-R-H₂O)

CL-R-H₂O was only mildly active on NF-κB transcription factor and it was the only active subextract. It was fractionated by Amberlite XAD-2 column chromatography.

Fractionation of CL-R-H₂O by Amberlite XAD-2 CC (CL_{R-H₂O} I)

Column size: 2.5 x 25 cm

Stationary phase: Amberlite XAD-2 (Sigma)

Procedure: 30 g. of Amberlite XAD-2 was mixed with H₂O and transferred into glass column. CL-R-H₂O (5 g) was dissolved in H₂O and applied to column. Elution was started with H₂O and MeOH was gradually increased to reach a final concentration of . Fractions are combined to give four main fractions: CL_{R-H₂O} I Fr. 1-4 (1,520 mg), CL_{R-H₂O} I Fr. 5-6 (1.5 g), CL_{R-H₂O} I Fr. 7-11 (418 mg), CL_{R-H₂O} I Fr. 12-17 (925 mg). None of the fractions exerted inhibitory activity against NF-κB so CL-R-H₂O was selected for further investigations.

Spectroscopic Methods: The IR spectra were recorded on a Perkin Elmer Spectrum One (in CHCl₃ or MeOH), and UV on Agilent 8453 spectrophotometers (in MeOH). Optical rotations were determined on a Opt. Act. Ltd. AA-5 polarimeter. The NMR (¹H, ¹³C, HSQC, HMBC) spectra were run in CDCl₃ or CD₃OD, and recorded on a JEOL Eclipse 500 MHz NMR (Virginia Tech). TMS was used as an internal standard and chemical shifts were given as δ (ppm), and the coupling constants (*J*) were reported as Hz. The mass measurements were carried out either at Virginia Tech or at MRC, TUBITAK, Gebze Turkey using different spectrometers.

3.2.2. Activity Studies

3.2.2.1. Cells and Cell Culture

The Raw 264.7 macrophages were obtained from American Type Culture Collection (ATCC TIB-71). Raw 264.7 cell line is a macrophage-like, Abelson leukemia virus transformed cell line derived from BALB/c mice by W. C. Raschke in 1978. The cells were grown in Dulbecco's modified Eagle's medium supplemented with 10% fetal bovine serum, 4 mM L-glutamin, 100 IU/mL penicillin and 100 µg/mL streptomycin at 37 °C in a humidified atmosphere containing 5% CO₂.

3.2.2.2. Cell Passaging and Counting

Cells were passaged when cells reach an approximate 70% confluency. After the removal of media, the cell monolayer was once rinsed with DPBS (pH 7.4). Cells were then detached with 2x Trypsin solution [0.1% (w/v)] in %5 CO₂ humidified incubator. The detached cells were collected in 10% (v/v) FBS containing media to inactivate trypsin and centrifuged at 300xg for 5 mins. The supernatant was discarded and cells were resuspended in the growth media and seeded into tissue culture flasks.

10 µl aliquots of the cell suspension were applied to the haemocytometer and the number of the cells was counted on the 5 squares in the large middle square of the haemocytometer using inverted phase contrast microscope (Nikon, USA). The cells were counted three times and an average of cell number per ml was calculated.

3.2.2.3. Cryopreservation of the Cell Line

Cells were trypsinised and centrifuged as described above. After discarding the supernatant, cell pellet was resuspended in the freezing media (FBS containing 10% DMSO). Cells were then transferred in 1 ml aliquots into cryovials and slowly frozen at (-80 °C) and then transferred to the liquid nitrogen for long term storage.

3.2.2.4. Cell Thawing

After the removal of the cells from liquid nitrogen, cells were rapidly thawed at 37 °C. The cell suspension was then transferred to a sterile centrifuge tube and 5 ml of serum supplemented media was added onto cells dropwise with gentle shaking. After that cells were centrifuged for 5 mins 300x g, supernatant was removed and cell pellet was suspended in growth media and then transferred to cell culture flasks. Following a 12-24 hr incubation, the media was changed with fresh media.

3.2.2.5. WST-1 Assay for Cell Viability

The non-toxic concentrations of the extracts and pure compounds were examined using a WST-1 assay kit (Roche Applied Sciences Cat. No: 05015944001) following the manufacturer's instructions. WST-1, a tetrazolium-based salt dye, is reduced by metabolically active cells, and a purple formazan salt is formed from this reaction which remains soluble within cells and it is directly quantified by spectrophotometric measurements. Briefly, Raw 264.7 cells (22,500 cells/well) in 10% (v/v) FBS-DMEM were seeded into 96-well plates. After incubation for 24 h for attachment of cells, various concentrations of test compounds or extracts were added to the wells with or without 1 µg/ml LPS, and the plates were incubated at 37 °C for additional 24 hr's. After the supernatant was removed, the cells were used in the WST-1 assay. WST-1 was then added directly to the cultures to a final concentration of 5% (v/v), and cells were incubated at 37 °C for an additional 60 mins. Absorbance was then read between 420-480 nm (λ_{max} 450 nm) using a plate reader. All test compounds were dissolved in DMSO and diluted with DMEM to the appropriate concentrations. The final concentration of DMSO in the culture medium was not more than 0.1% (v/v).

3.2.2.6. Preparation of Nuclear Proteins and Electromobility Shift Assay (EMSA)

Cells were scraped with ice-cold PBS and centrifuged. The pellets were resuspended in the hypotonic extraction buffer (20 mM HEPES, 0.4 M NaCl, 1 mM EDTA, 1mM DTT, 1 mM PMSF, pH 7.9) for 10 mins. on ice and then Igepal (Non-

Idet NP-40) was added into each sample to reach final concentration 1% and the samples were vortexed for an additional 20 mins on ice. The samples were then centrifuged at 450 x g for 3 mins. to participate the cell membrane. The supernatant was transferred to new tubes without disturbing the pellet and then centrifuged at 14.000 x g for 10 mins. then 16.000 x g for 3 mins. The supernatant cytosolic fraction was transferred to new tubes completely and then 25 µl of hypertonic solution (10 mM HEPES, 10mM KCl, 0.1 mM EDTA, 1mM DTT, 0.5 mM PMSF, pH 7.9) was added to pellets and were constantly shaken at 4 °C for 30 mins. The samples were then centrifuged 16.000 x g for 1 min. The resultant supernatants containing nuclear proteins were collected and stored at (-80 °C) until the EMSA was performed.

Nuclear proteins were analyzed for NF-κB binding activity by incubating 5 µg of nuclear protein with 3 pmol of biotin-labeled double-stranded oligomer probe and poly (dI-dC) in binding buffer for 30 mins at room temperature using LightShift™ Chemiluminescent EMSA Kit (Pierce). The probe used in electrophoretic mobility shift assay (EMSA) was forward 5'-ACAATCAGTTGAGGGGACTTTCCCAGGCAA-3' and reverse 5-TTGCCTGGGAAAGTCCCCTCAACTGATTGT-3', which was labeled using a Biotin 3' end DNA Labeling kit (Pierce) according to the manufacturer's instructions (Pierce cat no: 89818). Bound complexes were separated onto 6-15% nondenaturing two-step polyacrylamide gels, transferred onto nylon membrane, and detected by a LightShift chemiluminescent EMSA kit (Pierce) according to the manufacturer's protocol

3.2.2.7. Nitrite Assay

Raw 264.7 cells (22.500 cells/well) in 10% FBS-DMEM were seeded into 96-well plates. After incubation for 24 h for attachment of cells, various concentrations of test compounds were added to the wells. Following a one-hr pre-incubation, cells were stimulated with 1 µg/ml lipopolysaccharide (LPS) and the plates were incubated at 37 °C for additional 24 hr's. The nitrite accumulated in the culture medium was measured as an indicator of NO production based on the Griess reaction. Briefly, 50 µl of cell culture medium was mixed with 50 µl of 1% (w/v) sulfanilamide in 5% (v/v)

phosphoric acid and incubated for 10 mins and then 50 μ l of 0.1% (w/v) naphthylethylenediamine-HCl (Promega) and incubated at room temperature for another 10 mins, and then absorbance was read at 550 nm using a microplate reader. The amount of nitrite in the samples was calculated from the NaNO₂ serial dilution standard curve.

3.2.2.8. Enzyme Immunoassay for Quantification of PGE₂ and Cytokines (TNF α , IL-1 α , IL-1 β , IL-2, IL-6)

Sandwich ELISA was used to determine the inhibitory effects of the isolated compounds on the production of cytokines (TNF α , IL-1 α , IL-1 β , IL-2, IL-6) and PGE₂ in LPS-treated Raw 264.7 cells. The supernatant was harvested and assayed according to the manufacturer's protocol for the relevant ELISA kit.

3.2.2.9. Western Blotting

Cells were washed once with ice-cold PBS and extracted by RIPA lysis buffer (1x TBS, 1% Nonidet P-40, 0.5 % sodium deoxycholate, 0.1 % SDS, 0.004 % sodium azide-Santa Cruz) including 1mM phenylmethylsulfonyl fluoride 1 mM Na orthovanadate and 1% (v/v) protease inhibitor cocktail. The protein concentration was determined by Bradford assay after sonication. Fifty micrograms of cellular protein were separated by 8% SDS-polyacrylamide gel (PAGE) for iNOS and COX-2 and %10 (w/v) SDS-PAGE for MAPK's. After that proteins were electroblotted onto a nitrocellulose membrane. The immunoblot was incubated with primary antibodies overnight with blocking solution (5% skim milk) at 4 °C. Blots were washed three times with Tween 20/Tris-buffered saline (TBST) and incubated with a 1:1000 dilution of secondary antibodies for 2 h at room temperature. Blots were again washed three times with TBST (1M Tris-HCl, 9% NaCl, 0.5% Tween 20) and then visualised by ECL reagent (Amersham Life Science).

3.2.2.10. RNA Isolation and Quantification

Raw 264.7 macrophage cells were seeded in 6 well plates (675.000 cells/well). Cells were pre-treated with compounds and then induced with LPS (1 µg/ml) for 10h. At the end of the incubation total mRNA was isolated using PeqGOLD RNA Pure (Peqlab). The media was discarded and cell monolayer was rinsed with 1x PBS and 500 µl PeqGOLD RNA Pure reagent was added onto the cell monolayer. The cells were lysed and collected into sterile microcentrifuge tubes and 100 µl of chloroform was added. The tubes were then shaken vigorously and incubated for 5 mins at room temperature and then centrifuged at 12000 *x* g for 15 mins at 4 °C. The aqueous phase, which contains the RNA was transferred into a new tube and mixed with equal volumes of isopropanol. The samples were then incubated for 15 mins at 4 °C and centrifuged at 12000 *x* g for 15 mins (4°C). Afterwards the supernatant was removed and RNA pellet was rinsed with 75% (v/v) ethanol and centrifuged at 12000 *x* g for 10 mins at 4°C. RNA pellet was dried with vacuum-dry prior to the removal of supernatant and dissolved in 50 µl Rnase free water. RNA samples were stored at (-80 °C). RNA samples were quantified spectrophotometrically at 260 nm using Rnase free water as blank. Total RNA concentration calculated according to the formula “Concentration of RNA sample=40 x A260 x dilution factor”. The protein concentration in total RNA was checked by measuring the absorbans ratio A260/A280

3.2.2.11. cDNA synthesis

Target RNAs were reverse transcribed using the Quiagen Omniscript RT Kit. 1000 ng of total RNA was transferred into a new tube in 13 µl of Rnase free water. cDNA was synthesized at 37 °C for 1 h using Qiagen Senscript kit. Reaction mixture containing 2 µl 10x Buffer RT, 2 µl dNTP Mix (5 mM each dNTP), 2 µl Oligo-dT primer (10 µM), 1 µl Omniscript Reverse Transcriptase was added to make up a total volume of 20 µl. Samples were incubated at 37 °C for 60 mins. Samples store at (-20 °C).

3.2.2.12. Quantitative Polymerase Chain Reaction

The mRNA expression levels of iNOS and COX-2 genes in the cell line were determined using Quanti-Tech SYBR Green PCR kit in Bio-Rad iCycler iQ5 instrument. Thermal cycling conditions for all primers were as follows: 15 mins 94 °C denaturation followed by 40 cycles of 94 °C for 30 s, annealing at 55 °C for 60 s, and extension at 72 °C for 60 s. and extra extension at 72 °C for 10 mins. Primers were purchased from Quiagen (18SRNA QT02448075, iNOS QT001002275, COX-2 QT00165347).

3.2.2.13. Statistical Analysis

The experiments were performed in triplicate. The results were expressed as mean±standart deviation (SD). Statistical comparisons were made using Student's t-test or Mann Whitney U Test depending on the parametric and non-parametric distribution of the data, respectively, using the Graph Pad Prism 5. Statistically significant difference was defined as $p \leq 0.05$.

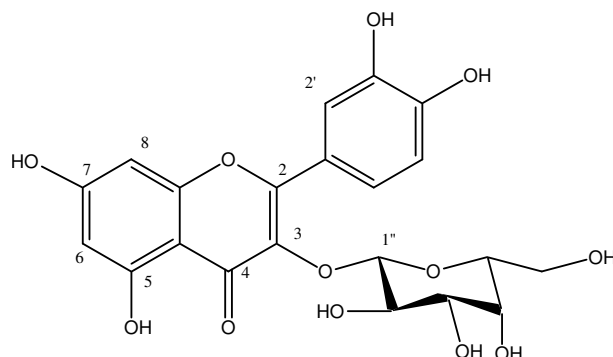
4. RESULTS

The results of the present study are compiled under two sections: Phytochemical Results and Activity Results. The first section includes an elaborate discussion of the structure elucidation of the compounds which were obtained by activity-guided fractionation method. The second section includes the biological activity data performed on extracts, fractions and isolates.

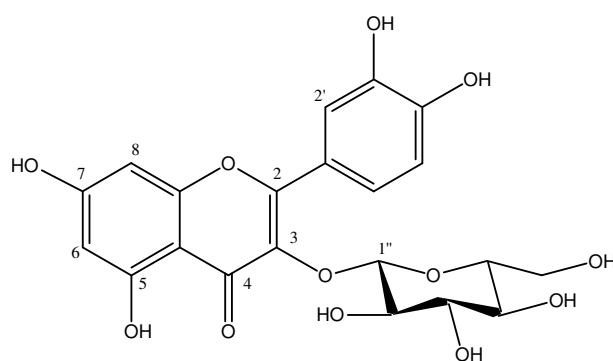
4.1. Phytochemical Results

This section includes structure elucidation of the isolated compounds discussed based on the spectroscopic data. Structure elucidation of the isolated active compounds was carried out by spectroscopic techniques namely; UV, ^1H -, ^{13}C -NMR and 2D-NMR (COSY, HSQC and HMBC) and MS. Structures of the compounds were identified as follows: a mixture of hyperoside (Quercetin-3-*O*- β -galactoside) (major constituent, 2/3 of mixture) and isoquercitrin (Quercetin-3-*O*- β -glucoside, minor, 1/3 of mixture) (**SE-1**); isorhamnetin-3-*O*- β -D-glucoopyranoside (**SE-2**); isorhamnetin-3-*O*-rutinoside (**SE-6**), a mixture of hyperoside (Quercetin-3-*O*- β -D-galactopyranoside, minor constituent, 1/3 of mixture) and isoquercitrin (major, 2/3 of mixture) (**SE-4**) from SE-EtOAc and two new iridoids; Sambulin A and Sambulin B from SE- CHCl_3 and SE-Hexane subextracts respectively.

4.1.1. Structure Elucidation of SE-1 and SE-4 (mixtures of Quercetin-3-O-β-D-glucopyranoside and Quercetin-3-O-β-D-galactopyranoside)



Quercetin-3-O-β-D-galactopyranoside: C₂₁H₂₀O₁₂ (MW:464.08)



Quercetin-3-O-β-D-glucopyranoside: C₂₁H₂₀O₁₂ (MW:464.08)

	SE-1	SE-4
UV λ_{max} (MeOH) nm	256, 266, 352	256, 266, 352
IR ν_{max} (KBr) cm⁻¹	3415, 1655, 1605,	3429, 1654, 1606
¹H-NMR (600 MHz, MeOD)	Figure 11	Figure 12
¹³C-NMR(150 MHz, MeOD)		Figure 13
Positive ion ESI-MS	Figure 14	Figure 15

Compound **SE-1** was obtained as yellow amorphous powder. The molecular formula was assigned to be $C_{21}H_{20}O_{12}$ based on the pseudomolecular ion peak at m/z 487.0847 ($[M+Na]^+$) in HR-ESI-MS spectrum (calculated: 487.0852). The absorption bands at 266 and 356 nm were characteristics of a flavonoid backbone. IR spectrum revealed bands at 3409 cm^{-1} (OH), 1653 cm^{-1} (α, β unsaturated C=O) and aromatic ring (1608 cm^{-1}).

Inspection of the $^1\text{H-NMR}$ spectrum revealed that it was a mixture of two flavonoid glycosides (**Figure 11, Table 56**). The $^1\text{H-NMR}$ spectrum displayed proton resonances of the ABX system of a 3', 4' disubstituted phenol ring at δ 7.66 (d, J: 2.2 Hz); 6.84 (d, J: 8.5 Hz), 7.63 (dd J: 8.5 Hz, J: 2.2 Hz) and the characteristic signals of 5,7 disubstituted A rings of flavones at δ 6.20 and δ 6.39 (d, 1.7 Hz) indicating the presence of flavonol moiety. This was supported by the signals at δ 163.11, 166.74 and at δ 145.96 and 150.00 which were interpreted to be the oxygenated carbons at 5 and 7 positions of the A ring and 3' and 4' positions of the B ring, respectively in the $^{13}\text{C-NMR}$ spectrum. The $^{13}\text{C-NMR}$ signal at 179.57 was assigned to be the carbon atom of the carbonyl group at the 4 position while the resonance at 136.0 was ascribed to C-3. The proton signal at δ 5.25 which was determined to be the anomeric proton of a sugar moiety and the coupling constant revealed the β -anomeric (J: 7.6 Hz) configuration. The other protons of the sugar moiety were determined by COSY spectrum and corresponding carbon atoms were determined by HSQC spectrum. These data were compared with literature and the characteristic signals of quercetin-3-*O*- β -D-glucopyranoside were assigned (201).

The $^{13}\text{C-NMR}$ revealed total of 42 signals including ten signals at sugar region (60-80 ppm). A second β -anomeric proton signal at δ 5.15 (d, J=7.7) along with an extra proton signal at δ 7.84 were appeared in $^1\text{H-NMR}$ spectrum. The ratio of intensities of the β -anomeric proton signal at δ 5.25 and δ 5.15 were calculated to be 3/2. These data indicated that **SE-1** was not completely pure and besides quercetin-3-*O*- β -D-glucopyranoside existence of an additional quercetin hexoside was discussed. The additional signal at δ 7.83 (d, J=2.2) was assigned to be the proton at 2' position of the other quercetin aglycone. When the other carbon signals at the sugar region of the $^{13}\text{C-}$

NMR was examined the second sugar moiety was identified to be β -galactopyranose thus structure of the compound was elucidated to be quercetin-3-*O*- β -D-galactopyranoside. Eventually **SE-1** was identified as a mixture of quercetin-3-*O*- β -D-glucopyranoside and quercetin-3-*O*- β -D-galactopyranoside at a ratio of 2/3. As the molecular weight of the compounds were the same, ESI-MS spectrum proposed a molecular weight of 464.37 as shown in **Figure 14**.

Compound **SE-4** was also obtained as a yellow amorphous powder. The TLC examination of the compounds showed the same *R_f* values with that of SE-1, but yellow color intensities of the spots (characteristic for flavonoids) after spraying with vanillin-sulphuric acid reagent were different. The molecular formula of **SE-4** was also assigned to be C₂₁H₂₀O₁₂ based on the ion peak at *m/z* 487.0847 ([M+Na]⁺) by HR-ESI-MS spectrum. When the ¹H-NMR and ¹³C-NMR spectra were compared to those of **SE-1**, all the spectra were the same except for the ratio of the intensities of the β -anomeric proton signals. A careful inspection of the spectra led to the identification of quercetin-3-*O*- β -D-glucopyranoside and quercetin-3-*O*- β -D-galactopyranoside (3/2 ratio), but this time, quercetin-3-*O*- β -D-glucopyranoside being the major one. The data was consistent with the published data (201).

Table 56: ^1H (600 MHz, MeOD) and ^{13}C -NMR (150 MHz, MeOD) data of Quercetin-3-*O*- β -D-glucopyranoside

	Quercetin-3- <i>O</i> - β -D-glucopyranoside		Quercetin-3- <i>O</i> - β -D-galactopyranoside	
Position	δ_{H} ,ppm (J, Hz)	δ_{C} , ppm	δ_{H} ,ppm (J, Hz)	δ_{C} , ppm
2		158.81		158.53
3		136.00		136.00
4		179.57		179.53
5		163.11		163.07
6	6.20 <i>d</i> (2.4)	99.97	6.20 <i>d</i> (2.1)	99.97
7		166.74		164.11
8	6.39 <i>d</i> (1.7)	94.76	6.39 <i>d</i> (4.1,1.7)	94.76
9		158.58		156.32
10		105.51		103.92
1'		123.14		102.31
2'	δ 7.66 <i>d</i> (2.2)	116.12	7.84 <i>d</i> (2.3)	116.03
3'		145.96		145.86
4'		150.00		149.90
5'	6.84 <i>d</i> (8.5 Hz)	117.58	6.86 <i>dd</i> (8.8,2.9)	117.81
6'	7.63 <i>dd</i> (8.5, 2.2)	123.20	7.59 <i>dd</i> (8.8,2.3)	121.76
1''	5.25 <i>d</i> (7.6)	104.53	5.15 <i>d</i> (8.2)	102.31
2''	3.42 <i>dd</i> (7.6, 5)	75.77	3.53 <i>dd</i> (8;9.3)	73.22
3''	3.48 <i>m</i>	78.44	3.22-3.34 <i>m</i>	75.14
4''	3.35 <i>m</i>	71.26	3.61 <i>d</i> (3.2)	70.07
5''	3.22 <i>m</i>	78.16	3.22-3.34 <i>m</i>	77.23
6''	3.58 <i>dd</i> (12;5)	62.59	3.22-3.34 <i>m</i>	61.98
	3.71 <i>dd</i> (12;2.5)		3.71 <i>dd</i> (12;2.5)	

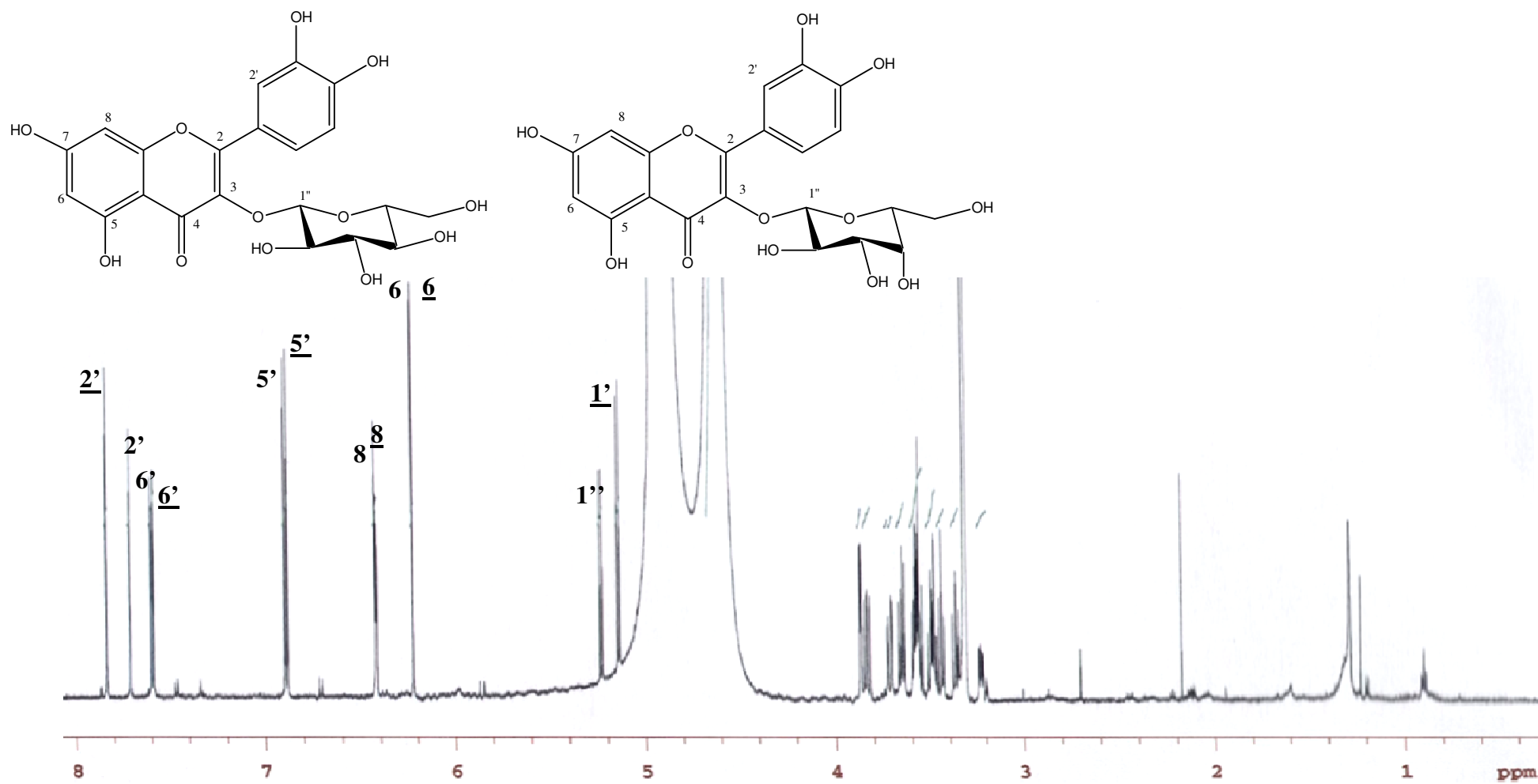


Figure 11: ¹H-NMR (600 MHz, MeOD) spectrum of SE-1 (Quercetin-3-O-β-D-glucopyranoside/Quercetin-3-O-β-D-galactopyranoside (3/2)). The signals of Quercetin-3-O-β-D-galactopyranoside were shown with underlined numbers.

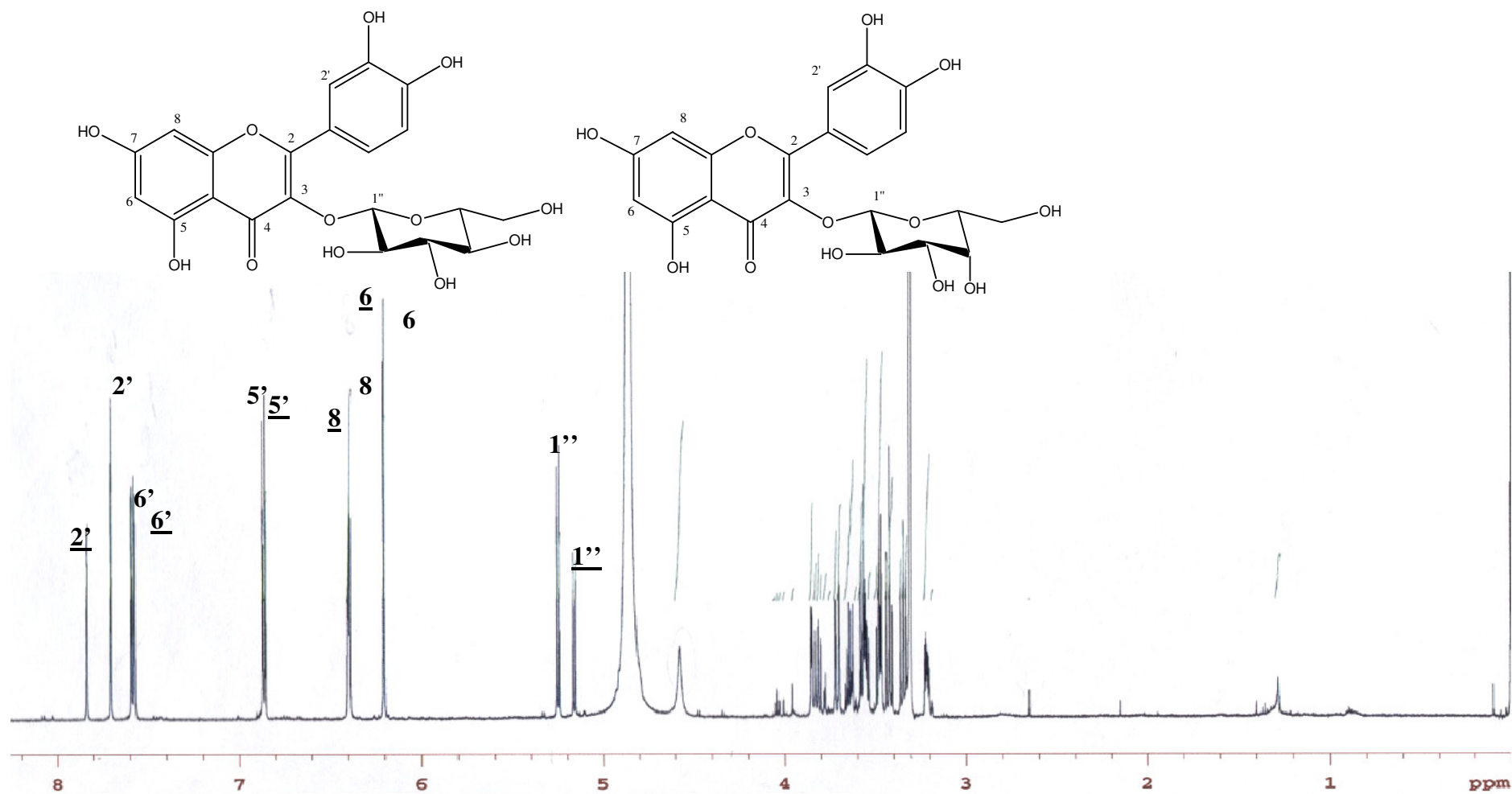


Figure 12: $^1\text{H-NMR}$ (600 MHz, MeOD) spectrum of SE-4 (Quercetin-3-*O*- β -D-glucopyranoside/Quercetin-3-*O*- β -D-galactopyranoside (2/3)). The signals of Quercetin-3-*O*- β -D-galactopyranoside were shown with underlined numbers.

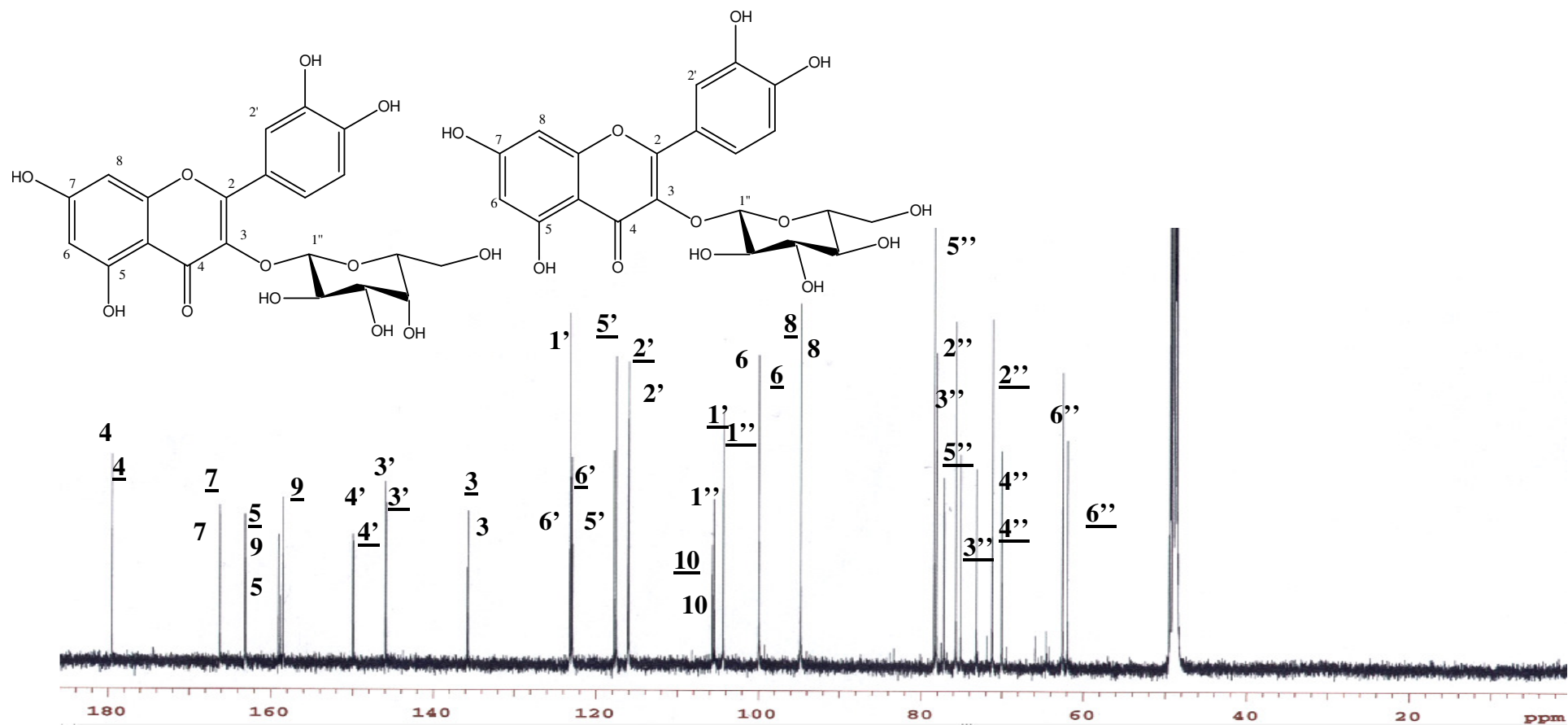


Figure 13: ¹³C-NMR (150 MHz, MeOD) spectrum of SE-4 (Quercetin-3-O-β-D-glucopyranoside/Quercetin-3-O-β-D-galactopyranoside (2/3)). The signals of Quercetin-3-O-β-D-galactopyranoside were shown with underlined numbers.

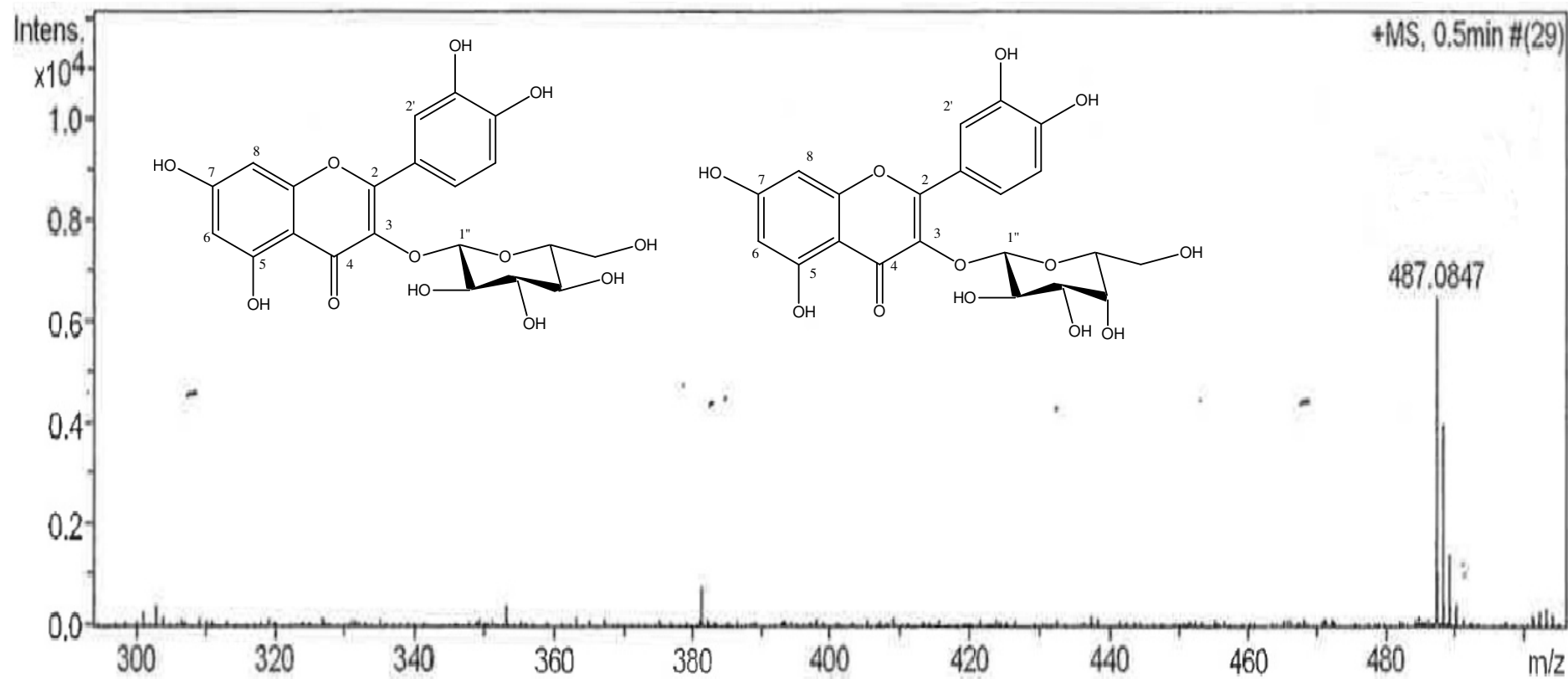


Figure 14: HR-ESI-MS spectra of SE-1 (Quercetin-3-O- β -D-glucopyranoside/Quercetin-3-O- β -D-galactopyranoside (3/2)).

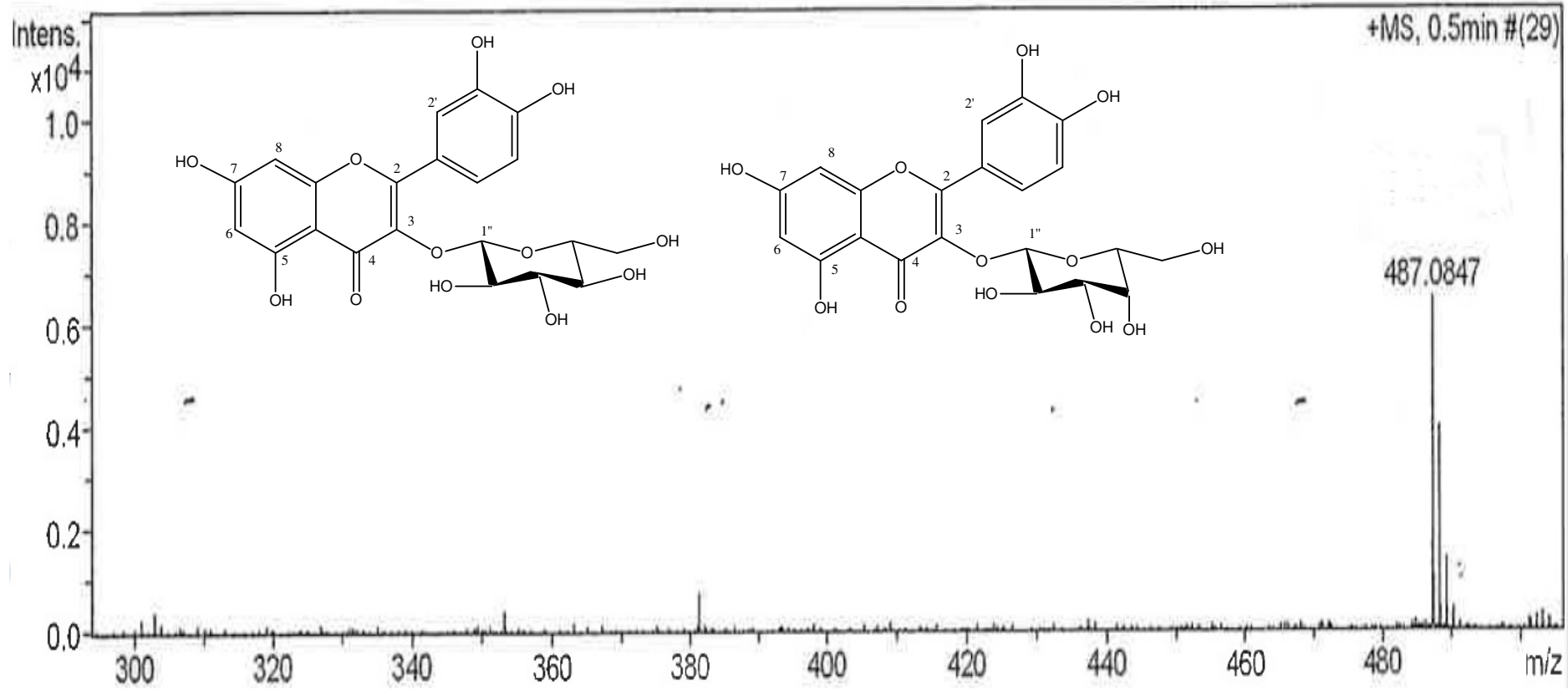
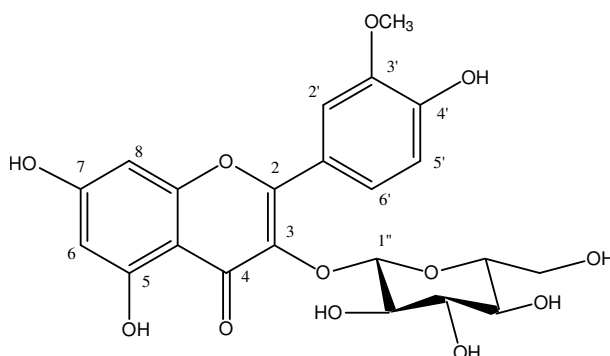


Figure 15: HR-ESI-MS spectra of SE-4 (Quercetin-3-O- β -D-glucopyranoside/Quercetin-3-O- β -D-galactopyranoside (2/3)).

4.1.2. Structure Elucidation of SE-2 (Isorhamnetin-3-O-β-D-glucopyranoside)



Isorhamnetin-3-O-β-D-glucopyranoside: C₂₂H₂₂O₁₂ (MW: 478.11)

UV λ_{max} (MeOH) nm	255, 264, 300, 354
IR ν_{max} (KBr) cm⁻¹	3409, 1653, 1607, 1294, 1057
¹H-NMR (600 MHz, MeOD):	Figure 16
¹³C-NMR(150 MHz, MeOD):	Figure 17

Compound **SE-2** was obtained as a yellow amorphous powder. The molecular formula was assigned to be $C_{22}H_{22}O_{12}$ based on the pseudomolecular ion peak at m/z 501.1003 ($[M+Na]^+$) in HR-ESI-MS spectrum and by NMR spectra (calculated: 501.111). The characteristic UV absorption bands of flavonoids were observed ($\lambda_{max}=264, 354$ nm). IR absorption bands were observed at 3409 cm^{-1} (OH), 1653 cm^{-1} (α, β unsaturated C=O), 1608 cm^{-1} (aromatic ring).

The proton resonances of an ABX system at δ 7.91 (d, J: 2.1 Hz); 6.92 (d, J: 7.9 Hz) and 7.59 (dd J: 7.9 Hz, J: 2.1 Hz) were assigned to the aromatic protons of 2', 5' and 6' positions. These signals indicated the presence of a 3', 4' disubstituted benzen ring. The coupling constants of the signals at δ 6.21 and δ 6.41 (2.1 Hz) were interpreted to be the characteristic signals for 5,7 disubstituted A ring of flavonols. The ^{13}C -NMR signals at δ 160.5 and 165.1 were interpreted to be the carbons at 5 and 7 positions of the A ring and chemical shifts suggested these carbons to be oxygenated. These findings were close to those of **SE-1**. But an additional methoxy signal at 3.94 was observed at the ^1H -NMR spectrum of **SE-2**. All these findings indicated that the aglycone part of **SE-2** was isorhamnetin. The signal at δ 5.37 was determined to be the anomeric proton of a sugar unit and carbon data arising from sugar unit led to the identification of the sugar unit as β -glucose. The large $J_{H1, H2}$ coupling constant (7.3 Hz) of the anomeric proton indicated the β -anomeric configuration of the sugar unit. The elucidation of interconnectivities and correlations between β -glucose and aglycone were accomplished by using 2D NMR (COSY, HMBC) spectra.

Thus, structure of the compound was identified as isorhamnetin-3-*O*- β -glucopyranoside. The ^1H - and ^{13}C - NMR data were also consistent with the published data (202).

Table 57: ^1H (600 MHz, MeOD) and ^{13}C -NMR (150 MHz, MeOD) datas of SE-2 (Isorhamnetin-3-*O*- β -D-glucopyranoside)

Position	δ_{H},ppm (<i>J</i>, Hz)	δ_{C}, ppm
2		157.2
3		130.9
4		178.0
5		160.5
6	6.21 <i>d</i> (2.1)	98.8
7		165.1
8	6.41 <i>d</i> (2.1)	93.6
9		157.0
10		104.1
1'		121.8
2'	7.91 <i>d</i> (2.1)	112.9
3'		149.5
4'		147.0
5'	6.92 <i>d</i> (7.9)	114.7
6'	7.58 <i>dd</i> (7.9, 2.1)	122.4
1''	5.37 <i>d</i> (7.3)	100.2
2''	3.24 <i>dd</i> (7.3, 5.2)	74.4
3''	3.46 <i>t</i> (7.3)	76.6
4''	3.30 <i>m</i>	69.9
5''	3.30 <i>m</i>	77.5
HA-6''	3.56 <i>dd</i> (12.0, 5.6)	61.2
HB-6''	3.72 <i>dd</i> (12.0, 2.3)	
OCH₃	3.94 <i>s</i>	55.4

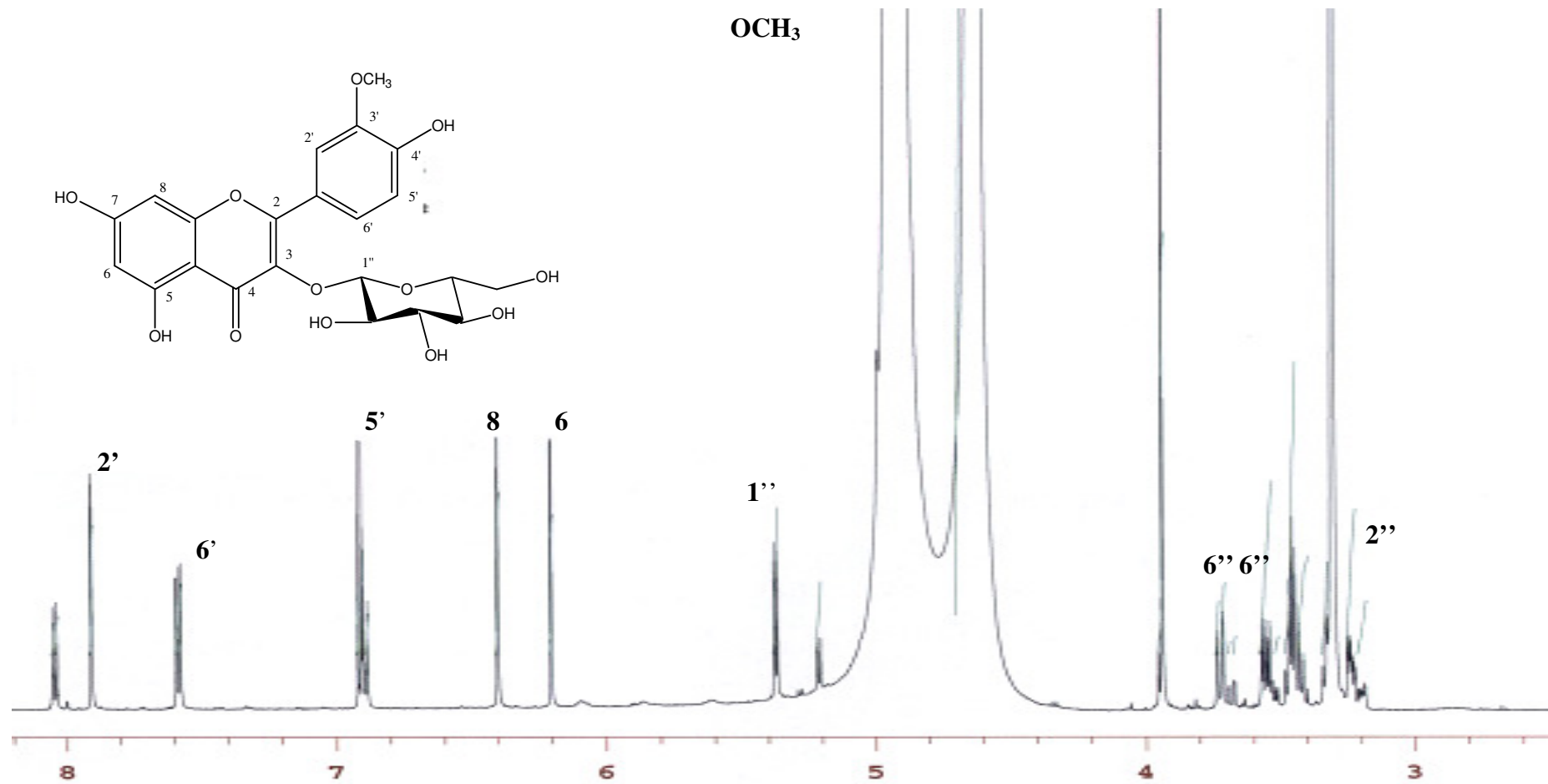


Figure 16: ¹H-NMR (600 MHz, MeOD) spectrum of SE-2 (Isorhamnetin-3-O-β-D-glucopyranoside).

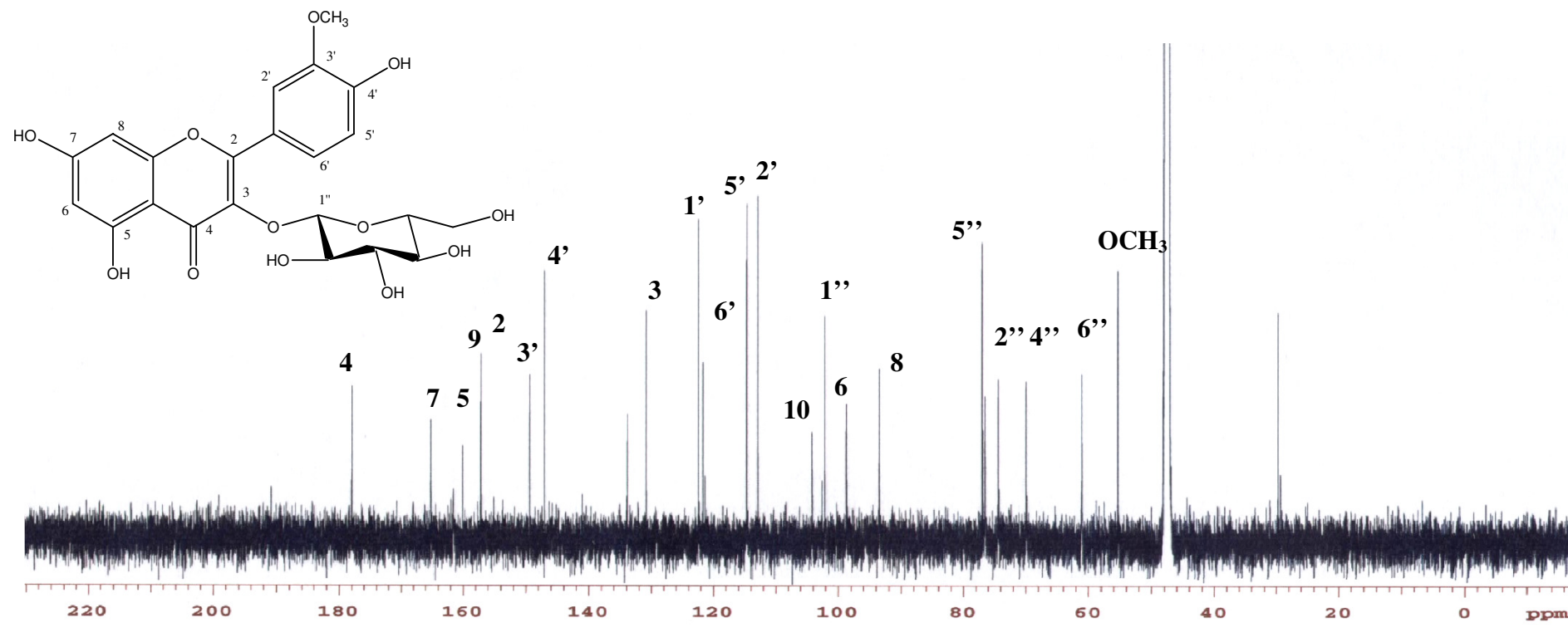
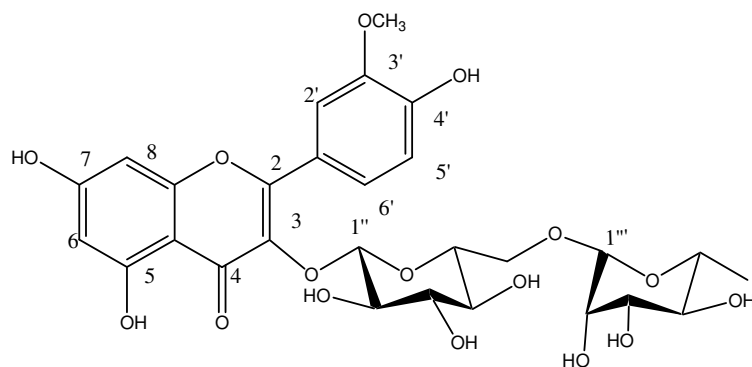


Figure 17: ¹³C-NMR (150 MHz, MeOD) spectrum of SE-2 (Isorhamnetin-3-O-β-D-glucopyranoside).

4.1.3. Structure Elucidation of SE-6 (Isorhamnetin-3-O-rutinoside)



Isorhamnetin-3-O-rutinoside: $C_{28}H_{32}O_{16}$ (MW: 624.16)

UV λ_{\max} (MeOH) nm	254, 266, 354
IR ν_{\max} (KBr) cm^{-1}	3452, 2934, 1665, 1608
1H-NMR (600 MHz, MeOD)	Figure 18
^{13}C-NMR(150 MHz, MeOD)	Figure 19

Compound **SE-6** was obtained as a yellow amorphous powder. The molecular formula of **SE-6** was assigned to be $C_{28}H_{32}O_{16}$ based on the pseudomolecular ion peak at m/z 647.1583 ($[M+Na]^+$) in HR-ESI-MS spectrum (calculated: 647.1690) and by NMR spectra. The characteristic UV absorption bands of flavonoids (λ_{max} = 264, 354 nm) were identified. The UV and IR spectra were also indicative of a flavonoid structure like **SE-1** and **SE-2**.

When the proton and carbon NMR resonances of the compound **SE-6** were examined, it was noticeable that the signals of the aglycone was identical to the compound **SE-2** (isorhamnetin-3-*O*- β -D-glucopyranoside). The ABX system [δ 7.94 (d, J: 1.5 Hz); 6.90 (d, J: 8.5 Hz) 7.63 (dd J: 8.5 Hz, J: 1.5 Hz)], two meta-coupled signal systems [δ 6.20 and δ 6.39 (J: 1.7 Hz)] as well as a methoxyl signal (δ 3.94) were the characteristics of isorhamnetin backbone (**Table 58**). The main difference between two spectra was observed at the sugar region. In addition to the signal at δ 5.22 (7.6 Hz) which was determined to be the β -anomeric proton of glucose moiety, a signal at 4.53 (d, J: 1.7 Hz) was interpreted to be the anomeric proton of α -rhamnosyl moiety. The secondary methyl signal (1.1 d J: 6 Hz) in the up-field region was assigned to be the protons of the 6''' position of the rhamnose. The C-6'' signal (68.57) of glucose showed a downfield shift of 7 ppm in comparison with the corresponding C-6'' signal (61.2) of isorhamnetin-3-*O*- β -glucopyranoside in the ^{13}C -NMR spectrum revealing the glycosidation point of rhamnose to be at C-6'' (OH). These data along with the ESI-MS spectrum which proposed a molecular weight of 624.55 for the compound was consistent with the published literature. Thus SE-6 was identified as isorhamnetin-3-*O*-rutinoside (202).

Table 58: ^1H (600 MHz, MeOD) and ^{13}C -NMR (150 MHz, MeOD) datas of SE-6 (Isorhamnetin-3-*O*- β -rutinoside)

Posisyon	δ_{H} ,ppm (J, Hz)	δ_{C} , ppm
2		159.2
3		132.99
4		179.94
5		164.00
6	6.20 <i>d</i> (1.7)	100.71
7		163.5
8	6.39 (1.7)	95.57
9		159.00
10		104.95
1'		123.40
2'	7.94 <i>d</i> (1.5)	116.40
3'		151.20
4'		148.89
5'	6.90 <i>d</i> (8.5)	116.50
6'	7.63 <i>dd</i> (8.5, 1.5)	124.50
1''	5.22 <i>d</i> (7.6)	103.01
2''	3.45-3.48 <i>m</i>	76.40
3''		78.68
4''	3.35 <i>m</i>	72.10
5''	3.22 <i>ddd</i> (10; 5; 2)	77.86
6''	3.55 <i>dd</i> (12; 5)	68.57
	3.72 <i>dd</i> (12;2.5)	
OCH ₃	3.94 <i>s</i>	57.24
1'''	4.53(<i>d</i> 1.7)	102.93
2'''	3.20-3.80 <i>m</i>	72.45
3'''	3.20-3.80 <i>m</i>	72.80
4'''	3.20-3.80 <i>m</i>	74.38
5'''	3.20-3.80 <i>m</i>	70.28
6'''	1.1 <i>d</i> (6.5)	18.20

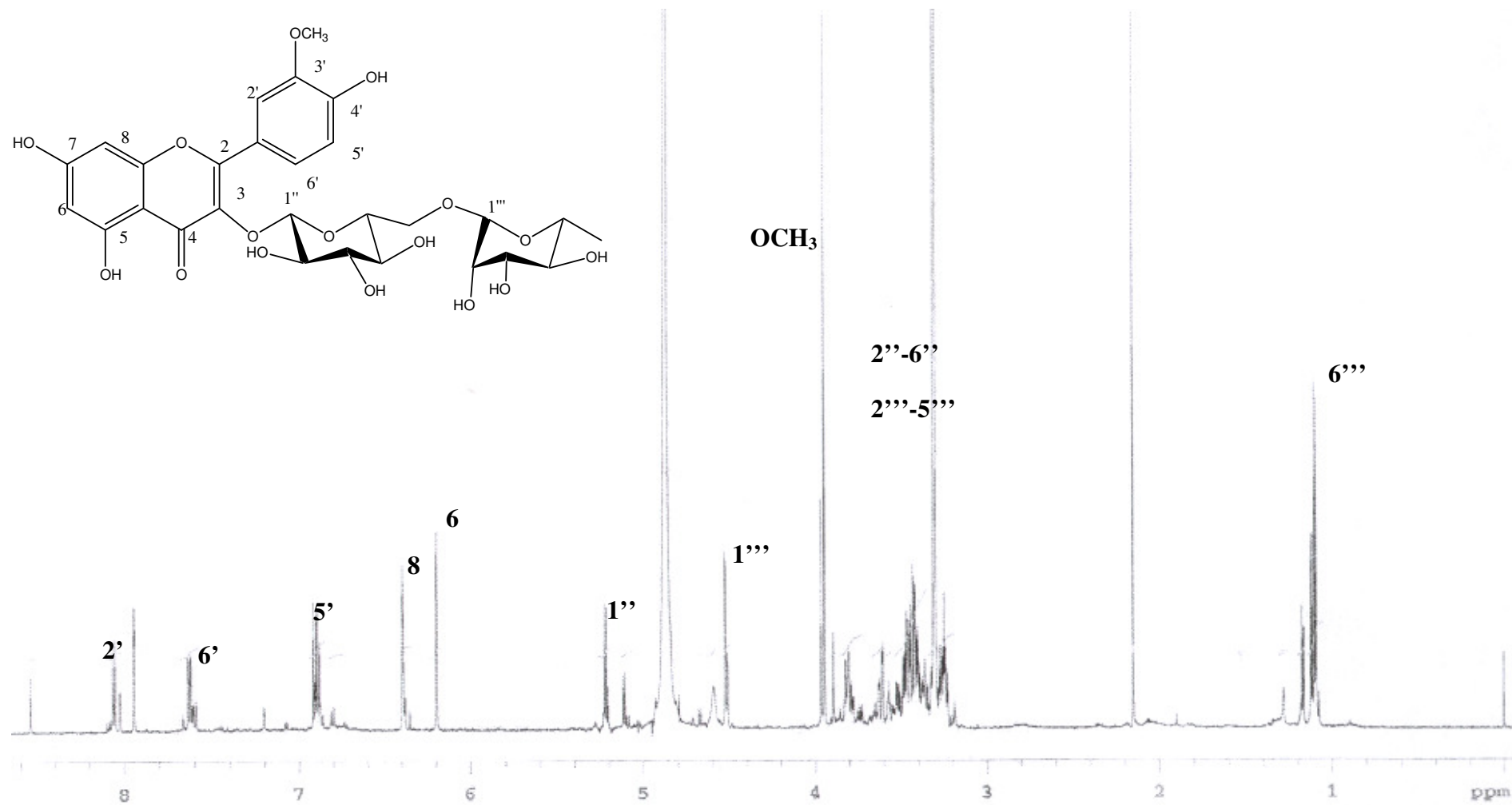


Figure 18: ¹H-NMR (600 MHz, MeOD) spectrum of SE-6 (Isorhamnetin-3-O-rutinoside).

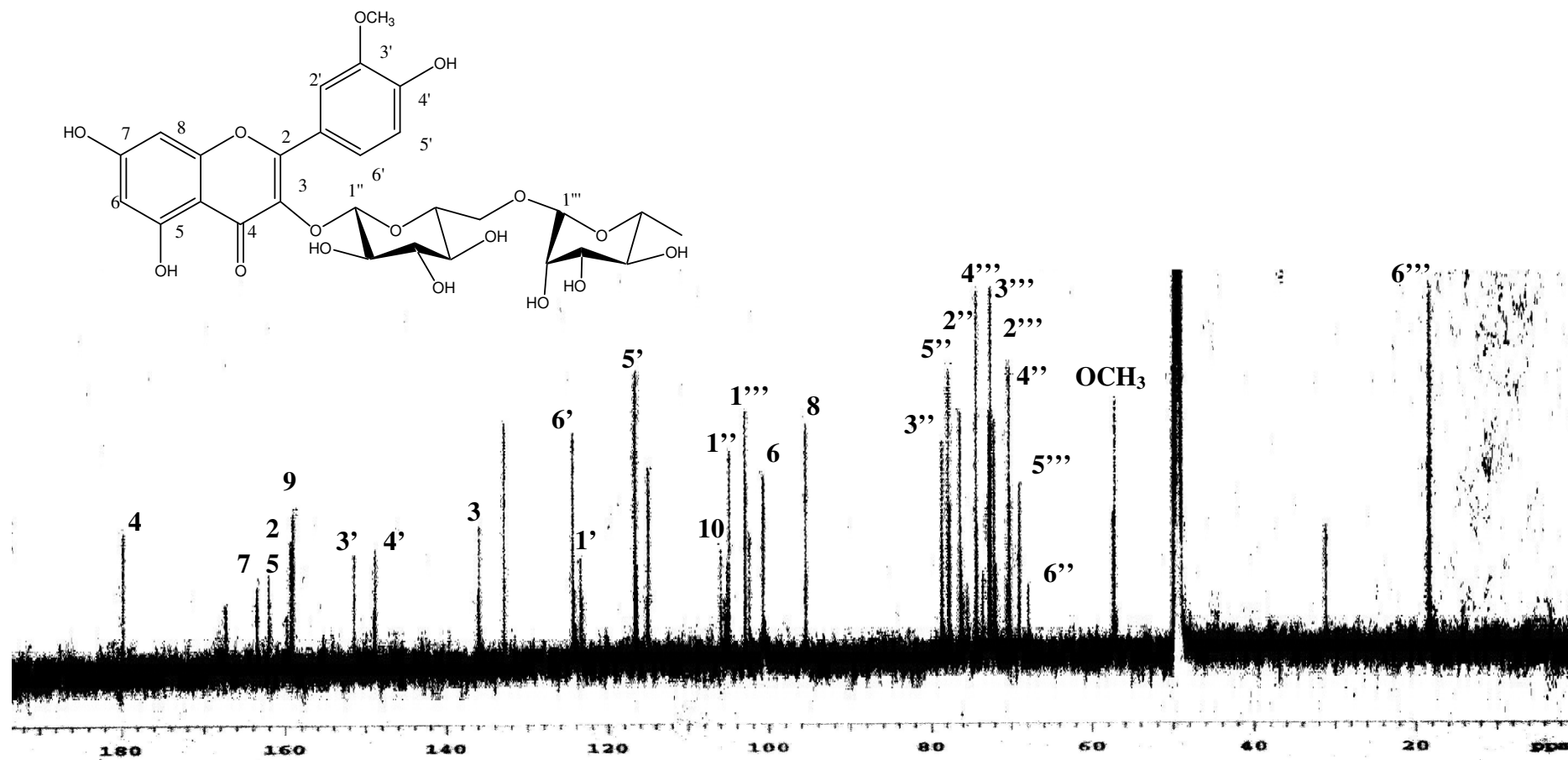
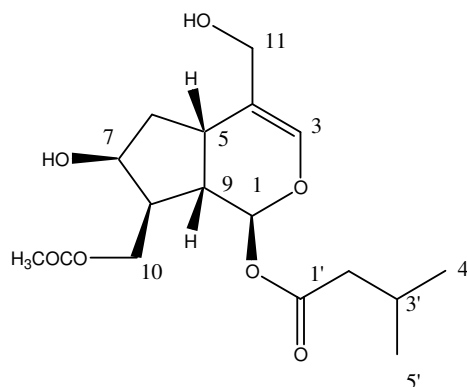
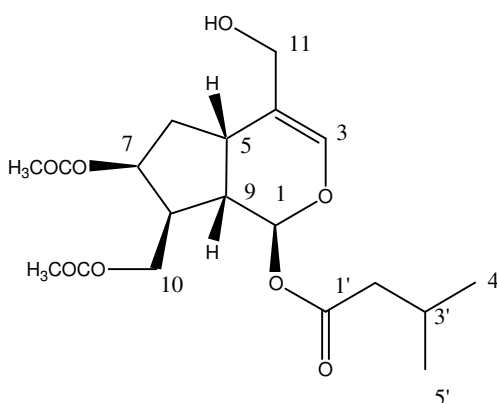


Figure 19: ¹³C-NMR (150 MHz, MeOD) spectrum of SE-6 (Isorhamnetin-3-O-rutinoside).

4.1.4. Structure Elucidation of SECP-2 and SEH-1 (Sambulin A and Sambulin B)



SECP-2 (Sambulin A): $C_{17}H_{26}O_7$ (MW: 342)



SEH-1 (Sambulin B): $C_{19}H_{28}O_8$ (MW: 384)

	SECP-2	SEH-1
UV λ_{\max} ($CHCl_3$) nm	241, 274, 282	241, 274, 282
IR ν_{\max} (KBr) cm^{-1}	3418, 1736, 1235, 1372	3678, 3100, 1738, 1235
$[\alpha]_D^{20}$	-4.6($c=0.33$, $CHCl_3$)	+39.1($c=0.41$, $CHCl_3$)
1H -NMR (600 MHz, MeOD)		Figure 21
^{13}C -NMR(150 MHz, MeOD)	Figure 24	Figure 22
Positive ion ESI-MS	Figure 27	Figure 23
HMBC	Figure 25	
HSQC	Figure 26	

SECP-2 was obtained as a colorless oily substance. The molecular formula, $C_{17}H_{26}O_7$ was deduced from the pseudomolecular ion peak at m/z 343 $[M+H]^+$ in the ESI-MS. It exhibited UV maxima at 241, 274, and 282 nm. IR spectrum suggested the presence of hydroxyl group (3418 cm^{-1}).

Its $^1\text{H-NMR}$ spectrum contained one olefinic (δ_{H} 6.39), two hydroxymethylene (δ_{H} 4.14 and 4.49, δ_{H} 4.10 and 4.02), one methylene (δ_{H} 2.15, 1.96), one oxymethylene (δ_{H} 4.20), two methyne (δ_{H} 3.07, δ 2.60) as well as a hemiacetal (δ_{H} 5.96) signals (**Table 59**). Moreover the $^1\text{H-NMR}$ spectrum displayed two equivalent secondary methyl resonances at δ 0.98 d (J: 6.4 Hz), one methyne and one methylene signal (δ_{H} 2.26) conjugated to a carbonyl function which were observed in a spin system in COSY spectrum, were indicative of the presence of an isovaleryl moiety in **SECP-2**. The signal at 22.2 (2C), 25.6, 43.1 and 171.7 in the $^{13}\text{C-NMR}$ spectrum supported this assumption (120). The signals at δ_{H} 2.09 and the corresponding carbon resonances at δ_{C} 21.0 and 171.8 were attributed to the acetyl moiety. The $^{13}\text{C-NMR}$ spectrum totally contained 17 signals, five of which were ascribed to an isovaleryl unit, while two of which were arising from an acetyl group. The remaining 10 carbon atoms were consistent with C-10 iridoid core. The esterification sites of the acyl units were established by the long range correlations in the HMBC (**Table 59**). Thus, cross peaks between carbonyl carbon of isovaleryl (δ_{C} 171.7) with H-1 (δ_{H} 5.96) and carbonyl carbon of acetyl unit with H₂-10 (δ_{H} 4.49, 4.14) revealed the locations of acyl units to be at C-1 and C-10, respectively. A detailed inspection of 2D-NMR (COSY, HSQC and HMBC) suggested that **SECP-2** is a non-glycosidic iridoid ester resembling to the structure of 10-*O*-acetylpatrinoside-aglycone (120).

To determine the relative stereochemistry of the chiral centers in **SECP-2**, ROESY experiment was performed. ROe cross-peaks were observed between H-1 α / H-8 α , H-7 α / H-8 α showed that these protons lie on the same side (α) of the molecule. Contrary, correlations were observed between H-3/H-11 β , H-5/H-9, H-5/H-6 β , H-5/ H-11 β indicating these protons was at the same side (β). Based on these findings **SECP-2** was identified as a new iridoid and was named as Sambulin A.

SEH-1 (Sambulin B) was also obtained as colorless oily substance, and the molecular formula was interpreted to be $C_{19}H_{28}O_8$ (ESI-MS: $m/z = 407 [M+Na]^+$, $791 [2M+Na]^+$). When the 1H -NMR spectrum of the compound was inspected, it was revealed that this compound was structurally similar to **SECP-2** (Table 59). Its molecular weight was 42, higher than **SECP-2**, indicating the presence of an additional acetyl unit. The signals observed at the 1H -NMR spectrum of the molecule; 5.97 (d J: 4.7), 6.34 (d J:6.5), 3.01 *m*, 5.30 *m*, 2.13 *m* was assigned to be the proton signals of 1, 3, 5, 7 and 9 positions of the iridoid moiety. The signals at δ 22.3, 25.6, 42.9, 171.7' of ^{13}C -NMR spectrum indicated the presence of an isovaleryl group similar to **SECP-2** but the overlapping signals at δ 20.8, δ 21 and 170.2' showed that this molecule has two acetyl groups. The correlation observed in HMBC spectrum between H-1 (δ 5.97) signal of the iridoid and carbonyl group of the isovaleryl moiety (δ 171.7) indicated that esterification with isovaleric acid occurred at the C-1 (OH) of the iridoid part. The second correlation between H2-10 (δ 4.20, 4.16) and carbonyl group (δ 171.8) showed that aglycone was esterified with acetic acid from the C-10 position. Compared to the spectrum of Sambulin A, H-7 signal of this compound shifted to down field about 1 ppm (δ 5.30). Besides ^{13}C -NMR spectrum of **SEH-1** showed that C-7 signal shifted to 1.5 ppm down field, while C-6 and C-8 signals shifted 3 ppm to up field comparing to Sambulin A. Therefore, the second acetyl group was attached to C-7 (OH). Based on these findings the structure of **SEH-1** was elucidated as 7-O-Acetyl derivative of **SECP-2**. A literature survey revealed that **SEH-1** was also new and named as Sambulin B.

Table 59: ^1H (600 MHz, MeOD) and ^{13}C -NMR (150 MHz, MeOD) data of SEH-1 (Sambulin B) and SECP-2 (Sambulin A)

Position	SEH-1 (Sambulin B)		SECP-2 (Sambulin A)		HMBC (C→H)
	δ_{C} (ppm)	δ_{H} (ppm), <i>J</i> (Hz)	δ_{C} (ppm)	δ_{H} (ppm), <i>J</i> (Hz)	
1	91.1	5.97 <i>d</i> (4.7)	91.9	5.96 <i>d</i> (4.7)	H-3/H-8
3	138.4	6.34 <i>s</i>	138.0	6.39 <i>s</i>	H-1/H-5/H ₂ -11
4	116.9	-	118.0	-	H-3/H-5/H ₂ -6/H ₂ -11
5	32.0	3.01 <i>m</i>	32.5	3.07 <i>m</i>	H-1/H-3/H-7/H ₂ -11
6 α	37.2	2.15 <i>m</i>	39.6	2.19 <i>m</i>	H-5
6 β		1.96 <i>m</i>		1.70 <i>m</i>	
7	74.0	5.30 <i>m</i>	71.5	4.20 <i>m</i>	H-9/H ₂ -10
8	43.2	2.34 <i>m</i>	46.6	2.60 <i>m</i>	H ₂ -6
9	42.3	2.13 <i>m</i> †	41.1	2.16 <i>m</i> †	H ₂ -6/H-8/H ₂ -10
10a	62.2	4.20 <i>dd</i> (11.2, 6.9)	62.8	4.49 <i>dd</i> (11.1, 6.9)	H-8
10b		4.16 <i>dd</i> (11.2, 6.9)		4.14 <i>dd</i> (11.1, 6.9)	
11a	62.6	4.09 <i>d</i> (12.3)	62.5	4.10 <i>d</i> (12.3)	H-3
11b		4.00 <i>d</i> (12.3)		4.02 <i>d</i> (12.3)	
7-COCH ₃	21.0	2.05 <i>s</i>			
7-COCH ₃	170.2	-			
10-COCH ₃	20.8	2.04 <i>s</i>	21.0	2.09 <i>s</i>	
10-COCH ₃	170.2	-	171.8	-	H ₂ -10/COCH ₃ (10)
1'	171.7	-	171.7	-	H-1/H ₂ -2'
2'	42.9	2.26 <i>m</i>	43.1	2.26 <i>m</i>	H ₃ -4'/H ₃ -5'
3'	25.6	2.30-2.22 <i>m</i> †	25.6	2.20-2.10 <i>m</i> †	H ₂ -2'/H ₃ -4'/H ₃ -5'
4'	22.3	0.97 <i>d</i> (6.4)	22.4	0.98 <i>d</i> (6.4)	H ₂ -2'/H-3'
5'	22.3	0.97 <i>d</i> (6.4)	22.4	0.98 <i>d</i> (6.4)	H ₂ -2'/H-3'

^a All signals were assigned by 2D NMR (COSY, HSQC, HMBC and ROESY).

†: Overlapping signals

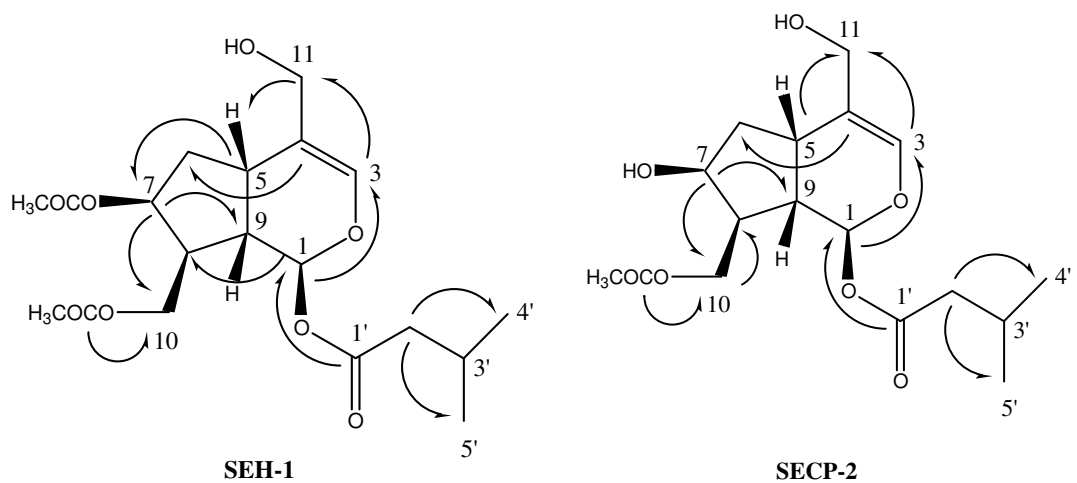


Figure 20: The HMBC correlations of SEH-1 (Sambulin B) and SECP-2 (Sambulin A) (C→H).

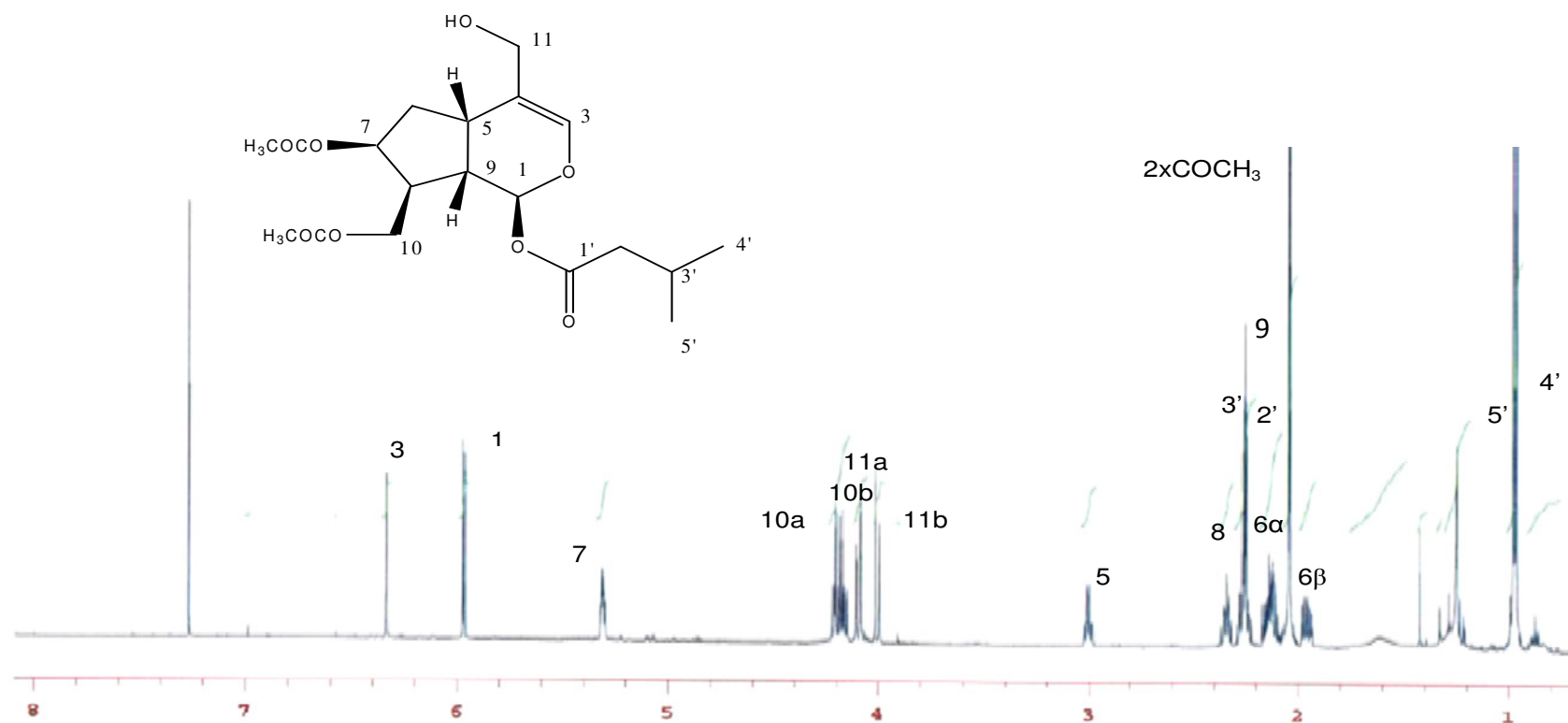


Figure 21: The ¹H-NMR (300 MHz, CDCl₃) spectrum of SEH-1 (Sambulin B) .

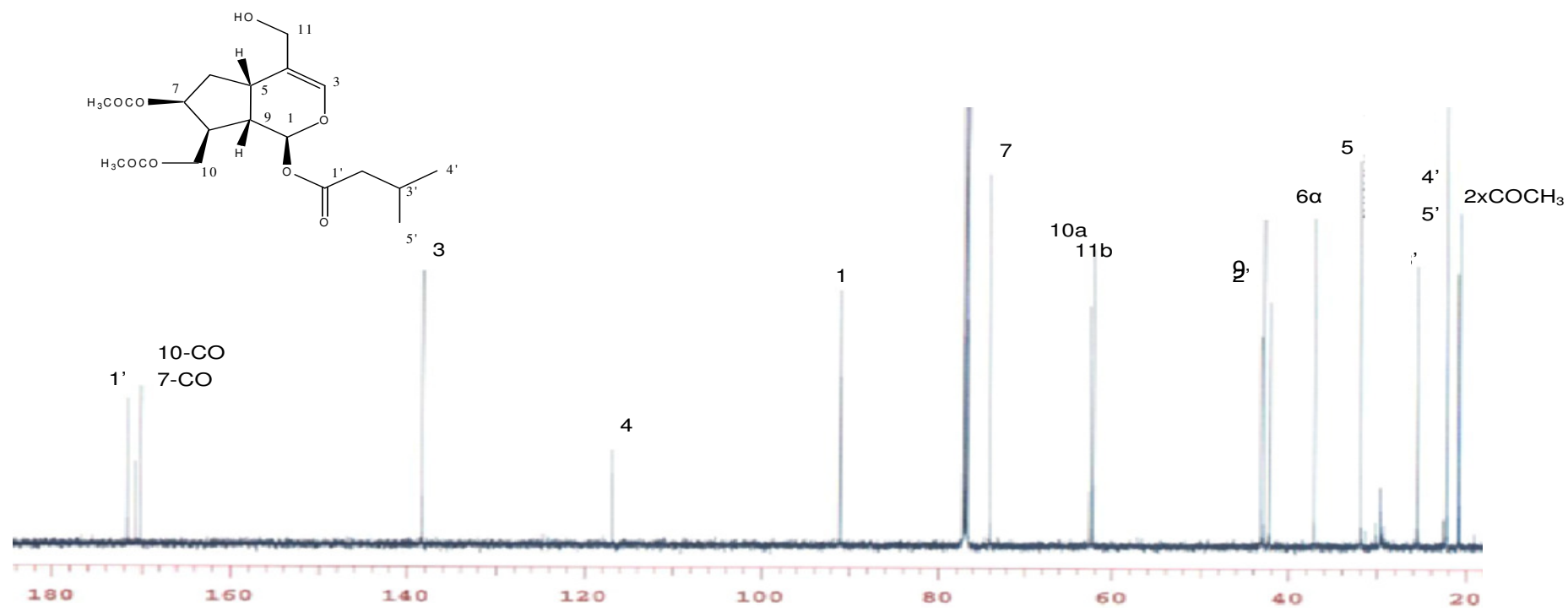


Figure 22: The ¹³C-NMR (150 MHz, CDCl₃) of SEH-1 (Sambulin B).

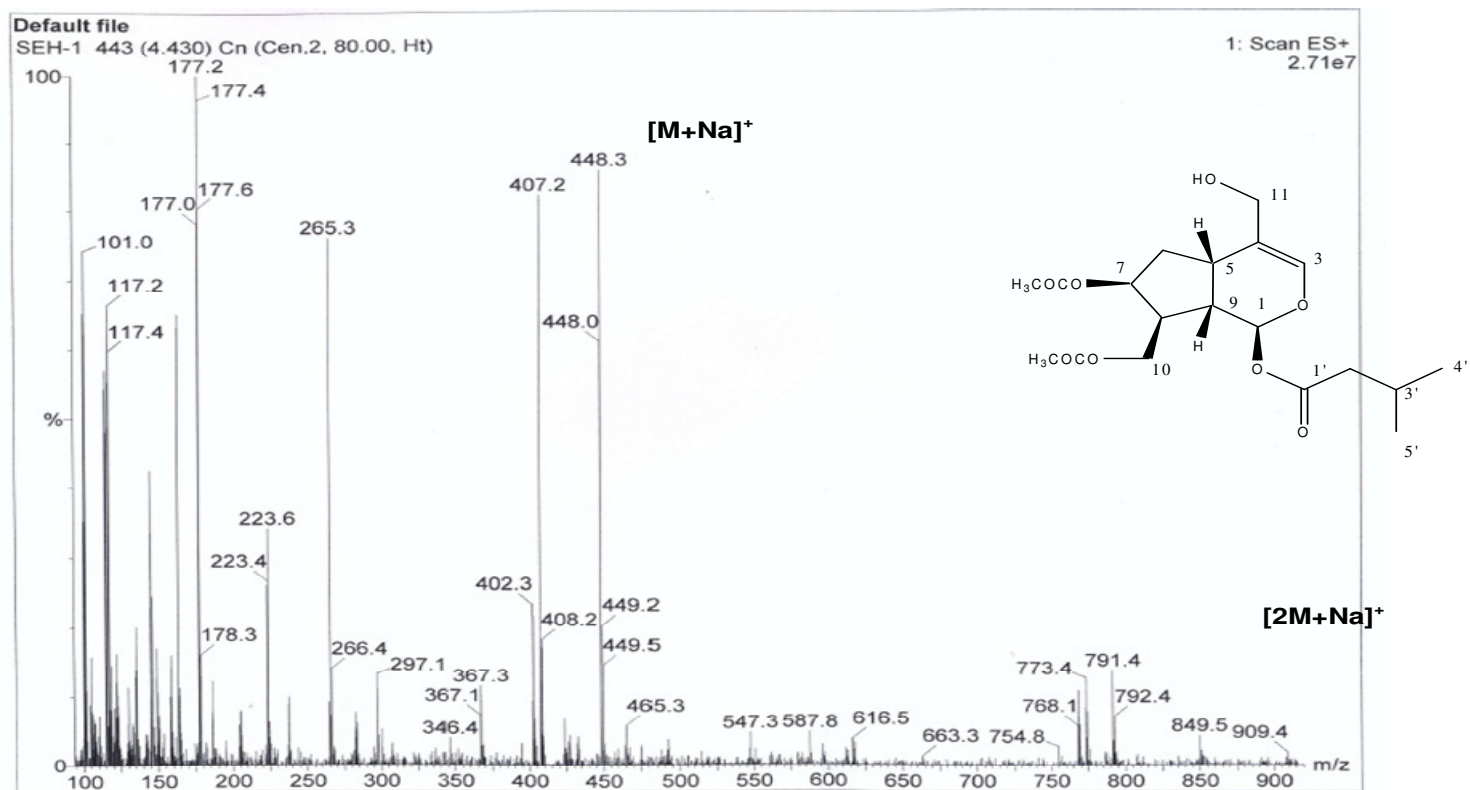


Figure 23: The ESI-MS spectrum of SEH-1 (Sambulin B)

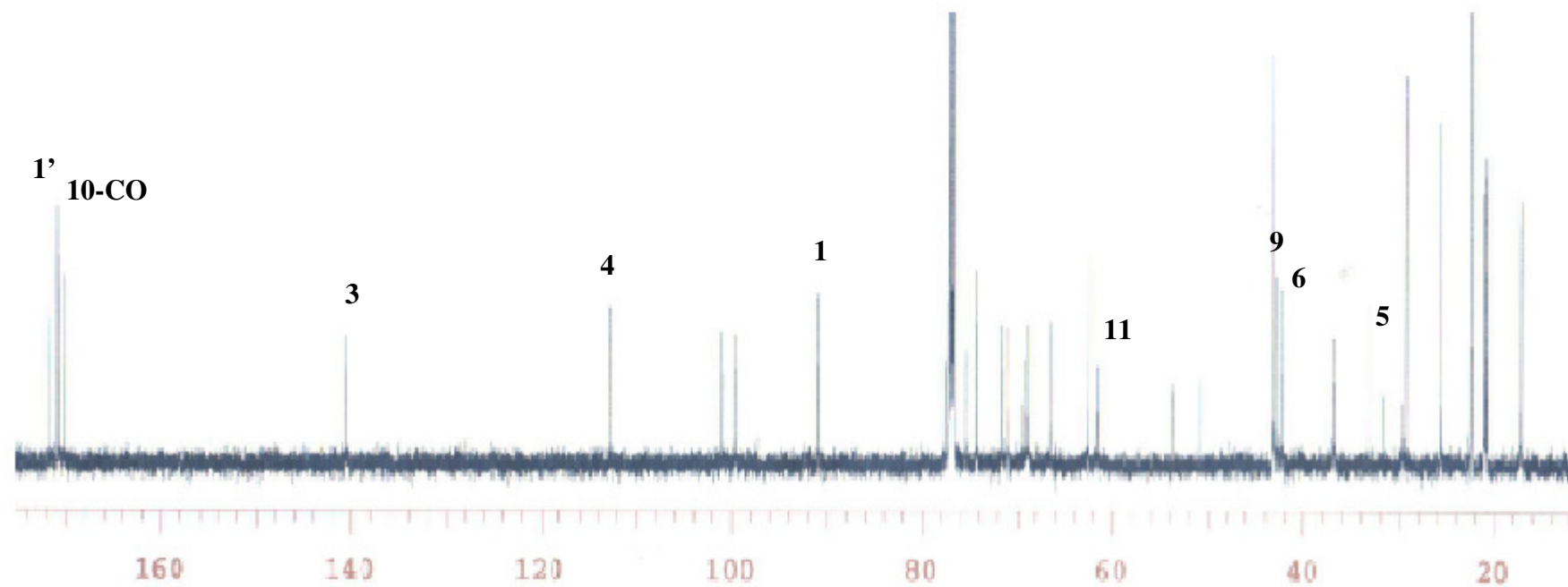


Figure 24: The ^{13}C -NMR (150 MHz, CDCl_3) of SECP-2 (Sambulin A).

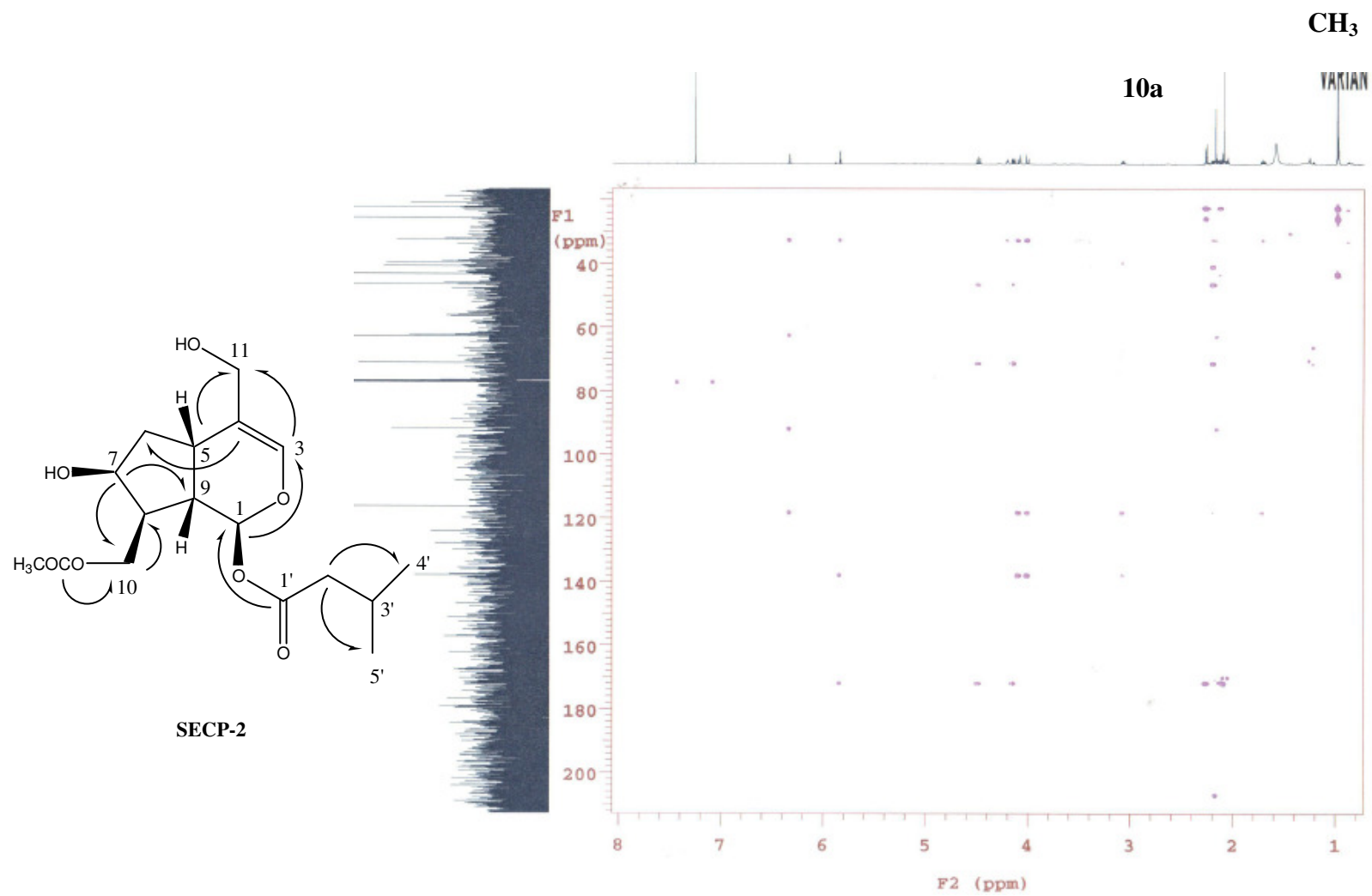


Figure 25: The HMBC spectrum of SECP-2 (Sambulin A)

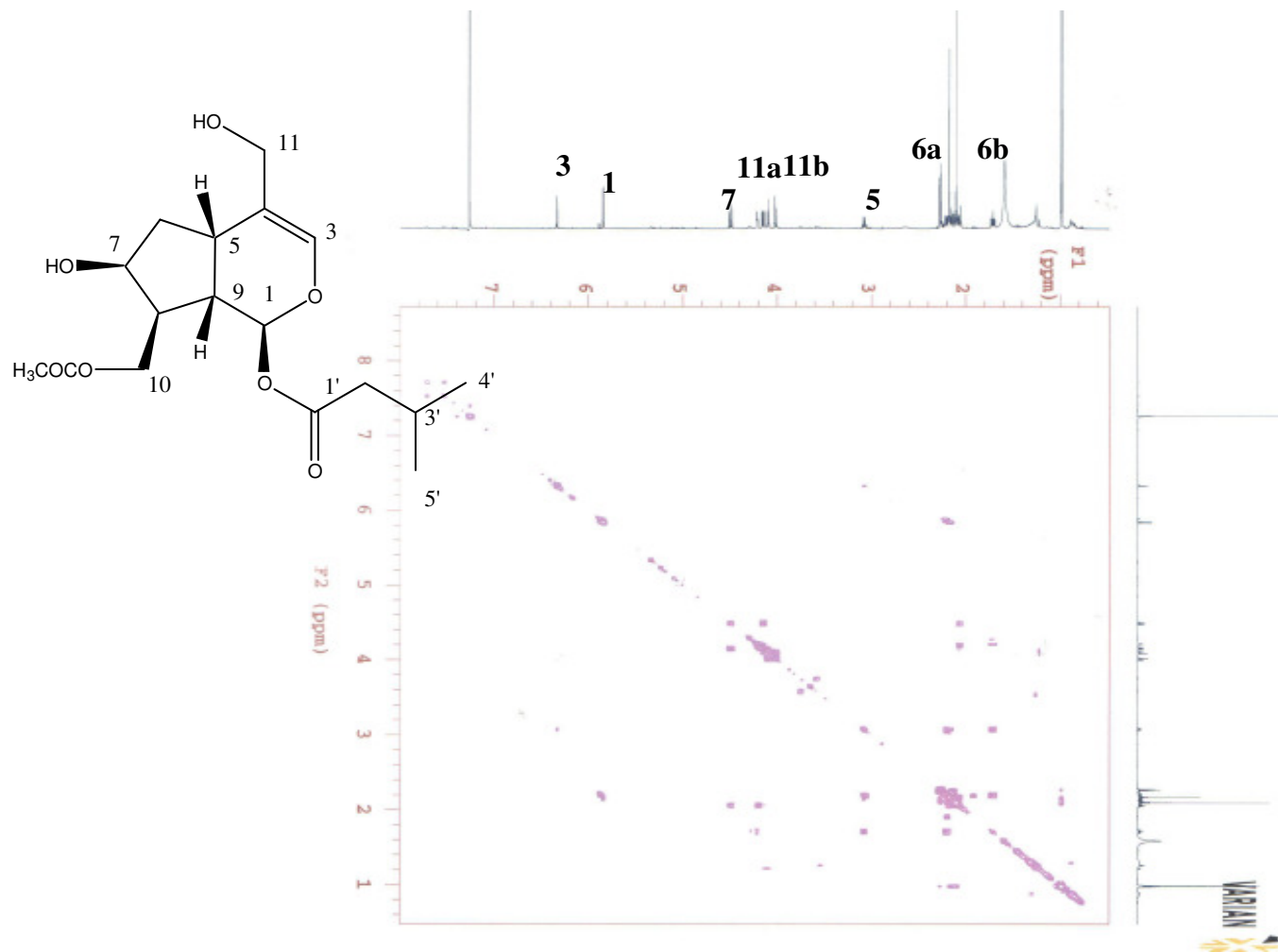


Figure 26: The HSQC spectrum of SECP-2 (Sambulin A)

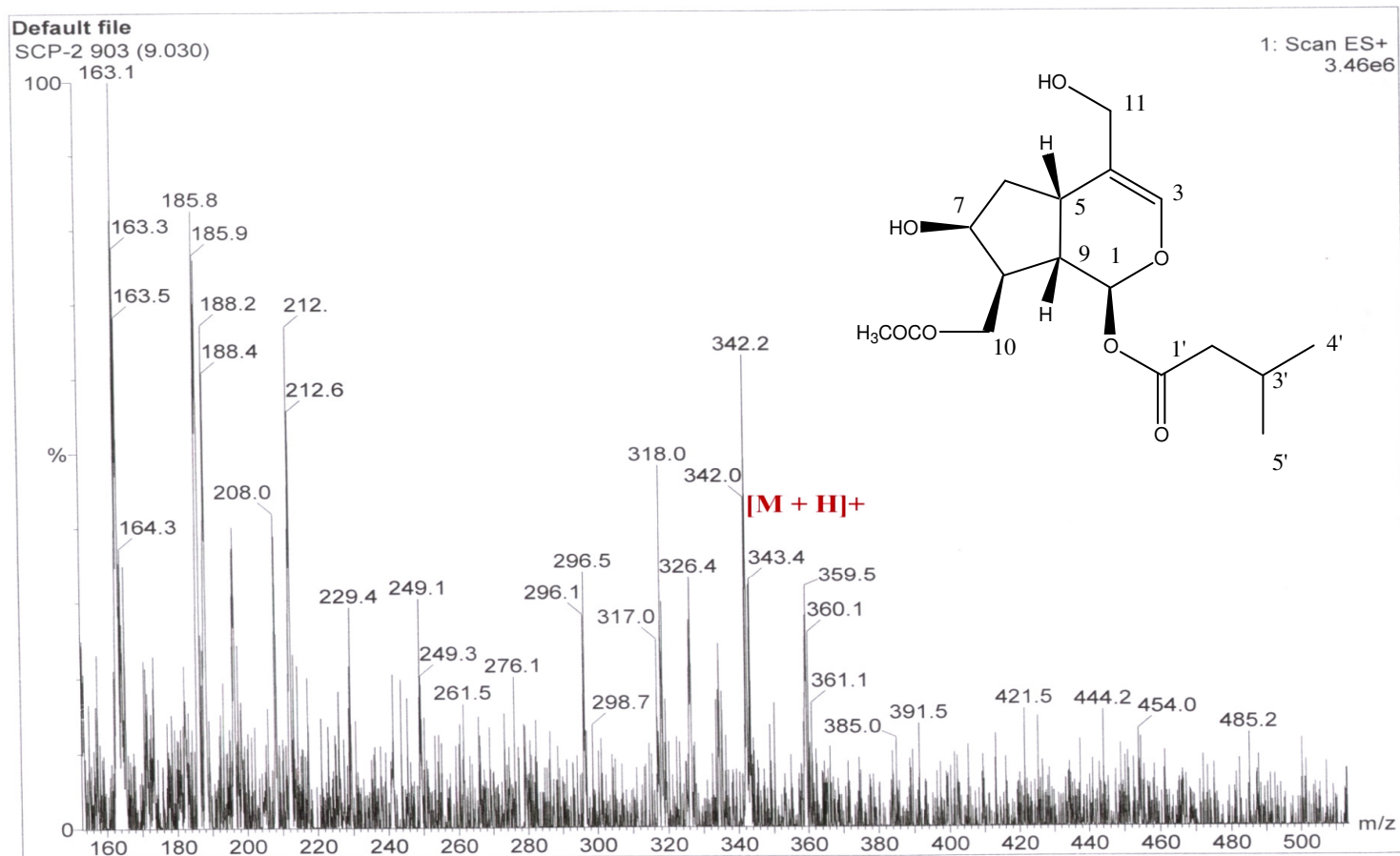


Figure 27: The ESI-MS spectrum of SECP-2 (Sambulin A)

4.1.5. The structure elucidations of SECP-1, SECP-3 and SECP-4

Two compounds were obtained from the active fraction of SE-CHCl₃ (SE_{CHCl₃} II Fr 59-63); **SECP-1** and **SECP-2**. The structure of SECP-2 was elucidated and named as Sambulin A (see 4.1.4. Structure Elucidation of SECP-2 and SEH-1 (Sambulin A and Sambulin B). NMR spectrum of the second compound (**SECP-1**) revealed that it was a mixture which contains **SECP-2** (Sambulin A) as the major component with minor impurities. Similarly, the NMR spectra of **SECP-3** and **SECP-4** were found to be identical which were obtained from the second active fraction of SE-CHCl₃ (SE_{CHCl₃} II Fr.71-72). This spectrum was interpreted to belong to a mixture which was also including **SECP-2** and an additional major iridoid. In spite of successive attempts for the separation of these compounds with similar polarity characteristics we could not achieve to isolate them. Therefore activity studies were performed on **SECP-4** as an active fraction

4.1.6. The structure Elucidation of SNH-1 and SNH-2

The hexane subextract of *S. nigra* was rich in chlorophylls and oily substances. When **SNH-2** was examined on Thin Layer Chromatography, a single spot was observed. However NMR spectrum of the substance revealed that **SNH-2** was not pure but an intense mixture. Due to problems in detection and isolation of the components in such nonpolar mixtures, this fraction was not further processed and submitted to activity studies as an active fraction.

SNH-1 generated a single spot on TLC, but NMR spectrum revealed that it is a mixture of two steroidal compounds with very similar chemical structures. The purification of the compounds could not have been achieved due the similar chemical characteristics of the compounds. Activity studies were conducted with this unidentified steroidal mixture.

4.2. Biological Activity Results

This section includes the results obtained during activity-guided fractionation (AGF) as well as the results obtained from the anti-inflammatory assays conducted on the pure compounds. Extracts and subextracts prepared from the leaves of three plant materials: *S. ebulus*, *S. nigra* (Caprifoliaceae) and *C. laurifolius* (Cistaceae) which are used in Turkish folk medicine for the treatment of rheumatism and related inflammatory diseases were submitted to activity-guided fractionation (AGF) procedures by using Electromobility Shift Assay (EMSA) to evaluate their inhibitory activity on NF- κ B transcription factor in LPS-induced RAW 264.7 macrophages. After the preliminary activity screening performed on these extracts and subextracts, those exerted the highest activities were selected for the following investigations. The activity-guided fractionation and isolation of the active compounds from the extracts achieved through successive chromatographic techniques such as column chromatography, medium pressure liquid chromatography. The structural characterization of the isolated compounds was performed by spectroscopic techniques such as UV, IR, NMR (1D, 2D) and MS as explained in the section “4.1. Phytochemical Results”. The inhibitory activity of the isolated compounds on NF- κ B activation was investigated. In order to determine the anti-inflammatory activity profile of the isolated compounds, their effects on several *in vitro* parameters including: NO, PGE₂, TNF α , IL-1 α , IL-1 β , IL-2, IL-6 were further determined by Griess Assays for NO and ELISA for the rest. The effects of the samples on COX-2 and iNOS protein and mRNA expressions were also analyzed by RT-PCR and Western Blotting. The mechanisms of the anti-inflammatory effects of the most potent compounds were investigated by their effects on I κ B α phosphorylation as well as the effects on the phosphorylation of MAP Kinases; extracellular signal-regulated kinases (ERK1/2), c-JUN-N-terminal kinases (JNK) ve p38 kinases by Western blotting.

4.2.1. Cytotoxicity Assay

All extracts, subextracts, fractions, purified compounds and known inhibitors such as L-NIL, NS-398, parthenolide were evaluated for their non-toxic concentrations using WST-1 cell proliferation assay. None of the tested compounds decreased cell viability more than 20% at their highest concentrations tested as shown in **Table 60**. Samples were not toxic to Raw 264.7 cells at tested concentrations for 24 hr's.

Table 60: Non-toxic concentrations of samples

*Cell viability is not less than %80

Sample	Non-toxic concentrations* (µg/ml)	Non-toxic concentrations* (µM)
SE-MeOH	12.5, 25, 50	
SE-Hex	12.5, 25, 50	
SE-CHCl ₃	25,50,100	
SE-EtOAc	25,50,100	
SE- <i>n</i> -BuOH	25,50,100	
SE-R-H ₂ O	25,50,100	
SN-MeOH	12.5, 25, 50	
SN-Hex	12.5, 25, 50	
SN-CHCl ₃	25,50,100	
SN-EtOAc	25,50,100	
SN- <i>n</i> -BuOH	25,50,100	
SN-R-H ₂ O	25,50,100	
CL-MeOH	25,50,100	
CL-Hex	12.5, 25, 50	
CL-CHCl ₃	12.5, 25, 50	
CL-EtOAc	25,50,100	
CL- <i>n</i> -BuOH	25,50,100	
CL-R-H ₂ O	25,50,100	
SE _{EtOAc} I Fr. 1-4	25,50,100	
SE _{EtOAc} I Fr. 5-10	25,50,100	
SE _{EtOAc} I Fr. 12-14	25,50,100	
SE _{EtOAc} I Fr. 15-20	25,50,100	
SE _{EtOAc} II Fr. 26-34	25,50,100	
SE _{EtOAc} II Fr. 35-49	25,50,100	
SE _{CHCl₃} I Fr. 2-7	25,50,75	

Sample	Non-toxic concentrations* (µg/ml)	Non-toxic concentrations* (µM)
SE _{CHCl3} I Fr. 8-13	25,50,100	
SE _{CHCl3} I Fr. 14-16	25,50,100	
SE _{CHCl3} I Fr. 17-23	25,50,100	
SE _{CHCl3} II Fr. 59-63	25,50,100	
SE _{CHCl3} II Fr. 71-71	25,50,100	
SE _{CHCl3} II Fr. 73-74	25,50,100	
SE _{CHCl3} II Fr. 78-86	25,50,100	
SE _{Hexane} I Fr. 9-12	12.5, 25, 50	
SE _{Hexane} I Fr. 13-15	12.5, 25, 50	
SE _{Hexane} II Fr. 41-49	12.5, 25, 50	
SE _{Hexane} III Fr. 16-19	12.5, 25, 50	
SE _{Hexane} III Fr. 23-25	12.5, 25, 50	
SE _{Hexane} III Fr. 49-52	6.25, 12.5, 25	
SN _{Hexane} I Fr. 1-6	25,50,100	
SN _{Hexane} I Fr. 7-10	25,50,100	
SN _{Hexane} I Fr. 11-16	25,50,100	
SE-1	25,50,100	
SE-2	25,50,100	
SE-4	25,50,100	
SE-6	25,50,100	
SECP-2	12.5, 25, 50	
SECP-4	12.5, 25, 50	
SEH-1	6.25, 12.5, 25	
SNH-1	25,50,100	
SNH-2	25,50,100	
Parthenolide		5,10,20
L-NIL		3,5,10
NS-398		3,5,10
Dexamethasone		5,10,20

4.2.2. Activity-guided Isolation Procedures

Three plant materials (*S. ebulus*, *S. nigra* and *C. laurifolius*) were first extracted with alcoholic solvents and then the alcoholic extracts were partitioned with successive solvent extractions in increasing polarities to obtain subextracts. EMSA was used to evaluate their inhibitory activity on NF- κ B transcription factor on LPS-induced RAW 264.7 macrophages. After the preliminary screening performed on these extracts and subextracts, the subextracts with higher activities were selected for further studies. The activity-guided fractionation (AGF) and isolation of the active compounds were achieved through chromatographic techniques.

Raw 264.7 macrophage cells were pre-treated with extracts and fractions for two hr's followed by LPS (1 μ g/ml) was treatment for 1 hr's. Nuclear fractions were isolated and NF- κ B activity in these nuclear extracts were investigated by EMSA. The specificity of the binding was tested by competition experiment using 200x unlabelled DNA prob.

The effects of the total extracts and subextracts on NF- κ B activation was summarised in **Figure 28** and **Figure 29**. While none of the total extracts from the plants exerted inhibitory effect on NF- κ B activation, some of their subextracts demonstrated significant activities. Among these *S. ebulus* ethyl acetate [SE-EtOAc] (32% NF- κ B inhibition), hexane [SE-Hex] (48% NF- κ B inhibition) and chloroform [SE-Hex] (29% NF- κ B inhibition) subextracts, *S. nigra* hexane [SN-Hex] (30%) subextract and *C. laurifolius* remaining water (20% NF- κ B inhibition) subextract [CL-R-H₂O] were selected for further experimentation. The percentage NF- κ B inhibition was calculated with respect to the control sample treated with LPS only, which represents 100% NF- κ B activation.

The remaining water subextract of *C. laurifolius* (CL-R-H₂O) was fractionated through Amberlite XAD-2 column chromatography, however the fractions obtained were found to be inactive. Therefore, CL-R-H₂O was evaluated for testing the anti-inflammatory activity profile without further fractionation, but increasing the incubation time to four hr's (**Figure 30**). Raw 264.7 macrophage cells were pre-incubated with CL-

R-H₂O at 25, 50 and 100 µg/ml for four hr's. The inhibitory activity of the extract on NF-κB showed a significant increase depending upon the concentration by 45%, 49% and 58% of the control, respectively. A representative image of the experiment was given at **Figure 31**.

S. ebulus EtOAc subextract (SE-EtOAc) was further fractionated by polyamide column chromatography to give four fractions. EMSA was conducted to determine their activities on NF-κB. Three fractions; SE_{EtOAc} I Fr.5-10, Fr.12-14 and Fr.15-20 exerted an inhibition higher than 90% (**Figure 32**). These fractions were then fractionated by successive column chromatography to yield two flavonoid mixtures [a mixture of hyperoside (major constituent, 2/3 of mixture) and isoquercitrin (minor, 1/3 of mixture)] (**SE-1**) and [a mixture of hyperoside (minor constituent, 1/3 of mixture) and isoquercitrin (major, 2/3 of mixture)] (**SE-4**) and two flavonoid glycosides [isorhamnetin-3-*O*-β-D-glucopyranoside] (**SE-2**) and [isorhamnetin-3-*O*-rutinoside] (**SE-6**). These compounds were tested for their inhibitory effects on NF-κB activation using LPS-induced Raw 264.7 cells. These compounds inhibited the activation of NF-κB at a rate of 56%, 52% and 68% of the control, respectively (**Figure 33**). The significantly active compounds were examined for their concentration-dependent activities. The activity of all compounds showed a concentration-dependent increase.. At tested concentrations (25, 50, 100 µg/ml) **SE-4** [a mixture of hyperoside (minor constituent, 1/3 of mixture) and isoquercitrin major, 2/3 of mixture] exhibited the highest activity at the lowest concentration, providing a 35% inhibition (**Figure 36**). While at higher concentrations (50, and 100 µg/ml) **SE-4** provided 53.84% and 64.80% inhibitions of NF-κB activity. On the other hand, **SE-1** [a mixture of hyperoside (major constituent, 2/3 of mixture) and isoquercitrin minor, 1/3 of mixture] was almost inactive at 25 µg/ml concentration, while at 50 and 100 µg/ml concentrations it inhibited the activity of NF-κB by 39.29% and 56.10% as summarised in the **Figure 34**. As shown in **Figure 35**, **SE-2** (isorhamnetin-3-*O*-D-glucopyranoside) provided 22.14, 26.18 and 46.42% of NF-κB inhibition at 25, 50, 100 µg/ml concentrations, respectively. Another flavonoid isolated (**SE-6**: isorhamnetin-3-*O*-rutinoside) from SE-EtOAc, also decreased LPS induced activity of NF-κB at 25, 50, 100 µg/ml concentrations in a concentration-

dependent manner as can be seen at **Figure 37** (15.99, 20.04 and 45.62% of NF- κ B activity obtained for the only LPS treated control sample, respectively).

Among the fractions obtained from the Silica Gel CC of the CHCl₃ subextract of *S. ebulus* (SE-CHCl₃) only SE_{CHCl₃} I Fr.14-16 inhibited NF- κ B activation at 100 μ g/ml (79%) as can be seen at **Figure 38** and **Figure 39**. A rich secondary metabolites profile was observed on TLC control of this fraction (SE_{CHCl₃} I Fr.14-16). Thus this fraction was further fractionated by silica gel column chromatography into four subfractions. The activity was observed only in two subfractions: SE_{CHCl₃} II Fr.59-63 and SE_{CHCl₃} II Fr.71-72 which decreased the NF- κ B activation significantly at 100 μ g/ml. These fractions caused 47% and 43% inhibitions respectively. The first of these fractions yielded **SECP-2** (Sambulin A). Raw 264.7 macrophage cells pre-incubated with Sambulin A for 2 hr's. This molecule decreased the activation of NF- κ B at 44.73, 55.84, 82.50% at 12.5, 25 and 50 μ g/ml concentrations respectively. A representative EMSA image is given at **Figure 42**. The second subfraction yielded **SECP-4**. At 50 μ g/ml concentration **SECP-4** exerted substantial inhibition (74%). At 12.5 and 25 μ g/ml concentrations it provided 53.70 and 69.03% inhibitions. Both compounds exerted concentration-dependent activities (**Figure 43**). Both compounds were significantly active on the lowest concentration tested (12.5 μ g/ml).

The hexane subextract of *S. ebulus* (SE-Hex) fractionated through sephadex column chromatography and MPLC to obtain four fractions; (SE_{Hexane} III Fr. 16-19, SE_{Hexane} III Fr. 23-25, SE_{Hexane} II Fr. 41-49, SE_{Hexane} III Fr. 49-52) along with a pure compound coded as **SEH-1** (Sambulin B). As shown in **Figure 44** and **Figure 45**, out of these fractions only **SEH-1** inhibited LPS-induced NF- κ B activation at 50 μ g/ml (54%). The cell viability was 60% at 50 μ g/ml concentration for that reason the concentration-dependent experiments were conducted at 6.25, 12.5 and 25 μ g/ml concentrations. Sambulin B exerted a concentration-dependent activity; at 12.5 μ g/ml it provided an inhibition of 29.14% and at 25 μ g/ml the inhibition increased to 31.82%. The EMSA image of the concentration-dependent experiment is laid out at **Figure 46**. Parthenolide; a known NF- κ B inhibitor of natural origin, which was applied at 10 μ M and 20 μ M concentrations led to 67% and 83% inhibitions respectively.

Only two of the fractions from *S. nigra*; SN_{Hexane} I Fr.11-16 and Fr.17-25 led to an inhibition of 70% and 79% at 100 µg/ml concentration, respectively (**Figure 38, Figure 39**). **SNH-1** and **SNH-2** were identified as the subfractions responsible for the activity of these fractions. The activities of both subfractions were higher than 70% at 50 µg/ml concentration. For that reason both fractions were evaluated for their concentration-dependent activities. **SNH-1** exerted a concentration-dependent inhibitory activity against LPS-induced NF-κB activity at 12.5, 25 and 50 µg/ml concentrations (42.25, 62.00 and 73.35% inhibitions). **SNH-2** also inhibited the activity of LPS-induced NF-κB but the activity did not change substantially with increasing concentrations (66.00, 77.69 and 78.38%) (**Figure 40, Figure 41**).

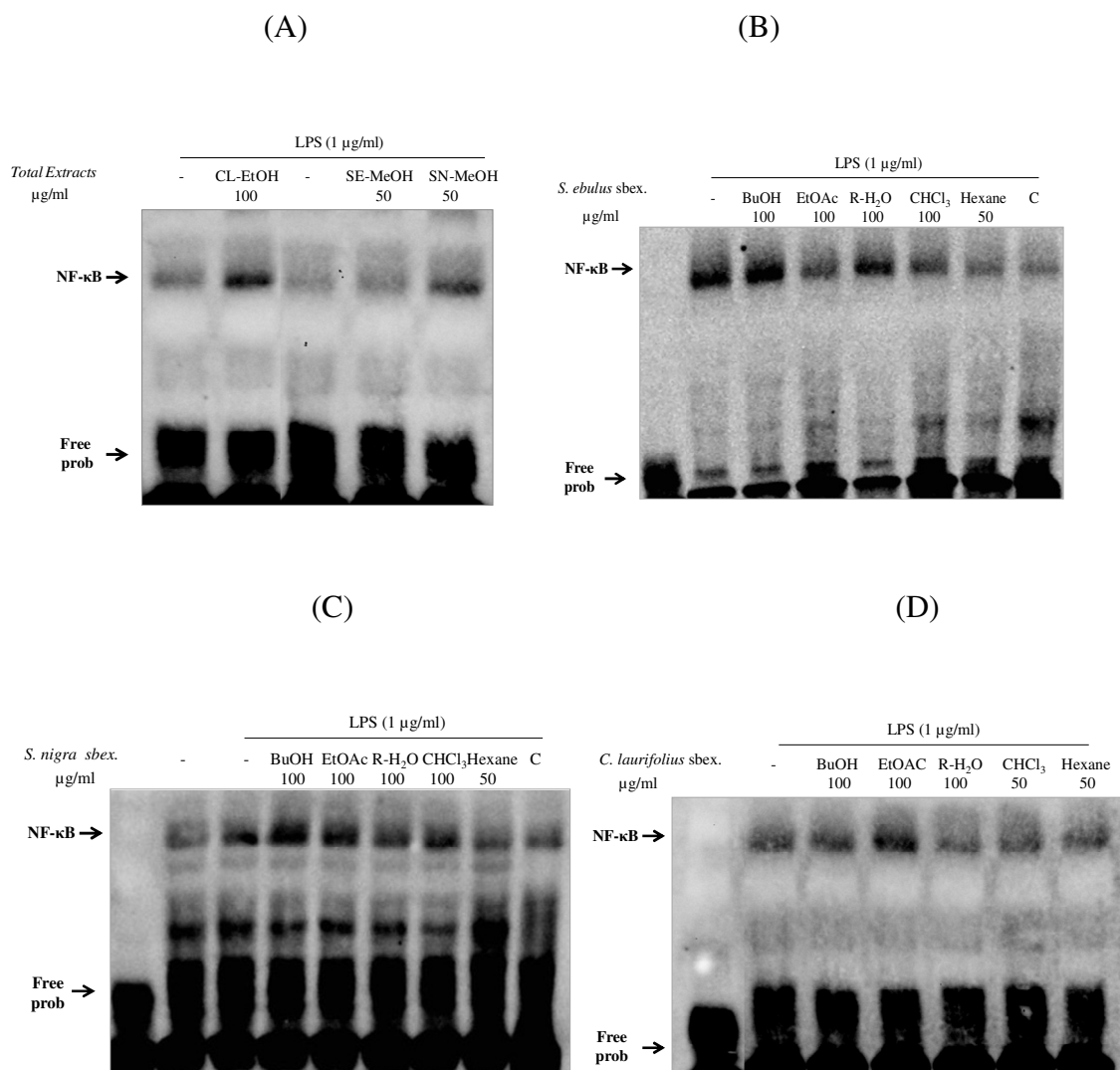
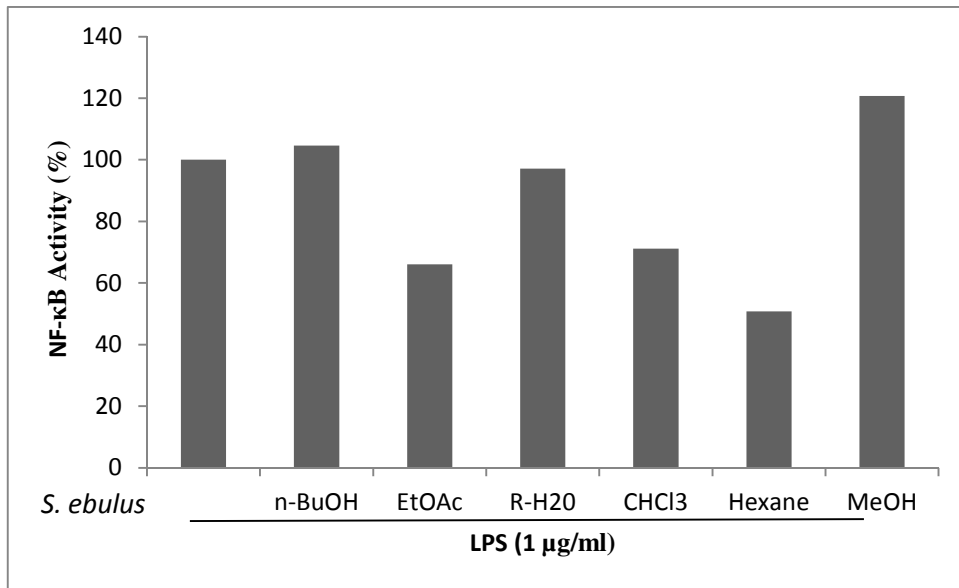
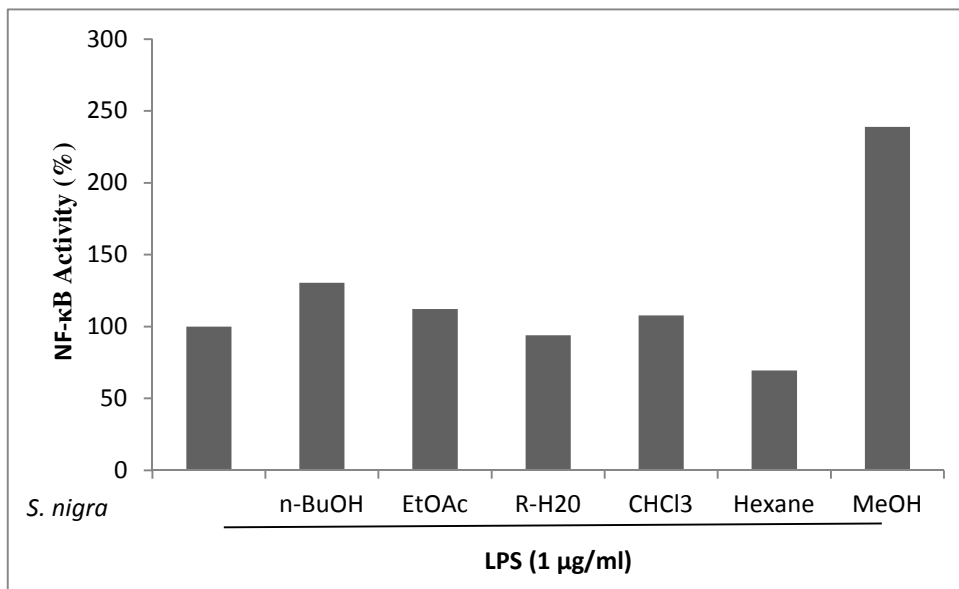


Figure 28: EMSA images of the total extracts and subextracts. Effects of total extracts (A) and subextracts of *S. ebulus* (B), *S. nigra* (C), *C. laurifolius* (D) on the activation of NF-κB. Raw 264.7 macrophage cells were pre-treated with extracts and subextracts for two hr's and then induced with LPS (1 μg/ml) for 1 hr. Nuclear fractions were isolated and evaluated by EMSA. C: 200x unlabelled prob.

A)



B)



C)

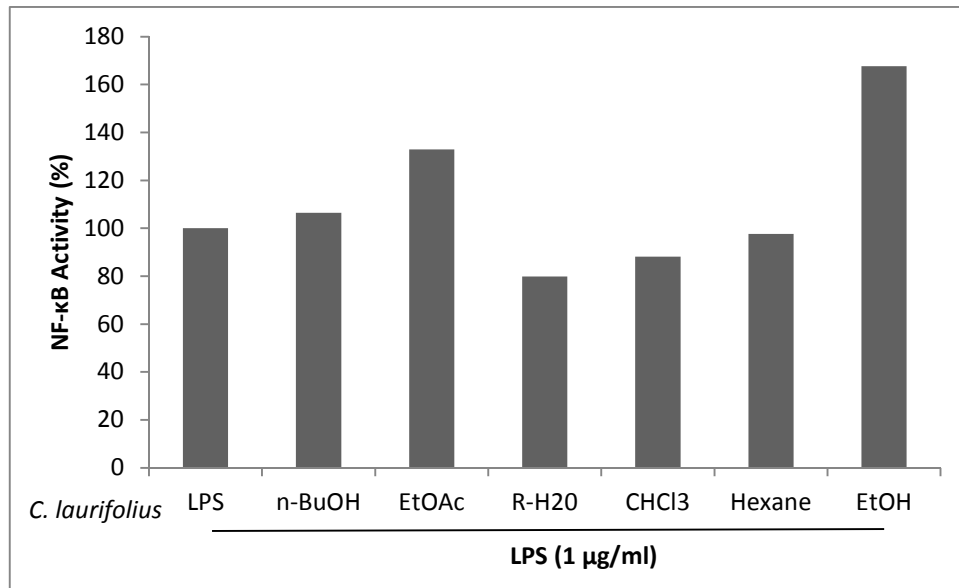
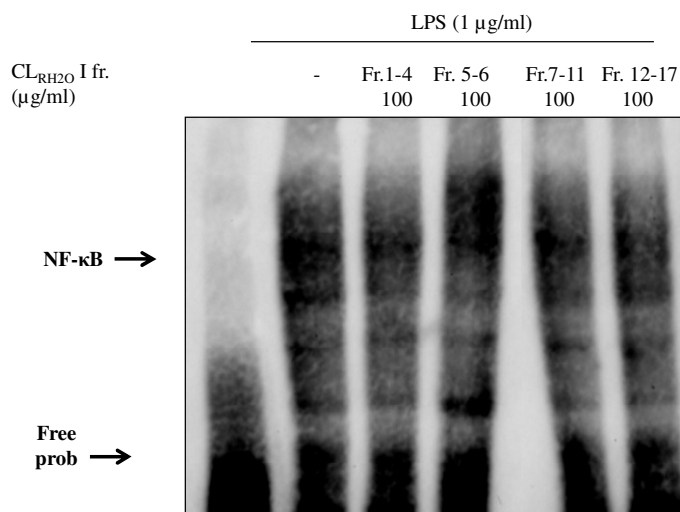


Figure 29: Densitometric analysis of NF-κB inhibitory activities obtained for total extracts and subextracts. Band intensities were evaluated by densitometric analysis using Image J and relative intensities were calculated; subextracts of *S. ebulus* (A), *S. nigra* (B), *C. laurifolius* (C). NF-κB activity recorded for Raw 264.7 cells treated only with LPS represents 100%.

A)



B)

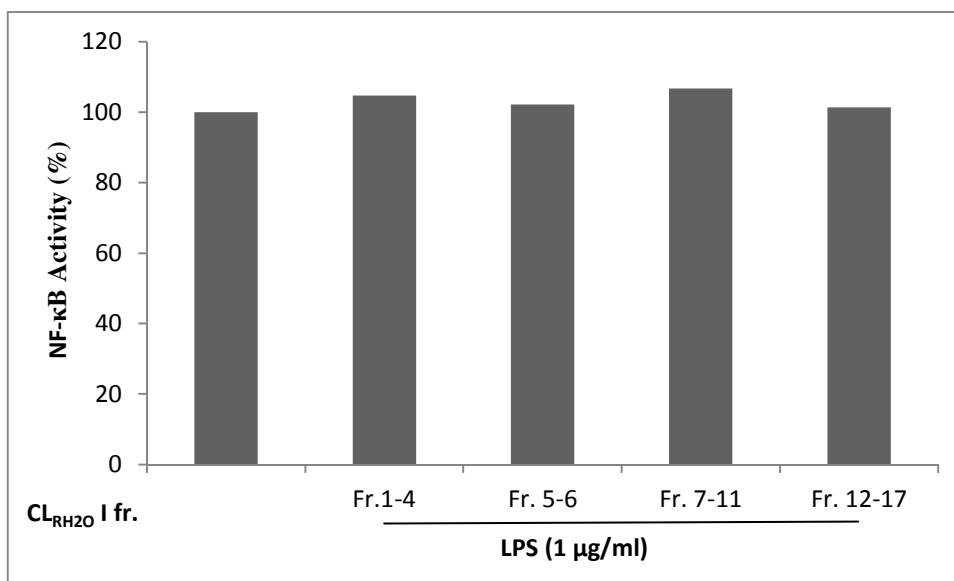
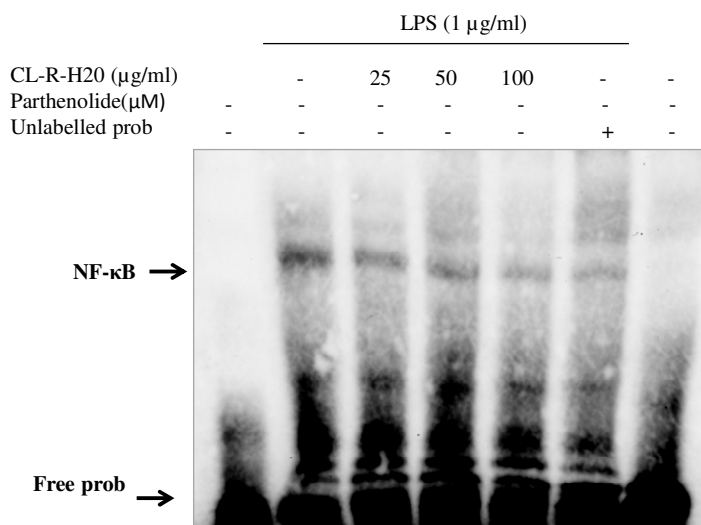


Figure 30: The NF-κB inhibitory activities of the fractions obtained from CL-R-H₂O. (A) EMSA image of the fractions obtained from CL-R-H₂O through Amberlite XAD-2 column chromatography on the activation of NF-κB. (B) The NF-κB inhibitory effects of fractions obtained from *C. laurifolius* remaining water Amberlite XAD-2 column chromatography. Band intensities were evaluated by densitometric analysis using Image J and relative intensities were calculated. NF-κB activity recorded for Raw264.7 cells treated only with LPS represents 100%. Raw 264.7 macrophage cells were pre-treated with extracts and fractions for two hr's and then induced with LPS (1 μg/ml) for one hr. Nuclear fractions were isolated and evaluated by EMSA.

A)



B)

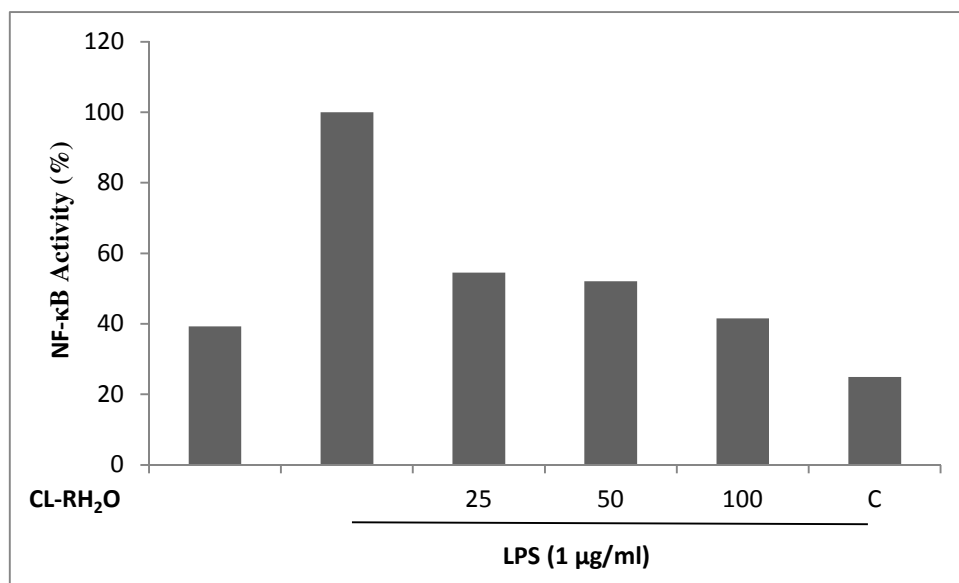
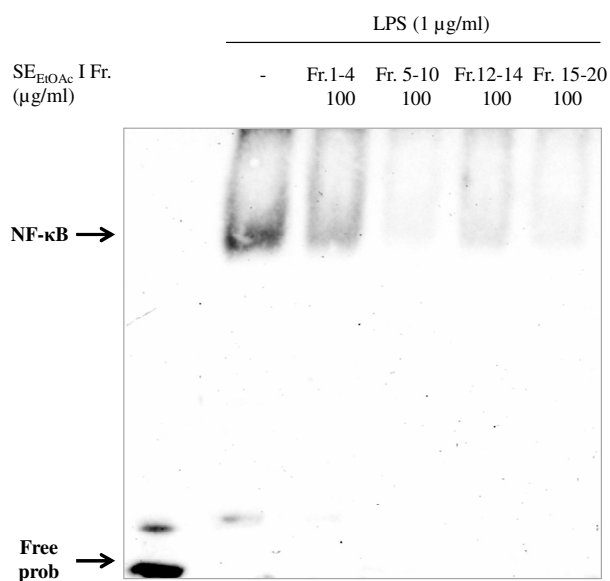


Figure 31: The concentration-dependent NF- κ B inhibitory activity of CL-R-H₂O. (A) The EMSA image of the concentration-dependent effects of CL-R-H₂O. (B) The inhibitory effects of CL-R-H₂O on the activation of NF- κ B. Band intensities were evaluated by densitometric analysis using Image J and relative intensities were calculated. NF- κ B activity recorded for Raw264.7 cells treated only with LPS represents 100%. C: competition experiment with 200x unlabelled probe. Raw 264.7 macrophage cells were pre-treated with the fraction for two hr's and then induced with LPS (1 $\mu\text{g/ml}$). Nuclear fractions were isolated and evaluated by EMSA.

A)



B)

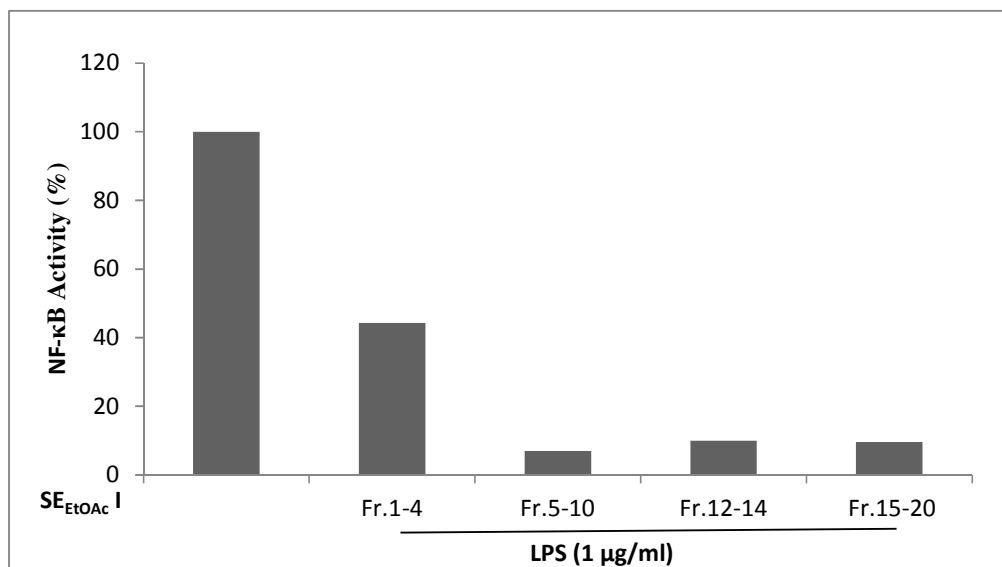


Figure 32: The NF-κB inhibitory activities of the fractions obtained from polyamide column chromatography of SE-EtOAc. (A) EMSA images showing the effects of the fractions on the activation of NF-κB. (B) The inhibitory effects of SE_{EtOAc} I fractions on the activation of NF-κB. Band intensities were evaluated by densitometric analysis using Image J and relative intensities were calculated. NF-κB activity recorded for Raw264.7 cells treated only with LPS represents 100%. Raw 264.7 macrophage cells were pre-treated with fractions for two hr's and then induced with LPS (1 μg/ml) for one hr. Nuclear fractions were isolated and investigated by EMSA

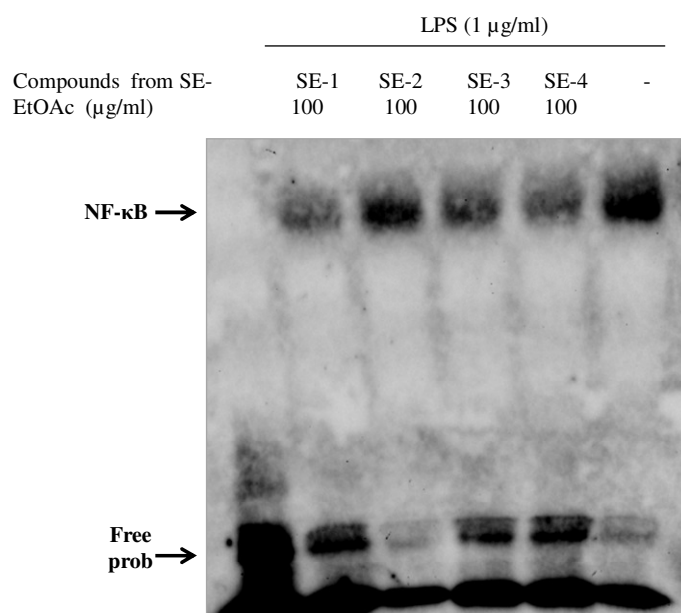
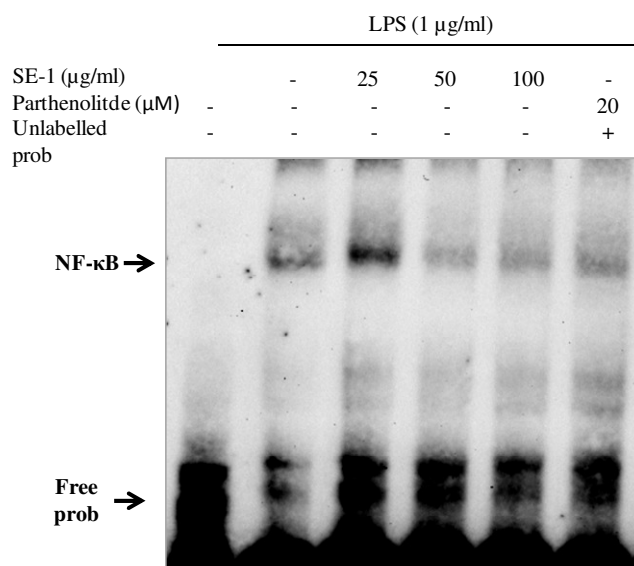


Figure 33: EMSA image showing the effects of the flavonoids obtained from SE-EtOAc on the activation of NF- κ B. Raw 264.7 macrophage cells were pre-treated with extracts and fractions for two hr's and then induced with LPS ($1 \mu\text{g/ml}$) for one hr. Nuclear fractions were isolated and investigated by EMSA. SE-1: mixture of hyperoside (major constituent, $2/3$ of mixture) and isoquercitrin (minor, $1/3$ of mixture), SE-2: isorhamnetin-3-*O*-D-glucopyranoside, SE-4: a mixture of hyperoside (minor constituent, $1/3$ of mixture) and isoquercitrin (major, $2/3$ of mixture), SE-6: isorhamnetin-3-*O*-rutinoside.

A)



B)

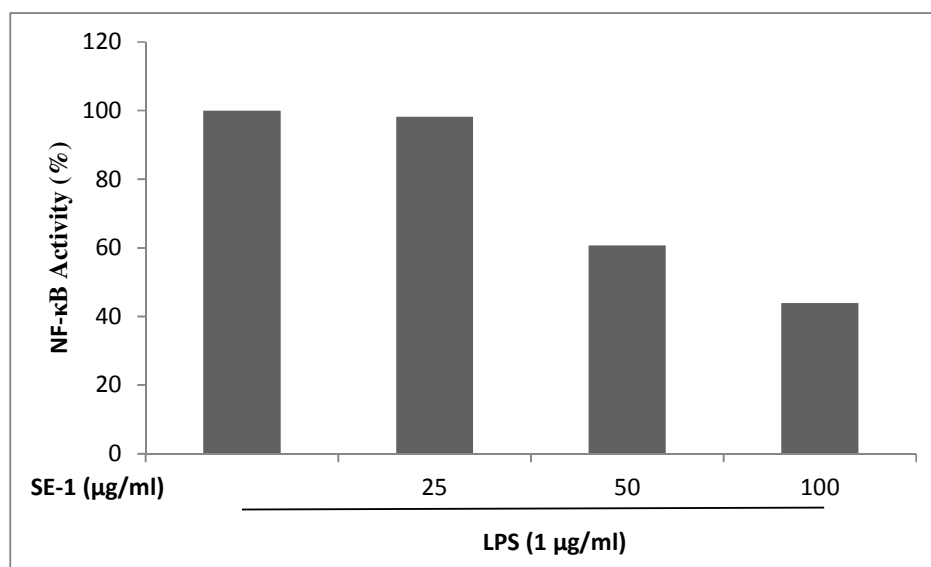
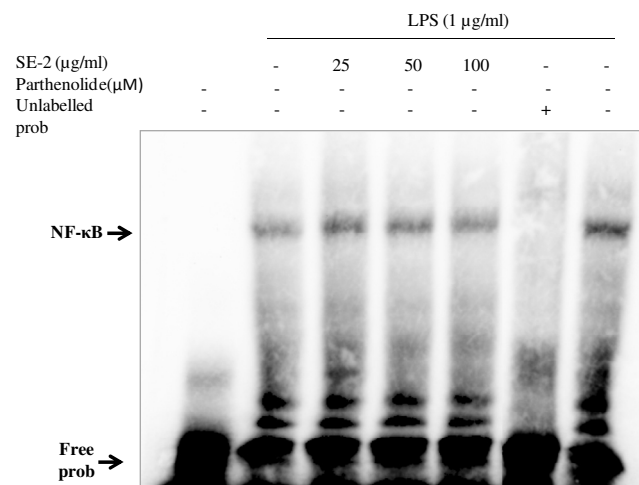


Figure 34: The concentration-dependent NF- κ B inhibitory activity of the flavonoid mixture SE-1. (A) The EMSA image of the concentration-dependent activity of the flavonoid mixture SE-1. (B) The concentration-dependent inhibitory activity of SE-1 on the activation of NF- κ B. Band intensities were evaluated by densitometric analysis using Image J and relative intensities were calculated. NF- κ B activity recorded for Raw264.7 cells treated only with LPS represents 100%. Raw 264.7 macrophage cells were pre-treated with extracts and fractions for two hr's and then induced with LPS (1 $\mu\text{g/ml}$) for one hr. Nuclear fractions were isolated and evaluated by EMSA. SE-1: mixture of hyperoside (major constituent, 2/3 of mixture) and isoquercitrin (minor, 1/3 of mixture).

A)



B)

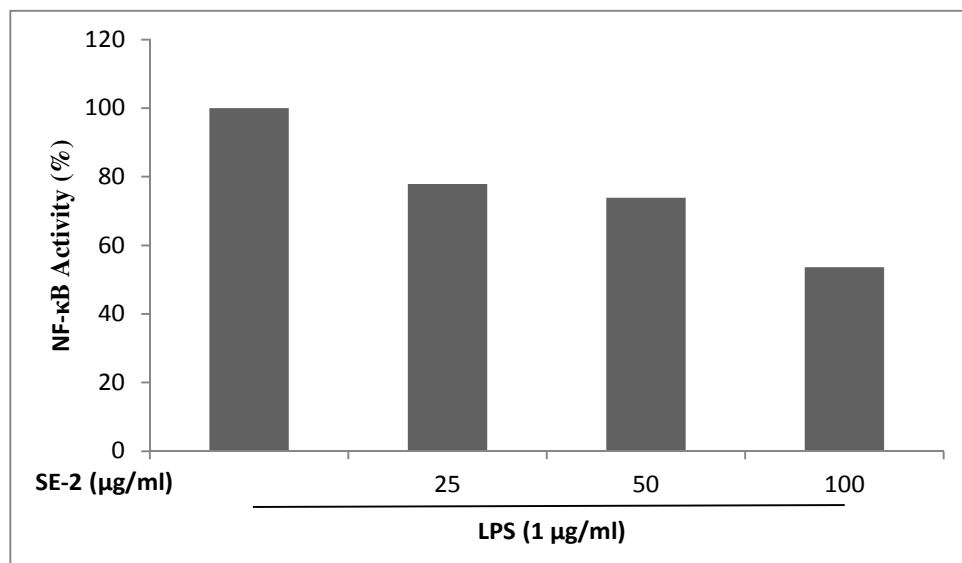
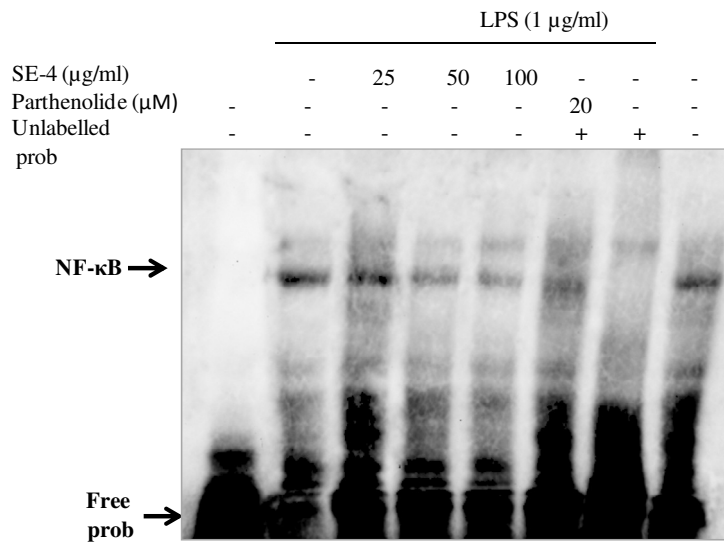


Figure 35: The concentration-dependent NF- κ B inhibitory activity of the SE-2. (A) The EMSA image of the concentration-dependent activity of the SE-2. (B) The concentration-dependent inhibitory activity of SE-2 on the activation of NF- κ B. Band intensities were evaluated by densitometric analysis using Image J and relative intensities were calculated. NF- κ B activity recorded for Raw264.7 cells treated only with LPS represents 100%. Raw 264.7 macrophage cells were pre-treated with extracts and fractions for two hr's and then induced with LPS (1 $\mu\text{g/ml}$) for one hr. Nuclear fractions were isolated and evaluated by EMSA. SE-2: isorhamnetin-3-*O*-D-glucopyranoside

A)



B)

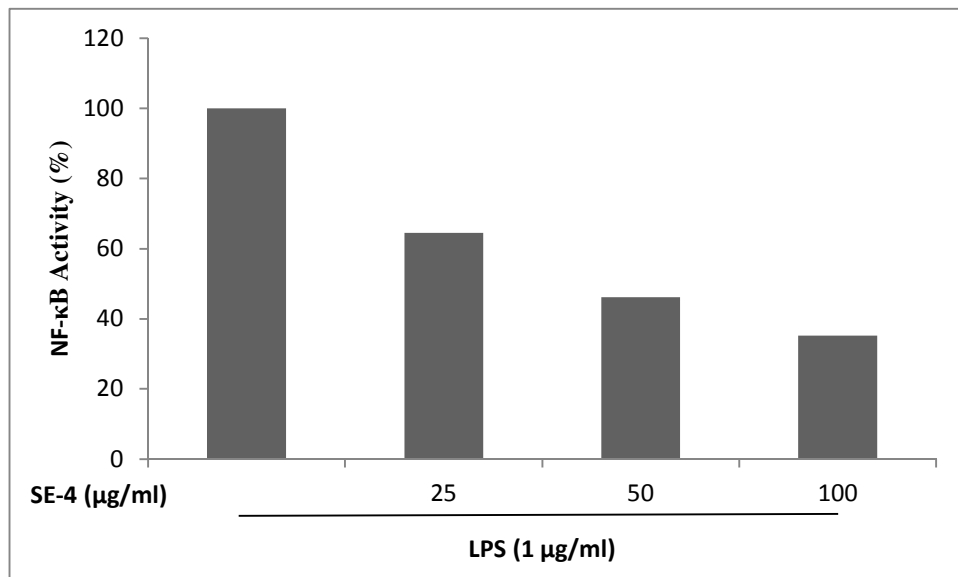
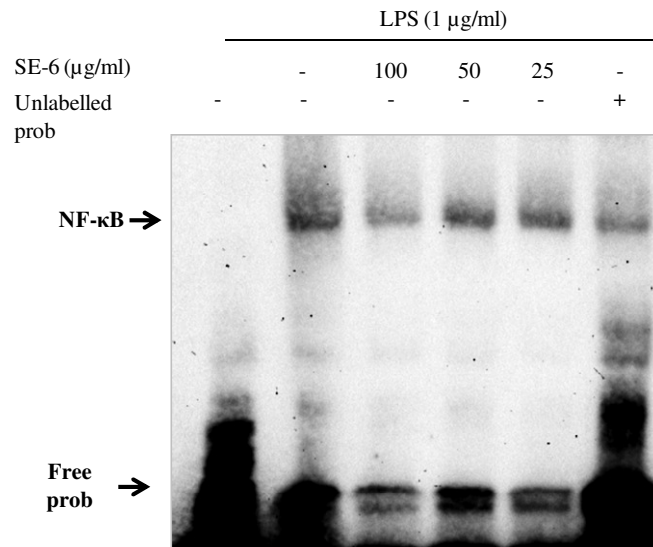


Figure 36: The concentration-dependent NF- κ B inhibitory activity of the flavonoid mixture SE-4. (A) The EMSA image of the concentration-dependent activity of the flavonoid mixture SE-1. (B) The concentration-dependent inhibitory activity of SE-4 on the activation of NF- κ B. Band intensities were evaluated by densitometric analysis using Image J and relative intensities were calculated. NF- κ B activity recorded for Raw264.7 cells treated only with LPS represents 100%. Raw 264.7 macrophage cells were pre-treated with extracts and fractions for two hr's and then induced with LPS (1 $\mu\text{g/ml}$) for one hr. Nuclear fractions were isolated and evaluated by EMSA. SE-4: a mixture of hyperoside (minor constituent, 1/3 of mixture) and isoquercitrin (major, 2/3 of mixture)

A)



B)

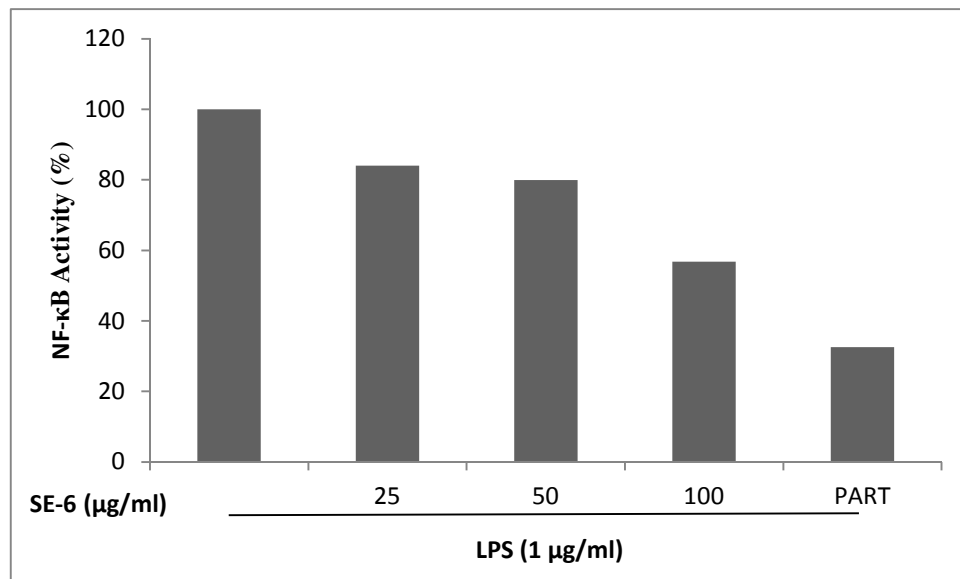
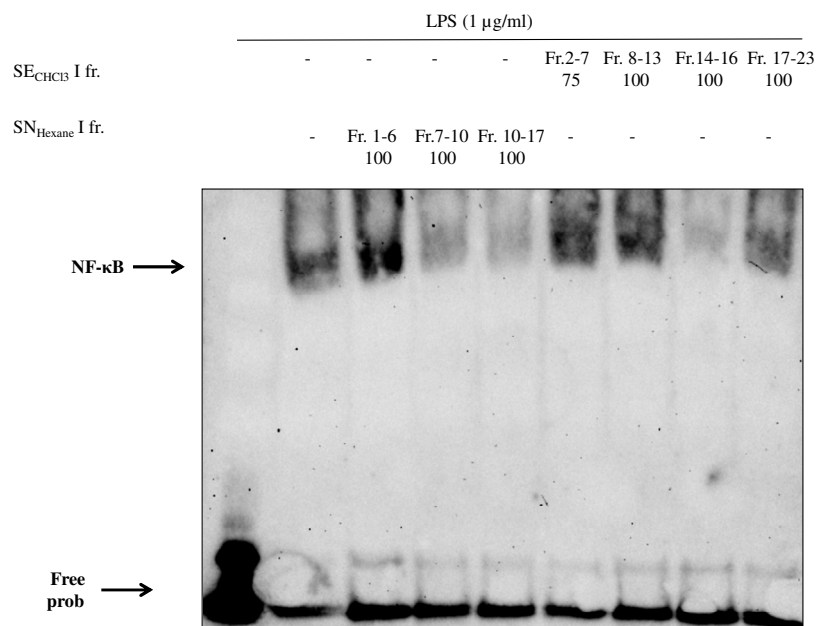


Figure 37: The concentration-dependent NF- κ B inhibitory activity of SE-6. (A) The EMSA image of the concentration-dependent activity of SE-6. (B) The concentration-dependent inhibitory activity of SE-6 on the activation of NF- κ B. Band intensities were evaluated by densitometric analysis using Image J and relative intensities were calculated. NF- κ B activity recorded for Raw264.7 cells treated only with LPS represents 100%. Raw 264.7 macrophage cells were pre-treated with extracts and fractions for two hr's and then induced with LPS (1 $\mu\text{g/ml}$) for one hr. Nuclear fractions were isolated and evaluated by EMSA. SE-6: isorhamnetin-3-*O*-rutinoside

A)



B)

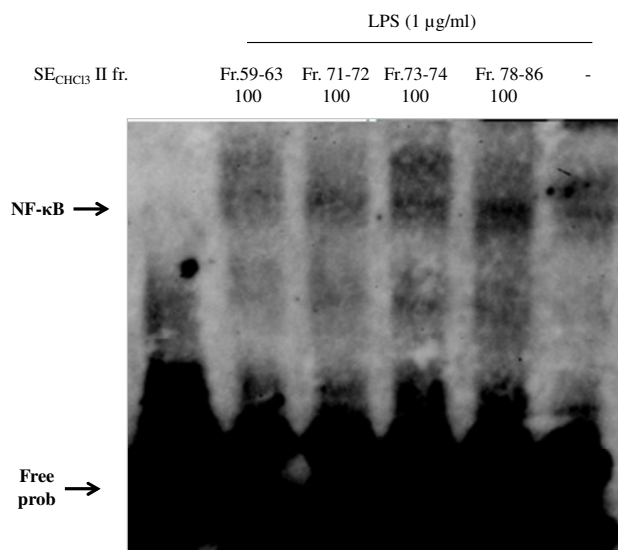
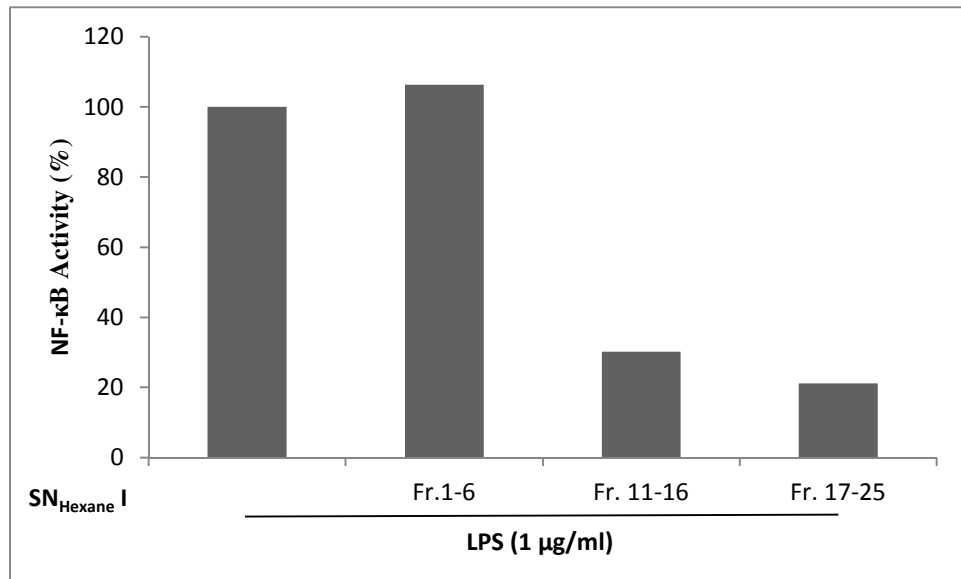
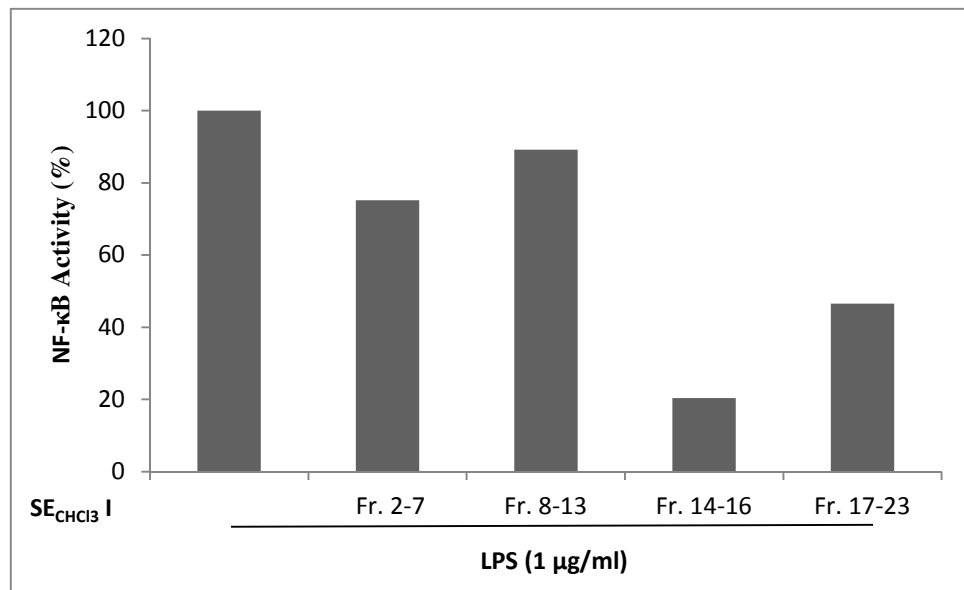


Figure 38: The EMSA images showing the NF- κ B inhibitory activities of the fractions obtained from SE-CHCl₃, SN-Hex by silica gel column chromatographies. (A) and subfractions obtained from fraction SE_{CHCl₃} I Fr 14-16 (B). Raw 264.7 macrophage cells were pre-treated with extracts and fractions for two hr's and then induced with LPS (1 $\mu\text{g/ml}$) for one hr. Nuclear fractions were isolated and evaluated by EMSA.

A)



B)



C)

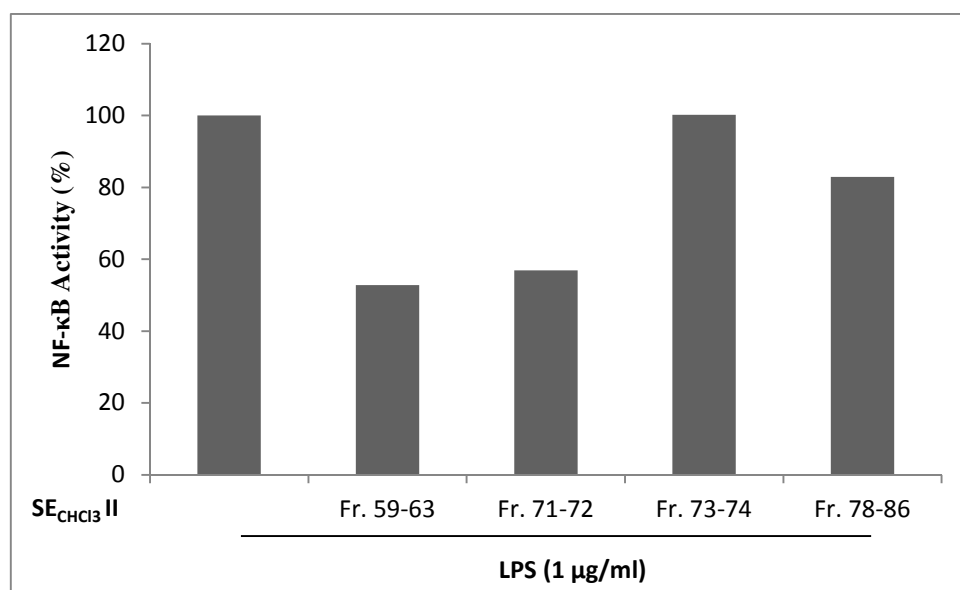
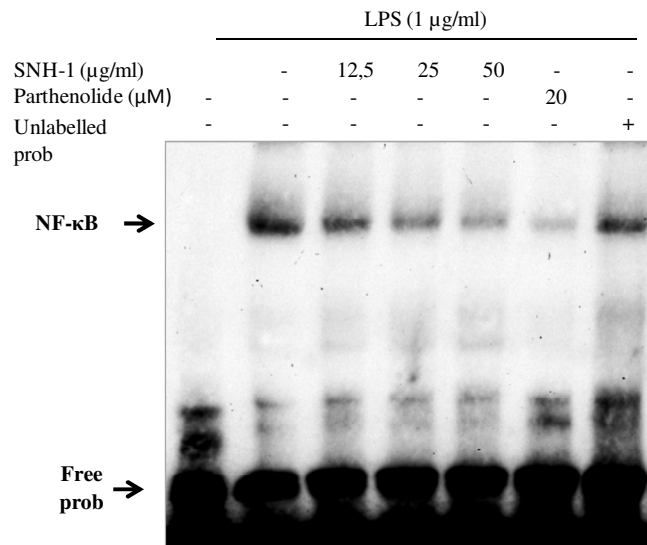


Figure 39: The NF-κB inhibitory effects of the fractions obtained from SE-CHCl₃, SN-Hex by silica gel column chromatographies and subfractions obtained from fraction SE_{CHCl3} I Fr 14-16. Band intensities were evaluated by densitometric analysis using Image J and relative intensities were calculated. NF-κB activity recorded for Raw264.7 cells treated only with LPS represents 100%. SN_{Hexane} I (A), SE_{CHCl3} I (B) and SE_{CHCl3} II (C) Raw 264.7 macrophage cells were pre-treated with fractions for two hr's and then induced with LPS (1 μg/ml) for one hr. Nuclear fractions were isolated and investigated by EMSA.

A)



B)

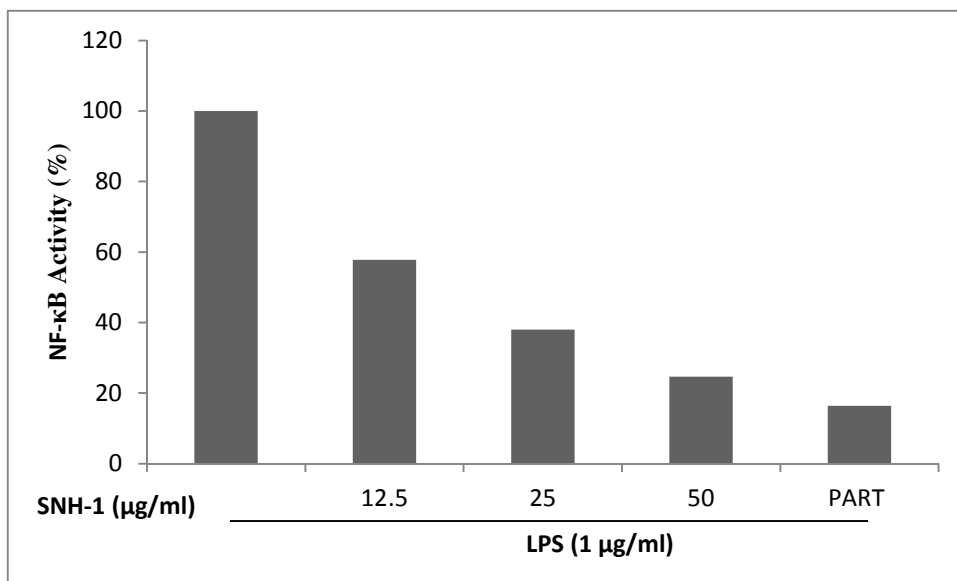
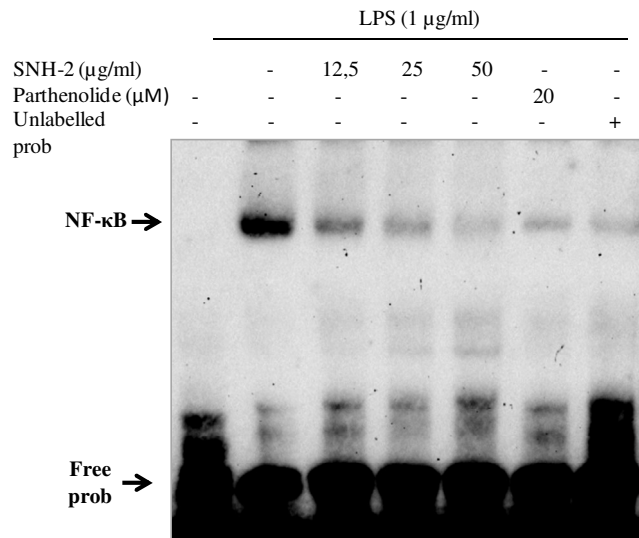


Figure 40: The concentration-dependent NF- κ B inhibitory activity of SNH-1. (A) The EMSA image of the concentration-dependent activity of SNH-1.(B) The concentration-dependent inhibitory activity of SNH-1 on the activation of NF- κ B. Band intensities were evaluated by densitometric analysis using Image J and relative intensities were calculated. NF- κ B activity recorded for Raw264.7 cells treated only with LPS represents 100%. Raw 264.7 macrophage cells were pre-treated with extracts and fractions for two hr's and then induced with LPS (1 $\mu\text{g/ml}$) for one hr. Nuclear fractions were isolated and evaluated by EMSA.

A)



B)

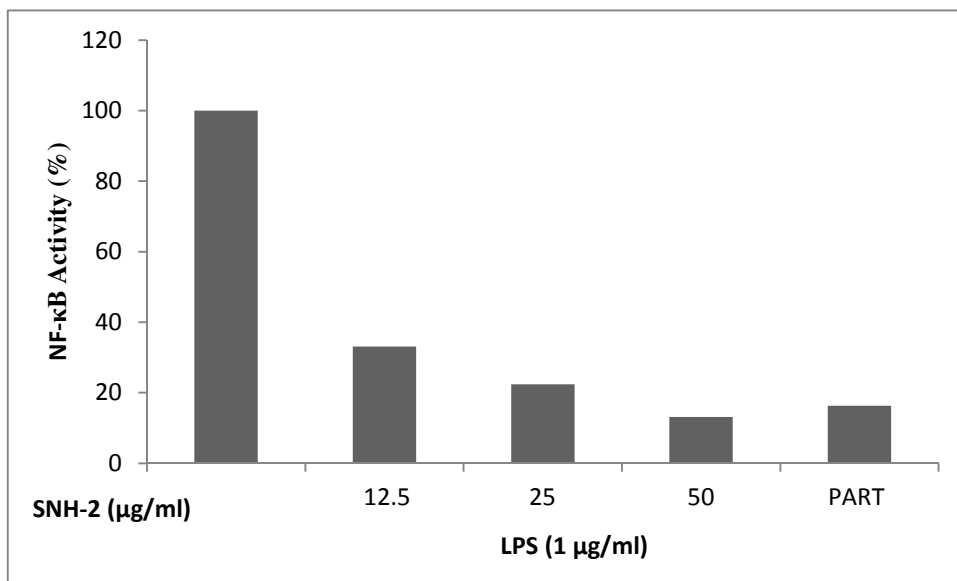
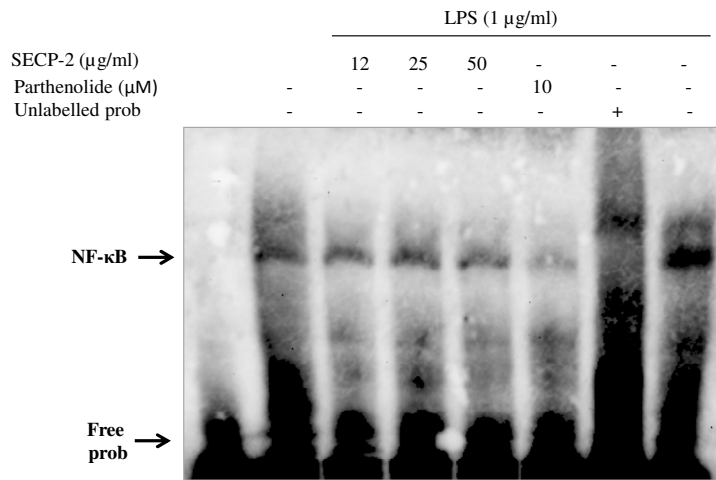


Figure 41: The concentration-dependent NF- κ B inhibitory activity of SNH-2. (A) The EMSA image of the concentration-dependent activity of SNH-2. (B) The concentration-dependent inhibitory activity of SNH-2 on the activation of NF- κ B. Band intensities were evaluated by densitometric analysis using Image J and relative intensities were calculated. NF- κ B activity recorded for Raw264.7 cells treated only with LPS represents 100%. Raw 264.7 macrophage cells were pre-treated with extracts and fractions for two hr's and then induced with LPS (1 $\mu\text{g/ml}$) for one hr. Nuclear fractions were isolated and evaluated by EMSA.

A)



B)

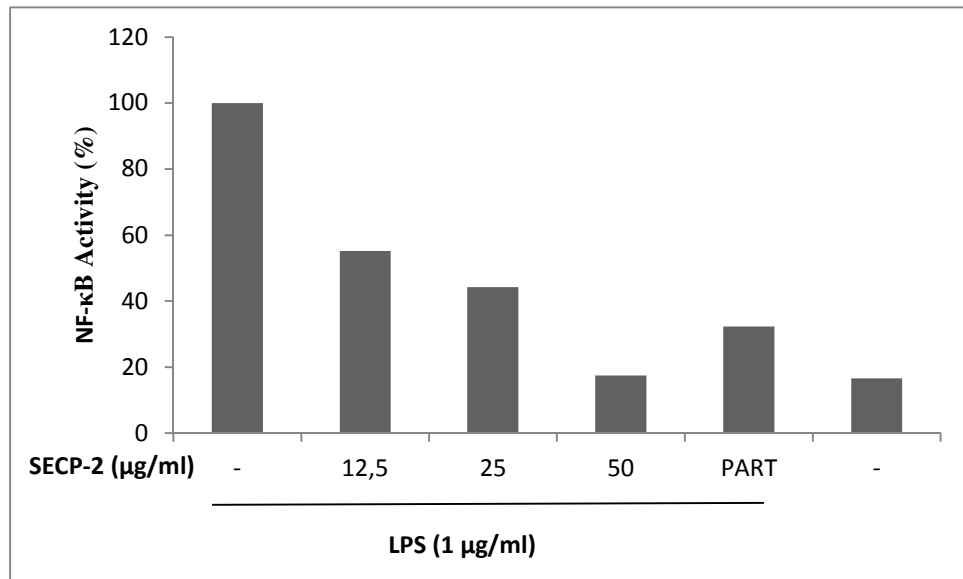
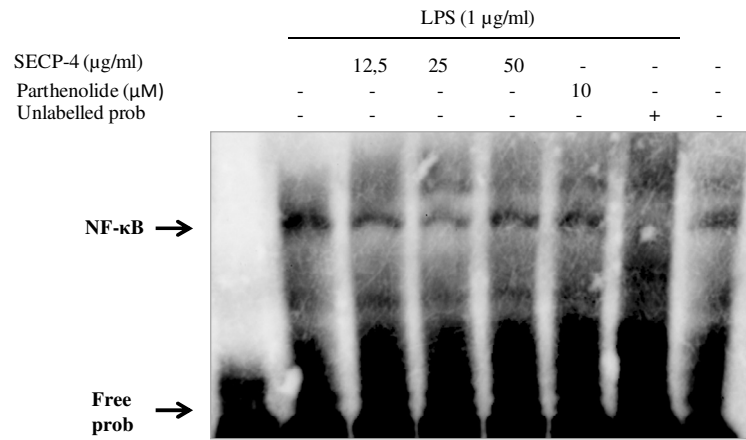


Figure 42: The concentration-dependent NF-κB inhibitory activity of SECP-2. (A) The EMSA image of the concentration-dependent activity of SECP-2. (B) The concentration-dependent inhibitory activity of SECP-2 on the activation of NF-κB. Band intensities were evaluated by densitometric analysis using Image J and relative intensities were calculated. NF-κB activity recorded for Raw264.7 cells treated only with LPS represents 100%. Raw 264.7 macrophage cells were pre-treated with extracts and fractions for two hr's and then induced with LPS (1 μg/ml) for one hr. Nuclear fractions were isolated and evaluated by EMSA. SECP-2: Sambulin A.

A)



B)

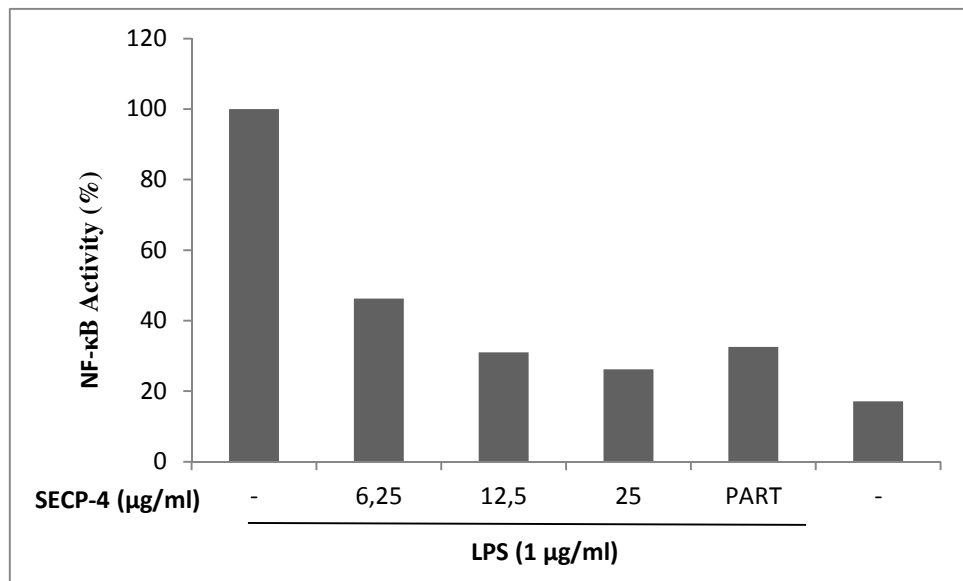
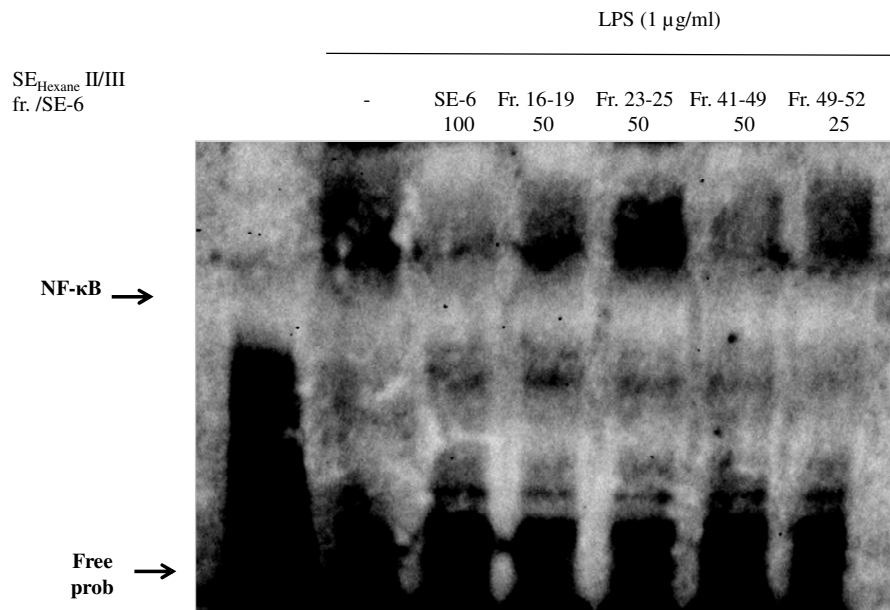


Figure 43: The concentration-dependent NF-κB inhibitory activity of SECP-4. (A) The EMSA image of the concentration-dependent activity of SECP-4. (B) The concentration-dependent inhibitory activity of SECP-4 on the activation of NF-κB. Band intensities were evaluated by densitometric analysis using Image J and relative intensities were calculated. NF-κB activity recorded for Raw264.7 cells treated only with LPS represents 100%. Raw 264.7 macrophage cells were pre-treated with extracts and fractions for two hr's and then induced with LPS (1 µg/ml) for one hr. Nuclear fractions were isolated and evaluated by EMSA.

A)



B)

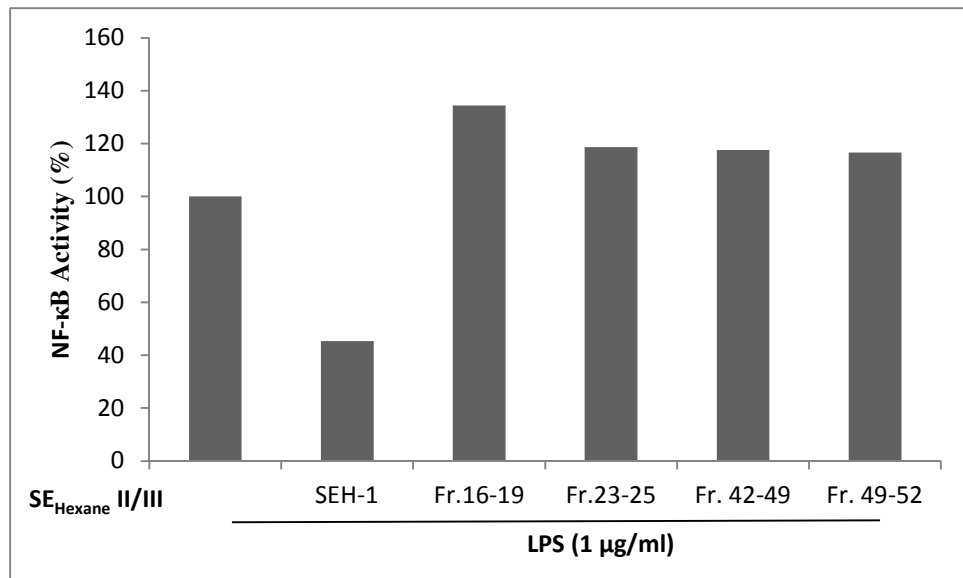


Figure 44: The NF-κB inhibitory effects of the fractions obtained from SE-Hex. (A) The EMSA image showing the NF-κB inhibitory activities of the fractions. (B) The NF-κB inhibitory effects of the fractions obtained from SE_{Hexane} II. Band intensities were evaluated by densitometric analysis using Image J and relative intensities were calculated. NF-κB activity recorded for Raw264.7 cells treated only with LPS represents 100%. Raw 264.7 macrophage cells were pre-treated with extracts and fractions for two hr's and then induced with LPS (1 μg/ml) for 1hr. Nuclear fractions were isolated and evaluated by EMSA.

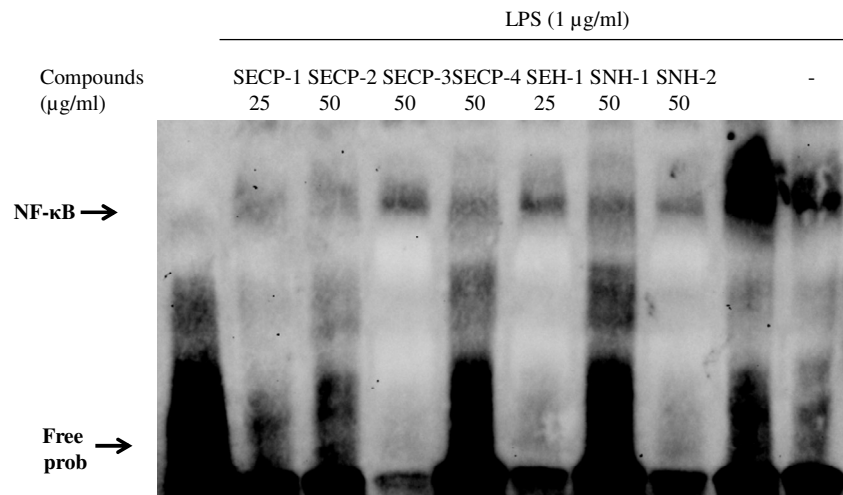
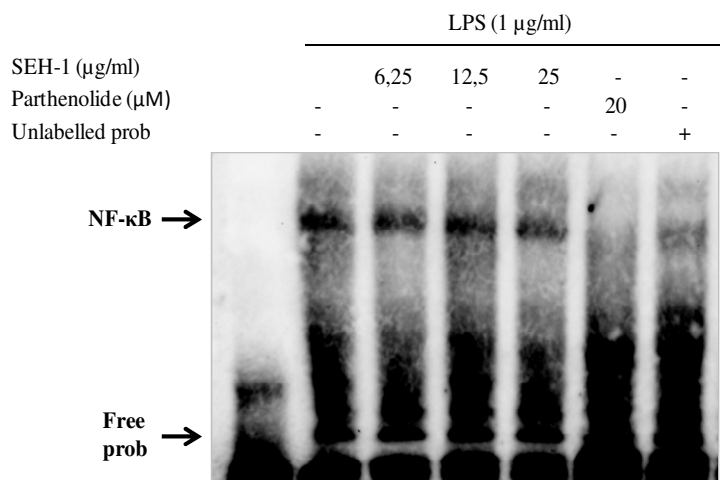


Figure 45: EMSA image showing the effects of the compounds obtained from SE-CHCl₃ and SN-Hex on the activation of NF-κB. Raw 264.7 macrophage cells were pre-treated with compounds for two hr's and then induced with LPS (1 µg/ml) for one hr. Nuclear fractions were isolated and investigated by EMSA. SEH-1: Sambulin B, SECP-2: Sambulin A

A)



B)

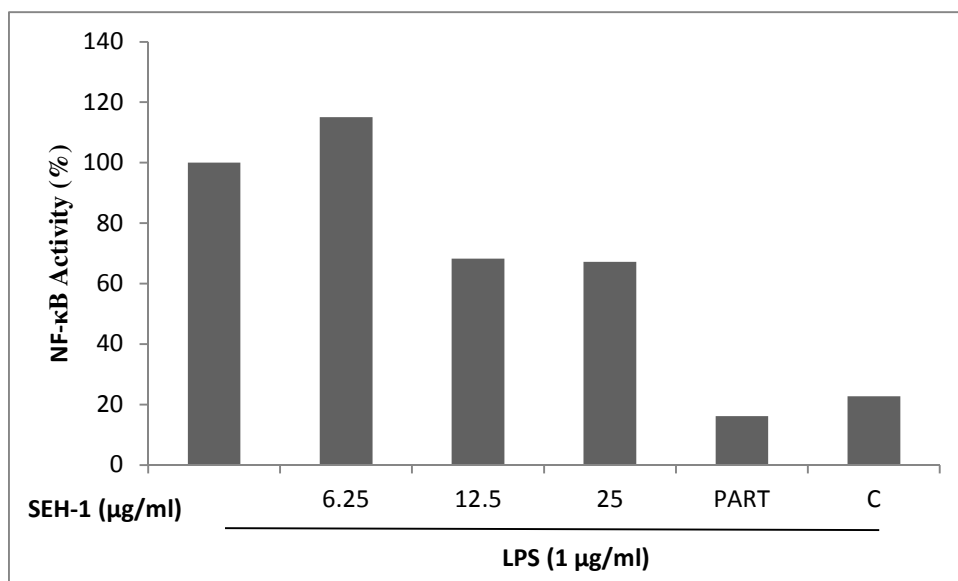


Figure 46: The concentration-dependent NF- κ B inhibitory activity of SEH-1. (A) The EMSA image of the concentration-dependent activity of SEH-1. (B) The concentration-dependent inhibitory activity of SEH-1 on the activation of NF- κ B. Band intensities were evaluated by densitometric analysis using Image J and relative intensities were calculated. NF- κ B activity recorded for Raw264.7 cells treated only with LPS represents 100%. Raw 264.7 macrophage cells were pre-treated with extracts and fractions for two hr's and then induced with LPS (1 $\mu\text{g/ml}$) for 1hr. Nuclear fractions were isolated and evaluated by EMSA. SEH-1: Sambulin B

4.2.3. The Effects of the Compounds on PGE₂, Nitric Oxide Productions and Protein and mRNA levels of Related Enzymes

The molecules which caused a significant decrease of the activity of NF- κ B on LPS induced Raw 264.7 cells, were further investigated for their activity on prostaglandin E₂ (PGE₂) and nitric oxide (NO) productions and enzymes responsible for their production (COX-2, iNOS). Molecules were initially screened at their highest non-toxic concentrations and the active compounds were selected for further studies. COX-2 and iNOS levels in the total cell lysates were determined by Western Blotting.

Raw 264.7 macrophage cells pre-treated with molecules or fractions (**SE-1**, **SE-2**, **SE-4**, **SE-6**, **SEH-1**, **SECP-2**, **SECP-4**, **SNH-1**, **SNH-2** and **CL-R-H₂O**) for one hr and then cells were induced with 1 μ g/ml LPS for a total of 24 hr's. The molecules which exerted NO inhibition more than 20% of only LPS treated control group were as follows: **SE-2** (59 %), **SE-6** (81.12%), **SEH-1** (81.2%), **SECP-2** (70%), **SNH-1** (28%) and **CL-R-H₂O** (58%). The PGE₂ inhibiting molecules were identified as: **SE-6** (41% inhibition of the control), **SECP-2** (42% inhibition of the control), **SEH-1** (83% inhibition of the control), **CL-R-H₂O** (52% inhibition of the control), and **SNH-1** (29.01% inhibition of the control). The active molecules and fractions were evaluated for their concentration-dependent activities and their effects on iNOS and COX-2 protein levels.

Cells were pre-incubated with 25, 50, 75 and 100 μ g/ml concentrations of isorhamnetin-3-*O*-rutinoside (**SE-6**). The compound inhibited the production of NO by 30.68%, 43.30%, 67.27% and 81.12% at the specified concentrations, respectively (**Figure 47**). **SE-6** at 100 μ g/ml concentration was more active than the known NO inhibitor L-NIL at 10 μ M, which provided a 58% inhibition. The PGE₂ production of Raw 264.7 macrophage cells was significantly increased with the addition of LPS. The molecule was also concentration-dependently inhibited the production of PGE₂ in LPS induced Raw 264.7 macrophage cells. The inhibition was up to 40% at the highest concentration tested for **SE-6**. NS-398 which is a selective COX-2 inhibitor at 20 μ M

concentration provided a 99% inhibition of PGE₂. Western Blot analysis of the cells under same conditions revealed a concentration-dependent decrease in both COX-2 and iNOS protein levels which was well correlated with NO and PGE₂ results. **SE-6** at 50, 75 and 100 µg/ml concentrations decreased the levels of iNOS by 29%, 44%, 62%. Compared to only LPS treated group, this molecule decreased the levels of COX-2 protein by 44%, 55% and 60%. Raw 264.7 macrophage cells were pre-treated with **SE-6** for one hr and then induced with 1 µg/ml LPS for 10 hr's. Total RNA was isolated and iNOS and COX-2 mRNA levels were determined by Real-Time PCR. It was revealed that at the end of 10 hr's iNOS mRNA levels were decreased only at the highest concentration (100 µg/ml). COX-2 mRNA levels were decreased at 25 and 50 µg/ml concentrations, but remained unchanged at 100 µg/ml. The decrease of the protein levels were not confirmed by mRNA levels as determined at the end of 10 hr's induction with LPS. The investigation of mRNA levels at different time points might be beneficial to explain the decreases of protein levels of iNOS and COX-2 (**Figure 54**).

Isorhamnetin-3-*O*-D-glucopyranoside (**SE-2**) led to a decrease of 15.18%, 23.33%, 42% and 59.29% in the NO levels compared to LPS treated group at 25, 50, 75 and 100 µg/ml concentrations, respectively. The decrease of NO levels in the cell culture might be due to the decrease of the iNOS levels as can be seen in **Figure 48**. **SE-2** decrease the levels of iNOS protein levels by 13%, 35%, 45% compared to only LPS treated group at 50, 75 and 100 µg/ml. At the end of 10 hr's induction with LPS, mRNA levels of iNOS was slightly decreased (**Figure 53**). However, this molecule was ineffective on LPS induced PGE₂ and COX-2 levels.

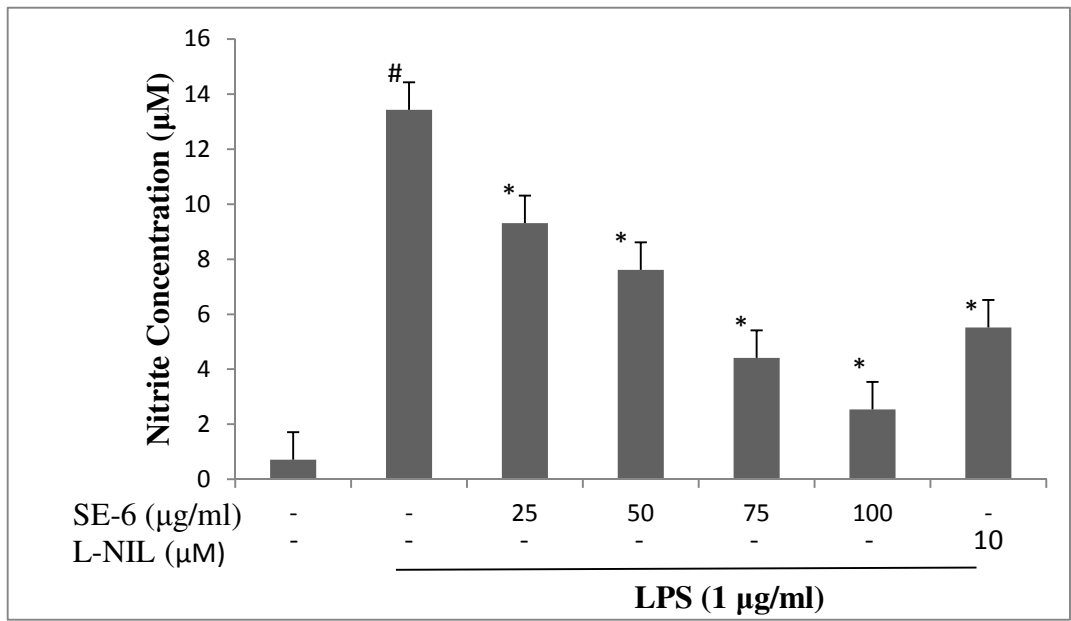
Sambulin B (**SEH-1**) was found to be toxic at higher concentrations. Therefore it was tested at 6.25, 12.5 and 25 µg/ml concentrations leading to an inhibition up to 80% of production of NO and PGE₂. When Sambulin B applied to cells at 12.5 µg/ml and more, it was more effective than L-NIL (10 µM). Western Blot analysis of the cell lysates showed that this effect might be due to a decrease of iNOS and COX-2 levels (**Figure 49**). **SEH-1** at 12.5 and 25 µg/ml completely inhibited the productions in iNOS protein in Raw 264.7 cells. At the end of 10 hr's of induction with LPS, iNOS mRNA

levels were found to be decreased by 44% at the highest concentration. COX-2 mRNA levels remained unchanged except the 53% decrease at 6.25 µg/ml (**Figure 55**).

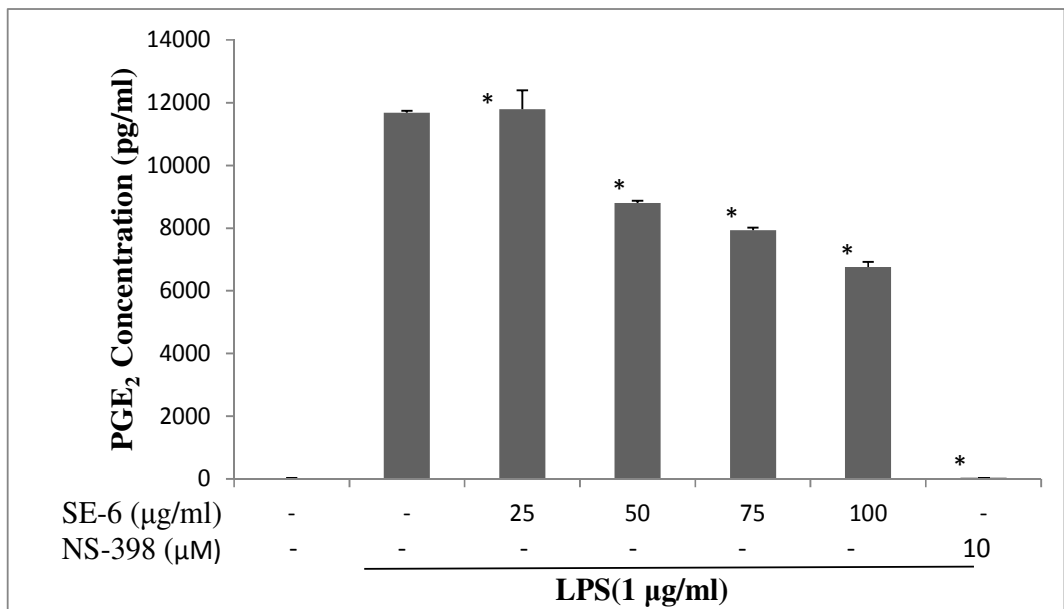
Sambulin A (**SECP-2**) provided a 23%, 52% and 70% decrease in the levels of NO compared to the control at 12.5, 25 and 50 µg/ml concentrations. The inhibitory activity of Sambulin A at 50 µg/ml concentration was close to L-NIL (10 µM). This effect might be due to the decrease of iNOS levels. At highest concentration this compound provided a 42% decrease in the levels of PGE₂, which was also correlated with the decrease of COX-2 levels shown by Western Blotting. **SECP-2** decreased the levels of iNOS protein up to 66% at the highest concentration (50 µg/ml). At highest concentration COX-2 inhibition was 60% compared to only LPS treated group. A representative western image was laid out in **Figure 50**. The mRNA levels of iNOS and COX-2 was not affected at the end of 10 hr's of induction (**Figure 56**).

CL-R-H₂O decreased the levels of NO and PGE₂ only at the highest concentration. This extract caused a 52% decrease of PGE₂ level and 57% decrease in NO production which was correlated with the decrease of the protein levels of COX-2 and iNOS observed in Western Blotting (**Figure 51**). At 100 µg/ml concentrations **CL-R-H₂O** provided 38% inhibition for iNOS and 28.7 inhibition for COX-2 protein.

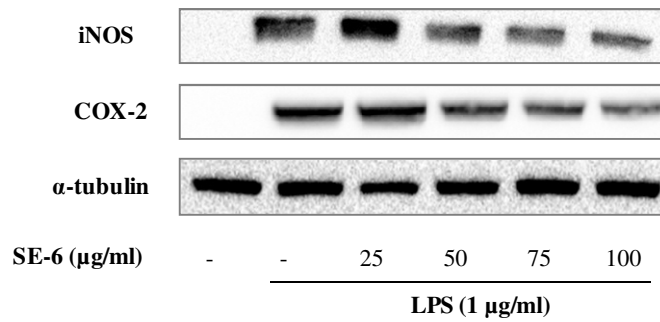
SNH-1 was slightly active on both parameters as shown in **Figure 52**. Although the inhibitory activity of the compound increased with the increasing concentrations reaching up to 40% at the highest concentration (100 µg/ml). The inhibitory effect on PGE₂ was 29.01%. At 25, 50 and 100 µg/ml concentrations **SNH-1** decreased the levels of iNOS by 6.2%, 25.7% and 35.4% and COX-2 by 28.2%, 58.4%, 59.2% compared to only LPS treated group.



B)



C)



(D)

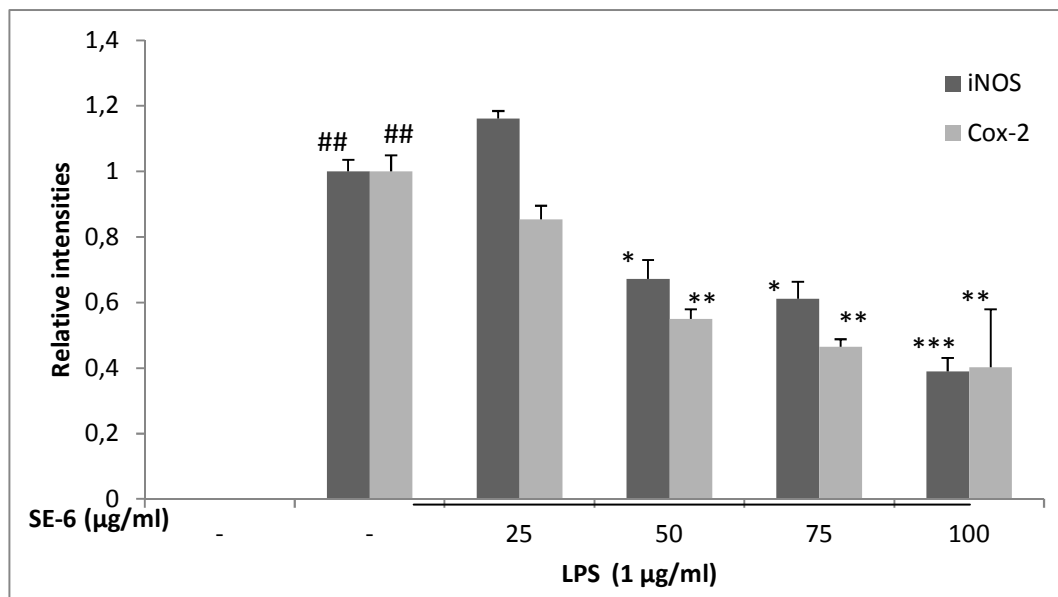
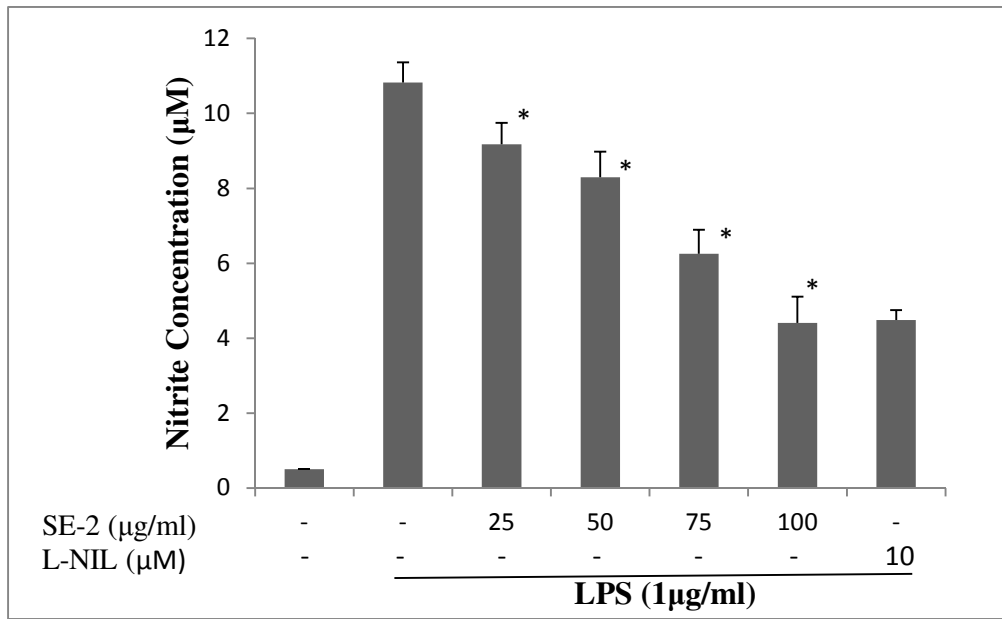
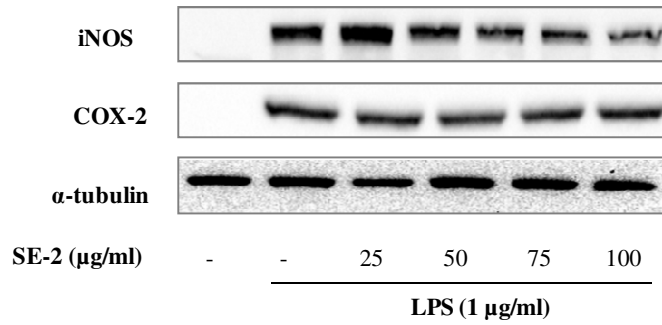


Figure 47: Effects of isorhamnetin-3-*O*-rutinoside (SE-6) on the productions of NO, PGE₂ and iNOS/COX-2 protein expression levels. Raw 264.7 cells were pre-incubated with indicated concentrations of isorhamnetin-3-*O*-rutinoside and induced with LPS (1 μ g/ml) for a total of 24 h. Media collected and NO (A) and PGE₂ (B) levels were measured by Griess Assay and ELISA. (C) At the end of the 24 hr's cells were lysed and iNOS and COX-2 proteins were detected with Western Blot using specific antibodies. Equal loading was verified by α -tubulin antibody. (D) Relative band intensities measured by Image J. The figures shows the representative of three experiments. * $p \leq 0.05$ ** $p \leq 0.01$ *** $p \leq 0.001$ compared to LPS treated group # $p \leq 0.05$ ## $p \leq 0.01$ ### $p \leq 0.001$ compared to non-induced group

A)



B)



(C)

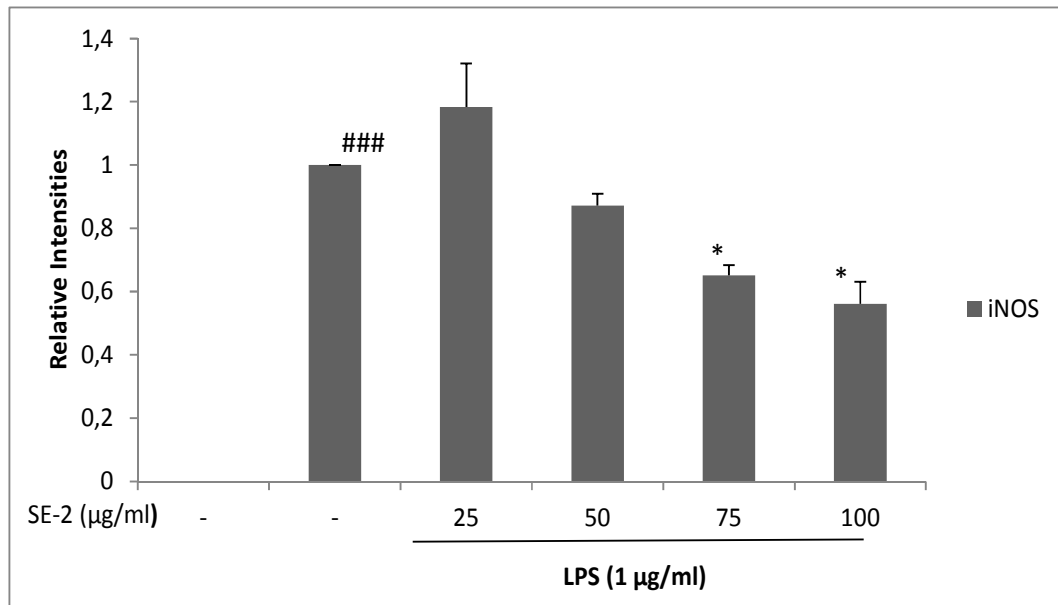
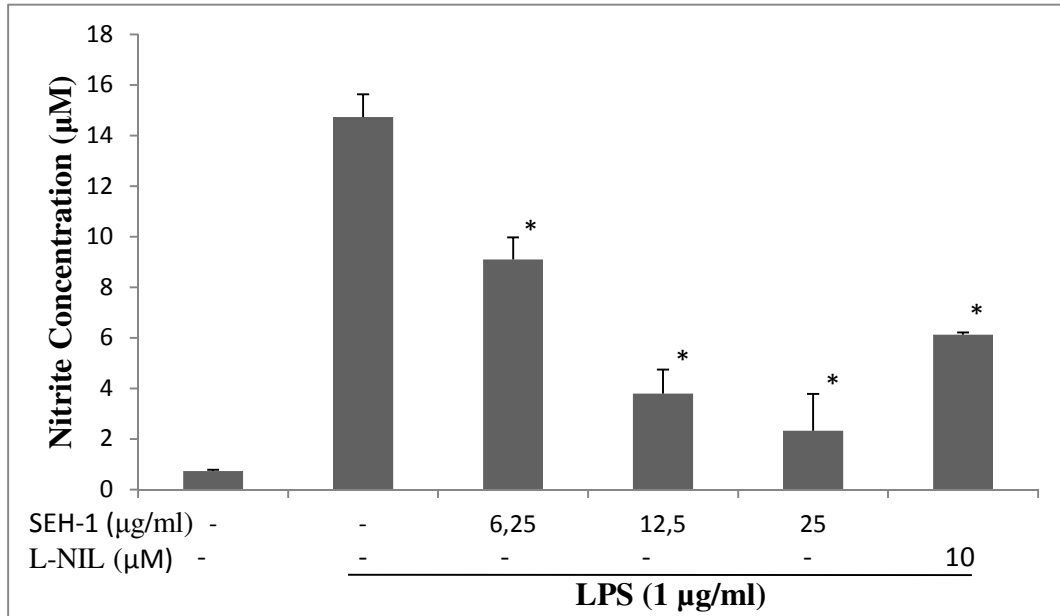
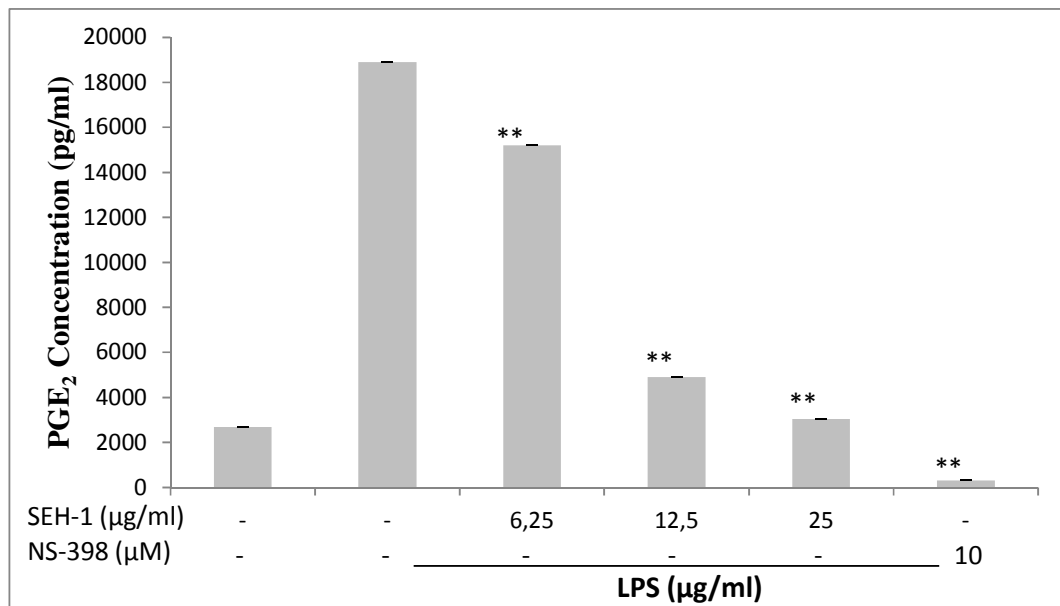


Figure 48: Effects isorhamnetin-3-*O*-β-D-glucopyranoside (SE-2) on the productions of NO, PGE2 and iNOS/COX-2 protein expression levels. Raw 264.7 cells were pre-incubated with indicated concentrations of isorhamnetin-3-*O*-β-D-glucopyranoside and induced with LPS (1 µg/ml) for a total of 24 h. Media collected and NO (A) levels were measured by Griess Assay. (B) At the end of 24 hr's cells were lysed and iNOS and COX-2 proteins were detected with Western Blot using specific antibodies. (C) Relative band intensities measured by Image J. The figures show the representative of three experiments. * $p \leq 0.05$ ** $p \leq 0.01$ *** $p \leq 0.001$ compared to LPS treated group # $p \leq 0.05$ ## $p \leq 0.01$ ### $p \leq 0.001$ compared to non-induced group.

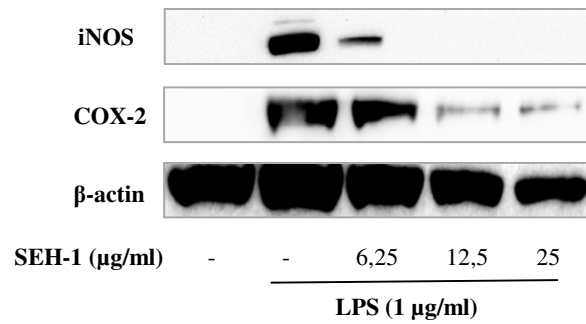
A)



B)



C)



D)

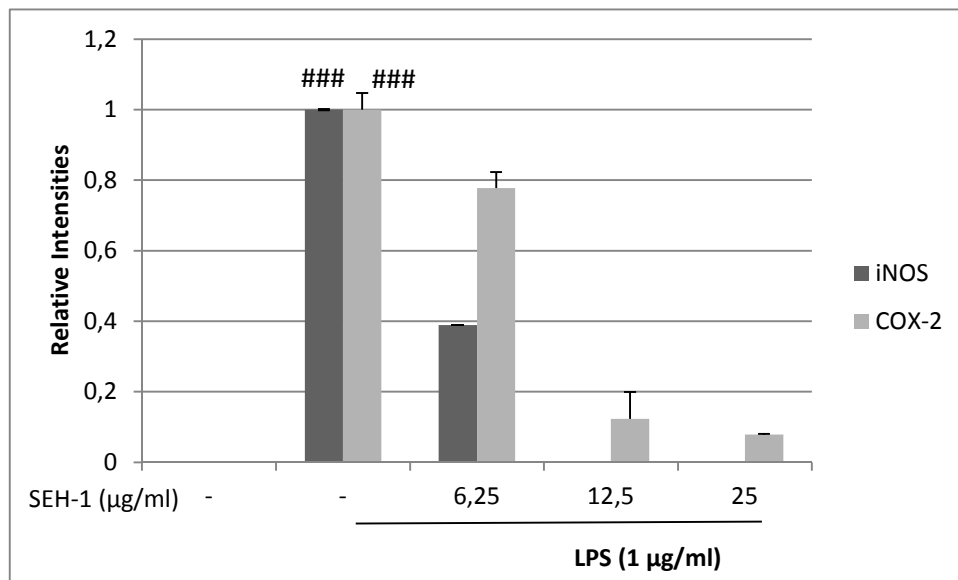
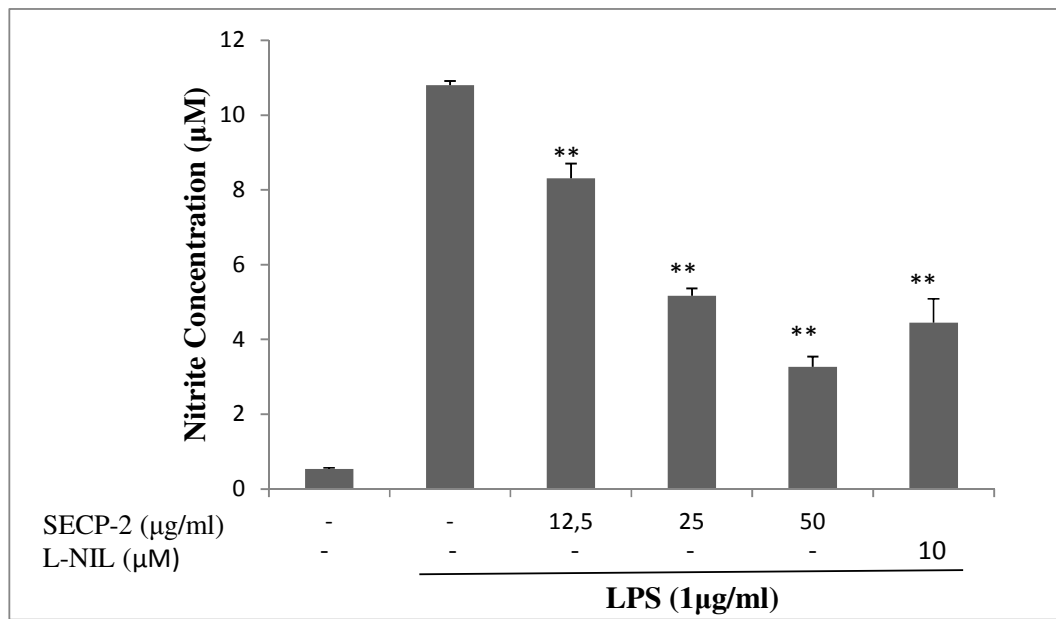
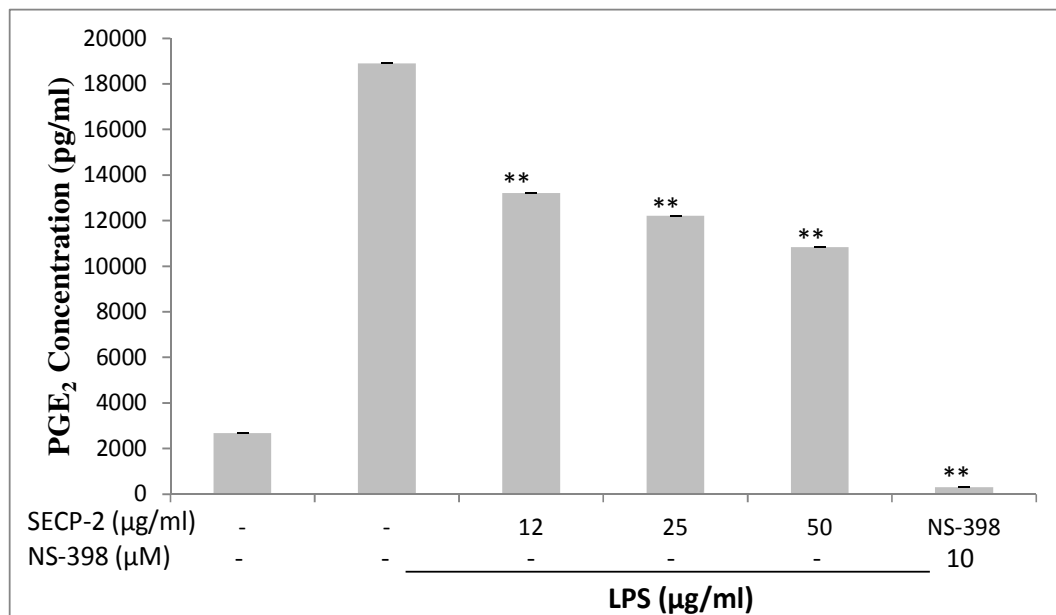


Figure 49: Effects of Sambulin B (SEH-1) on the productions of NO, PGE₂ and iNOS/COX-2 protein expression levels. Raw 264.7 cells were pre-incubated with indicated concentrations of Sambulin B (SEH-1) and induced with LPS (1 μg/ml) for a total of 24 h. Media collected and NO (A) and PGE₂ (B) levels were measured by Griess Assay and ELISA. (C) At the end of the 24 hr's cells were lysed and iNOS and COX-2 proteins were detected with Wester Blot using specific antibodies. Equal loading was verified by β-actin antibody. (D) Relative band intensities measured by Image J. The figures show the representative of three experiments. * p ≤ 0.05 **p ≤ 0.01 ***p ≤ 0.001 compared to LPS treated group # p ≤ 0.05 ##p ≤ 0.01### p ≤ 0.001 compared to non-induced group

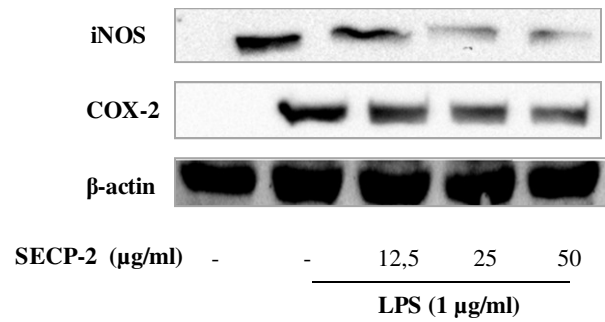
A)



B)



C)



D)

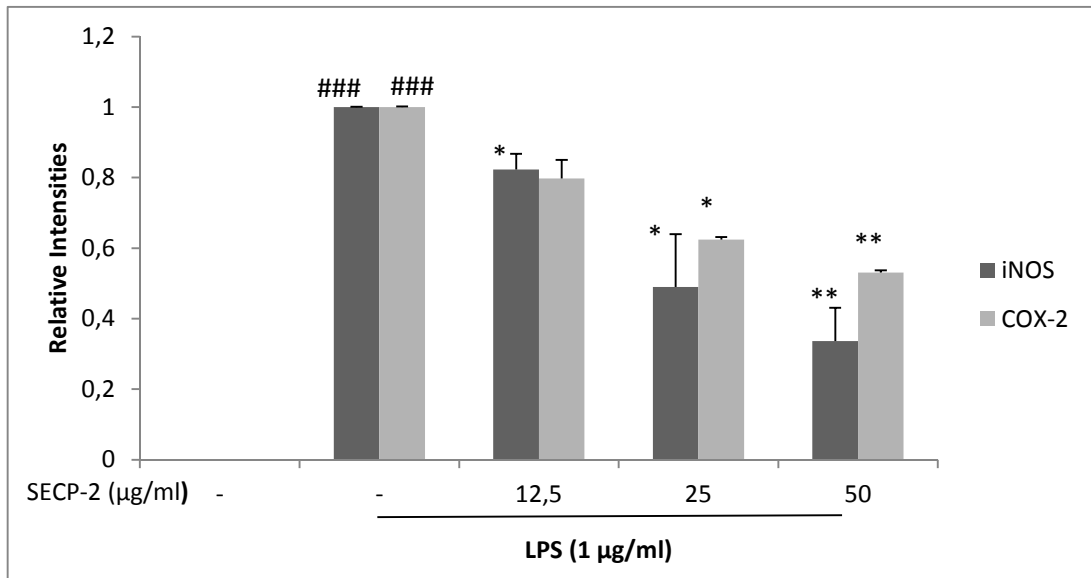
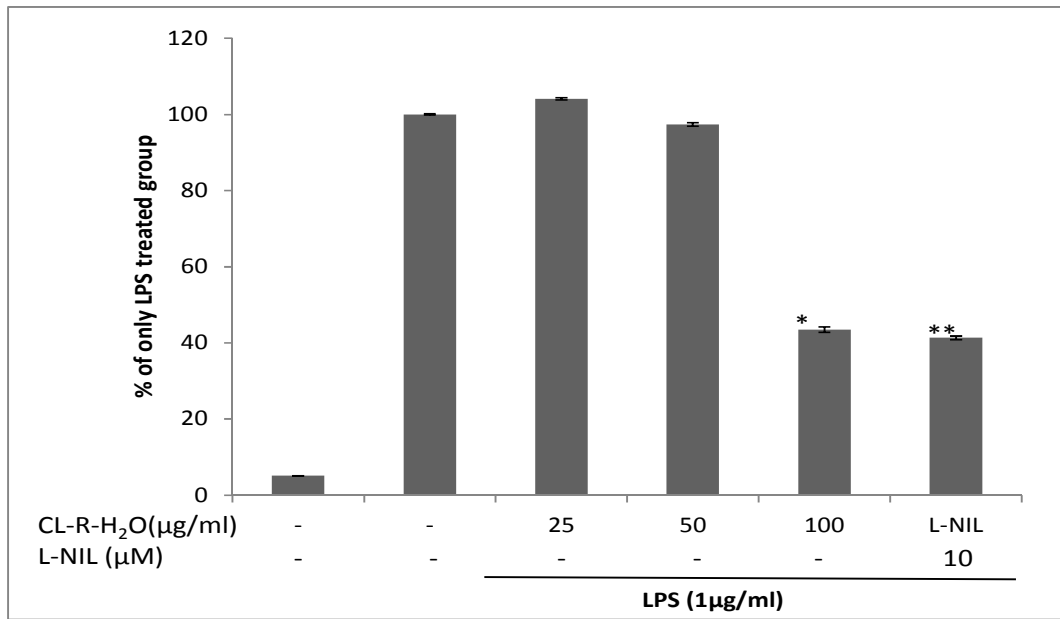
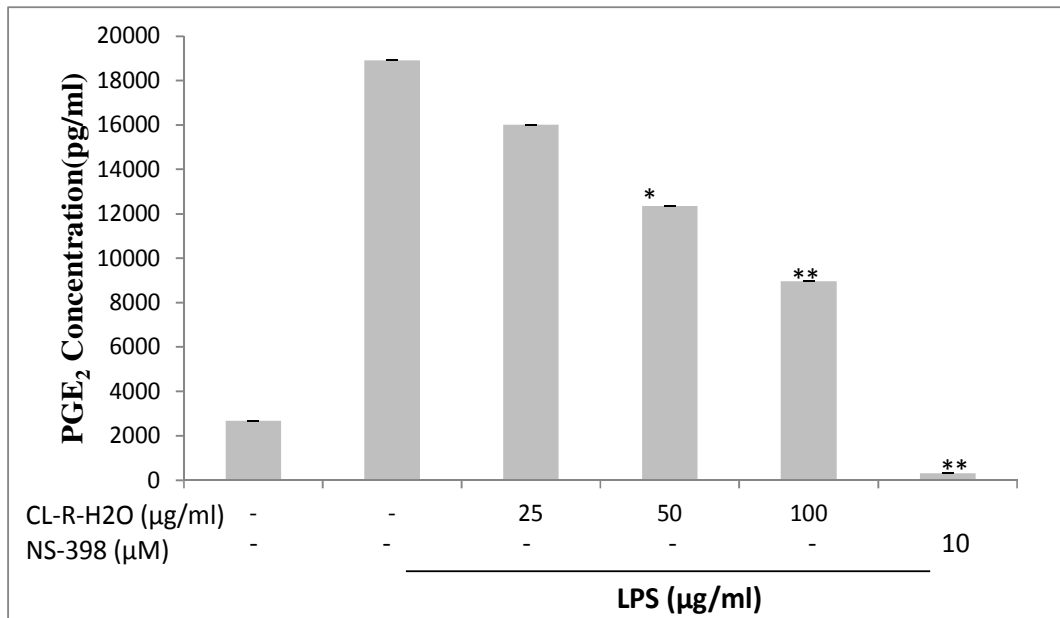


Figure 50: Effects of Sambulin A (SECP-2) on the productions of NO, PGE₂ and iNOS/COX-2 protein expression levels. Raw 264.7 cells were pre-incubated with indicated concentrations Sambulin A (SECP-2) and induced with LPS (1 µg/ml) for a total of 24 h. Media collected and NO (A) and PGE₂ (B) levels were measured by Griess Assay and ELISA. (C) At the end of the 24 hr's cells were lysed and iNOS and COX-2 proteins were detected with Western Blot using specific antibodies. Equal loading was verified by β-actin antibody. (D) Relative band intensities measured by Image J. The figures show the representative of three experiments. * p ≤ 0.05 **p ≤ 0.01 ***p ≤ 0.001 compared to LPS treated group # p ≤ 0.05 ##p ≤ 0.01### p ≤ 0.001 compared to non-induced group

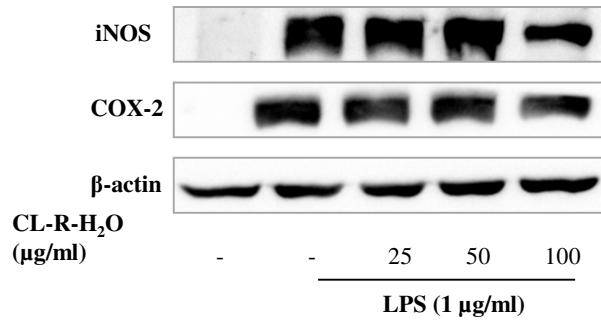
A)



B)



C)



D)

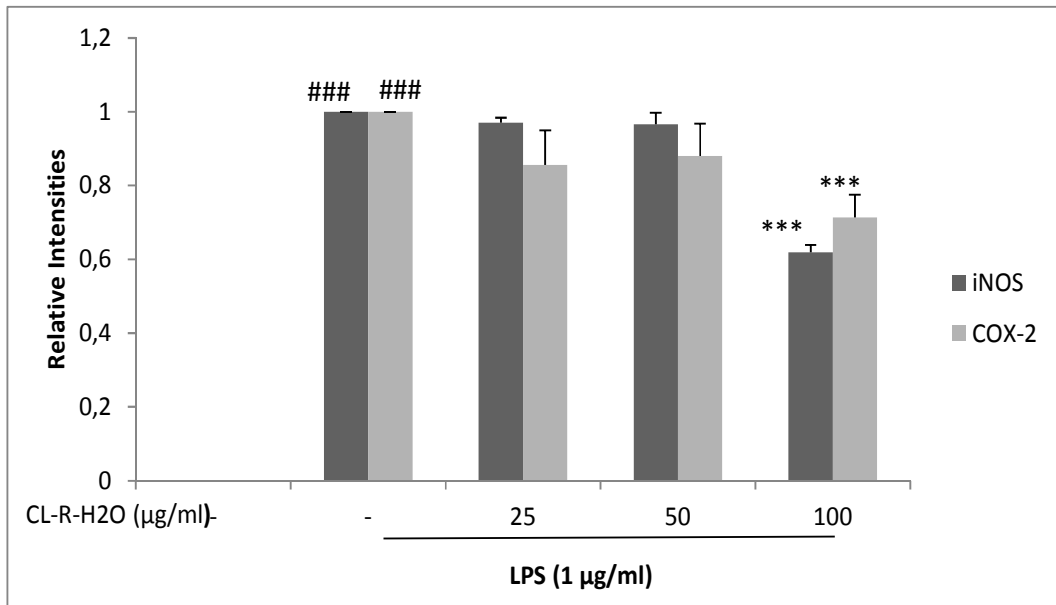
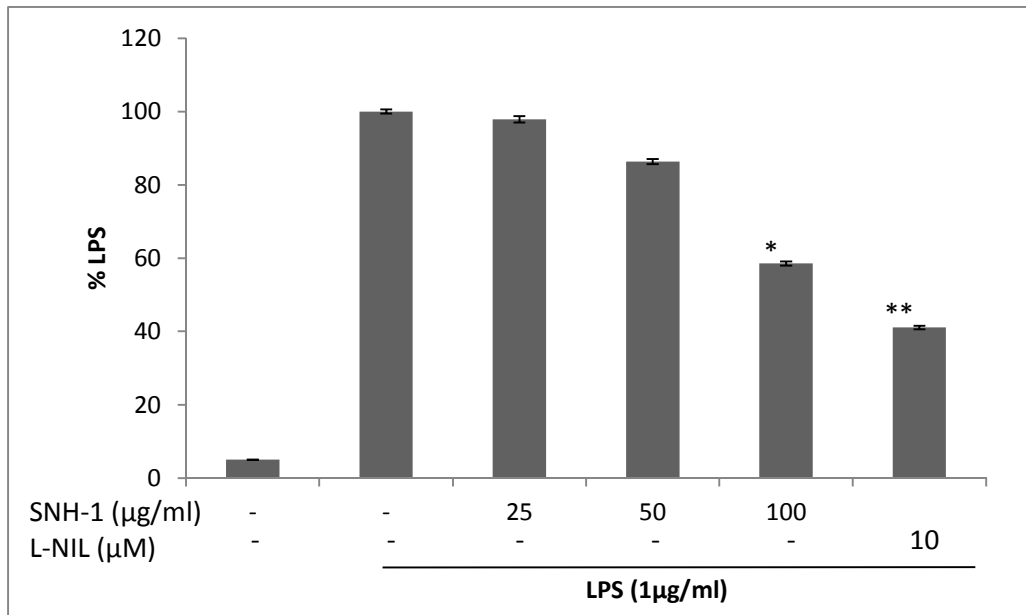
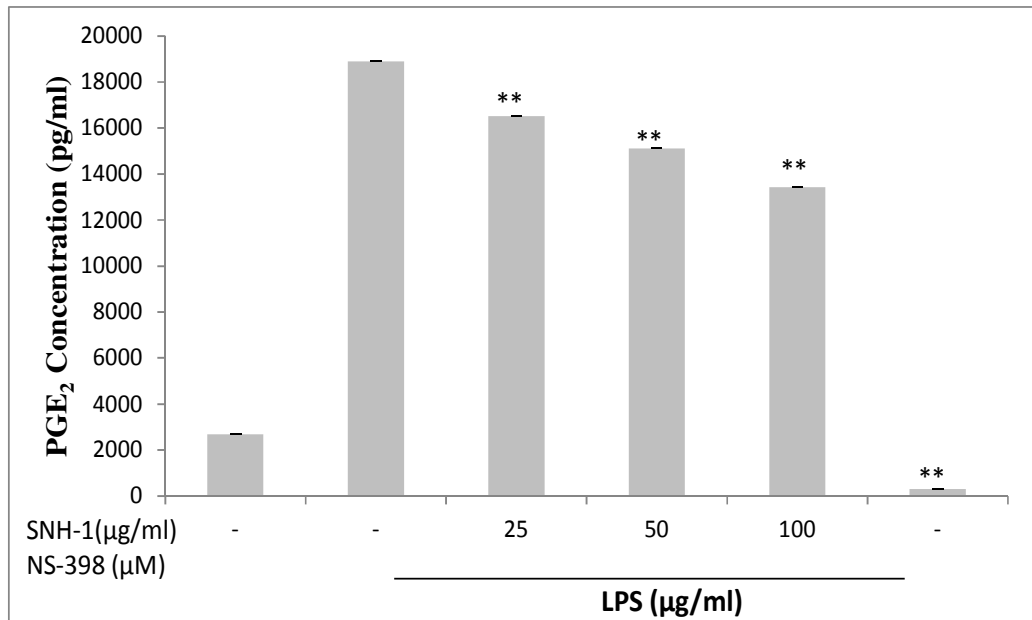


Figure 51: Effects of CL-R-H₂O on the productions of NO, PGE₂ and iNOS/COX-2 protein expression levels. Raw 264.7 cells were pre-incubated with indicated concentrations CL-R-H₂O and induced with LPS (1 μg/ml) for a total of 24 h. Media collected and NO (A) and PGE₂ (B) levels were measured by Griess Assay and ELISA. (C) At the end of the 24 hr's cells were lysed and iNOS and COX-2 proteins were detected with Western Blot using specific antibodies. Equal loading was verified by β-actin antibody. (D) Relative band intensities measured by Image J. The figures show the representative of three experiments. * p ≤ 0.05 **p ≤ 0.01 ***p ≤ 0.001 compared to LPS treated group # p ≤ 0.05 ##p ≤ 0.01 ### p ≤ 0.001 compared to non-induced group

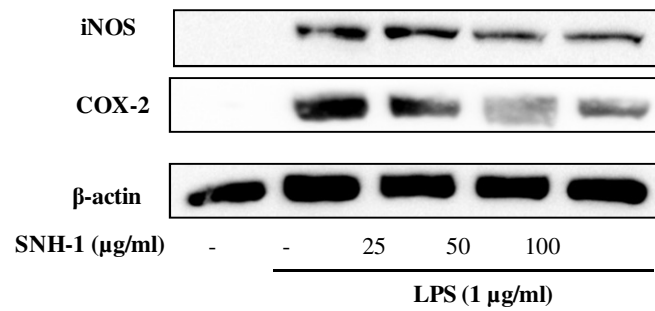
A)



B)



C)



D)

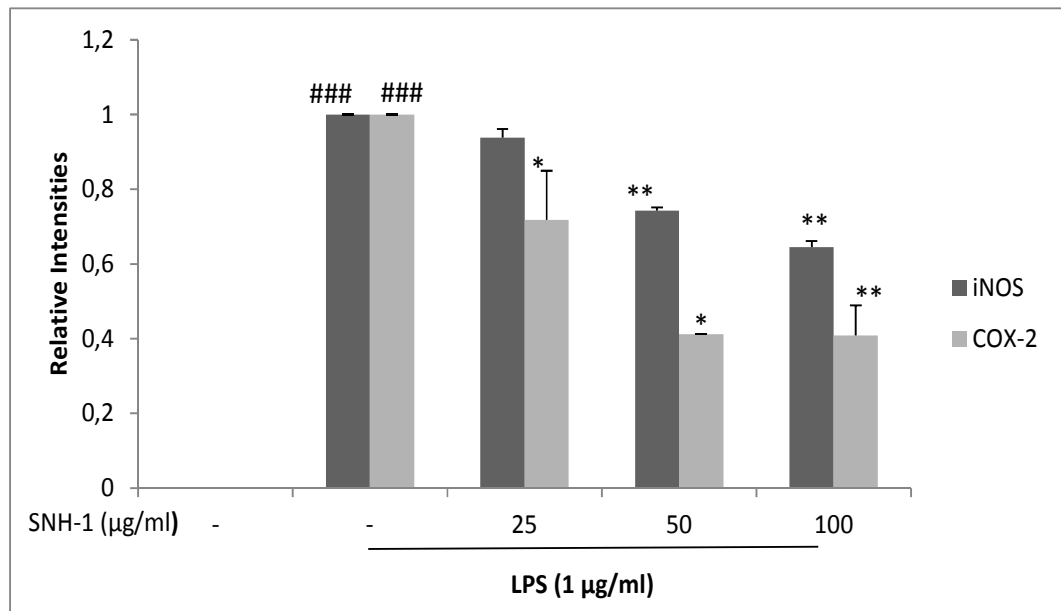


Figure 52: Effects of SNH-1 on the productions of NO, PGE₂ and iNOS/COX-2 protein expression levels. Raw 264.7 cells were pre-incubated with indicated concentrations SNH-1 and induced with LPS (1 µg/ml) for a total of 24 h. Media collected and NO (A) and PGE₂ (B) levels were measured by Griess Assay and ELISA. (C) At the end of the 24 hr's cells were lysed and iNOS and COX-2 proteins were detected with Western Blot using specific antibodies. Equal loading was verified by β-actin antibody. (D) Relative band intensities measured by Image J. The figures show the representative of three experiments. * p ≤ 0.05 **p ≤ 0.01 ***p ≤ 0.001 compared to LPS treated group # p ≤ 0.05 ##p ≤ 0.01 ### p ≤ 0.001 compared to non-induced group

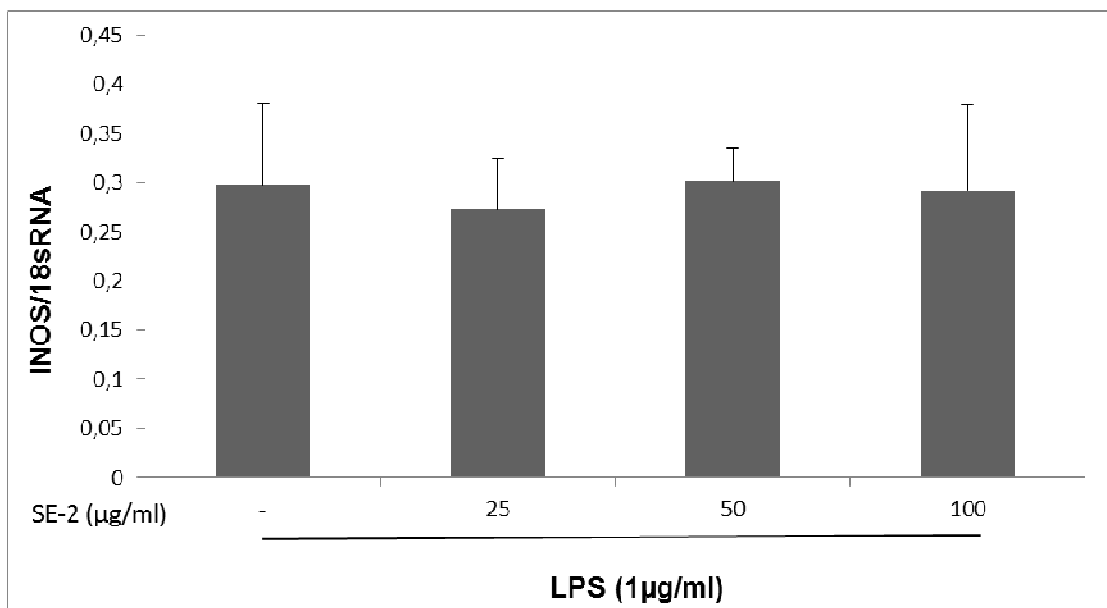
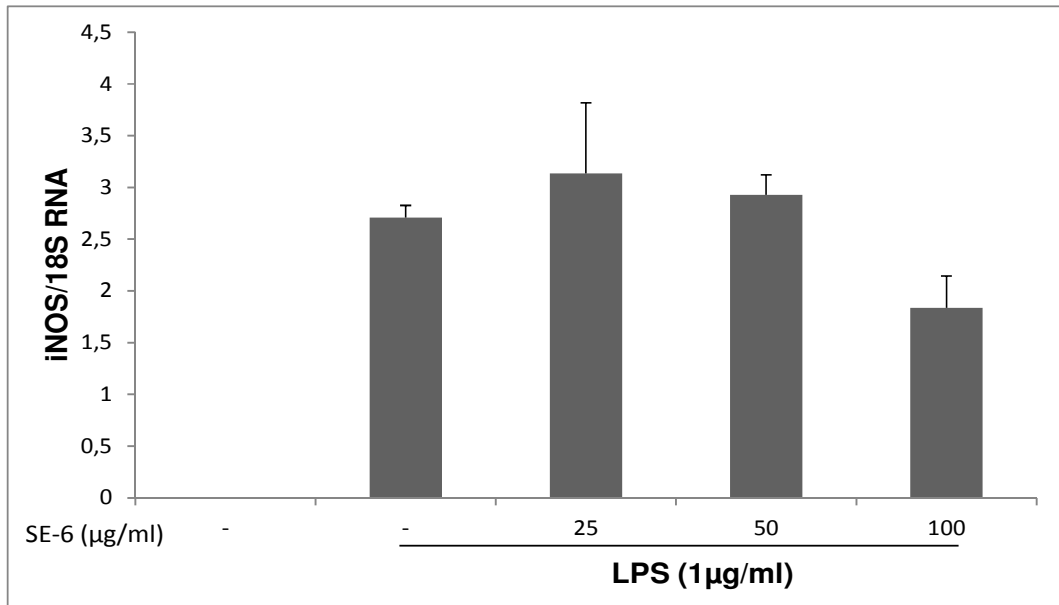


Figure 53: The effects of SE-2 (isorhamnetin-3-*O*-*D*-glucopyranoside) on mRNA levels of iNOS. The RAW 264.7 cells pre-treated with indicated concentrations of SE-2 and induced with LPS (1 µg/ml) for 10 hr's. Total RNA's were isolated and iNOS and COX-2 mRNA levels were measured by RT-PCR.

A)



B)

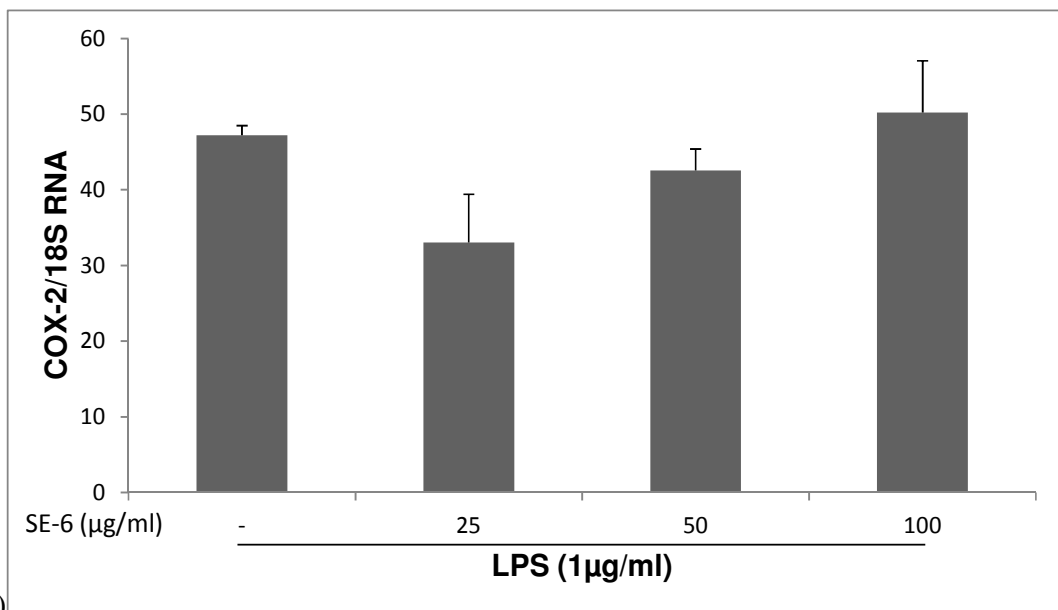
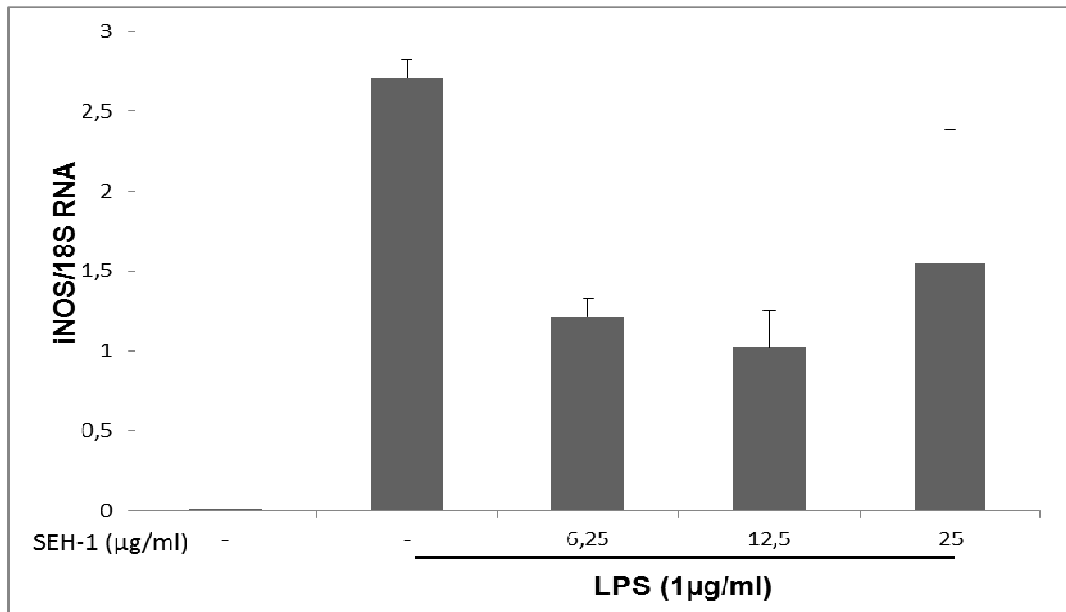


Figure 54: The effects of SE-6 (isorhamnetin-3-O-rutinoside) on mRNA levels of iNOS and COX-2. The RAW 264.7 cells pre-treated with indicated concentrations of SE-6 and induced with LPS (1 µg/ml) for 10 hr's. Total RNA's were isolated and iNOS and COX-2 mRNA levels were measured by RT-PCR.

A)



B)

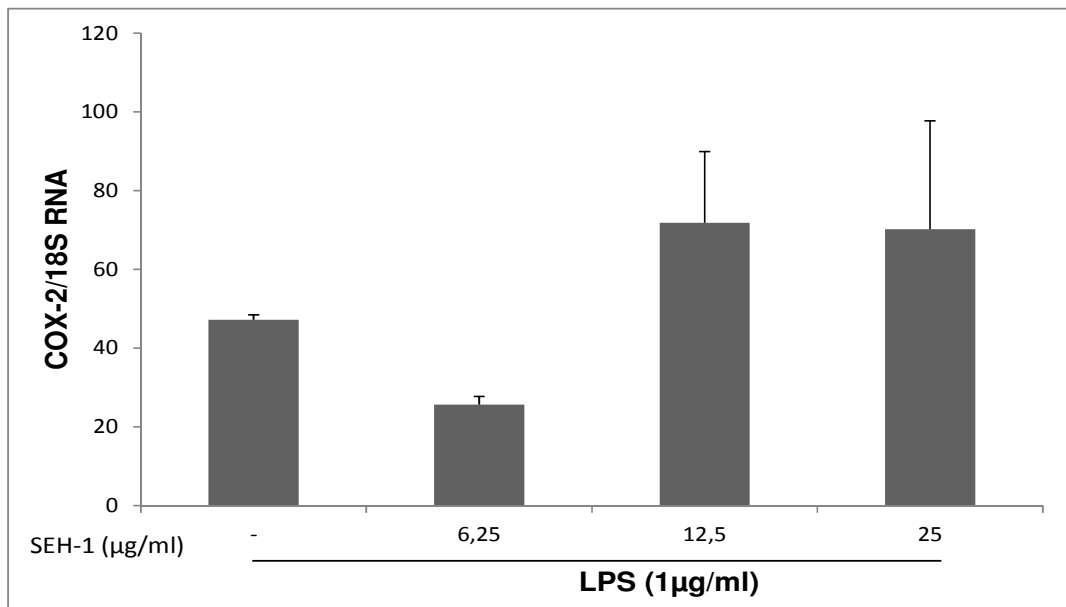
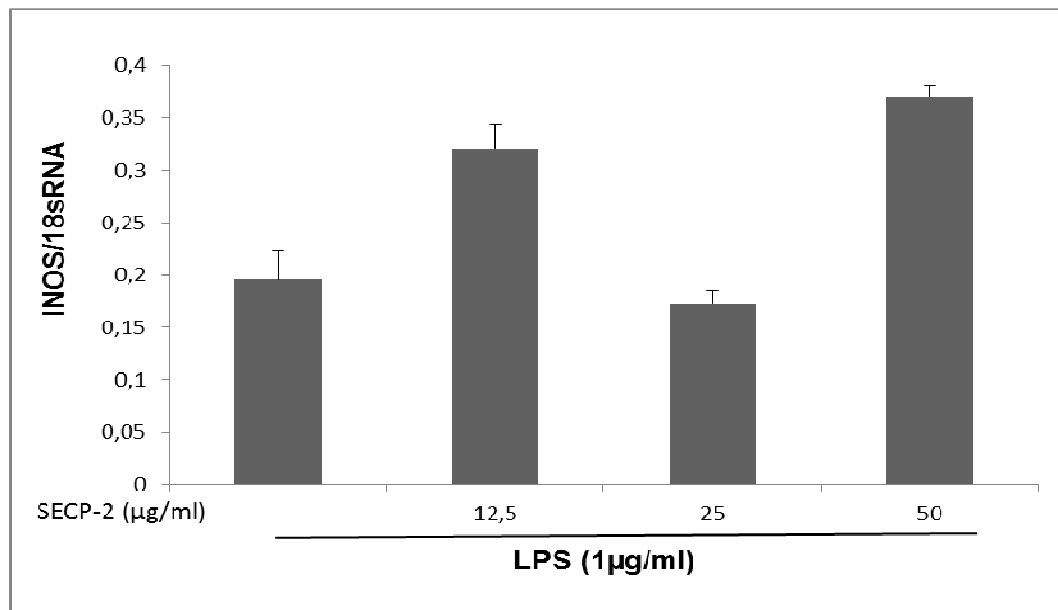


Figure 55: The effects of SEH-1 (Sambuln B) on mRNA levels of iNOS and COX-2. The RAW 264.7 cells pre-treated with indicated concentrations of SEH-1 and induced with LPS (1 µg/ml) for 10 hr's. Total RNA's were isolated and iNOS and COX-2 mRNA levels were measured by RT-PCR.

A)



B)

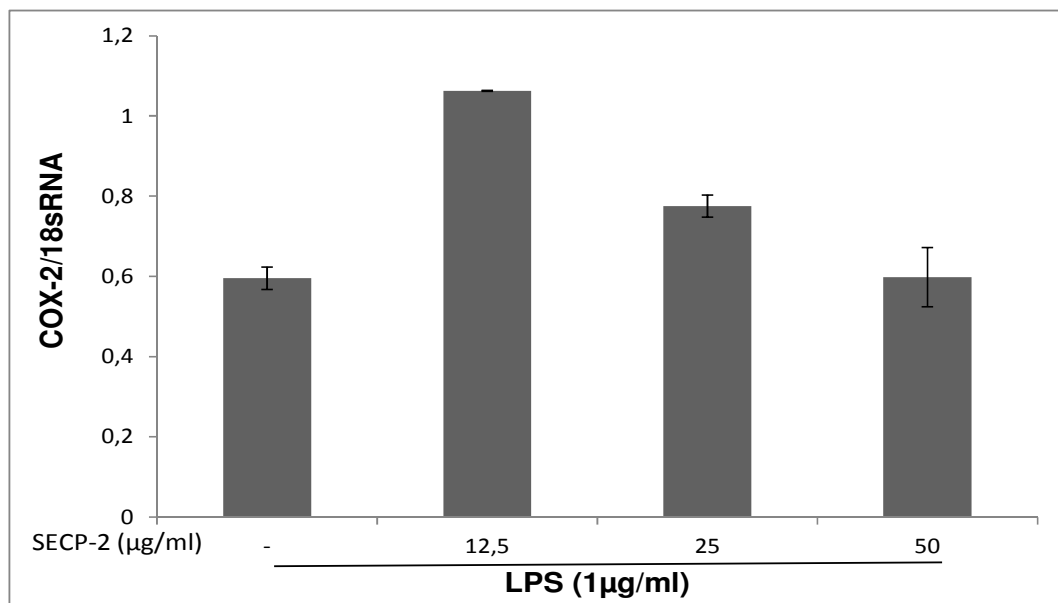


Figure 56: The effects of SECP-2 (Sambuln A) on mRNA levels of iNOS and COX-2. The RAW 264.7 cells pre-treated with indicated concentrations of SECP-2 and induced with LPS (1 µg/ml) for 10 hr's. Total RNA's were isolated and iNOS and COX-2 mRNA levels were measured vy RT-PCR.

4.2.4. Effects of the Active Compounds on Inflammatory Cytokines

The effect of the compounds obtained by activity-guided fractionation were tested for their inhibitory activities on LPS induced TNF α , IL-1 α , IL-1 β , IL-2, IL-6 productions on LPS-induced Raw 264.7 macrophage cells using ELISA assay. The molecules which were found to be effective at their highest concentrations were selected for concentration-dependent experiments.

The preliminary screening conducted with single concentrations revealed the TNF α inhibitor molecules to be; **SE-2**, **SE-6**, **SECP-2** and **SEH-1** (**Figure 57**). **CL-R-H₂O** also exerted inhibitory activity. Dexamethasone inhibited 45% of TNF α secretion of the LPS-induced Raw 264.7 cells at 10 μ M concentration.

The results of the concentration-dependent effects of the compounds were summarised in **Figure 58**. Only **CL-R-H₂O** provided an inhibition more than 40%. All other compounds exerted inhibitions around 40% at their highest concentrations. The activities of all compounds increased with concentration except for isorhamnetin-3-*O*-rutinoside. Both **SEH-1** and **SECP-2** were more active at lower concentrations than the flavonoids and other fractions tested. **SEH-1** provided a decrease of 17%, 21% and 33% of TNF α levels compared to only LPS treated group at 6.25, 12.5 and 25 μ g/ml concentrations. **SECP-2** exerted 25%, 31%, 38% inhibition (12.5, 25 50 μ g/ml). Isorhamnetin-3-*O*- β -D-glucopyranoside (**SE-2**) concentration-dependently inhibited TNF α secretion of the cells up to 40% at 100 μ g/ml. The effect observed for **SECP-2**, **SE-6** and **CL-R-H₂O** was comparable to the effect of 10 μ M of dexamethasone.

Only Sambulin B (**SEH-1**) exerted inhibition of IL-6 secretion on LPS-induced Raw 264.7 macrophage cells. At 25 μ g/ml concentration, it inhibited 59.12% of IL-6 amount in the cell culture media (**Figure 59**). **SECP-2**, **SE-2** and **SE-4** displayed weak activities on IL-6 production which was around 20% for each molecule at their highest concentrations.

As shown in **Figure 61**, **Figure 62** and **Figure 63** none of the molecules was active on IL-1 α , IL-1 β and IL-2.

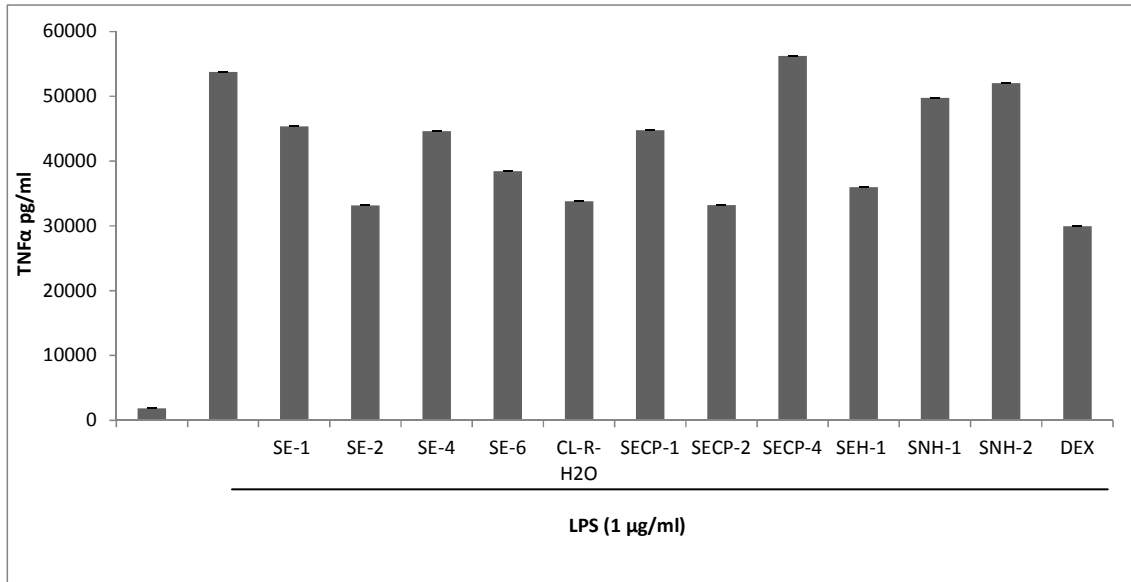
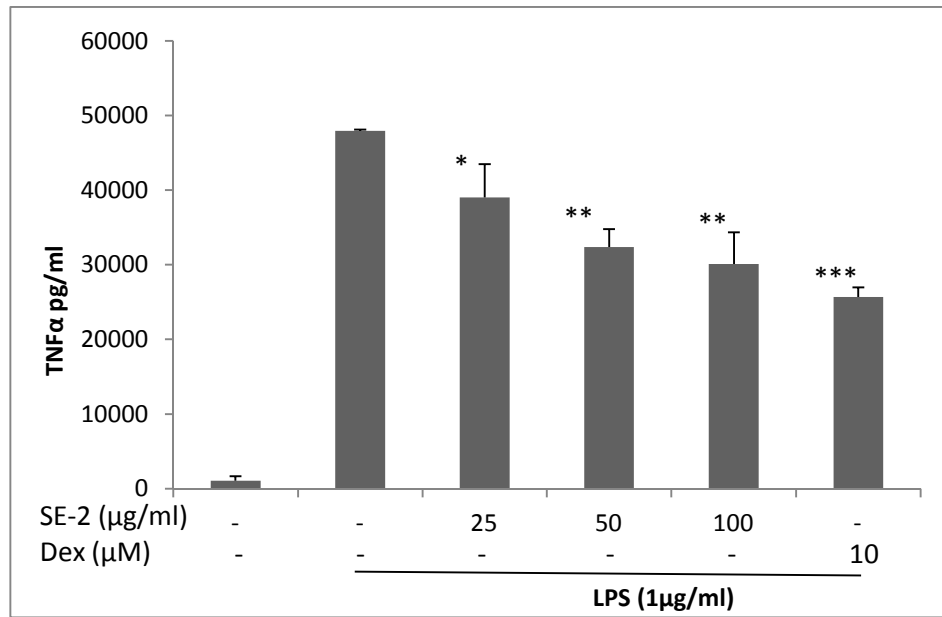
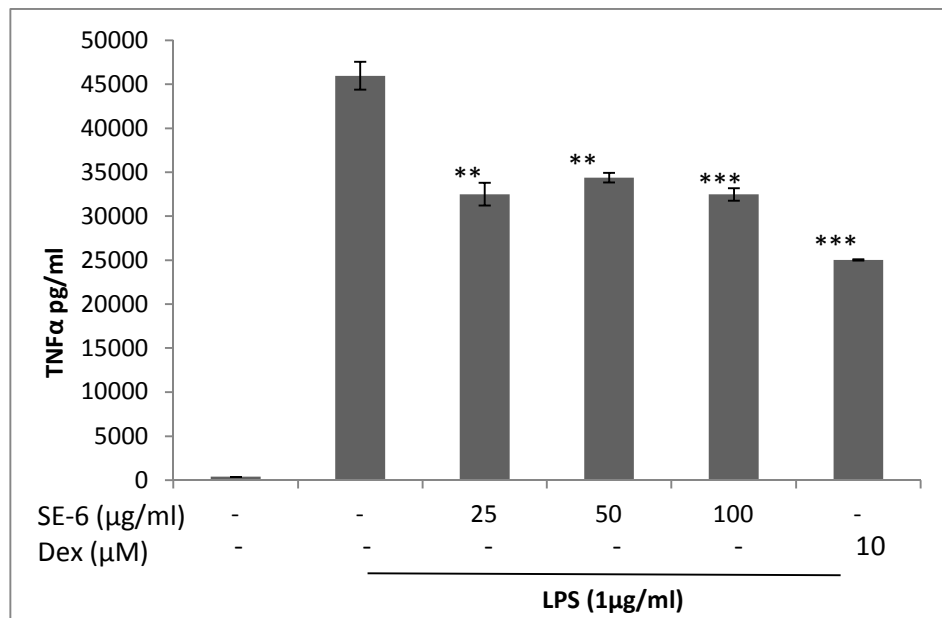


Figure 57: The inhibitory effects of the isolates on LPS induced TNF α secretion. Raw 264.7 macrophages were pre-incubated with the compounds for 1h. And then the cells were induced with 1 μ g/ml LPS for a total of 24 h. Media were collected and TNF α levels were measured by ELISA. SE-1 (100 μ g/ml), SE-2 (100 μ g/ml), SE-4 (100 μ g/ml), SE-6 (100 μ g/ml), SEH-1 (25 μ g/ml), SECP-2(50 μ g/ml), SECP-4 (50 μ g/ml), SNH-1 (50 μ g/ml), SNH-2 (50 μ g/ml), CL-ksu (100 μ g/ml), Dex: Deksametazon (10 μ M)

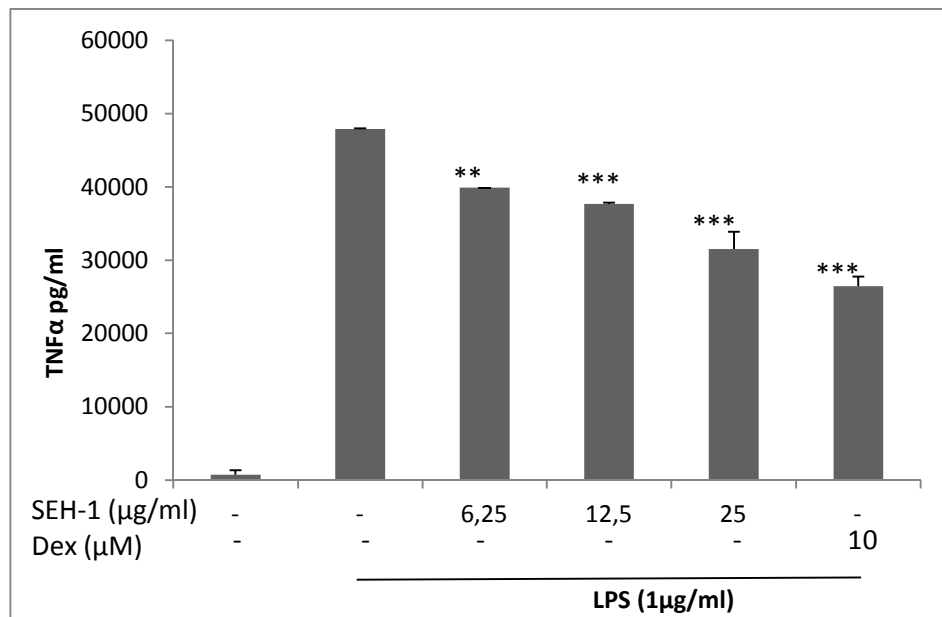
A)



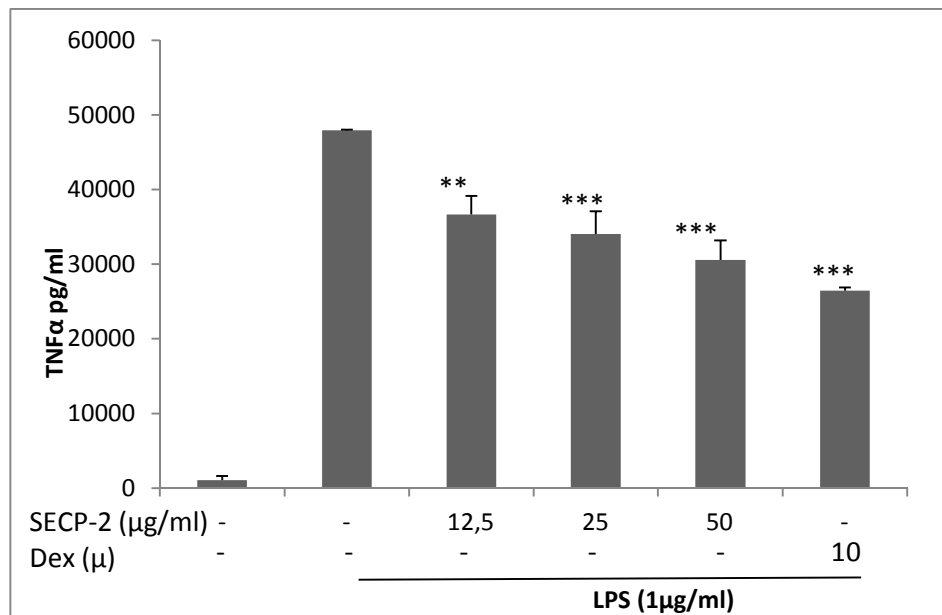
B)



C)



D)



E)

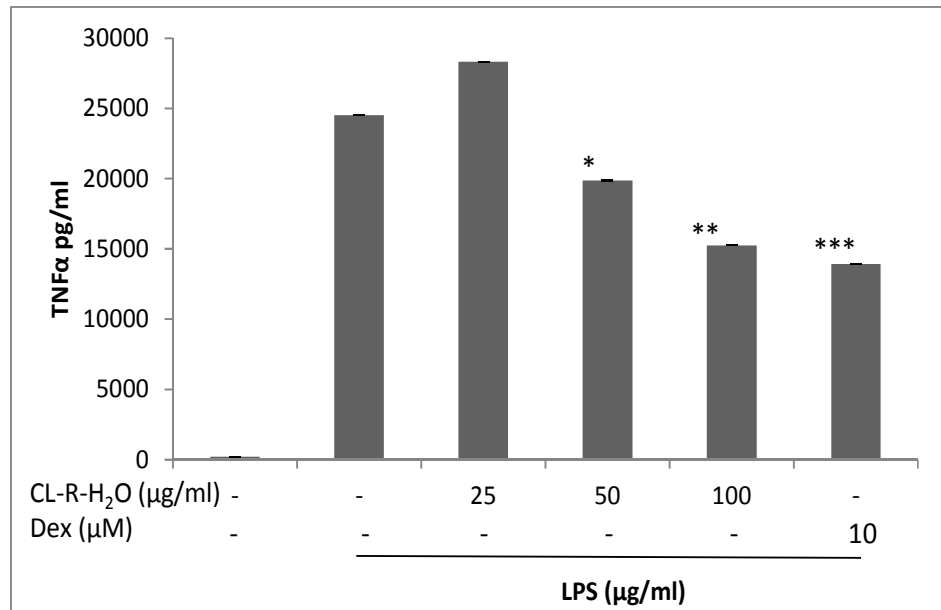


Figure 58: The concentration-dependent inhibitory effects of the active compounds on LPS-induced TNF α secretion. SE-2.(A), SE-6 (B), SEH-1 (C), SECP-2 (D) and CL-R-H₂O (E). Raw 264.7 macrophages were pre-incubated with the indicated concentrations of compounds for 1h. And then the cells were induced with 1 μ g/ml LPS for a total of 24 h. Media was collected and TNF α levels were measure by ELISA. Dex: Dexametazon (10 μ M) * $p \leq 0.05$ ** $p \leq 0.01$ *** $p \leq 0.001$ compared to LPS induced group

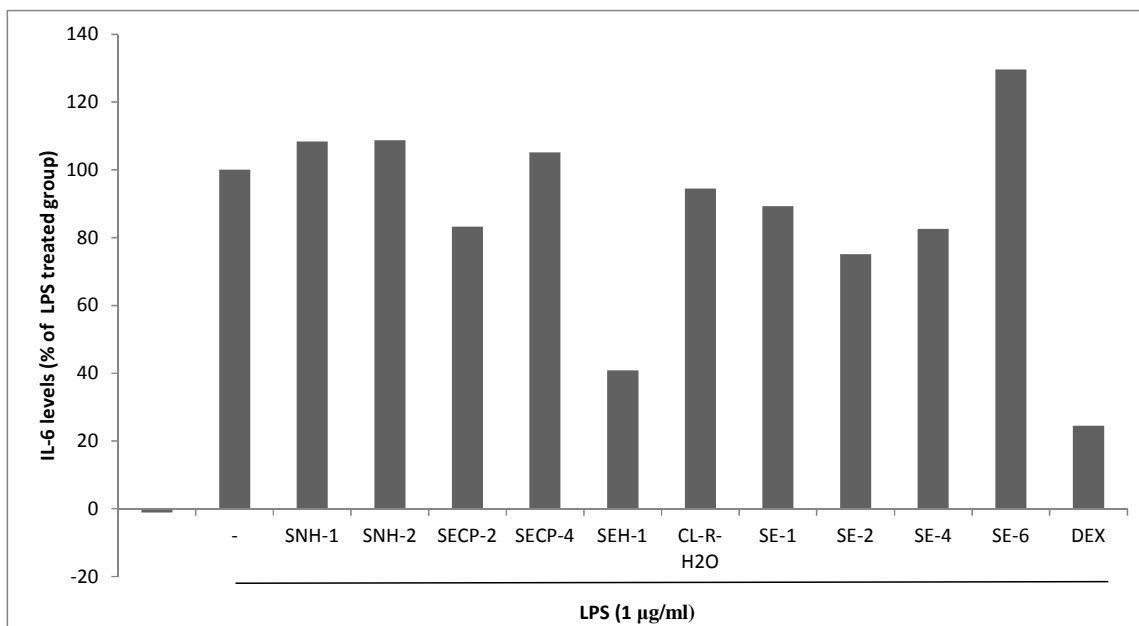


Figure 59: The inhibitory effects of the isolates on LPS induced IL-6 secretion. Raw 264.7 macrophages were pre-incubated with the compounds for 1h. And then the cells were induced with 1 µg/ml LPS for a total of 24 h. Media were collected and IL-6 levels were measured by ELISA. SE-1 (100 µg/ml), SE-2 (100 µg/ml), SE-4 (100 µg/ml), SE-6 (100 µg/ml), SEH-1 (25 µg/ml), SECP-2(50 µg/ml), SECP-4 (50 µg/ml), SNH-1 (50 µg/ml), SNH-2 (50 µg/ml), CL-ksu (100 µg/ml), Dex: Dexametazon (10 µM)

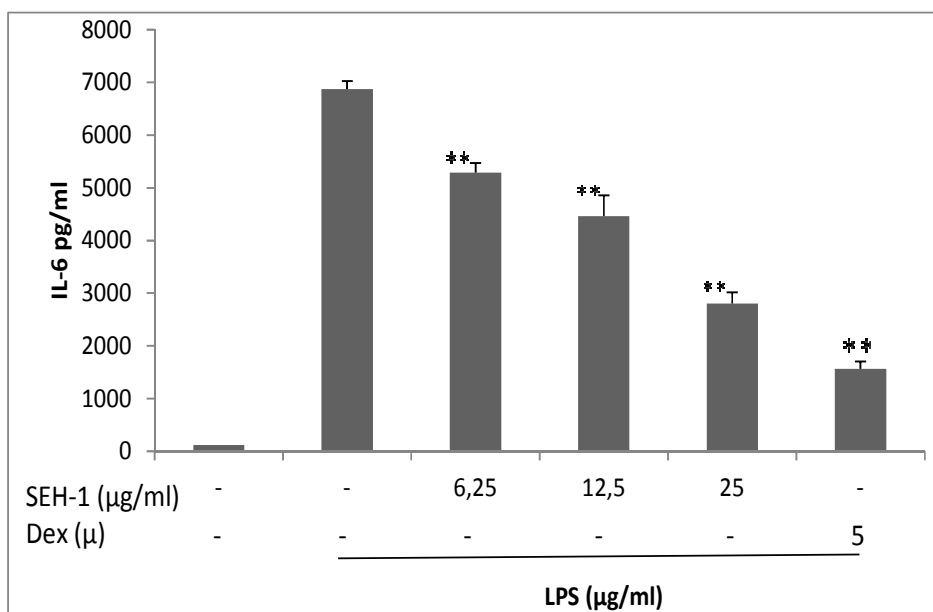


Figure 60: The concentration-dependent inhibitory effects of the SEH-1 (Sambulin B) on LPS induced IL-6 secretion. Raw 264.7 macrophages were pre-incubated with the compounds for 1h. And then the cells were induced with 1 µg/ml LPS for a total of 24 h. Media was collected and IL-6 levels were measured by ELISA. Dex: Dexametazon (10 µM) * $p \leq 0.05$ ** $p \leq 0.01$ compared to LPS induced group.

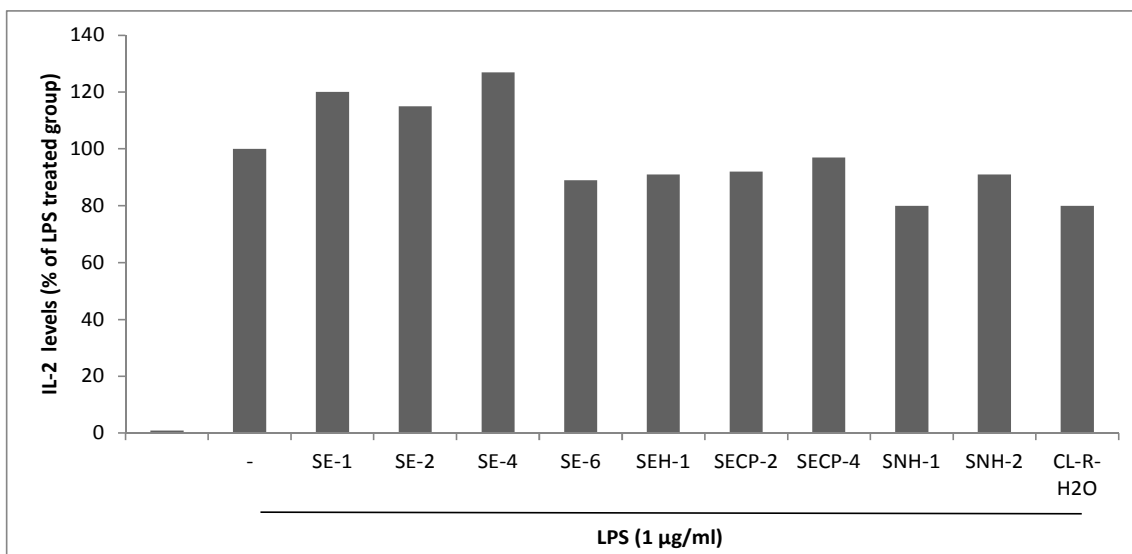


Figure 61: The inhibitory effects of the isolates on LPS induced IL-2 secretion. Raw 264.7 macrophages were pre-incubated with the compounds for 1h. And then the cells were induced with 1 µg/ml LPS for a total of 24 h. Media were collected and IL-2 levels were measure by ELISA. SE-1 (100 µg/ml), SE-2 (100 µg/ml), SE-4 (100 µg/ml), SE-6 (100 µg/ml), SEH-1 (25 µg/ml), SECP-1(25 µg/ml), SECP-2(50 µg/ml), SECP-3 (50 µg/ml),SNH-1 (50 µg/ml), SNH-2 (50 µg/ml), CL-ksu (100 µg/ml), Dex: Deksametazon (10 µM)

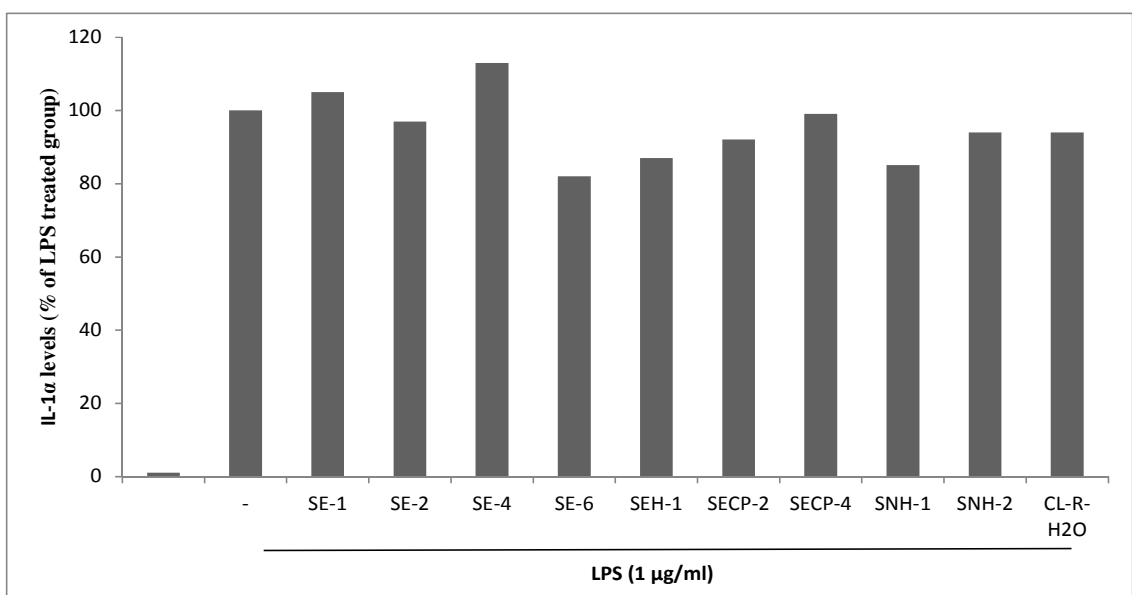


Figure 62:The inhibitory effects of the isolates on LPS induced IL-1α secretion. Raw 264.7 macrophages were pre-incubated with the compounds for 1h. And then the cells were induced with 1 µg/ml LPS for a total of 24 h. Media were collected and IL-1α levels were measure by ELISA. SE-1 (100 µg/ml), SE-2 (100 µg/ml), SE-4 (100 µg/ml), SE-6 (100 µg/ml), SEH-1 (25 µg/ml), SECP-1(25 µg/ml), SECP-2(50 µg/ml), SECP-3 (50 µg/ml),SNH-1 (50 µg/ml), SNH-2 (50 µg/ml), CL-ksu (100 µg/ml), Dex: Deksametazon (10 µM)

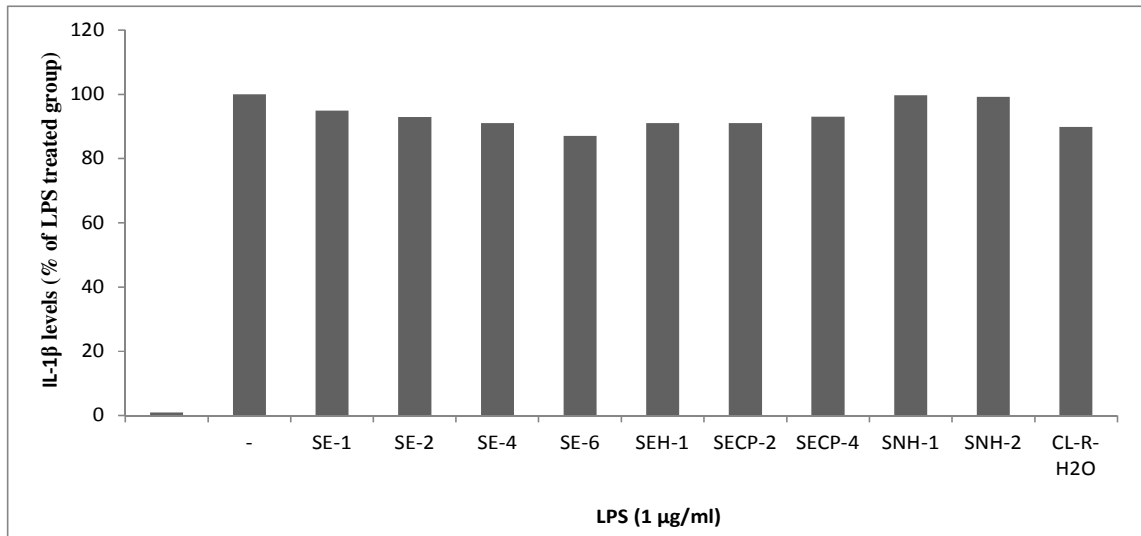


Figure 63: The inhibitory effects of the isolates on LPS induced IL-1 β secretion. Raw 264.7 macrophages were pre-incubated with the compounds for 1h. And then the cells were induced with 1 μ g/ml LPS for a total of 24 h. Media were collected and IL-1 β levels were measured by ELISA. SE-1 (100 μ g/ml), SE-2 (100 μ g/ml), SE-4 (100 μ g/ml), SE-6 (100 μ g/ml), SEH-1 (25 μ g/ml), SECP-1(25 μ g/ml), SECP-2(50 μ g/ml), SECP-3 (50 μ g/ml), SNH-1 (50 μ g/ml), SNH-2 (50 μ g/ml), CL-ksu (100 μ g/ml), Dex: Dexametazon (10 μ M)

4.2.5. The Effects of Bioactive Compounds on MAPK's and I κ -B α phosphorylation

The compounds which significantly inhibited the activity of NF- κ B and other inflammatory parameters were chosen to be investigated for their mechanism of action. For that reason their effects on phosphorylation of MAPK including ERK, JNK and p38 was investigated by Western Blotting using LPS-induced Raw 264.7 macrophages. In order to further investigate the mechanism of action of active compounds, their effects on I κ -B α phosphorylation which leads to NF- κ B activation were also investigated.

Raw 264.7 macrophage cells were pre-incubated with compounds for two hr's and then induced with LPS (1 μ g/ml) for 30 mins. 50 μ g of total cellular protein was extracted, electrophoresed and transferred onto nitrocellulose membrane. Membranes were incubated overnight with specific antibodies and visualised by CCD camera.

Isorhamnetin-3-*O*-D-glucopyranoside (**SE-2**) applied to Raw 264.7 cells for 2 hr's at 25, 50 and 100 μ g/ml concentrations. After 30 mins of induction with LPS, the cells were lysed and 50 μ g of total cellular proteins were electrophoresed. The results of the Western Blot analysis showed that isorhamnetin-3-*O*-D-glucopyranoside inhibited ERK phosphorylation at its lowest concentration (25 μ g/ml) by 66.57% but had no effect on ERK phosphorylation at the higher concentrations. At 100 μ g/ml compared to only LPS treated group this molecule significantly reduced p38 and JNK phosphorylations by 30.09% and 63.47% respectively. The results suggest that at low concentrations inhibitions of ERK and at higher concentrations inhibition of p38 and JNK pathways might be responsible for the anti-inflammatory activity of this molecule (**Figure 64**). Isorhamnetin-3-*O*- β -D-glucopyranoside inhibited I κ -B α phosphorylation and that compound also decreased the levels of I κ -B α (100 μ g/ml). At 50 and 100 μ g/ml concentrations **SE-2** prevented 47.36% and 49.35% of the phosphorylation of I κ -B α proteins.

Isorhamnetin-3-*O*-rutinoside had no effect on JNK phosphorylation at the concentrations tested (25, 50, 100 µg/ml). ERK phosphorylation was reduced by 44.75% and 46.17% by pre-treatment of cells with 50 and 100 µg/ml isorhamnetin-3-*O*-rutinoside. At the highest concentration tested (100 µg/ml) this molecule inhibited 56.08% of p38 phosphorylation. Anti-inflammatory activity of this molecule might be through inhibition of p38 phosphorylation. Raw 264. 7 macrophage cells were pre-treated with compounds for 2 hr's and then the cells were induced with LPS (1 µg/ml) for 30 mins. As shown in **Figure 65**, LPS treatment of cells for 30 mins. significantly increased the Iκ-Bα phosphorylation. Iκ-Bα phosphorylation was almost completely inhibited by pre-treatment of cells with 50 and 100 µg/ml isorhamnetin-3-*O*-rutinoside (**SE-6**) for 2 hr's. Iκ-Bα levels remained unchanged.

As shown in **Figure 66**, **SECP-2** (Sambulin A) induced ERK phosphorylation at 12.5, 25 and 50 µg/ml concentrations more than only LPS treated group. However, Sambulin A provided a concentration-dependent inhibition of phosphorylation of JNK and p38. At 6.25 µg/ml **SECP-2** had no inhibitory effect on JNK phosphorylation but this molecule inhibited 24.28% and 69.93% of the phosphorylation of JNK at 25 and 50 µg/ml. At 50 µg/ml **SECP-2** inhibited 85.37% of the phosphorylation of p38. The mechanism underlying the anti-inflammatory effects of this molecule might be through blockage of p38 and JNK pathways. **SECP-2** provided a significant inhibition of the phosphorylation of Iκ-Bα at 50 µg/ml (43.61%) verifying the NF-κB inhibition caused by this molecule.

SEH-1 (Sambulin B) inhibited JNK phosphorylation in a concentration-dependent manner. **SEH-1** inhibited 38.26, 86.21, 92.79% of the phosphorylation of JNK at 6.25, 12.5 and 25 µg/ml concentrations respectively. This molecule inhibited ERK phosphorylation by 58.57% at 6.25 µg/ml concentration compared to only LPS treated group but showed no effect on p38 phosphorylation. Suppression of JNK and ERK phosphorylation might be responsible for the mechanism of anti-inflammatory effect of this molecule (**Figure 67**). Sambulin B (**SEH-1**) concentration-dependently inhibited the phosphorylation of Iκ-Bα. The effect of the compound at 25 µg/ml was remarkable (67.34%).

CL-R-H₂O inhibited JNK phosphorylation at 25, 50 and 100 µg/ml by 21.26, 48.81, 51.40% compared to only LPS treated group. The inhibitory effect increased with increasing concentrations (**Figure 69**). It inhibited p38 phosphorylation at 50 µg/ml by 27.25%. No effect had been observed at ERK phosphorylation. **CL-R-H₂O** almost totally prevented Iκ-Bα phosphorylation at 100 µg/ml concentrations (89.45% inhibition).

SNH-1, which was determined as the responsible fraction of *S. nigra* hexane subextract, was tested for its effect on MAPK phosphorylation. **SNH-1** had no effect on none of these parameters. The results of the experiment was laid out in **Figure 68**. **SNH-1** was only effective on Iκ-Bα phosphorylation at the highest (50 µg/ml) concentration tested providing 54.04% inhibition.

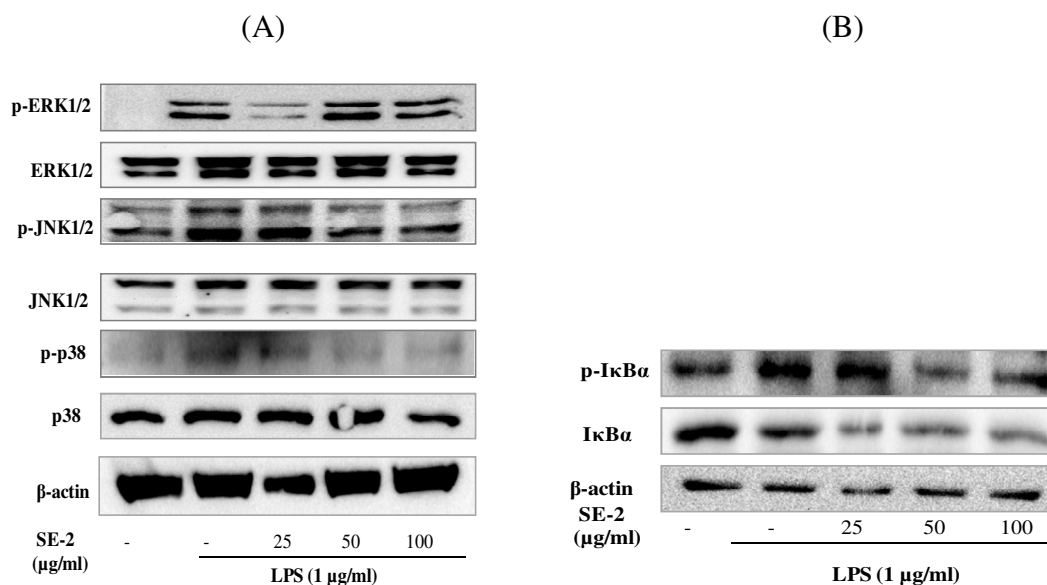


Figure 64: Effect of SE-2 (isorhamnetin-3-*O*-*D*-glucopyranoside) on MAPKs activation (p38, JNK and ERK phosphorylation) and IκBα phosphorylation. MAPKs activation (A), IκBα phosphorylation (B) Raw 264.7 macrophages were pre-incubated with the indicated concentrations of flavonoids for 2 h and then treated with LPS (1 μg/ml) for an additional 30 mins. 50 μg of cell lysate protein was prepared and subjected to Western blot using specific antibodies. Equal loading was verified using β-actin antibody.

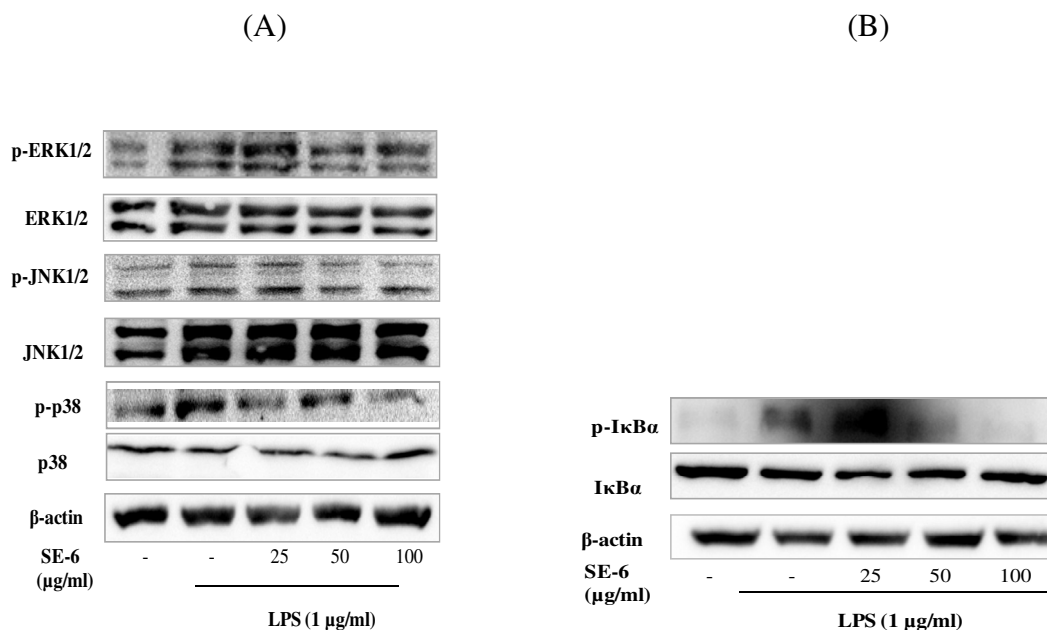


Figure 65: Effect of SE-6 (isorhamnetin-3-*O*-rutinoside) on MAPKs activation (p38, JNK and ERK phosphorylation) and IκBα phosphorylation. (A) MAPKs activation (B). IκBα phosphorylation. The figure shows the representative of three experiments. Raw 264.7 macrophages were pre-incubated with the indicated concentrations of flavonoids for 2 h and then treated with LPS (1 μg/ml) for an additional 30 mins. 50 μg of cell lysate protein was prepared and subjected to Western blot using specific antibodies. Equal loading was verified using β-actin antibody.

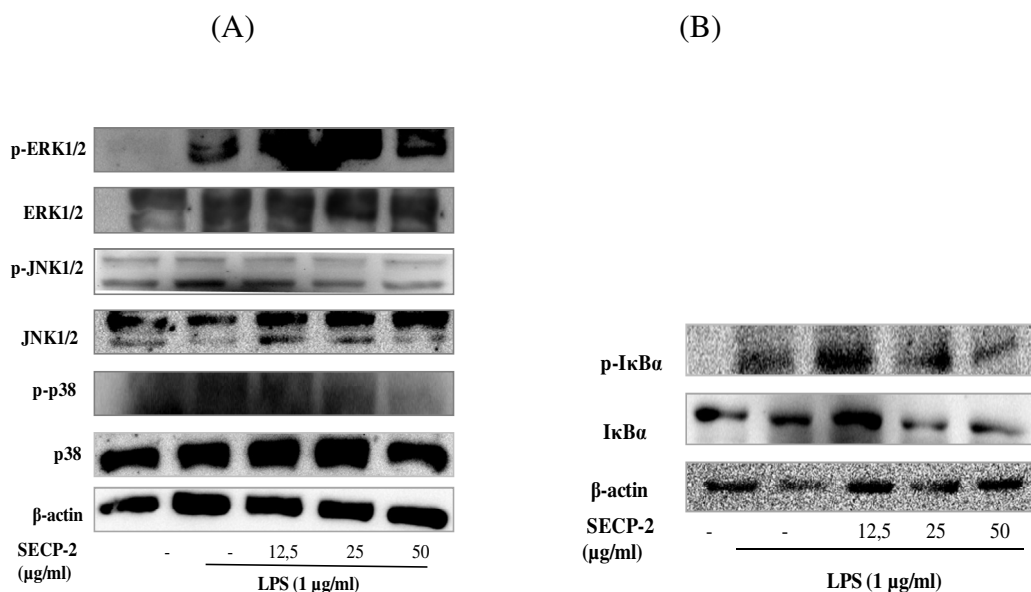


Figure 66: Effect of SECP-2 (Sambulin A) on MAPKs activation (p38, JNK and ERK phosphorylation) and IκBα phosphorylation. (A) MAPKs activation (B) IκBα phosphorylation. The figure shows the representative of three experiments. Raw 264.7 macrophages were pre-incubated with the indicated concentrations of flavonoids for 2 h and then treated with LPS (1 μg/ml) for an additional 30 mins. 50 μg of cell lysate protein was prepared and subjected to Western blot using specific antibodies. Equal loading was verified using β-actin antibody.

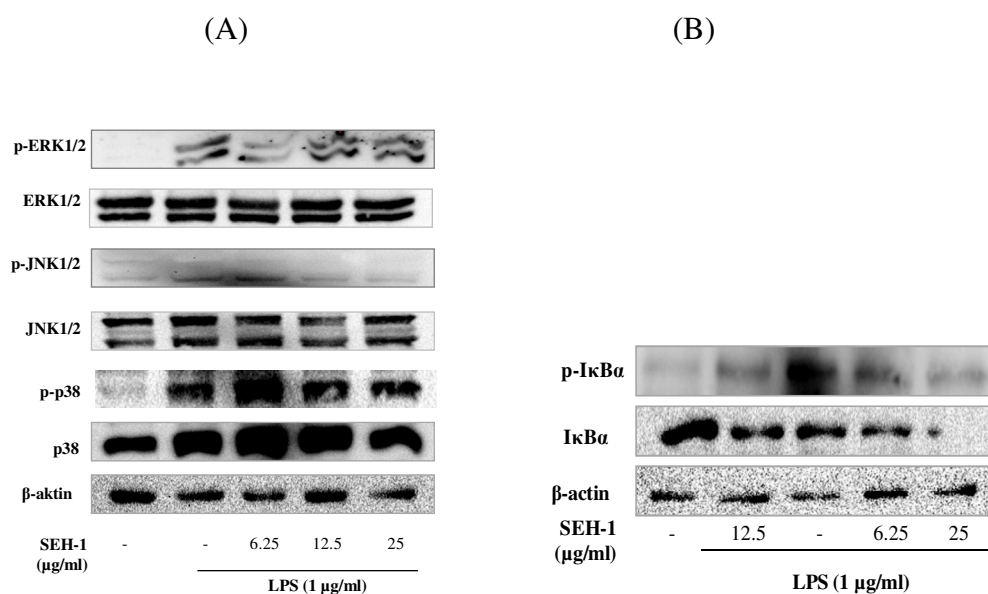


Figure 67: Effect of SEH-1 (Sambulin B) on MAPKs activation (p38, JNK and ERK phosphorylation) and IκBα phosphorylation. (A) MAPKs activation (B) IκBα phosphorylation. The figure shows the representative of three experiments. Raw 264.7 macrophages were pre-incubated with the indicated concentrations of flavonoids for 2 h and then treated with LPS (1 μg/ml) for an additional 30 mins. 50 μg of cell lysate protein was prepared and subjected to Western blot using specific antibodies. Equal loading was verified using β-actin antibody.

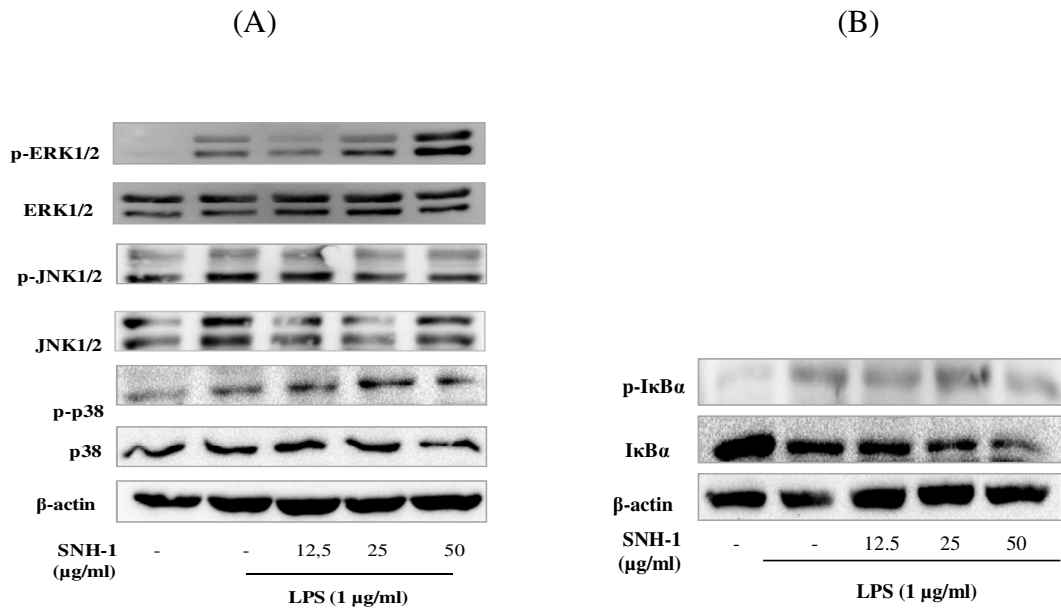


Figure 68: Effect of SNH-1 on MAPKs activation (p38, JNK and ERK phosphorylation) and IκBα phosphorylation. (A) MAPK's activation (B) IκBα phosphorylation. The figure shows the representative of three experiments. Raw 264.7 macrophages were pre-incubated with the indicated concentrations of SNH-1 for 2 h and then treated with LPS (1 μg/ml) for an additional 30 mins. 50 μg of cell lysate protein was prepared and subjected to Western blot using specific antibodies. Equal loading was verified using β-actin antibody.

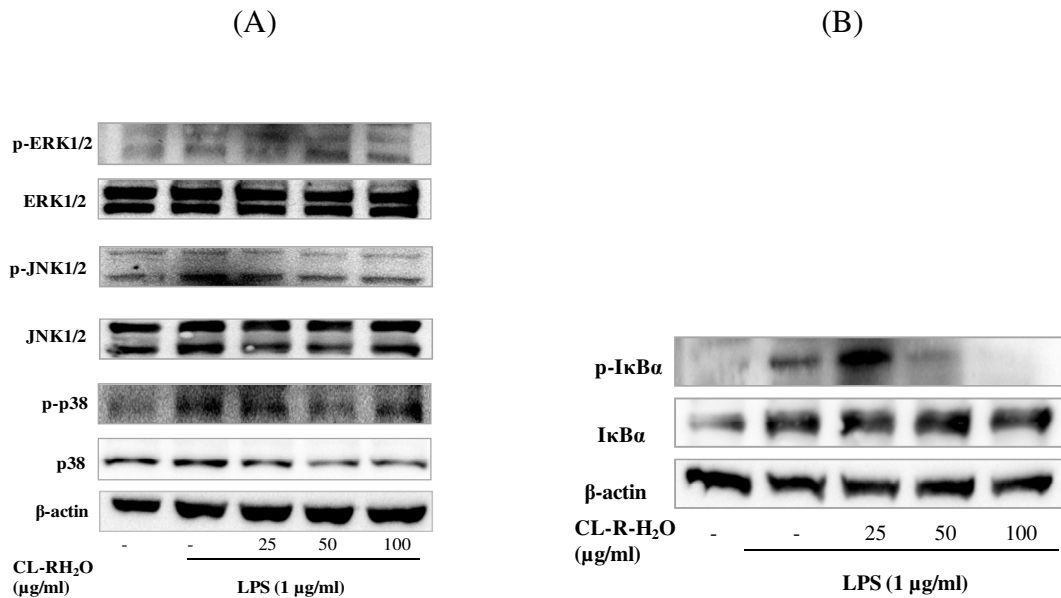


Figure 69: Effect of CL-R-H₂O on MAPKs activation (p38, JNK and ERK phosphorylation) and IκBα phosphorylation (A) MAPK' phosphorylation (B) IκBα phosphorylation. The figure shows the representative of three experiments. Raw 264.7 macrophages were pre-incubated with the indicated concentrations of fraction for 2 h and then treated with LPS (1 μg/ml) for an additional 30 mins. 50 μg of cell lysate protein was prepared and subjected to Western blot using specific antibodies. Equal loading was verified using β-actin antibody.

5. DISCUSSION & CONCLUSION

DISCUSSION

Acute and chronic inflammatory diseases are still one of the major health problems among world's population. Chronic inflammation may lead to the development of diseases such as chronic asthma, rheumatoid arthritis, multiple sclerosis and inflammatory bowel disease (203). These diseases are debilitating and are becoming increasingly common in society. Although several chemical agents are known for the treatment of these type of diseases, long term usage of these agents might be unsafe due to severe adverse/side effects and high costs (203, 204). Therefore, there is a growing need to develop new anti-inflammatory agents with minimum side effects (204).

Plants used in folk medicine have been accepted as an indispensable source in new drug discovery (203). Ethnobotanical field surveys on Anatolian folk medicine revealed that traditional medicine in Turkey is a rich source for herbal remedies with possible anti-inflammatory activity. As a consequence; three plants which are widely used in folk medicine for the treatment of rheumatism and related inflammatory diseases in Turkey, were selected; two species of *Sambucus*; *S. ebulus*, *S. nigra* (Caprifoliaceae) and *Cistus laurifolius* (Cistaceae) as the subject of this experimental study (205-209). Besides their widespread utilization in traditional medicine, these plants were also demonstrated to exert significant *in vitro* and *in vivo* anti-inflammatory activity in the previous studies and several active constituents were isolated. However, the mechanisms behind these activities and their active components have not been investigated thoroughly so far.

To prove the claimed effect of these plants (*S. ebulus*, *S.nigra* and *C. laurifolius*) and to isolate the compounds responsible for the *in vitro* activity, activity-guided fractionation (AGF) technique was used monitoring with convenient *in vitro* methods. For that purpose total extracts were prepared from these plants with EtOH or MeOH and then they were partitioned with successive solvent-solvent extractions with solvents of increasing polarities. Consequently hexane, CHCl₃, EtOAc, *n*-BuOH and remaining water subextracts were obtained from each total extract. These extracts were then

monitored for their inhibitory activities on NF- κ B transcription factor in LPS-induced Raw 264.7 macrophages.

NF- κ B is a transcription factor that regulates the expression of several molecules that has a critical role in inflammatory and immune responses such as interleukines (IL-1, IL-2, IL-6) and TNF α , enzymes such as iNOS, COX-2 (210). NF- κ B pathway involves in the pathogenesis of chronic inflammatory diseases such as rheumatoid arthritis and asthma as well as several cancers. Also high levels of NF- κ B activity was observed in Alzheimer's disease and atherosclerosis (203, 211-214). In addition to its regulator role in inflammation and immune response, NF- κ B is an important regulator of tumorigenesis, apoptosis and cellular proliferation (215). Several anti-inflammatory drugs in the practice were shown to inhibit NF- κ B pathway (216). Therefore NF- κ B and signalling pathways that regulates its activity have become an important target for drug discovery and development. In a recent review, it was reported that, 785 NF- κ B inhibitory synthetic or natural compounds had been defined by the end of 2006 (217).

Inflammation is a complex process that involves various pathways. Prostaglandines, leukotrienes, platelet activating factors and cytokines such as IL-1 and TNF α are known to be involved in the inflammatory response of the body (204). The inflammatory response may be inhibited by antagonizing the inflammatory pathway and blockage of the productions of these inflammatory mediators. Therefore such pathways are accepted as potential targets in anti-inflammatory drug discovery. The main targets include enzymes such as COX-2 or cytokines such as IL-1 β or TNF α (218). Besides these mediators, transcriptions factors responsible for the transcription of inflammatory mediators such as NF- κ B and signalling pathways such as mitogen active protein kinases (MAPK) are also known to be important targets for anti-inflammatory research (219).

Although the crude (MeOH or EtOH) extracts of all three species had no inhibitory effect on the activation of NF- κ B transcription factor on these experimental set up, some of the subextracts obtained by solvent-solvent extraction, exerted significant activity. This situation might be due to the antagonistic effect of some of the

components in the extract or their low concentrations in the crude extracts. The most active subextracts were determined to be the hexane (SE-Hex) , EtOAc (SE-EtOAc) and CHCl₃ (SE-EtOAc) subextracts of *S. ebulus* and hexane subextract of *S. nigra* (SN-Hex). The remaining water subextract of *C. laurifolius* (CL-R-H₂O) was also active on NF-κB transcription factor. Activity-guided fractionation of these active subextracts yielded active compounds which were then investigated for their activity profiles on several inflammatory parameters.

SE-EtOAc was fractionated by polyamide column chromatography and MPLC. Two flavonoids (isorhamnetin-3-*O*-β-D-glucopyranoside and isorhamnetin-3-*O*-rutinoside) and a mixture of these flavonoids in different ratios [isoquercitrin (quercetin-3-*O*-β-D-glucopyranoside) and hyperoside (quercetin-3-*O*-β-D-galactopyranoside)] were isolated as the active components. They were highly active on NF-κB, whereas the mixture was inactive on the other inflammatory parameters investigated when cells were pre-incubated with the compounds for 1 hr. In a recent study it was reported that at 100 μM concentrations hyperoside, isoquercetin and quercetin (aglycone of these molecules) inhibited LPS induced nitric oxide production of the cells at the ratios of 49.8, 47.5 and 66.1% respectively (220). Aglycone of these compounds were found to be more active than the glycosidic forms in that study. It is noteworthy that these compounds were pre-incubated with cells for 4 hr's. Since we applied 1 hr pre-incubation for the flavonoid mixture, the activity of these molecules might possibly be increased over long incubation times. In the same study these molecules were also found to inhibit the phosphorylations of ERK, JNK and p38 when pre-incubated with cells for 4 hr's (220).

The same mixture of hyperoside and isoquercitrin (hyperoside 2/3 of the mixture) was previously determined to be anti-inflammatory component from the leaves of *Rhododendron ponticum*, which exerted high activity on TPA-induced ear eadema in mice and carrageenan-induced hind paw eadema (221). In the present study, the same mixture inhibited the activity of NF-κB activation in LPS-induced Raw 264.7 macrophage cells. Therefore we can suggest the underlying mechanism of the anti-inflammatory activity for this mixture might be due to its inhibition on NF-κB pathway.

The other two active NF- κ B inhibitory components of *S. ebulus*, isorhamnetin-3-*O*- β -D-glucopyranoside and isorhamnetin-3-*O*-rutinoside, were also found active on the other inflammatory parameters investigated. Isorhamnetin-3-*O*- β -D-glucopyranoside inhibited 49% of the nitric oxide production of the cells compared to only LPS treated control group. But the molecule had no effect on PGE₂ production. Nitric oxide inhibition correlated with the reduction of the iNOS protein levels of the cells but no effect was observed on COX-2 levels. This latter result determined for isorhamnetin-3-*O*- β -D-glucopyranoside, i.e. ineffective on COX-2 level, was consistent with previous data (222). The inhibitory activity of the compound on TNF α was around 40% of the LPS treated group at the highest concentration, but it was only slightly active on IL-6 levels. In an attempt to explain the mechanism of these effects, we further investigated their effects on phosphorylation of MAPK's and I κ B α . This molecule prevented ERK phosphorylation at low concentration (25 μ g/ml) and p38 at high concentrations (50, 100 μ g/ml). The reduction of the phosphorylation levels of I κ B α at 50 and 100 μ g/ml confirmed the inhibitory effect observed on NF- κ B.

The other active component, isorhamnetin-3-*O*-rutinoside inhibited 41% of the LPS induced activation of NF- κ B at 100 μ g/ml concentration and provided a 73% reduction in NO levels. The only structural difference between isorhamnetin-3-*O*- β -D-glucopyranoside and this molecule is the attachment of a rhamnose unit at the 6th position of the glucose moiety. Therefore different ratios in the inhibitory effects of these molecules on NO might be related with the presence of a second sugar in its structure. Isorhamnetin-3-*O*-rutinoside inhibited 41% of the PGE₂ levels. The reduction in the levels of iNOS and COX-2 was in accordance with the decreased levels observed at NO and PGE₂ productions. This molecule exerted up to 30% inhibition on LPS induced TNF α production in Raw 264.7 cells. This effect was not concentration-dependent. The studies aimed to explain the anti-inflammatory mechanism of this compound demonstrated that the reduction on the phosphorylation of p38 and I κ B α might be the mechanism behind the activity. Hamalainen et al. investigated the effect of isorhamnetin, the aglycone of both molecules that was isolated in this study, on nitric oxide production in LPS-induced J774 macrophage cells and reported that isorhamnetin significantly inhibited nitric oxide production (IC₅₀ 30 μ M), iNOS protein levels and

NF- κ B activation (223). Same flavonoids were previously isolated from the alcoholic extract of the fresh flowers of *Opuntia dillenii* as the active anti-inflammatory components on carrageenan- induced rat paw edema, through bioactivity-guided procedures (224). Eventually, results of the present survey would also contribute to explain the anti-inflammatory activity of the *Opuntia* extract.

TLC examination of SE-CHCl₃ revealed that this extract was rich in secondary metabolites. Therefore the components of this extract was further partitioned by successive column chromatographic processes and active fractions and subfractions were determined. Finally through MPLC a new iridoid compound was isolated and its chemical structure was elucidated and named as Sambulin A.

The other active subextract of *S. ebulus*, SE-Hex was further partitioned into five fractions by MPLC. The other new iridoid was isolated from the active fraction and named as Sambulin B. Sambulin B differs from Sambulin A by the presence of an additional acetyl unit attached at the C-7 (OH) position. Both molecules were more active than the flavonoid components at low concentrations. Sambulin A applied to Raw 264.7 macrophages at 12.5, 25 and 50 μ g/ml concentrations. At highest concentration, it inhibited the activation of NF- κ B at a ratio of 83% compared to only LPS treated group. This compound was also found effective on LPS-induced NO production. The nitric oxide production was inhibited from 23% to 70%, concentration-dependently in accordance with the reduction in iNOS protein levels. This molecule led to a 40% reduction in PGE₂ levels at 100 μ g/ml and COX-2 protein levels were well correlated with PGE₂ levels. It was one of the most potent inhibitor of TNF α among the isolated compounds and provided a reduction between 25% and 38% depending on the concentration. On the other hand, it was only slightly active on IL-6 levels. JNK and p38 pathways might be the underlying mechanism of the anti-inflammatory effect of these molecules. The effects observed on I κ -B α phosphorylations were well correlated with NF- κ B results. Raw 264.7 macrophage cells were pre-incubated with 6.25, 12.5 and 25 μ g/ml Sambulin B (SEH-1). At 25 μ g/ml concentration Sambulin B inhibited 32% of LPS induced NF- κ B activation. This effect is probably due to the inhibitions observed on the phosphorylation of MAPK especially on JNK and at low concentrations

ERK. Consistent with the results of NF- κ B inhibition this molecule exerted a concentration-dependent inhibition of I κ B α phosphorylation. This molecule is a potent NO and PGE₂ inhibitor exerting inhibitions up to 80%. NO inhibitory effect of Sambulin B was twice as much potent as Sambulin A. Sambulin B also decreased PGE₂ levels in the cell culture more than twice as much potent as Sambulin A when applied at the half of its concentration. Eventually it can be concluded that the presence of an additional acetyl group at C-7 of the iridoid skeleton as in Sambulin B increased the inhibitory activity against both NO and PGE₂. Moreover Sambulin B provided up to 33% decrease of the TNF α amount in the cell culture media and it was the only molecule which was effective on IL-6 levels. At 25 μ g/ml concentration, this molecule provided a 48% inhibition. Sambulin B at concentrations higher than 25 μ g/ml concentration resulted in more than 30% decrease of the viability of Raw 264.7 macrophages, but Sambulin A was not toxic to cells up 100 μ g/ml concentration suggesting that the acetyl group had also affected cell viability.

The results obtained from the experiments conducted on active components were summarized in **Table 61**: and **Table 62**. All flavonoids inhibited LPS induced activation of NF- κ B ranging from 46% to 64% at their highest concentrations. However, **SE-1** and **SE-2** (mixtures of hyperoside and isoquercitrin in different ratios) were not active on other parameters tested (NO, PGE₂, cytokines). Accordingly, they were not further evaluated for their effects on MAPK's and I κ B α phosphorylations. On the other hand, **SE-2** (isorhamnetin-3-*O*- β -D-glucopyranoside) and **SE-6** (isorhamnetin-3-*O*-rutinoside) were active on more parameters. Isorhamnetin-3-*O*- β -D-glucopyranoside decreased the LPS induced levels of NO and this effect was found to be correlated with the decrease in the protein levels of iNOS. Isorhamnetin-3-*O*-rutinoside was active on NO and iNOS productions and in addition this molecule was found to decrease PGE₂ and COX-2 levels. While isorhamnetin-3-*O*- β -D-glucopyranoside exerted its anti-inflammatory effect by inhibiting the phosphorylations of JNK and p38 pathways, isorhamnetin-3-rutinoside slightly inhibited ERK and significantly inhibited p38 pathway. Both molecules inhibited TNF α production but had no effect on the other cytokines.

SEH-1 (Sambulin B) and **SECP-2** (Sambulin A) which were isolated as new iridoids were toxic to Raw 264.7 cells at high concentrations. The highest non-toxic concentration for Sambulin B was 25 and 50 $\mu\text{g/ml}$ for Sambulin A. Sambulin B inhibited 32% of the activation of NF- κ B at the highest concentration. Sambulin A at 50 $\mu\text{g/ml}$ inhibited 82% of the activity of NF- κ B. These iridoids were more active than all the active flavonoids isolated in the present study at lower concentrations. These molecules were also highly active on NO and PGE₂ productions. The inhibitions observed at iNOS and COX-2 levels proved their effects on NO and PGE₂. Besides, Sambulin A and Sambulin B inhibited TNF α productions. Out of the tested compounds Sambulin B was the only active molecule on IL-6 production. Although iridoid molecules were more toxic to Raw 264.7 cells than flavonoids, they exerted wider anti-inflammatory spectrum. Sambulin B exerted its effect through inhibiting JNK phosphorylation. Sambulin A inhibited both JNK and p38 phosphorylations. Although the presence of an additional acetyl group at C-7 of Sambulin B increased the inhibitory activity against LPS-induced NO production, acetyl group might possibly prevented the inhibitory effect of the molecule on p38 phosphorylation.

Comparing to *S. ebulus*, *S. nigra* extract was found less active. Through activity-guided fractionation procedures, two fractions were identified to be responsible for the activity of *S. nigra* hexane subextract; SNH-1 and SNH-2. Although they were active on NF- κ B, only SNH-1 exerted inhibitions on other inflammatory parameters. SNH-1 inhibited NO and PGE₂ productions and decreased iNOS and COX-2 protein levels. SNH-1 applied to Raw 264.7 cells at 50 $\mu\text{g/ml}$ concentration and inhibited 73% of NF- κ B activation. The effects observed on other parameters (NO, PGE₂) were lower at 50 $\mu\text{g/ml}$ concentration so SNH-1 applied to cells at 25, 50 and 100 $\mu\text{g/ml}$ concentrations for these experiments. SNH-1 exerted no inhibitions on MAP kinases.

As a result of Real-Time PCR experiments to detect the mRNA levels of iNOS and COX-2, it was shown that 10 hr's of induction with LPS was not causative for the decreases observed at protein levels. Therefore different time points for induction with LPS might lead to the observed inhibitions of iNOS and COX-2 protein levels. The anti-inflammatory and antiarthritic activities of methanol and water extracts of *S. ebulus*

were previously investigated orally and topically in mice. Both extracts were shown to be significantly active in carrageenan edema and chronic adjuvant arthritis models. Chlorogenic acid was isolated as one of the active principles of the MeOH extract of the plant (204). In another study, Ahmadiani et al. reported that root extract exerted significant activity on both acute and sub-acute *in vivo* models (44).

Iridoids are monoterpenic compounds bearing a cyclopentanopyranoid skeleton. This group of compounds has been shown to exert antihypertensive, antihepatotoxic, hepatoprotective, hypoglycaemic, hypolipidemic, antispasmodic, antiviral, immunomodulator and anti-inflammatory activities in the previous studies (225). Iridoids such as monotropein, catalposide, scopolioside and harpagoside have been shown to inhibit the activation of NF- κ B on LPS-induced macrophages. Moreover, these molecules provided a significant decrease in the levels of iNOS, COX-2 and certain cytokines (226-229). Our findings seem to corroborate the previous anti-inflammatory result of the iridoids.

S. nigra extract was fractionated by silica gel column chromatography to yield two active fractions encoded as **SNH-1** and **SNH-2**. Pre-treatment of the cells for two hours with both fractions led to significant inhibitions on NF- κ B but only **SNH-1** had a moderate activity on NO and PGE₂. These inhibitions were possibly due to the decreases of the levels of COX-2 and iNOS. While **SNH-1** had no effect on MAPK pathways, **SNH-2** almost completely inhibited p38 and JNK phosphorylations.

Table 61: Summary of the inhibitory activities of the active components on NF-κB and IκBα/MAPK phosphorylations

N.D.: Not Determined, **N.E.:** No Effects (+): low inhibitory effect (between 0-40%), (++): moderate inhibitory effect (between 40-60%), (+++): high inhibitory effect (more than 60%) *Cell viability is not less than %80

	Non-toxic concentrations*	NF-κB (% inhibition)	p-IκBα	MAPK		
				p-ERK	p-JNK	p-p38
SE-1 mixture of hyperoside (major constituent, 2/3 of mixture) and isoquercitrin (Quercetin-3-O-β-glucoside, minor, 1/3 of mixture)						
25 μg/ml	25 μg/ml	1.85	{ N.D. }	{ N.D. }	{ N.D. }	{ N.D. }
50 μg/ml	50 μg/ml	39.29				
100 μg/ml	100 μg/ml	56.10				
SE-2 isorhamnetin-3-O-β-D-glucopyranoside						
25 μg/ml	25 μg/ml	22.14	N.E.	(+++)	(+)	(+)
50 μg/ml	50 μg/ml	26.18	(++)	N.E.	(+)	(+++)
100 μg/ml	100 μg/ml	46.42	(++)	N.E.	(++)	(+++)
SE-4 hyperoside (Quercetin-3-O-β-D-galactopyranoside, minor constituent, 1/3 of mixture) and isoquercitrin (major, 2/3 of mixture)						
25 μg/ml	25 μg/ml	35.49	{ N.D. }	{ N.D. }	{ N.D. }	{ N.D. }
50 μg/ml	50 μg/ml	53.84				
100 μg/ml	100 μg/ml	64.80				
SE-6 isorhamnetin-3-O-rutinoside						
25 μg/ml	25 μg/ml	15.99	(+)	(++)	N.E.	(+)
50 μg/ml	50 μg/ml	20.04	(++)	(++)	N.E.	(+)
100 μg/ml	100 μg/ml	45.62	(+++)	(++)	N.E.	(++)

Continued (Table 61:)		NF-κB (% inhibition)	p-IκBα	MAPK		
				p-ERK	p-JNK	p-p38
SEH-1 Sambulin B						
6,25 µg/ml	6,25 µg/ml	-15,04	(++)	(++)	(++)	N.E.
12,5 µg/ml	12,5 µg/ml	29.14	(++)	N.E.	(+++)	N.E.
25 µg/ml	25 µg/ml	31.82	(+++)	N.E.	(+++)	N.E.
SECP-2 Sambulin A						
12,5 µg/ml	12,5 µg/ml	44.73	N.E.	N.E.	(+)	(+)
25 µg/ml	25 µg/ml	55.84	(++)	N.E.	(++)	(++)
50 µg/ml	50 µg/ml	82.50	(++)	N.E.	(+++)	(+++)
CL-R-H₂O Remaining water subextract of <i>C. laurifolius</i>						
25 µg/ml	25 µg/ml	45	N.E.	N.E.	(+)	N.E.
50 µg/ml	50 µg/ml	49	(+)	N.E.	(++)	(+)
100 µg/ml	100 µg/ml	58	(+++)	N.E.	(++)	N.E.
SNH-1 Active fraction of <i>S. nigra</i> hexane extract						
12,5 µg/ml	25 µg/ml	42.2	N.E.	N.E.	N.E.	N.E.
25 µg/ml	50 µg/ml	62.00	N.E.	N.E.	N.E.	N.E.
50 µg/ml	100 µg/ml	73.35	(++)	N.E.	N.E.	N.E.

Continued (Table 61:)		NF-κB (% inhibition)	p-IκBα	MAPK		
				p-ERK	p-JNK	p-p38
SNH-2 Active fraction of <i>S. nigra</i> hexane extract						
12,5 μg/ml	12,5 μg/ml	66.00	{ N.D. }	{ N.D. }	{ N.D. }	{ N.D. }
25 μg/ml	25 μg/ml	77.69				
50 μg/ml	50 μg/ml	78.38				
Parthenolide						
10 μM	10 μM	67				
20 μM	20 μM	83				

Table 62: Summary of the results of the *in vitro* inhibitory activities of the active components on inflammatory parameters

N.D.: Not Determined, **N.E.:** No Effects

	(% inhibition of protein expression)		% inhibition (\pm %STD)					
	iNOS	COX-2	NO	PGE ₂	TNF α	IL-1	IL-2	IL-6
SE-1 mixture of hyperoside (major constituent, 2/3 of mixture) and isoquercitrin (Quercetin-3- <i>O</i> - β -glucoside, minor, 1/3 of mixture)								
25 μ g/ml	N.D.	N.D.	N.D.	N.D.	N.D.	N.D.	N.D.	N.D.
50 μ g/ml	N.D.	N.D.	N.D.	N.D.	N.D.	N.D.	N.D.	N.D.
100 μ g/ml	N.E.	N.E.	N.E.	N.E.	N.E.	N.E.	N.E.	N.E.
SE-2 isorhamnetin-3- <i>O</i> - β -D-glucopyranoside								
25 μ g/ml	-18.35 \pm 11.60		15.18 \pm 6.18					
50 μ g/ml	12.83 \pm 4.30	N.D.	23.33 \pm 8.26	N.D.	18.63 \pm 11.43	N.D.	N.D.	N.D.
75 μ g/ml	34.94 \pm 5.10	N.D.	42.19 \pm 10.17	N.D.	32.49 \pm 7.4	N.D.	N.D.	N.D.
100 μ g/ml	43.90 \pm 12.46	N.E.	59.28 \pm 15.93	N.E.	37.21 \pm 14.06	N.E.	N.E.	N.E.
SE-4 hyperoside (Quercetin-3- <i>O</i> - β -D-galactopyranoside, minor constituent, 1/3 of mixture) and isoquercitrin (major, 2/3 of mixture)								
25 μ g/ml	N.D.	N.D.	N.D.	N.D.	N.D.	N.D.	N.D.	N.D.
50 μ g/ml	N.D.	N.D.	N.D.	N.D.	N.D.	N.D.	N.D.	N.D.
100 μ g/ml	N.E.	N.E.	N.E.	N.E.	N.E.	N.E.	N.E.	N.E.

Continued (Table 62)	(% inhibition of protein expression)		% inhibition (\pm %STD)					
	iNOS	COX-2	NO	PGE ₂	TNF α	IL-1	IL-2	IL-6
SE-6 isorhamnetin-3-O-rutinoside								
25 μ g/ml	-16.11 \pm 2.90	14.59 \pm 2.90	30.68 \pm 1.52	N.E.				
50 μ g/ml	32.80 \pm 12.82	44.96 \pm 4.96	43.30 \pm 1.64	26.08 \pm 1.99	29.30 \pm 3.93	N.D.	N.D.	N.D.
75 μ g/ml	38.87 \pm 12.58	53.57 \pm 4.83	67.27 \pm 1.15	31.30 \pm 1.52	25.23 \pm 1.56	N.D.	N.D.	N.D.
100 μ g/ml	61.07 \pm 15.66	59.74 \pm 25.81	81.12 \pm 1.53	39.13 \pm 12.31	29.43 \pm 2.22	N.E.	N.E.	N.E.
SEH-1 Sambulin B								
6,25 μ g/ml	61.12 \pm 0.38	22.24 \pm 0.045	38.28 \pm 9.70	19.59 \pm 0.001	16.75 \pm 0.08	N.D.	N.D.	22.96 \pm 5.90
12,5 μ g/ml	100	87.66 \pm 0.07	74.23 \pm 24.93	74.08 \pm 0.005	21.32 \pm 0.39	N.D.	N.D.	35.03 \pm 15.39
25 μ g/ml	100	92.10 \pm 0.01	84.20 \pm 62.18	83.92 \pm 0.008	34.20 \pm 7.47	N.E.	N.E.	59.12 \pm 12.64
SECP-2 Sambulin A								
12,5 μ g/ml	17.70 \pm 5.82	20.23 \pm 8.04	23.02 \pm 4.62	30.11 \pm 0.01	23.53 \pm 6.82	N.D.	N.D.	N.D.
25 μ g/ml	53.17 \pm 1.42	53.17 \pm 1.42	52.13 \pm 3.66	35.35 \pm 0.001	28.96 \pm 8.89	N.D.	N.D.	N.D.
50 μ g/ml	60.73 \pm 1.42	60.73 \pm 1.42	69.72 \pm 8.14	42.63 \pm 0.01	36.21 \pm 8.50	N.E.	N.E.	N.E.
CL-R-H₂O Remaining water subextract of <i>C. laurifolius</i>								
25 μ g/ml	2.97 \pm 1.36	14.40 \pm 10.93	-4.11 \pm 2.51	15.32 \pm 0.05	-17.22 \pm 0.03	N.D.	N.D.	N.D.
50 μ g/ml	3.45 \pm 3.23	12.00 \pm 9.88	2.61 \pm 4.34	37.98 \pm 0.01	18.96 \pm 0.05	N.D.	N.D.	N.D.
100 μ g/ml	38.12 \pm 3.26	28.70 \pm 8.68	56.55 \pm 15.80	54.84 \pm 0.01	37.81 \pm 0.006	N.E.	N.E.	N.E.
SNH-1 Active fraction of <i>S. nigra</i> hexane extract								
25 μ g/ml	6.21 \pm 2.40	28.20 \pm 18.31	2.13 \pm 8.43	12.63 \pm 0.01	N.D.	N.D.	N.D.	N.D.
50 μ g/ml	25.76 \pm 1.20	58.79 \pm 1.41	13.64 \pm 7.46	20.01 \pm 0.01	N.D.	N.D.	N.D.	N.D.
100 μ g/ml	35.49 \pm 2.49	59.21 \pm 19.91	41.47 \pm 9.56	29.01 \pm 0.01	N.E.	N.E.	N.E.	N.E.

Continued (Table 62)	(% inhibition of protein expression)		% inhibition (\pm %STD)					
	iNOS	COX-2	NO	PGE ₂	TNF α	IL-1	IL-2	IL-6
SNH-2 Active fraction of <i>S. nigra</i> hexane extract								
12,5 μ g/ml	N.D.	N.D.	N.D.	N.D.	N.D.	N.D.	N.D.	N.D.
25 μ g/ml	N.D.	N.D.	N.D.	N.D.	N.D.	N.D.	N.D.	N.D.
50 μ g/ml	N.E.	N.E.	N.E.	N.E.	N.E.	N.E.	N.E.	N.E.
Dexamethasone								
10 μ M					45.60 \pm 0.28			
5 μ M								77.24 \pm 17.79
NS-398								
10 μ M				97.20 \pm 0.07				
L-NIL								
10 μ M			58.56 \pm 5.85					

Among the subextracts obtained from solvent partition of the ethanol extract of *C. laurifolius*, only CL-R-H₂O provided 20% inhibition of NF- κ B activation. However, further fractionation of this subextract resulted in the loss of this activity. Therefore *in vitro* detailed investigations for the anti-inflammatory activity profile of *C. laurifolius* were carried out on CL-R-H₂O subextract. This subextract led up to 58% decrease of NO, and 52% of PGE₂ productions. iNOS protein level was significantly decreased at 100 μ g/ml. Phosphorylation levels of I κ -B α remarkably decreased upon pre-treatment of cells with 50 and 100 μ g/ml extract. JNK pathway might also contribute to the anti-inflammatory activity of this extract. This extract was also inhibited TNF α production (40%). In a recent study, K peli et al. investigated the anti-inflammatory effect of the EtOH extract of *C. laurifolius* against *in vivo* carrageenan edema model and acetic acid induced capillary permeability models. Through bioactivity-guided fractionation 3-*O*-methylquercetin, 3,7-*O*-dimethylquercetin and 3,7-*O*-dimethylkaempferol were isolated as active components (83). In another previous study, *C. laurifolius* extract yielded several compounds possessing *in vitro* PGE₂ inhibitory activity (82).

The extracts and subextracts prepared with successive solvent extractions from the leaves of *C. laurifolius*, and leaves and flowers of *S. ebulus* and *S. nigra* were evaluated for their effects on several inflammatory cytokines, *i.e.*, IL-1 α , IL-1 β and TNF α on isolated human monocytes in a previous study. In the mentioned study, the remaining water subextract of *C. laurifolius* at 30 μ g/ml concentration was only active on IL-1 α and provided up to 27% inhibition. This extract inhibited 7% of TNF α production (6). In the present study, CL-R-H₂O inhibited 40% of TNF α secretion in LPS-induced Raw 264.7 macrophages. At 25 μ g/ml concentration we observed no inhibition confirming the previous study conducted on human monocytes.

CONCLUSION

The present study aimed to isolate compounds responsible for the activity of three plants which are widely used against inflammatory diseases in Turkish folk medicine. Four flavonoids; isorhamnetin-3-*O*- β -D-glucopyranoside, isorhamnetin-3-*O*-D-rutinoside, isoquercitrin, hyperoside and two new iridoids; Sambulin A, Sambulin B were isolated through activity-guided fractionation procedures as the active components and their anti-inflammatory effects on NF- κ B and several parameters such as proinflammatory cytokines (TNF α and IL-1 α , IL-1 β , IL-2 ve IL-6), mediators (NO, PGE₂) and enzymes (iNOS and COX-2) were evaluated. In addition, in order to explain the mechanism underlying the anti-inflammatory effects of these compounds, their effects on MAPK (ERK, JNK ve p38) and I κ B α pathways were investigated. The data provide an *in vitro* scientific explanation for the traditional use of these three plants in a molecular and mechanistic approach. Besides, two new iridoid compounds with anti-inflammatory activity were identified.

It has long been suggested that there is a link between inflammation and cancer (230). This hypothesis depends on the presence of uncontrolled cellular proliferation on the inflammatory sites and the presence of inflammatory cells on cancerous sites (231). The discovery of the fact that chronic inflammation leads to tumorigenesis supported this hypothesis (232). Epidemiologic studies demonstrated that people with chronic inflammatory diseases are more prone to cancers. Chronic inflammation is linked to proliferation and metastasis (233). Besides its involvement in inflammatory processes, NF- κ B plays important roles in cell proliferation, tumorigenesis and apoptosis (211). Therefore NF- κ B inhibiting molecules identified in this study might be further evaluated for their cytotoxic and anticancer activities in the future.

Several mediators such as lipoxygenases, phospholipases and elastases are known to involve in the development of chronic inflammation. Therefore further investigations should be carried out with the subextracts, fractions and compounds, particularly with those found to be not active on the parameters studied here for detailed explanation of the ethnopharmacological usage. Besides the chloroform subextract of *S. ebulus* which was very rich in secondary metabolites yielded two highly active iridoids.

Profound phytochemical investigation of *S. ebulus* chloroform subextract may yield new and active compounds with different activities.

6. REFERENCES

1. Feldmann M, Maini RN. TNF defined as a therapeutic target for rheumatoid arthritis and other autoimmune diseases. *Nat Med*, 9: 1245-1250, 2003.
2. Heller RA, Schena M, Chai A, Shalon D, Bedilion T, Gilmore J, Woolley DE, Davis RW. Discovery and analysis of inflammatory disease-related genes using cDNA microarrays. *P Natl A Sci USA*, 94: 2150-2155, 1997.
3. Gabay C. Interleukin-6 and chronic inflammation. *Arthritis Res Ther*, 6: 1-6, 2006.
4. Coussens LM, Werb Z. Inflammation and cancer. *Nature*, 420 (6917): 860-867, 2002.
5. Prete AD, Allavena P, Santoro G, Fumarulo R, Corsi MM, Mantovani A. Molecular pathways in cancer-related inflammation. *Biochem Medica*, 21 (3): 264-275, 2011.
6. Yesilada E, Ustun O, Sezik E, Takaishi Y, Ono Y, Honda G. Inhibitory effects of Turkish folk remedies on inflammatory cytokines: interleukin-1 alpha, interleukin-1 beta and tumor necrosis factor alpha. *J Ethnopharmacol*, 58 (1): 59-73, 1997.
7. Gauatam R, Jachak SM. Recent developments in anti-inflammatory natural products. *Med Res Rev*, 5: 767-820, 2009.
8. Gerondakis S, Grumont R, Rourke I, Grossmann M. The regulation and roles of Rel/NF- κ B transcription factors during lymphocyte activation. *Curr Opin Immunol*, 10 (3): 353-359, 1998.
9. Li Q, Verma IM. NF-kappaB regulation in the immune system. *Nat Rev Immunol*, 2 (10): 725-734, 2002.
10. Tak PP, Firestein GS. NF-kappaB: a key role in inflammatory diseases. *J Clin Invest*, 107 (1): 7-11, 2001.
11. Tuzlacı E, Tolon E. Turkish folk medicinal plants , part III. *Fitoterapia*, 71 (6): 673-685, 2000.
12. Kultur S. Medicinal plants used in Kırklareli province (Turkey). *J Ethnopharmacol*, 111: 341-364, 2007.
13. Yesilada E, Sezik E, Honda G, Takaishi Y, Takeda Y, Tanaka T. Traditional medicine in Turkey IX : Folk medicine in north-west Anatolia. *J Ethnopharmacol*, 64: 195-210, 1999.

14. Eriksson T, Donoghue MJ. Phylogenetic relationships of *Sambucus* and *Adoxa* (Adoxoideae, Adoxaceae) based on nuclear ribosomal ITS sequences and preliminary morphological data. *Syst Bot*, 22: 555-573, 1997.
15. Donoghue M, Eriksson T, Reeves P, Olmstead R. Phylogeny and phylogenetic taxonomy of Dipsocales, with special reference to *Sinadoxa* and *Tetradoxa* (Adoxaceae). *Harvard Papers in Botany*, 6: 459-479, 2001.
16. II AAPG. An update of the Angio-sperm Phylogeny Group classification for the orders and families of flowering plants: APG II. *Bot J Linn Soc* 141:399–436.: 399–436, 2003.
17. Bell C, Edwards E, Kim S, Donoghue M. Dipsacales phylogeny based on chloroplast DNA sequences. *Harvard Papers in Botany*, 6: 481-499, 2001.
18. Chamberline D, Phill D, Victoria A. Flora of Turkey and the East Aegean islands. Davis P (ed). Edinburg Univ. Press., Edinburg, pp 541-543, 1972.
19. Baytop T. Türkçe Bitki Adları Sözlüğü. (3. baskı. ed.) Türk Dil Kurumu. Ankara, 2007.
20. Schwaiger S, Zeller I, Polzelbauer P, Frotschnig S, Laufer G, Messner B, Pieri V, Stuppner H, Bernhard D. Identification and pharmacological characterization of the anti-inflammatory principal of the leaves of dwarf elder (*Sambucus ebulus* L.). *J Ethnopharmacol*, 133 (2): 704-709, 2011.
21. Leporatti ML, Ivancheva S. Preliminary comparative analysis of medicinal plants used in the traditional medicine of Bulgaria and Italy. *J Ethnopharmacol*, 87 (2-3): 123-142, 2003.
22. Scherrer AM, Motti R, Weckerle CS. Traditional plant use in the areas of Monte Vesole and Ascea, Cilento National Park (Campania, Southern Italy). *J Ethnopharmacol*, 97 (1): 129-143, 2005.
23. Lev E, Amar Z. Ethnopharmacological survey of traditional drugs sold in Israel at the end of the 20th century. *J Ethnopharmacol*, 72 (1–2): 191-205, 2000.
24. Cavero RY, Akerreta S, Calvo MI. Pharmaceutical ethnobotany in Northern Navarra (Iberian Peninsula). *J Ethnopharmacol*, 133 (1): 138-146, 2011.
25. Miraldi E, Ferri S, Mostaghimi V. Botanical drugs and preparations in the traditional medicine of West Azerbaijan (Iran). *J Ethnopharmacol*, 75 (2–3): 77-87, 2001.
26. Cullen J, Coode MJE. The Flora of Turkey and East Aegean Islands. Davis P (ed). Edinburg Univ. Press., Edinburg, pp 506-508, 1965.
27. Sezik E, Zor M, Yesilada E. Traditional medicine in Turkey. II. Folk medicine in Kastamonu. *Int J Pharmacogn*, 30: 233–239, 1992.

28. Polat R, Satıl F. An ethnobotanical survey of medicinal plants in Edremit Gulf (Balıkesir – Turkey). *J Ethnopharmacol*, 139 (2): 626-641, 2012.
29. Sezik E, Yesilada E, Tabata M, Honda G, Takaishi Y, Fujita T, Tanaka T, Takeda Y. Traditional medicine in Turkey VIII. Folk medicine in east anatolia; Erzurum, Erzincan, Agri, Kars, Iğdir provinces. *Econ Bot*, 51 (3): 195-211, 1997.
30. Cakilcioglu U, Turkoglu I. An ethnobotanical survey of medicinal plants in Sivrice (Elazığ-Turkey). *J Ethnopharmacol*, 132 (1): 165-175, 2010.
31. LEPORATTI ML, Ivancheva S. Preliminary comparative analysis of medicinal plants used in the traditional medicine of Bulgaria and Italy. *J Ethnopharmacol*, 87 (2–3): 123-142, 2003.
32. Pieroni A, Quave CL. Traditional pharmacopoeias and medicines among Albanians and Italians in southern Italy: A comparison. *J Ethnopharmacol*, 101 (1–3): 258-270, 2005.
33. Baytop T. *Therapy with plants in Turkey (past & present)*, (2nd ed.) Nobel Medical Bookhouse, Istanbul, pp 301, 1999.
34. Jaric S, Popović Z, Mačukanović-Jocić M, Djurdjević L, Mijatović M, Karadžić B, Mitrović M, Pavlović P. An ethnobotanical study on the usage of wild medicinal herbs from Kopaonik Mountain (Central Serbia). *J Ethnopharmacol*, 111 (1): 160-175, 2007.
35. Cano JH, Volpato G. Herbal mixtures in the traditional medicine of Eastern Cuba. *J Ethnopharmacol*, 90 (2–3): 293-316, 2004.
36. Macía MJ, García E, Vidaurre PJ. An ethnobotanical survey of medicinal plants commercialized in the markets of La Paz and El Alto, Bolivia. *J Ethnopharmacol*, 97 (2): 337-350, 2005.
37. Sanz-Biset J, Campos-de-la-Cruz J, Epiquién-Rivera MA, Cañigueral S. A first survey on the medicinal plants of the Chazuta valley (Peruvian Amazon). *J Ethnopharmacol*, 122 (2): 333-362, 2009.
38. Goleniowski ME, Bongiovanni GA, Palacio L, Nuñez CO, Cantero JJ. Medicinal plants from the “Sierra de Comechingones”, Argentina. *J Ethnopharmacol*, 107 (3): 324-341, 2006.
39. Inta A, Shengji P, Balslev H, Wangpakapattanawong P, Trisonthi C. A comparative study on medicinal plants used in Akha's traditional medicine in China and Thailand, cultural coherence or ecological divergence. *J Ethnopharmacol*, 116 (3): 508-517, 2008.
40. Lee S, Xiao C, Pei S. Ethnobotanical survey of medicinal plants at periodic markets of Honghe Prefecture in Yunnan Province, SW China. *J Ethnopharmacol*, 117 (2): 362-377, 2008.

41. Fazio A, Plastina P, Meijerink J, Witkamp RF, Gabriele B. Comparative analyses of seeds of wild fruits of *Rubus* and *Sambucus* species from Southern Italy: fatty acid composition of the oil, total phenolic content, antioxidant and anti-inflammatory properties of the methanolic extracts. *Food Chem*, 4 (140): 817-824, 2012.
42. Ebrahimzadeh MA, Mahmoudi M, Pourmorad F, Saeidnia S, Salimi E. Anti-inflammatory and anti-nociceptive properties of fractionated extracts in different parts of *Sambucus ebulus*. *J Mazandaran Uni Med Sci*, 16 (54): 35-42, 2006.
43. Ebrahimzadeh MA, Mahmoudi M, Karami M, Saeedi S, Ahmadi AH, Salimi E. Separation of active and toxic portions in *Sambucus ebulus*. *Pak J Biol Sci*, 10 (22): 4171-4173, 2007
44. Ahmadiani A. FM, Semnanian S., Kamalinejad M., Saremi S. Antinociceptive and anti-inflammatory effects of *Sambucus ebulus* rhizome extract in rats. *J Ethnopharmacol*, 61: 229-235, 1998.
45. Yesilada E. Evaluation of the Anti-inflammatory activity of the Turkish medicinal plant *Sambucus ebulus* *Chem Nat Compd*, 33 (5), 1997.
46. E. Y. Antiinflammatory Activity of the Aerial Parts of *Sambucus ebulus*; Isolation of an Antiinflammatory Principle. . *Doğa Turkish Journal of Pharmacy*, 3 (4): 111-123 1992.
47. Shokrazadeh M, Mirzayi M, Saeedi S. Cytotoxic effects of ethyl acetate extract of *Sambucus ebulus* compared with etoposide on normal and cancer cell lines. *Pharmacogn Mag*, 5 (20): 316-319, 2009.
48. Hosseinimehr SJ, Pourmorad F, Shahabimajd N, Shahrbandy K, Hosseinzadeh R. *In vitro* antioxidant activity of *Polygonium hyrcanicum*, *Centaurea depressa*, *Sambucus ebulus*, *Mentha spicata* and *Phytolacca americana*. *Pak J Biol Sci*, 10 (4): 637-640, 2007.
49. Ebrahimzadeh MA, Nabavi SF, Nabavi SM. Antioxidant activities of methanol extract of *Sambucus ebulus* L. flower. *Pak J Biol Sci*, 12 (5): 447-450, 2009.
50. Yesilada E, Gurbuz I, Shibata H. Screening of Turkish anti-ulcerogenic folk remedies for anti-*Helicobacter pylori* activity. *J Ethnopharmacol*, 66 (3): 289-293, 1999.
51. Chatterjee A, Yasmin T, Bagchi D, Stohs SJ. Inhibition of *Helicobacter pylori* *in vitro* by various berry extracts, with enhanced susceptibility to clarithromycin. *Mol Cell Biochem*, 265 (1-2): 19-26, 2004.
52. Krawitz C, Mraheil MA, Stein M, Imirzalioglu C, Domann E, Pleschka S, Hain T. Inhibitory activity of a standardized elderberry liquid extract against clinically-relevant human respiratory bacterial pathogens and influenza A and B viruses. *BMC Complem Altern M*, 11: 16, 2011.

53. Glatthaar-Saalmuller B, Rauchhaus U, Rode S, Haunschild J, Saalmuller A. Antiviral activity *in vitro* of two preparations of the herbal medicinal product Sinupret(R) against viruses causing respiratory infections. *Phytomedicine*, 19 (1): 1-7, 2011.
54. Smee DF, Hurst BL, Wong MH. Effects of TheraMax on influenza virus infections in cell culture and in mice. *Antivir Chem Chemother*, 21 (6): 231-237, 2011.
55. Hwang B, Cho J, Hwang IS, Jin HG, Woo ER, Lee DG. Antifungal activity of lariciresinol derived from *Sambucus williamsii* and their membrane-active mechanisms in *Candida albicans*. *Biochem Biophys Res Commun*, 410 (3): 489-493, 2011.
56. Hwang B, Lee J, He-Liu Q, Eun-Rhan W, Lee DG. Antifungal Effect of Pinoresinol Isolated from *Sambucus williamsii*. *Molecules*, 15 (5): 3507-3516, 2010.
57. Uncini Manganelli RE, Zaccaro L, Tomei PE. Antiviral activity *in vitro* of *Urtica dioica* L., *Parietaria diffusa* M. et K. and *Sambucus nigra* L. *J Ethnopharmacol*, 98 (3): 323-327, 2005.
58. McCutcheon AR, Roberts TE, Gibbons E, Ellis SM, Babiuk LA, Hancock RE, Towers GH. Antiviral screening of British Columbian medicinal plants. *J Ethnopharmacol*, 49 (2): 101-110, 1995.
59. Roschek Jr B, Fink RC, McMichael MD, Li D, Alberte RS. Elderberry flavonoids bind to and prevent H1N1 infection *in vitro*. *Phytochemistry*, 70 (10): 1255-1261, 2009.
60. Kinoshita E, Hayashi K, Katayama H, Hayashi T, Obata A. Anti-influenza virus effects of elderberry juice and its fractions. *Biosci Biotechnol Biochem*, 76 (9): 1633-1638, 2012.
61. Zakay-Rones Z, Varsano N, Zlotnik M, Manor O, Regev L, Schlesinger M, Mumcuoglu M. Inhibition of several strains of influenza virus *in vitro* and reduction of symptoms by an elderberry extract (*Sambucus nigra* L.) during an outbreak of influenza B Panama. *J Altern Complement Med*, 1 (4): 361-369, 1995.
62. Zakay-Rones Z, Thom E, Wollan T, Wadstein J. Randomized study of the efficacy and safety of oral elderberry extract in the treatment of influenza A and B virus infections. *J Int Med Res*, 32 (2): 132-140, 2004.
63. Mlinaric A, Kreft S, Umek A, Strukelj B. Screening of selected plant extracts for *in vitro* inhibitory activity on HIV-1 reverse transcriptase (HIV-1 RT). *Pharmazie*, 55 (1): 75-77, 2000.
64. Barak V, Halperin T, Kalickman I. The effect of Sambucol, a black elderberry-based, natural product, on the production of human cytokines: I. Inflammatory cytokines. *Eur Cytokine Netw*, 12 (2): 290-296, 2001.

65. Xie F, Wu CF, Zhang Y, Yao XS, Cheung PY, Chan AS, Wong MS. Increase in bone mass and bone strength by *Sambucus williamsii* HANCE in ovariectomized rats. *Biol Pharm Bull*, 28 (10): 1879-1885, 2005.
66. Zhang Y, Li Q, Wan HY, Xiao HH, Lai WP, Yao XS, Wong MS. Study of the mechanisms by which *Sambucus williamsii* HANCE extract exert protective effects against ovariectomy-induced osteoporosis *in vivo*. *Osteoporos Int*, 22 (2): 703-709, 2011.
67. Xiao HH, Dai Y, Wan HY, Wong MS, Yao XS. Bone-protective effects of bioactive fractions and ingredients in *Sambucus williamsii* HANCE. *Br J Nutr*, 106 (12): 1802-1809, 2011.
68. Yang XJ, Wong MS, Wang NL, Chan SC, Yao XS. Lignans from the stems of *Sambucus williamsii* and their effects on osteoblastic UMR106 cells. *J Asian Nat Prod Res*, 9 (6-8): 583-591, 2007.
69. Suntar IP, Akkol EK, Yalcin FN, Koca U, Keles H, Yesilada E. Wound healing potential of *Sambucus ebulus* L. leaves and isolation of an active component, quercetin 3-*O*-glucoside. *J Ethnopharmacol*, 129 (1): 106-114, 2010.
70. Badescu L, Badulescu O, Badescu M, Ciocoiu M. Mechanism by *Sambucus nigra* extract improves bone mineral density in experimental diabetes. *Evid Based Complement Alternat Med*, 2012: 848269, 2012.
71. Sezik E, Tabata M, Yesilada E, Honda G, Goto K, Ikeshiro Y. Traditional medicine in Turkey I. Folk medicine in Northeast Anatolia. *J Ethnopharmacol*, 35 (2): 191-196, 1991.
72. Yesilada E, Honda G, Sezik E, Tabata M, Fujita T, Tanaka T, Takeda Y, Takaishi Y. Traditional medicine in Turkey. V. Folk medicine in the inner Taurus Mountains. *J Ethnopharmacol*, 46 (3): 133-152, 1995.
73. Agelet A, Valles J. Studies on pharmaceutical ethnobotany in the region of Pallars (Pyrenees, Catalonia, Iberian Peninsula) Part III; medicinal uses of non-vascular plants. *J Ethnopharmacol*, 84 (2-3): 229-234, 2003.
74. El Beyrouthy M, Arnold N, Delelis-Dusollier A, Dupont F. Plants used as remedies antirheumatic and antineuralgic in the traditional medicine of Lebanon. *J Ethnopharmacol*, 120 (3): 315-334, 2008.
75. Leto C, Tuttolomondo T, La Bella S, Licata M. Ethnobotanical study in the Madonie Regional Park (Central Sicily, Italy) medicinal use of wild shrub and herbaceous plant species. *J Ethnopharmacol*, 146 (1): 90-112, 2013.
76. Gurdal B, Kultur S. An ethnobotanical study of medicinal plants in Marmaris (Mugla, Turkey). *J Ethnopharmacol*, 146 (1): 113-126, 2013.

77. Bonet MÀ, Parada M, Selga A, Vallès J. Studies on pharmaceutical ethnobotany in the regions of L'Alt Empordà and Les Guilleries (Catalonia, Iberian Peninsula). *J Ethnopharmacol*, 68 (1–3): 145-168, 1999.
78. Uncini Manganelli RE, Tomei PE. Ethnopharmacobotanical studies of the Tuscan Archipelago. *J Ethnopharmacol*, 65 (3): 181-202, 1999.
79. Bruni A, Ballero M, Poli F. Quantitative ethnopharmacological study of the Campidano Valley and Urzulei district, Sardinia, Italy. *J Ethnopharmacol*, 57 (2): 97-124, 1997.
80. Carrio E, Valles J. Ethnobotany of medicinal plants used in Eastern Mallorca (Balearic Islands, Mediterranean Sea). *J Ethnopharmacol*, 141 (3): 1021-1040, 2012.
81. Benitez G, Gonzalez-Tejero MR, Molero-Mesa J. Pharmaceutical ethnobotany in the western part of Granada province (southern Spain): ethnopharmacological synthesis. *J Ethnopharmacol*, 129 (1): 87-105, 2010.
82. Sadhu SK, Okuyama E, Fujimoto H, Ishibashi M, Yesilada E. Prostaglandin inhibitory and antioxidant components of *Cistus laurifolius*, a Turkish medicinal plant. *J Ethnopharmacol*, 108 (3): 371-378, 2006.
83. Kupeli E, Yesilada E. Flavonoids with anti-inflammatory and antinociceptive activity from *Cistus laurifolius* L. leaves through bioassay-guided procedures. *J Ethnopharmacol*, 112 (3): 524-530, 2007.
84. Bremner P, Rivera D, Calzado MA, Obon C, Inocencio C, Beckwith C, Fiebich BL, Munoz E, Heinrich M. Assessing medicinal plants from South-Eastern Spain for potential anti-inflammatory effects targeting nuclear factor-Kappa B and other pro-inflammatory mediators. *J Ethnopharmacol*, 124 (2): 295-305, 2009.
85. Barrajon-Catalan E, Fernandez-Arroyo S, Saura D, Guillen E, Fernandez-Gutierrez A, Segura-Carretero A, Micol V. Cistaceae aqueous extracts containing ellagitannins show antioxidant and antimicrobial capacity, and cytotoxic activity against human cancer cells. *Food Chem Toxicol*, 48 (8-9): 2273-2282, 2010.
86. Matsingou C, Dimas K, Demetzos C. Design and development of liposomes incorporating a bioactive labdane-type diterpene. *In vitro* growth inhibiting and cytotoxic activity against human cancer cell lines. *Biomed Pharmacother*, 60 (4): 191-199, 2006.
87. Chinou I, Demetzos C, Harvala C, Roussakis C, Verbist JF. Cytotoxic and antibacterial labdane-type diterpenes from the aerial parts of *Cistus incanus* subsp. *creticus*. *Planta Med*, 60 (1): 34-36, 1994.
88. Demetzos C, Mitaku S, Couladis M, Harvala C, Kokkinopoulos D. Natural metabolites of ent-13-epi-manoyl oxide and other cytotoxic diterpenes from the resin "ladano" of *Cistus creticus*. *Planta Med*, 60 (6): 590-591, 1994.

89. Dimas K, Demetzos C, Marsellos M, Sotiriadou R, Malamas M, Kokkinopoulos D. Cytotoxic activity of labdane type diterpenes against human leukemic cell lines *in vitro*. *Planta Med*, 64 (3): 208-211, 1998.
90. Matsingou C, Hatziantoniou S, Georgopoulos A, Dimas K, Terzis A, Demetzos C. Labdane-type diterpenes: thermal effects on phospholipid bilayers, incorporation into liposomes and biological activity. *Chem Phys Lipids*, 138 (1-2): 1-11, 2005.
91. Dimas K, Demetzos C, Vaos V, Ioannidis P, Trangas T. Labdane type diterpenes down-regulate the expression of c-Myc protein, but not of Bcl-2, in human leukemia T-cells undergoing apoptosis. *Leuk Res*, 25 (6): 449-454, 2001.
92. Bouamama H, Noel T, Villard J, Benharref A, Jana M. Antimicrobial activities of the leaf extracts of two Moroccan *Cistus* L. species. *J Ethnopharmacol*, 104 (1-2): 104-107, 2006.
93. Droebner K, Ehrhardt C, Poetter A, Ludwig S, Planz O. CYSTUS052, a polyphenol-rich plant extract, exerts anti-influenza virus activity in mice. *Antiviral Res*, 76 (1): 1-10, 2007.
94. Ehrhardt C, Hrinčius ER, Korte V, Mazur I, Droebner K, Poetter A, Dreschers S, Schmolke M, Planz O, Ludwig S. A polyphenol rich plant extract, CYSTUS052, exerts anti influenza virus activity in cell culture without toxic side effects or the tendency to induce viral resistance. *Antiviral Res*, 76 (1): 38-47, 2007.
95. Kalus U, Grigorov A, Kadecki O, Jansen JP, Kiesewetter H, Radtke H. *Cistus incanus* (CYSTUS052) for treating patients with infection of the upper respiratory tract; a prospective, randomised, placebo-controlled clinical study. *Antiviral Res*, 84 (3): 267-271, 2009.
96. Ustun O, Ozcelik B, Akyon Y, Abbasoglu U, Yesilada E. Flavonoids with anti-*Helicobacter pylori* activity from *Cistus laurifolius* leaves. *J Ethnopharmacol*, 108 (3): 457-461, 2006.
97. Attaguile G, Perticone G, Mania G, Savoca F, Pennisi G, Salomone S. *Cistus incanus* and *Cistus monspeliensis* inhibit the contractile response in isolated rat smooth muscle. *J Ethnopharmacol*, 92 (2-3): 245-250, 2004.
98. Aziz M, Tab N, Karim A, Mekhfi H, Bnouham M, Ziyat A, Melhaoui A, Legssyer A. Relaxant effect of aqueous extract of *Cistus ladaniferus* on rodent intestinal contractions. *Fitoterapia*, 77 (6): 425-428, 2006.
99. Enomoto S, Okada Y, Guvenc A, Erdurak CS, Coskun M, Okuyama T. Inhibitory effect of traditional Turkish folk medicines on aldose reductase (AR) and hematological activity, and on AR inhibitory activity of quercetin-3-O-methyl ether isolated from *Cistus laurifolius* L. *Biol Pharm Bull*, 27 (7): 1140-1143, 2004.

100. Orhan N, Aslan M, Sukuroglu M, Deliorman Orhan D. *In vivo* and *in vitro* antidiabetic effect of *Cistus laurifolius* L. and detection of major phenolic compounds by UPLC-TOF-MS analysis. *J Ethnopharmacol*, 146 (3): 859-865, 2013.
101. Kupeli E, Orhan DD, Yesilada E. Effect of *Cistus laurifolius* L. leaf extracts and flavonoids on acetaminophen-induced hepatotoxicity in mice. *J Ethnopharmacol*, 103 (3): 455-460, 2006.
102. Akkol EK, Orhan IE, Yesilada E. Anticholinesterase and antioxidant effects of the ethanol extract, ethanol fractions and isolated flavonoids from *Cistus laurifolius* L. leaves. *Food Chem*, 131 (2): 626-631, 2012.
103. D'abrosca B, DellaGreca M, Fiorentino A, Monaco P, Previtera L, Simonet AM, Zarrelli A. Potential allelochemicals from *Sambucus nigra*. *Phytochemistry*, 58 (7): 1073-1081, 2001.
104. Barros L, Duenas M, Carvalho AM, Ferreira IC, Santos-Buelga C. Characterization of phenolic compounds in flowers of wild medicinal plants from Northeastern Portugal. *Food Chem Toxicol*, 50 (5): 1576-1582, 2012.
105. Chen X, Li G, Wu X, Huang Q, Zhang G. Chemical Study on *Sambucus adnata* Wall. *Chinese Journal of Applied Environmental Biology*, 16: 197-201, 2010.
106. Sasaki T, Li W, Morimura H, Li S, Li Q, Asada Y, Koike K. Chemical constituents from *Sambucus adnata* and their protein-tyrosine phosphatase 1B inhibitory activities. *Chem Pharm Bull*, 59 (11): 1396-1399, 2011.
107. Veberic R, Jakopic J, Stampar F, Schmitzer V. European elderberry (*Sambucus nigra* L.) rich in sugars, organic acids, anthocyanins and selected polyphenols. *Food Chem*, 114: 511-515, 2009.
108. Jordheim M, Giske NH, Andersen OM. Anthocyanins in Caprifoliaceae. *Biochem Syst Ecol*, 35: 153-159, 2007.
109. Johansen OP, Andersen OM, Nerdal W, Aksnes DW. Cyanidin 3-[6-(p-coumaroyl)-2-(xylosyl)-glucoside]-5-glucoside and other anthocyanins from fruits of *Sambucus canadensis*. *Phytochemistry*, 30 (12): 4137-4141, 1991.
110. Nakatani N, Kikuzaki H, Hikida J, Ohba M, Inami O, Tamura I. Acylated anthocyanins from fruits of *Sambucus canadensis*. *Phytochemistry*, 38 (3): 755-757, 1995.
111. Acuna UM, Atha DE, Ma J, Nee MH, Kennelly EJ. Antioxidant capacities of ten edible North American plants. *Phytother Res*, 16 (1): 63-65, 2002.
112. Machida K, Takano M, Kakuda R, Yaoita Y, Kikuchi M. A new lignan glycoside from the leaves of *Sambucus sieboldiana* (Miq.) Blume ex. Graebn. *Chem Pharm Bull*, 50 (5): 669-671, 2002.

113. Ouyang F, Liu Y, Xiao H, Yu H, Wang N, Yao X. Lignans from stems of *Sambucus williamsii*. *Zhongguo Zhong Yao Za Zhi*, 34 (10): 1225-1227, 2009.
114. Ouyang F, Liu Y, Li R, Li L, Wang N, Yao XS. Five Lignans and an Iridoid from *Sambucus williamsii*. *Chinese Journal of Natural Medicines*, 9 (1): 26-29, 2011.
115. Gross GA, Sticher O, Anklin C. Zwei weitere Iridoid-glycoside und ein neues monoterpen-glycosid aus *Sambucus ebulus* L. (Caprifoliaceae). *Helv Chim Acta*, 70: 91-101, 1987.
116. Wang Z-Y, Han H, Yang B-Y, Xia Y-G, Kuang H-X. Two new iridoid glycosides from the root barks of *Sambucus williamsii* Hance. *Molecules*, 16: 3869-3874, 2011.
117. Gross GA, Sticher O. Isosweroside, ein neues scoiridoidglucoside aus den Wurzeln des Zwergholunders *Sambucus ebulus* L. (Caprifoliaceae). *Helv Chim Acta*, 69: 1113-1119, 1986.
118. Gross G, Sticher O, Anklin C. Two new iridoid glycosides and a monoterpene glycoside from *Sambucus ebulus* L. (Caprifoliaceae). *Helv Chim Acta*, 70 (1): 901-101, 1987.
119. Gross GA, Sticher O, Anklin C. Ein neues esteriridoidglucoside aus *Sambucus ebulus* L (Caprifoliaceae). *Helv Chim Acta*, 69: 156-162, 1986.
120. Pieri V, Schwaiger S, Ellmerer EP, Stuppner H. Iridoid glycosides from the leaves of *Sambucus ebulus*. *J Nat Prod*, 72 (10): 1798-1803, 2009.
121. Yang X, Wong M, Wang N, Chan AS, Yao X. A new eudesmane derivative and a new fatty acid ester from *Sambucus williamsii*. *Chem Pharm Bull*, 54 (5): 676-678, 2006.
122. Guo X, Zhang L, Quan S, Hong Y, Liu M. Chemical constituents of Williams elder (*Sambucus williamsii*). *Zhongcaoyao*, 29 (11): 727-729, 1998.
123. Lawrie W, McLean J, Paton AC. Triterpenoids in the bark of elder (*Sambucus nigra*). *Phytochemistry*, 3: 267-268, 1963.
124. Rao VS, Melo CL, Queiroz MG, Lemos TL, Menezes DB, Melo TS, Santos FA. Ursolic acid, a pentacyclic triterpene from *Sambucus australis*, prevents abdominal adiposity in mice fed a high-fat diet. *J Med Food*, 14 (11): 1375-1382, 2011.
125. Riehle P, Vollmer M, Rohn S. Phenolic compounds in *Cistus incanus* herbal infusions; antioxidant capacity and thermal stability during the brewing process. *Food Res Int*, 53 (2): 891-889, 2013.
126. Danne A, Petereit F, Nahrstedt A. Proanthocyanidins from *Cistus incanus*. *Phytochemistry*, 34 (4): 1129-1133, 1993.

127. Chaves N, Escudero JC, Gutiérrez-Merino C. Quantitative variation of flavonoids among individuals of a *Cistus ladanifer* population. *Biochem Syst Ecol*, 25 (5): 429-435, 1997.
128. De Pascual TJ, Urones JG, Marcos IS, Núñez L, Basabe P. Diterpenoids and flavonoids from *Cistus palinhae*. *Phytochemistry*, 22 (12): 2805-2808, 1983.
129. Vogt T, Gulz PG, Wray V. Epicuticular 5-O-methyl flavonols from *Cistus laurifolius*. *Phytochemistry*, 27 (11): 3712-3713, 1988.
130. Danne A, Peterleit F, Nahrstedt A. Flavan-3-ols, prodelphinidins and further polyphenols from *Cistus salvifolius*. *Phytochemistry*, 37 (2): 533-538, 1994.
131. De Pascual TJ, Urones JG, Marcos IS, Bermejo F, Basabe P. A rearranged labdane: Salmantic acid from *Cistus laurifolius*. *Phytochemistry*, 22 (12): 2783-2785, 1983.
132. Calabuig MT, Cortés M, Francisco CG, Hernández R, Suárez E. Labdane diterpenes from *Cistus symphytifolius*. *Phytochemistry*, 20 (9): 2255-2258, 1981.
133. De Pascual JT, Bellido IS, Basabe P, Marcos IS, Ruano IF, Urones JG. Labdane diterpenoids from *Cistus ladaniferus*. *Phytochemistry*, 21 (4): 899-901, 1982.
134. Demetzos C, Mitaku S, Skaltsounis AL, Harvala C, Couladis M, Libot F. Diterpene esters of malonic acid from the resin 'Ladano' of *Cistus creticus*. *Phytochemistry*, 35 (4): 979-981, 1994.
135. De Pascual TJ, Urones JG, Marcos IS, Barcala PB, Garrido NM. Diterpenoid and other components of *Cistus laurifolius*. *Phytochemistry*, 25 (5): 1185-1187, 1986.
136. Urones J, Basabe P, Isidro SM, Jiménez A, Lithgow A, López M, Moro R, Gómez A. Ring a functionalized Neo-clerodane diterpenoids from *Cistus populifolius*. *Tetrahedron*, 50 (36): 10791-10802, 1994.
137. Urones JG, Basabe P, Marcos IS, Martín DD, Jiménez V, Sexmero MJ, Gómez B, Slawin AMZ, Williams DJ. (5S,8R,9R,10S,13S)-2-oxo-3-cleroden-15-oic acid from *Cistus palinhae*. *Phytochemistry*, 30 (10): 3471-3473, 1991.
138. Robles C, Garzino S. Essential oil composition of *Cistus albidus* leaves. *Phytochemistry*, 48 (8): 1341-1345, 1998.
139. Robles C, Garzino S. Intraspecific variability in the essential oil composition of *Cistus monspeliensis* leaves. *Phytochemistry*, 53 (1): 71-75, 2000.
140. Robles C, Bousquet-Mélou A, Garzino S, Bonin G. Comparison of essential oil composition of two varieties of *Cistus ladanifer*. *Biochem Syst Ecol*, 31 (3): 339-343, 2003.
141. Ogutveren M, Tetik SS. Composition of the essential oil of *Cistus laurifolius* L. from Turkey. *J Essent Oil Res*, 16 (1): 24-25, 2004.

142. Ogutveren M, Tetik SS. Composition of the essential oil of *Cistus parviflorus* L. from Turkey. *J Essent Oil Res*, 16 (2): 115-116, 2004.
143. Kumar V, Robbins SL. *Robbins Basic Pathology*. W.B. Saunders Company, Philadelphia, pp 401, 1992.
144. Harvey R, Champe P. *Pharmacology*. Lippincot Williams, Philadelphia, pp 401-408, 1998.

145. Kaminska B. MAPK signalling pathways as molecular targets for anti-inflammatory therapy from molecular mechanisms to therapeutic benefits. *Biochim Biophys Acta*, 1754 (1-2): 253-262, 2005.
146. Zang JM, An J. Cytokines, Inflammation and Pain. *Int Anesthesiol Clin*, 45 (2): 27-37, 2009.
147. Dinarello CA. Proinflammatory Cytokines. *Chest*, 118: 503-508, 2000.
148. Salek-Ardakani S, Croft M. Tumor necrosis factor receptor/tumor necrosis factor family members in antiviral CD8 T-cell immunity. *J Interferon Cytokine Res*, 30 (4): 205-218, 2010.
149. Herreweghe F, Festjens N, Declercq W, Vandenameele P. Tumor necrosis factor-mediated cell death: to break or to burst, that's the question. *Cell Mol Life Sci*, 67 (10): 1567-1579, 2010.
150. Hehlhans T, Pfeffer K. The intriguing biology of the tumour necrosis factor/tumour necrosis factor receptor superfamily: players, rules and the games. *Immunology*, 115 (1): 1-20, 2005.
151. Montfrans C, Peppelenbosch M, Velde AA, Deventer S. Inflammatory signal transduction in Crohn's disease and novel therapeutic approaches. *Biochem Pharmacol*, 64 (5-6): 789-795, 2002.
152. Berry M, Brightling C, Pavord I, Wardlaw A. TNF-alpha in asthma. *Curr Opin Pharmacol*, 7 (3): 279-282, 2007.
153. Leung L, Cahill CM. TNF-alpha and neuropathic pain. *J Neuroinflammation*, 7: 27, 2010.
154. Wu Y, Zhou BP. TNF-alpha/NF-kappaB/Snail pathway in cancer cell migration and invasion. *Br J Cancer*, 102 (4): 639-644, 2010.
155. Van Deventer SJ. Immunotherapy of Crohn's disease. *Scand J Immunol*, 51 (1): 18-22, 2000.

156. Sims J, March C, Cosman D, Widmer M, MacDonald H, McMahan C, Grubin C, Wignall J, Jackson J, Call S. cDNA expression cloning of the IL-1 receptor, a member of the immunoglobulin superfamily. *Science*, 241 (4865): 585-589, 1988.
157. Sweeney SE, Firestein GS. Signal transduction in rheumatoid arthritis. *Curr Opin Rheumatol*, 16 (3): 231-237, 2004.
158. Schielke GP, Yang GY, Shivers BD, Betz AL. Reduced ischemic brain injury in interleukin-1 beta converting enzyme-deficient mice. *J Cereb Blood Flow Metab*, 18 (2): 180-185, 1998.
159. Boutin H, LeFeuvre RA, Horai R, Asano M, Iwakura Y, Rothwell NJ. Role of IL-1alpha and IL-1beta in ischemic brain damage. *J Neurosci*, 21 (15): 5528-5534, 2001.
160. Nelson B. IL-2, regulatory T cells, and tolerance. *J Immunol*, 172 (7): 3983-3988, 2012.
161. Aktan F. iNOS-mediated nitric oxide production and its regulation. *Life Sci*, 75 (6): 639-653, 2004.
162. Sun J, Zhang X, Broderick M, Fein H. Measurement of nitric oxide production in biological systems by using griess reaction assay. *Sensors*, 3 (8): 276-284, 2003.
163. Szabo C, Ohshima H. DNA damage induced by peroxynitrite: subsequent biological effects. *Nitric Oxide*, 1 (5): 373-385, 1997.
164. Lahti A, Kankaanranta H, Moilanen E. P38 mitogen-activated protein kinase inhibitor SB203580 has a bi-directional effect on iNOS expression and NO production. *Eur J Pharmacol*, 454: 115-123, 2002.
165. Momose I, Terashima M, Nakashima Y, Sakamoto M. Phorbol ester synergistically increases interferon regulatory factor-1 and inducible nitric oxide synthase induction in interferon-Q-treated. *Biochim Biophys Acta*, 1498: 19-31, 2000.
166. Marks-Konczalik J, Chu SC, Moss J. Cytokine-mediated transcriptional induction of the human inducible nitric oxide synthase gene requires both activator protein 1 and nuclear factor kappa B-binding sites. *J Biol Chem*, 273: 22201-22208, 1998.
167. Müller M, Pfannes SDC, Ayoub M, Hoffmann P, Bessler GM, Markus R, Mittenbühler K. Immunostimulation by the synthetic lipopeptide P3 CSK 4 : TLR4-independent activation of the ERK1 /2 signal transduction pathway in macrophages. *Immunology*, 103 (1): 49-60, 2001.
168. Kleinert H, Wallerath T, Fritz G, Ihrig-Biedert I, Rodriguez-Pascual F, Geller D, Förstermann U. Cytokine induction of NO synthase II in human DLD-1 cells: roles of the JAK-STAT, AP-1 and NF-kappaB-signaling pathways. *Brit J Pharmacol*, 125: 193-201, 1998.

169. Kleinert H, Euchenhofer C, Ihrig-Biedert I, Förstermann U. In murine 3T3 fibroblasts, different second messenger pathways resulting in the induction of NO synthase II (iNOS) converge in the activation of transcription factor NF-kappaB. *J Biol Chem*, 271: 6039-6044, 1996.
170. Hecker M, Cattaruzza M, Wagner H. Regulation of inducible nitric oxide synthase gene expression in vascular smooth muscle cells. *Gen Pharmacol*, 32: 9-16, 1999.
171. Wang BS, Lin JK. Role of tyrosine kinase Activity in 2 , 2' , 2''- tripyridine-induced nitric oxide generation in macrophages. *Biochem Pharmacol*, 57: 1367-1373, 1999.
172. Xia YF, Liu LP, Zhong CP, Geng JG. NF-kappaB activation for constitutive expression of VCAM-1 and ICAM-1 on B lymphocytes and plasma cells. *Biochem Biophys Res Commun*, 289 (4): 851-856, 2001.
173. Huang KT, Kuo L, Liao JC. Lipopolysaccharide activates endothelial nitric oxide synthase through protein tyrosine kinase. *Biochem Biophys Res Commun*, 245: 33-37, 1998.
174. Obermeier F, Gross V, Falk W. Interleukin-1 production by mouse macrophages is regulated in a feedback fashion by nitric oxide Abstract : The pleiotropic cytokine interleukin-1 synthase (iNOS). *J Leucocyte Bio*, 66: 829-836, 1999.
175. Tsai SH, Lin-Shiau SY, Lin JK. Suppression of nitric oxide synthase and the down-regulation of the activation of NFkB in macrophages by resveratrol. *Brit J Pharmacol*, 126 (3): 673-680, 1999.
176. Chen YC, Shen SC, Lee WR, Hou WC, Yang LL, Lee TJF. Inhibition of nitric oxide synthase inhibitors and lipopolysaccharide induced inducible NOS and cyclooxygenase-2 gene expressions by rutin, quercetin, and quercetin pentaacetate in RAW 264.7 macrophages. *J Cell Biochem*, 82 (4): 537-548, 2001.
177. Kudo I, Murakami M. Prostaglandin E synthase, a terminal enzyme for prostaglandin E2 biosynthesis. *J Biochem Mol Biol*, 6 (30): 633-638, 2005
178. Rouzer CA, Marnett LJ. Cyclooxygenases: structural and functional insights. *J Lipid Res*, 50: 29-34, 2009.
179. Hata AN, Breyer RM. Pharmacology and signaling of prostaglandin receptors: multiple roles in inflammation and immune modulation. *Pharmacol Ther*, 103 (2): 147-166, 2004.
180. Giuliano F, Warner TD. Origins of prostaglandin E2: involvements of cyclooxygenase (COX)-1 and COX-2 in human and rat systems. *J Pharmacol Exp Ther*, 303 (3): 1001-1006, 2002.

181. Akira S, Takeda K. Toll-like receptor signalling. *Nat Rev Immunol*, 4 (7): 499-511, 2004.
182. Chen YC, Shen SC, Chen LG, Lee TJF, Yang LL. Wogonin, baicalin, and baicalein inhibition of inducible nitric oxide synthase and cyclooxygenase-2 gene expressions induced by nitric oxide synthase inhibitors and lipopolysaccharide. *Biochem Pharmacol*, 61 (11): 1417-1427, 2001.
183. O'Connel MA, Bennett BL, Mercurio F, Manning AM, Mackman N. Role of IKK1 and IKK2 in lipopolysaccharide signaling in human monocytic cells. *J Biol Chem*, 273 (46): 30410-30414, 1998.
184. Hawiger J, Veach RA, Liu XY, Timmons S, Ballard DW. IkappaB kinase complex is an intracellular target for endotoxic lipopolysaccharide in human monocytic cells. *Blood*, 94 (5): 1711-1716, 1999.
185. Napetschnig J, Wu H. Molecular basis of NF-kappaB signaling. *Annu Rev Biophys*, 42: 443-468, 2013.
186. Cooper GM, Hausman RE. *The cell : a molecular approach*. (5th ed.) ASM Press, Washington, D.C., pp 820, 2009.
187. Johnson GL, Lapadat R. Mitogen-activated protein kinase pathways mediated by ERK, JNK, and p38 protein kinases. *Science*, 298: 1911-1912, 2002.
188. Chen CC, Wang JK. p38 but not p44/42 mitogen-activated protein kinase is required for nitric oxide synthase induction mediated by lipopolysaccharide in Raw 264.7 macrophages. *Mol Pharmacol*, 55 (3): 481-488, 1999.
189. Schumann RR, Leong SR, Flaggs GW, Gray PW, Wright SD, Mathison JC, Tobias PS, Ulevitch RJ. Structure and function of lipopolysaccharide binding protein. *Science*, 249 (4975): 1429-1431, 1990.
190. Wright SD, Ramos RA, Tobias PS, Ulevitch RJ, Mathison JC. CD14, a receptor for complexes of lipopolysaccharide (LPS) and LPS binding protein. *Science*, 249 (4975): 1431-1433, 1990.
191. Hoshino K, Takeuchi O, Kawai T, Sanjo H, Ogawa T, Takeda Y, Takeda K, Akira S. Cutting edge: Toll-like receptor 4 (TLR4)-deficient mice are hyporesponsive to lipopolysaccharide: Evidence for TLR4 as the Lps gene product. *J Immunol*, 162 (7): 3749-3752, 1999.
192. Choi RJ, Shin EM, Jung HA, Choi JS, Kim YS. Inhibitory effects of kaurenoic acid from *Aralia continentalis* on LPS-induced inflammatory response in Raw 264.7 macrophages. *Phytomedicine*, 18: 677-682, 2011.

193. Yoon WJ, Moon JY, Song G, Lee YK, Han MS, Lee JS, Ihm BS, Lee WJ, Lee NH, Hyun CG. *Artemisia fukudo* essential oil attenuates LPS-induced inflammation by suppressing NF- κ B and MAPK activation in Raw 264.7 macrophages. *Food Chem Toxicol*, 48: 1222-1229, 2010.
194. Lu Y, Suh SJ, Kwak CH, Kwon KM, Seo CS, Li Y, Jin Y, Li X, Hwang SL, Kwon O, Chang YC, Park YG, Park SS, Son JK, Kim CH, Chang HW. Saucerneol F, a new lignan, inhibits iNOS expression via MAPKs, NF- κ B and AP-1 inactivation in LPS-induced Raw 264.7 cells. *Int Immunopharmacol*, 12: 175-181, 2012.
195. Liu SF, Adcock IM, Old RW, Barnes PJ, Evans TW. Lipopolysaccharide treatment *in vivo* induces widespread tissue expression of inducible nitric oxide synthase mRNA. *Biochem Biophys Res Commun*, 196 (3): 1208-1213, 1993.
196. Chan ED, Riches DWH. IFN- γ + LPS induction of iNOS is modulated by ERK, JNK/SAPK, and p38 Mapk in a mouse macrophage cell line. *American Journal of Physiology - Cell Physiology*, 280 (3): 441-450, 2001.
197. Hambleton J, Weinstein SL, Lem L, DeFranco AL. Activation of c-Jun N-terminal kinase in bacterial lipopolysaccharide-stimulated macrophages. *P Natl A Sci*, 93 (7): 2774-2778, 1996.
198. Swantek JL, Cobb MH. Protein kinase (JNK /SAPK) is required for lipopolysaccharide stimulation of tumor necrosis factor alpha (TNF-alpha) translation : glucocorticoids inhibit TNF-alpha translation by blocking JNK /SAPK . Jun N-Terminal Kinase /Stress-Activated Protein. *Microbiology*, 1997.
199. Geppert TD, Whitehurst CE, Thompson P, Beutler B. Lipopolysaccharide signals activation of tumor necrosis factor biosynthesis through the ras/raf-1/MEK/MAPK pathway. *Mol Med*, 1: 93-103, 1994.
200. Durando MM, Meier KE, Cook JA. Endotoxin activation of mitogen-activated protein kinase in THP-1 cells ; diminished activation following endotoxin desensitization. *J Leukocyte Biol*, 64: 259-264, 1998.
201. Olszewska M. Flavonoids from *Prunus serotonia* EHRH . *Acta Poloniae Pharmaceutica*, 62: 127-133, 2005.
202. Gutzeit D, Wray V, Winterhalter P, Jerz G. Preparative isolation and purification of flavonoids and protocatechuic acid from sea buckthorn juice concentrate (*Hippophaë rhamnoides* L. ssp. *rhamnoides*) by High-Speed Counter-Current Chromatography. *Chromatographia*, (1-2) (65): 1-7, 2007.
203. Gautam R, Jachak SM. Recent developments in anti-inflammatory natural products. *Med Res Rev*, 29 (5): 767-820, 2009.
204. Yesilada E. Evaluation of the Anti-inflammatory activity of the Turkish medicinal plant *Sambucus ebulus*. *Chem Nat Comp*, 5: 539-540, 1997.

205. Honda G, Yesilada E, Tabata M, Sezik E, Fujita T, Takeda Y, Takaishi Y, Tanaka T. Traditional medicine in Turkey. VI. folk medicine in West Anatolia: Afyon, Kutahya, Denizli, Mugla, Aydin provinces. *J Ethnopharmacol*, 53 (2): 75-87, 1996.
206. Fujita T, Sezik E, Tabata M, Yeşilada E, Honda G, Takeda Y, Tanaka T, Takaishi T. Traditional medicine in Turkey VII: folk medicine in Middle and West Black Sea regions. *Econ Bot*, 49: 406-422, 1995.
207. Sezik E, Yeşilada E, Tabata M, Honda G, Takaishi Y, Fujita T, Tanaka T, Takeda Y. Traditional medicine in Turkey VIII: folk medicine in east Anatolia; Erzurum, Erzincan, Ağrı, Kars, Iğdır provinces. *Econ Bot*, 51: 195-211, 1997.
208. Yesilada E, Honda G, Sezik E, Tabata M, Fujita T, Tanaka T, Takeda Y, Takaishi Y. Traditional medicine in Turkey. V. Folk medicine in the inner Taurus Mountains. *J Ethnopharmacol*, 46 (3): 133-152, 1995.
209. Yesilada E, Sezik E, Honda G, Takaishi Y, Takeda Y, Tanaka T. Traditional medicine in Turkey IX: folk medicine in North-West Anatolia. *J Ethnopharmacol*, 64 (3): 195-210, 1999.
210. Hwang BY, Lee JH, Nam JB, Hong YS, Lee JJ. Lignans from *Saururus chinensis* inhibiting the transcription factor NF-kappaB. *Phytochemistry*, 64 (3): 765-771, 2003.
211. Sun Z, Andersson R. NF-kappaB activation and inhibition: a review. *Shock*, 18 (2): 99-106, 2002.
212. Salminen A, Huuskonen J, Ojala J, Kauppinen A, Kaarniranta K, Suuronen T. Activation of innate immunity system during aging: NF-kB signaling is the molecular culprit of inflamm-aging. *Ageing Res Rev*, 7 (2): 83-105, 2008.
213. Nam J, Aguda BD, Rath B, Agarwal S. Biomechanical thresholds regulate inflammation through the NF-kappaB pathway: experiments and modeling. *PLoS One*, 4 (4): 5262, 2009.
214. Mattson MP, Meffert MK. Roles for NF-kappaB in nerve cell survival, plasticity, and disease. *Cell Death Differ*, 13 (5): 852-860, 2006.
215. Bharti AC, Aggarwal BB. Nuclear factor-kappa B and cancer: its role in prevention and therapy. *Biochem Pharmacol*, 64 (5-6): 883-888, 2002.
216. Makarov SS. NF-kappaB as a therapeutic target in chronic inflammation: recent advances. *Mol Med Today*, 6 (11): 441-448, 2000.
217. Gilmore TD, Herscovitch M. Inhibitors of NF-kappaB signaling: 785 and counting. *Oncogene*, 25 (51): 6887-6899, 2006.

218. Tincani A, Andreoli L, Bazzani C, Bosiso D, Sozzani S. Inflammatory molecules: a target for treatment of systemic autoimmune diseases. *Autoimmun Rev*, 7 (1): 1-7, 2007.
219. Schmitz ML, Bacher S. Novel molecular targets in the search for anti-inflammatory agents. *Phytochem Rev*, 4: 19-25, 2005.
220. Lee S, Park HS, Notsu Y, Ban HS, Kim YP, Ishihara K, Hirasawa N, Jung SH, Lee YS, Lim SS, Park EH, Shin KH, Seyama T, Hong J, Ohuchi K. Effects of hyperin, isoquercitrin and quercetin on lipopolysaccharide-induced nitrite production in rat peritoneal macrophages. *Phytother Res*, 22 (11): 1552-1556, 2008.
221. Erdemoglu N, Akkol EK, Yesilada E, Calis I. Bioassay-guided isolation of anti-inflammatory and antinociceptive principles from a folk remedy, *Rhododendron ponticum* L. leaves. *J Ethnopharmacol*, 119 (1): 172-178, 2008.
222. Son KHK, S.Y. Kim, H.P. Chang, H. W. Kang, S. S. Constituents from *Syzygium aromaticum* Merr. *et* Perry. *Nat Prod Sci*, 4 (4): 263-267, 1998.
223. Hamalainen M, Nieminen R, Vuorela P, Heinonen M, Moilanen E. Anti-inflammatory effects of flavonoids: genistein, kaempferol, quercetin, and daidzein inhibit STAT-1 and NF-kappaB activations, whereas flavone, isorhamnetin, naringenin, and pelargonidin inhibit only NF-kappaB activation along with their inhibitory effect on iNOS expression and NO production in activated macrophages. *Mediators Inflamm*, 2007: 45673, 2007.
224. Ahmed MS, Tanbouly NDE, Islam WT, Sleem AA, Senousy ASE. Antiinflammatory flavonoids from *Opuntia dillenii* (Ker-Gawl) Haw. flowers growing in Egypt. *Phytotherapy Research*, 19 (9): 807-809, 2005.
225. Ghisabelti EL. Biological and pharmacological activity of naturally occurring iridoids and secoiridoids. *Phytomedicine*, 5 (2): 147-163, 1998.
226. Shin JS, Yun KJ, Chung KS, Seo KH, Park HJ, Cho YW, Baek NI, Jang D, Lee KT. Monotropein isolated from the roots of *Morinda officinalis* ameliorates proinflammatory mediators in Raw 264.7 macrophages and dextran sulfate sodium (DSS)-induced colitis via NF- κ B inactivation. *Food Chem Toxicol*, 53 (0): 263-271, 2013.
227. An SJ, Pae HO, Oh GS, Choi BM, Jeong S, Jang SI, Oh H, Kwon TO, Song CE, Chung HT. Inhibition of TNF- α , IL-1 β , and IL-6 productions and NF- κ B activation in lipopolysaccharide-activated Raw 264.7 macrophages by catalposide, an iridoid glycoside isolated from *Catalpa ovata* G. Don (Bignoniaceae). *Int Immunopharmacol*, 2 (8): 1173-1181, 2002.
228. Bas E, Recio MC, Máñez S, Giner RM, Escandell JM, López-Ginés C, Rios JL. New insight into the inhibition of the inflammatory response to experimental delayed-type hypersensitivity reactions in mice by scopolioside A. *Eur J Pharmacol*, 555 (2-3): 199-210, 2007.

229. Huang THW, Tran VH, Duke RK, Tan S, Chrubasik S, Roufogalis BD, Duke CC. Harpagoside suppresses lipopolysaccharide-induced iNOS and COX-2 expression through inhibition of NF- κ B activation. *J Ethnopharmacol*, 104 (1–2): 149-155, 2006.
230. Mantovani A, Allavena P, Sica A, Balkwill F. Cancer-related inflammation. *Nature*, 454: 436-444, 2008.
231. Patel SA, Heinrich AC, Reddy BY, Rameshwar P. Inflammatory mediators: parallels between cancer biology and stem cell therapy. *J Inf Res*, 2: 13-19, 2009.
232. Cheon MS, Yoon T, Lee Y, Choi G, Moon BC, Lee AY, Choo BK, Kim HK. *Chrysanthemum indicum* Linne extract inhibits the inflammatory response by suppressing NF-kappaB and MAPKs activation in lipopolysaccharide-induced Raw 264.7 macrophages. *J Ethnopharmacol*, 122 (3): 473-477, 2009.
233. Tran K, Merika M, Thanos D. Distinct functional properties of IkappaB alpha and IkappaB beta. *Mol Cell Biol*, 17 (9): 5386-5399, 1997.

7. CURRICULUM VITAE

İrem Atay was born in April, 1985 in İstanbul, Turkey. She graduated from Bandırma Anadolu Lisesi in 2003. In the same year, she started her education at Marmara University Faculty of Pharmacy and graduated in 2007. She attended Yeditepe University Institute of Health Sciences Pharmacognosy PhD. Programme in 2007. She started working as a research and teaching assistant in Yeditepe University Faculty of Pharmacy Department of Pharmacognosy at the same year. She is currently employed in the same job.